THE ROLE OF

TUMOUR NECROSIS FACTOR ALPHA STIMULATED GENE-6

ON BONE

~

Sara Afrough
Wolfson College

A thesis submitted to
The Medical Sciences Division, University of Oxford
In partial fulfilment of the requirement
For the degree of Doctor of Philosophy
In Musculoskeletal Sciences
Through
The Kennedy Institute of Rheumatology,
Nuffield Department of Orthopaedics,
Rheumatology and Musculoskeletal Sciences,
University of Oxford

~

Hilary Term
2016

DECLARATION OF ORIGINALITY

No part of this thesis has previously been published or submitted elsewhere for any academic degree or qualification. Where other people have contributed to aspects of the study, they have been acknowledged. Information derived from alternative sources, other than my own study, have been acknowledged.

Signature:



Print: SARA AFROUGH

Date: 22 April 2016

WORD COUNT: 30,861

ACKNOWLEDGEMENTS

There is a long list of people I would like to thank for the past four years leading up to the completion of my D.Phil studies. Firstly, my supervisors Prof. Nicole Horwood, Prof. Afsie Sabokbar and Dr. David Mahoney, I thank you for enabling me to undertake this project, your guidance throughout my time as a student has been indispensable. Nikki and Afsie, I cannot thank you enough for your untiring support, words of wisdom, and the many discussions shedding light on aspects of osteoimmunology and bone biology. David, you have given so much of your time teaching techniques and scientific concepts in the most creative and thought-provoking way possible, thank you for being a dedicated mentor and planting the seeds for this project.

I would next like to thank Dr. Sarah Wythe, your mentorship and insights into the study of immunology have been an asset during my studies. Dr. Andrew Freidin, thank you for the hours, days and weeks you invested in teaching and carrying out micro-CT on bone samples. Dr. James Dunford, I appreciate the time you patiently spent sharing your expertise on protein production.

During my time as a D.Phil student the past and present staff at the Kennedy Institute of Rheumatology and the Botnar Research Centre have been instrumental in developing my scientific thinking. In no particular order I would like the thank the following people; Mrs. Patricia Green, Mrs. Parisa Amjadi, Dr. Simon Kollnberger, Dr. Anastasios Chanalaris, Dr. Heba Ismail, Dr. Allahdad Zarei, Dr. Xiaodi Tang, Dr. Mohammad Nickdel, Dr. Lynett Danks, Mr. Albertino Bonifacio and Mrs. Mino Medghalchi. I would also like to thank Dr. Jadwiga Zarebska and Prof. Tonia Vincent for the TSG-6 mouse line. Similarly, the team of histologists have been a great support to our research. I would therefore like to thank Ms. Geethanjali Bahal, Ms. Angela Seedhar, Dr. Bryony Stott, Dr. Samuel Bullers, Dr. Ida Parisi and Ms. Marcia Curtinha.

My College, Wolfson, have been wonderful throughout the course of my stay in Oxford. A special thank you to Sir Professor Anthony Epstein, Ms. Gillian Hamnet and Ms. Rachael Connelly. I would also like to thank Prof. Chris Murphy for student-related matters and acknowledge the Kennedy Institute of Rheumatology Trustees for funding my studies.

This journey would not have been complete without all my dear friends, some old, others new, yet all great. Dr. Christine Doherty, Ms. Lorena Zulliani, Mr. Sean Giblin, Dr. Mona Alinejad, Dr. Kristian Sørbo, Mr. Jonas Fuchs, and Dr. Mohammad Bahar. I thank you for listening, supporting, offering advice and forming my team of proof readers.

I also wanted to thank the people that made it possible for me to progress onto this D.Phil program. This largely rest with Prof. David Gary, Dr. Steven Jenkins and Prof. Judith Allen for building foundations during my years as an undergraduate student.

Lastly, but by no mean least, I would like to thank my family Saltanat Barideh, Sima Bajdanzadeh, Mohammad Afrough, Babak Afrough, Simin Hough, Jack Rooney, Richard Hough, Marie Soetens, Molly Foster, and Darius Hough. You have all been an unbelievable support system and I am forever indebted.

For Babak Afrough and Simin Hough,

Always.

“…If you can dream - and not make dreams your master;
If you can think - and not make thoughts your aim,
If you can meet with Triumph and Disaster
And treat those two impostors just the same.
If you can bear to hear the truth you've spoken
Twisted by knaves to make a trap for fools,
Or watch the things you gave your life to, broken,
And stoop and build'em up with worn-out tools…”

Rudyard Kipling

1895

ABSTRACT

Thesis Title: The Role of Tumour Necrosis Factor Alpha Stimulated Gene-6 on Bone

Candidate: Sara Afrough

College: Wolfson

Degree: Doctor of Philosophy (D.Phil)

Term and year: Hilary 2016

Osteoporosis, a metabolic disorder of the skeletal system, currently affects 200 million people worldwide. Osteoporosis is caused by an imbalance in bone resorption and formation due to either molecular mutations, oestrogen reduction at menopause, oxidative stress, as well as life style, leading to a characteristic low bone density and/or thinning that predisposes patients to skeletal fracture and breakage upon minimal physical trauma. Depending on the severity of the disease, most patients are often treated with calcium/vitamin D and anti-resorptive drugs such as bisphosphonates or calcitonin. However, there are few options for bone formation using anabolic agents- such as Teriparatide (PTH_{1-34}), which have limited success, creating an unmet need for novel anabolic interventions.

The rapidly-advancing field of osteoimmunology recognises the close and finely-tuned interaction between the immune system and musculoskeletal organisation. In an attempt to identify immune-derived cells and soluble factors that induce the differentiation of stem cells towards the osteoblast lineage, the interaction between monocytes and osteoblast precursors has proven a potentially promising approach.

One of the factors identified from this screening was TSG-6 – a secreted protein with immunomodulatory and chondroprotective properties.

This study aimed to generate adequate amounts of biologically active TSG-6 protein to test its role on bone formation *in vivo* during physiology and disease - using oestrogen-

deficiency induced bone loss in mice as a model of osteoporosis. TSG-6 was not found to protect bone tissue against the effects of oestrogen-deficiency induced bone loss, as determined by global TSG-6 knockout and systemic exogenous administration studies. However, local delivery of full-length TSG-6 significantly enhanced mineral apposition rate in a dose-dependent manner, and *in vitro* studies found TSG-6 significantly enhanced alkaline phosphatase levels of primary bone marrow-derived human mesenchymal stem cells *in vitro,* in the presence of BMP-2.

Contrary to its previously reported inhibitory effects on osteoblastogenesis, this thesis shows, for the first time, that TSG-6 displays context-specific anabolic properties. This finding implies a therapeutic value for the protein, with possibilities of being used in conjunction with BMP-2 to treat local bone injuries such as fractures.

TABLE OF CONTENTS

DECLARATION OF ORIGINALITY 1

ACKNOWLEDGEMENTS 2

ABSTRACT 5

LIST OF FIGURES 10

LIST OF TABLES 14

LIST OF ABBREVIATIONS 16

CHAPTER 1: LITERATURE REVIEW 21

1.1 BONE TISSUE 22
1.1.1 Bone Function 22
1.1.2 Bone Structure 22
1.1.3 Bone Composition 22
1.1.4 Bone Ossification 24

1.2 CELLS OF THE SKELETAL SYSTEM 25
1.2.1 Osteoclast Origin, Function and Characteristics 26
1.2.2 Osteoblast Origin, Function and Characteristics 27
1.2.3 Osteocyte Origin, Function and Characteristics 29
1.2.4 Bone Lining Cells 31

1.3 MOLECULAR CONTROL OF BONE CELLS 32
1.3.1 Osteoclastogenesis 32
1.3.2 Osteoblastogenesis 40
1.3.3 Other Important Interactions Orchestrating Bone Remodelling 45

1.4 BONE REMODELLING 48
1.4.1 Physiological Bone Remodelling 48
1.4.2 Pathological Bone Remodelling 54

1.5 OSTEOPOROSIS 55
1.5.1 Glucocorticoid-Induced Osteoporosis 55
1.5.2 Postmenopausal Osteoporosis 56
1.5.3 Treating Osteoporosis 58

1.6 TSG-6 61
1.6.1 The Structure of TSG-6 Protein 61
1.6.2 TSG-6: Pattern of Expression 63
1.6.3 TSG-6 Expression in Non-Pathological Processes 64
1.6.4 TSG-6 Expression in Pathological Processes 65
1.6.5 Understanding the Function of TSG-6 through its Ligands 66
1.6.6 The Significance of TSG-6 in Murine Models of Inflammatory Arthritis 68
1.6.7 TSG-6 and the Therapeutic Effects of MSCs 70

1.7 THESIS AIMS AND HYPOTHESIS 72

CHAPTER 2: EXPRESSION AND PURIFICATION OF BIOLOGICALLY ACTIVE FULL-LENGTH RECOMBINANT HUMAN TSG-6 PROTEIN..... 73

2.1 INTRODUCTION..... 74

2.2 MATERIALS AND METHODS..... 77
2.2.1 Expression, Purification, Quantification of Full-Length rhTSG-6 Protein..... 77
2.2.2 Preparation of High-Titer Passage 3 Viral Stock for Protein Expression..... 81
2.2.3 Baculovirus-Sf9 Cell Expression System..... 83
2.2.4 Affinity Chromatography..... 83
2.2.5 TEV Digestion of His-FLAG Tag..... 84
2.2.6 Size Exclusion Chromatography..... 84
2.2.7 Sodium Dodecyl Sulphate Polyacrylamide Gel Electrophoresis Analysis..... 84
2.2.8 Western Blot Analysis..... 85
2.2.9 Bicinchoninic Acid Assay: Quantification of Total Protein in Preparations..... 86
2.2.10 Chromogenic Limulus Amebocyte Lysate Assay: Quantification of LPS Endotoxin Contaminate in TSG-6 Protein Preparations..... 86
2.2.11 Osteoclast Formation Assay: *In Vitro* test of TSG-6 Biological Activity..... 86

2.3 RESULTS..... 88
2.3.1 Determination of TSG-6 Vector Sequence and its Corresponding Peptide Sequence Using Bioinformatics Tools..... 88
2.3.2 Optimisation of Baculovirus-Mediated Expression of Full-length rhTSG-6 Protein..... 93
2.3.3 Affinity Purification of Full-Length rhTSG-6 Fusion Protein..... 96
2.3.4 Cleavage of Full-Length rhTSG-6 Fusion Protein..... 100
2.3.5 Size Elusion Chromatography Purification of Full-Length rhTSG-6 Protein..... 101
2.3.6 Quantification and Quality Control of Full-Length rhTSG-6 Protein Preparation..... 104
2.3.7 Full-length TSG-6 Inhibits Osteoclast Activity *In Vitro*..... 105

2.4 DISCUSSION..... 106

CHAPTER 3: THE ROLE OF TSG-6 ON BONE MARROW-DERIVED MESENCHYMAL STEM CELLS' OSTEOGENESIS *IN VITRO*..... 110

3.1 INTRODUCTION..... 111

3.2 MATERIALS AND METHODS..... 114
3.2.1 Chromogenic LAL Assay: Quantification of LPS Endotoxin Contaminant in Reagents..... 114
3.2.2 *In Vitro* Expansion and Maintenance of BM-hMSCs..... 114
3.2.3 Isolation of Human Monocytes from Peripheral Blood Mononuclear Cells..... 115
3.2.4 *In Vitro* Osteogenic Differentiation of BM-hMSCs..... 116
3.2.5 Human TSG-6 ELISA..... 117
3.2.6 Knockdown of tsg-6 Gene in Primary Human Monocytes..... 118
3.2.7 Statistical analysis..... 122

3.3 RESULTS..... 123
3.3.1 *In Vitro* Osteogenic Differentiation of BM-hMSCs..... 123
3.3.2 TSG-6 Protein is Significantly Upregulated in Human Monocytes Following Contact with BM-hMSCs *In Vitro*..... 126
3.3.3 Addition of the Monoclonal Antibody against TSG-6 (A38.1.20) into BM-hMSC-Monocyte Co-Culture does not Influence ALP activity of primary BM-hMSCs..... 131
3.3.4 Silencing *tsg-6* Gene in Human Monocytes Prior to their *In Vitro* Co-Culture with BM-hMSCs does not Affect ALP Activity of Primary BM-hMSCs..... 134
3.3.5 TSG-6 does not Directly Enhance ALP Activity of Primary BM-hMSCs *In Vitro*..... 138
3.3.6 TSG-6 displays additive effects on BMP-2 mediated enhancement of ALP Activity of Primary BM-hMSCs *In Vitro*..... 140

3.4 DISCUSSION..... 143

CHAPTER 4: THE *IN VIVO* ROLE OF TSG-6 ON OESTROGEN DEFICIENCY-INDUCED OSTEOPOROSIS 148

4.1 INTRODUCTION 149

4.2 MATERIALS AND METHODS 151
4.2.1 Breeding and Maintenance of TSG-6 Knockout and Transgenic Murine Colonies 151
4.2.2 TSG-6 Knockout Colony Genotyping 152
4.2.3 Murine Calvarial Model: An In Vivo Test of Full-length TSG-6 Bone Anabolic Activity 156
4.2.4 Surgical Bilateral Removal of Mouse Ovaries: Bilateral Ovariectomy – A Murine Model of Postmenopausal Osteoporosis 158
4.2.5 Phenotypic Characterisation of Bone Tissue 159
4.2.6 Statistical Analysis 167

4.3 RESULTS 168
4.3.1 Determination of Mice Genotypes Derived from the TSG-6 Heterozygous Colony 168
4.3.2 Twelve and Twenty Week-Old TSG-6 Deficient Female Mice Exhibit Lower Bone Mass Relative to their Wild-Type Littermates 168
4.3.3 TSG-6 Significantly Increases Local MAR in a Dose-Dependent Manner During Physiological Bone Modelling 172
4.3.4 Global TSG-6 Deficiency does not Influence Bone Loss during Oestrogen-Deficiency-Induced Osteoporosis 180
4.3.5 Global TSG-6 deficiency does not influence osteoblast or osteoclast numbers at four weeks post oestrogen-deficiency induced osteoporosis 187
4.3.6 Systemic Administration of the Link domain of TSG-6 does not Influence Bone Loss during Oestrogen-Deficiency Induced Osteoporosis 191
4.3.7 The Link Domain of TSG-6 does not Enhance Local MAR 200
4.3.8 Systemic Administration of Full-Length rhTSG-6 Protein does not Influence Bone Loss during Oestrogen-Deficiency Induced Osteoporosis 202

4.4 DISCUSSION 204

CHAPTER 5: DISCUSSION 208

CHAPTER 6: BIBLIOGRAPHY 217

LIST OF FIGURES

CHAPTER 1: LITERATURE REVIEW

Figure 1. 1 The main anatomical features of a typical long bone 23

Figure 1. 2 Constituent cells of the bone/bone marrow 25

Figure 1. 3 Sequential gene expression during osteoblast differentiation. 27

Figure 1. 4 M-CSF signaling pathway in osteoclast precursors..... 33

Figure 1. 5 RANKL-mediated signaling controlling osteoclast lineage commitment and activation 35

Figure 1. 6 Signalling pathways controlling osteoblastogensis 44

Figure 1. 7 Bone remodeling unit and its cellular components. 50

Figure 1. 8 The phases of bone remodelling 53

Figure 1. 9 The structure of TSG-6 protein 63

CHAPTER 2: EXPRESSION AND PURIFICATION OF BIOLOGICALLY ACTIVE FULL-LENGTH RECOMBINANT HUMAN TSG-6 PROTEIN

Figure 2. 1 Map of the baculovirus transfer vector showing the location of vector elements and annealing sites of primers 78

Figure 2. 2 Overview of steps taken to generate high titer P3 recombinant baculovirus for the expression of full-length rhTSG-6 protein..... 80

Figure 2. 3 Overview of workflow in expressing and purifying full-length rhTSG-6 protein. 82

Figure 2. 4 BLAST pairwise alignment of full-length rhTSG-6 sequencing results against existing full-length TSG-6 sequence on the NCBI database. 89

Figure 2. 5 EMBOSS Transeq translation of full-length TSG-6 nucleic acid into the corresponding peptide sequence in all six reading frames..... 91

Figure 2. 6 TSG-6 protein sequence alignment using Clustal Omega program 92

Figure 2. 7 Western blot showing optimisation of baculovirus-mediated expression of rhTSG-6 protein. 95

Figure 2. 8 Representative SDS-PAGE gel and its corresponding Western blot showing fractions containing the rhTSG-6 protein following gravity-flow affinity separation. 97

Figure 2. 9 Chromatography trace showing affinity purification of full-length rhTSG-6 protein and its corresponding fractions as visualised by SDS-PAGE and Western blot. 99

Figure 2. 10 Western blot showing TEV-mediated removal of the N-terminal FLAG-tag peptide sequence of the rhTSG-6 fusion protein. 100

Figure 2. 11 Size exclusion chromatography trace showing purification of rhTSG-6 protein and its corresponding fractions on SDS-PAGE and Western blot. 103

Figure 2. 12 Full-length rhTSG-6 inhibits RANKL induced osteoclast activity. 105

CHAPTER 3: THE ROLE OF TSG-6 ON BONE MARROW-DERIVED MESENCHYMAL STEM CELLS' OSTEOGENESIS *IN VITRO*

Figure 3. 1 Monocytes significantly enhances ALP activity of primary BM-hMSCs 125

Figure 3. 2 TSG-6 protein expression is significantly upregulated following monocyte contact with BM-hMSCs 130

Figure 3. 3 Monoclonal antibody to TSG-6 (A38.1.20) in BM-hMSC-monocyte co-cultures does not inhibit ALP activity of primary BM-hMSCs. 133

Figure 3. 4 Optimising TSG-6 target siRNA 136

Figure 3. 5 Silencing *tsg-6* gene in monocytes does not affect early BM-hMSC osteogenesis in co-culture assays. 137

Figure 3. 6 TSG-6 does not directly enhance ALP activity of primary BM-hMSCs. 139

Figure 3. 7 TSG-6 enhances ALP activity of primary BM-hMSCs in the presence of BMP-2. 142

CHAPTER 4: THE IN VIVO ROLE OF TSG-6 ON OESTROGEN DEFICIENCY-INDUCED OSTEOPOROSIS

Figure 4. 1 Schematic of the *in vivo* calvarial assay used to test the local anabolic activity of TSG-6..... 157

Figure 4. 2 Representative fluorescent micrograph of a calvaria section showing how 2-D quantification of calvariae were carried out using bone histomorphometry. 161

Figure 4. 3 Agarose gel electrophoresis showing PCR products used to determine the genotype of offspring derived from heterozygous TSG-6 crosses..... 169

Figure 4. 4 Micro-CT derived morphological parameters from the lumbar vertebrae of wild-type and TSG-6 gene-targeted mice at 12 and 20 weeks of age..... 170

Figure 4. 5 Micro-CT generated images showing baseline bone morphology of the lumbar vertebrae of wild-type and TSG-6 gene targeted mice at 12 and 20 weeks of age. 171

Figure 4. 6 Histomorphometry-derived parameters showing local administration of full-length rhTSG-6 significantly increases local calvarial MAR. 173

Figure 4. 7 Enumerating local calvaria osteoblasts and osteoclasts following local treatment with full-length rhTSG-6. 175

Figure 4. 8 Micro-CT quantification of calvarial bone volume following treatment with different doses of full-length rhTSG-6. 177

Figure 4. 9 Histomorphometry parameters showing local administration of full-length rhTSG-6 increases local MAR significantly in a dose-dependent manner..... 178

Figure 4. 10 Representative fluorescent micrograph of calvarial sections following treatment with different doses of full-length rhTSG-6. 179

Figure 4. 11 Micro-CT derived parameters from the lumbar vertebrae of global TSG-6 targeted and wild-type mice following bilateral ovareictomy..... 182

Figure 4. 12 Representative images of vertebral sections from 17 week old wild-type and TSG-6 knockout female mice, with and without ovariectomy. 186

Figure 4. 13 Histology sections showing osteoblast and osteoclasts on lumbar vertebrae of TSG-6 deficint mice four weeks post-ovariectomy. 188
Figure 4. 14 Osteoblast and osteoclast counts from the lumbar vertebrae of TSG-6 deficient mice four weeks post ovariectomy. 190
Figure 4. 15 Total body mass before and after treatment with the Link module of TSG-6. 193
Figure 4. 16 Three-point bend testing showing the Link module of TSG-6 does not influence mechanical properties of the femoral diaphysis following ovareictomy. 195
Figure 4. 17 Micro-CT data showing the Link module of TSG-6 does not protect cortical bone against ovariectomy-induced bone loss. 197
Figure 4. 18 Micro-CT data showing the Link module of TSG-6 does not protect trabecular bone from ovariectomy-induced bone loss. 199
Figure 4. 19 Link module of TSG-6 does not enhance local calvarial MAR. 201
Figure 4. 20 Micro-CT data showing systemic administration of full-length TSG-6 does not protect lumbar vertebrae from ovariectomy-induced bone loss. 203

LIST OF TABLES

CHAPTER 1: LITERATURE REVIEW

Table 1. 1 Osteoblast markers and their associated functions 28

Table 1. 2 Osteocyte markers and their associated functions 30

Table 1. 3 Stimulatory factors on osteoclastogenesis 38

Table 1. 4 Inhibitory factors on osteoclastogenesis 39

CHAPTER 2: EXPRESSION AND PURIFICATION OF BIOLOGICALLY ACTIVE FULL-LENGTH RECOMBINANT HUMAN TSG-6 PROTEIN

Table 2. 1 TSG-6 protein quantification values as determined by BCA assay, with levels of LPS contamination, as determined by LAL assay 104

CHAPTER 3: THE ROLE OF TSG-6 ON BONE MARROW-DERIVED MESENCHYMAL STEM CELLS' OSTEOGENESIS *IN VITRO*

Table 3. 1 Constituents of the RT-PCR reaction mix 121

Table 3. 2 Top fifty most up-regulated gene transcripts within the human monocyte population 2 and 8 h post contact with BM-hMSCs 127

CHAPTER 4: THE IN VIVO ROLE OF TSG-6 ON OESTROGEN DEFICIENCY-INDUCED OSTEOPOROSIS

Table 4. 1 Cycling conditions used to amplify the TSG-6 wild-type allele. 153

Table 4. 2 Cycling conditions used to amplify the target TSG-6 (knockout) allele 154

Table 4. 3 Constituents of the PCR reaction mix 154

Table 4. 4 Processing decalcified tissues within paraffin blocks. 162

Table 4. 5 Steps taken to stain tissue sections with toluidine blue stain. 163

Table 4. 6 Summary of the steps taken to process tissue sections in preparation for immunohistochemistry. 165

Table 4. 7 Quantitative micro-CT parameters from the lumbar vertebrae of 17 week-old TSG-6 global knockout, heterozygote, and wild-type with and without bilateral ovariectomy. 183

Table 4. 8 Experimental groups and treatment conditions within the Link_TSG-6 ovariectomy study. 192

Table 4. 9 Quantitative micro-CT parameters from the left tibia of mice systemically treated with Link module of the TSG-6 protein following bilateral ovariectomy. 198

LIST OF ABBREVIATIONS

Abbreviation	
A	
AIA	Antigen-induced arthritis
ALP	Alkaline phosphatase
B	
BLAST®	Basic Local Alignment Search Tool
BMD	Bone mineral density
BM-hMSCs	Bone marrow-derived human mesenchymal stem cells
BMP	Bone morphogenetic protein
BMU(s)	Basic multicellular unit(s)
bp	Base pair
BSU	Biomedical services unit
C	
c-Fms	Colony-stimulating factor-1 receptor
CHO	Chinese hamster ovarian
CIA	Collagen-induced arthritis
COC	Cumulus cell-oocyte complex
COX-2	Cyclooxygenase-2
CUB	**C**omplement C1r/C1s, **U**egf, **B**mp1
D	
DBP	Dibutyl-phthalate
DKK	Dickkopf
DMEM	Dulbecco's Modified Eagle Medium
DNA	Deoxyribonucleic acid
E	
E.coli	*Escherichia coli*
ECL	Enhanced chemiluminescence

ECM	Extracellular matrix
EDTA	Ethylenediaminetetraacetic acid
ELISA	Enzyme-linked immunosorbent assay
EU	Endotoxin units
F	
FCS	Foetal calf serum
FGF	Fibroblast growth factors
FZD	Frizzled
G	
GAGs	Glycosaminoglycan(s)
H	
HA	Hyaluronan
HBSS	Hank’s balanced salt solution
HC	Heavy chain
HCL	Hydrochloric acid
His	Histidine
HRP	Horseradish peroxidase
HSC(s)	Haematopoietic stem cells
I	
IGF	Insulin-like growth factor
K	
kDa	kilodalton
L	
LAL	Limulus amebocyte lysate
LPS	Lipopolysaccharide
LRP	Lipoprotein receptor-related protein
M	
mAb	Monoclonal antibody
MAFIA	Macrophage Fas-induced apoptosis
MAR	Mineral apposition rate
M-CSF	Macrophage-colony stimulating factor

Micro-CT	Micro-computed tomography
(d) MMA	(destabilised) methyl methacrylate
MMP	Matrix metalloprotease
MOPS	3-Morpholinopropane-1-sulfonic acid
mRNA	Messenger ribonucleic acid
MSC(s)	Mesenchymal stem cells
MW	Molecular weight

N

NaCl	Sodium chloride
NBF	Neutral buffered formalin
NCBI	National Center for Biotechnology Information
NCP(s)	Non collagenous protein(s)

O

OPG	Osteoprotegerin
ORF(s)	Open reading frame(s)
OSM	Oncostatin M
OSX	Osterix

P

PBMC(s)	Peripheral blood mononuclear cell(s)
PBS	Phosphate buffered saline
PCR	Polymerase chain reaction
PGIA	Proteoglycan-induced arthritis
PTH	Parathyroid hormone

R

RA	Rheumatoid arthritis
RANK	Receptor activator of nuclear factor kappa-B
RANKL	Receptor activator of nuclear factor kappa-B ligand
rh	Recombinant human
rpm	Revolutions per minute
RT	Room temperature
RUNX2	Runt-related transcription factor 2

S

SDS-PAGE	Sodium dodecyl sulphate polyacrylamide gel electrophoresis
SERM(s)	Selective oestrogen receptor modulator(s)
Sf9	*Spodoptera frugiperda* 9
SH2	Src Homology 2
siRNA	Small interfering RNA
SMI	Structure model index
SOST	Sclerostin gene
STAT	Signal transducer and activator of transcription

T

TEV	Tobacco Etch virus
TGF-β	Transforming growth factor-beta
TNF-α	Tumour necrosis factor-alpha
TRAP	Tartrate-resistant acid phosphatase
TSG-6	Tumour necrosis factor alpha stimulated gene-6

W

Wnt	Wingless

Units used

Abbreviation	Unit of measure
µg	Microgram
µL	Microliter
µm	Micrometre
EU/mL	Endotoxin unit per milliliter
g	Gram
h	Hour
mg	Milligram per millilitre
min	Minute
mL	Millilitre
mM	Millimolar
mm	Millimetre
Mpa	Megapascal
ng	Nanogram/millilitre
nM	Nanomolar
nm	Nanometers
^{o}C	Degrees Celsius
rpm	Revolutions per minute
s	Second
v/v	Volume per volume
w/v	Weight per volume

1

CHAPTER 1: LITERATURE REVIEW

1.1 BONE TISSUE

1.1.1 Bone Function

Bone is believed to have originated, in the sea, about 500 million years ago (Carter and Beaupré, 2001), giving rise to the internal (endoskeletal) and external (exoskeletal) systems. These skeletal tissues, composed primarily of cartilage and bone, offer structural support, mobility, and protect softer organs from mechanical harm. It also functions as a storage site for vital minerals and nutrients and provides a niche for immune cell development.

1.1.2 Bone Structure

Broadly, there are four types of human bone; (i) long bones, (ii) short bones (iii) flat bones, and (iv) irregular bones. Structurally, bone is organised into layers. The outer layer consists of cortical bone (also called compact bone) surrounding the trabeculae (also called cancellous or spongy bone) which, in turn, encloses the bone marrow space (**Fig. 1.1**). Cortical and trabecular bone are discriminated based on porosity, density, and microstructure, where the former is denser than the latter, and found primarily at the diaphysis shaft of long bones or surrounding the trabecular regions (Clarke, 2008).

1.1.3 Bone Composition

Mature bone is a living and growing vascularised connective tissue with a heterogeneous matrix composition consisting of; predominately type I collagen (Col1), calcium-phosphate minerals (hydroxyapatite), non-collagenous proteins (NCPs), lipids, and water (Wang et al., 2012). While the collagen plays a structural and mechanical role, the minerals such as; calcium, phosphate and magnesium ions, strengthen the scaffold and serve as a reservoir of vital nutrients (Moe, 2008). The NCPs include proteoglycans, glycosylated and γ-carboxylated (gla) proteins (Lamoureux et al., 2007). These are in-

volved in various metabolic processes such as; mineralisation, cell/mineral-matrix interactions and extracellular matrix (ECM) organisation (Yanagishita, 1993).

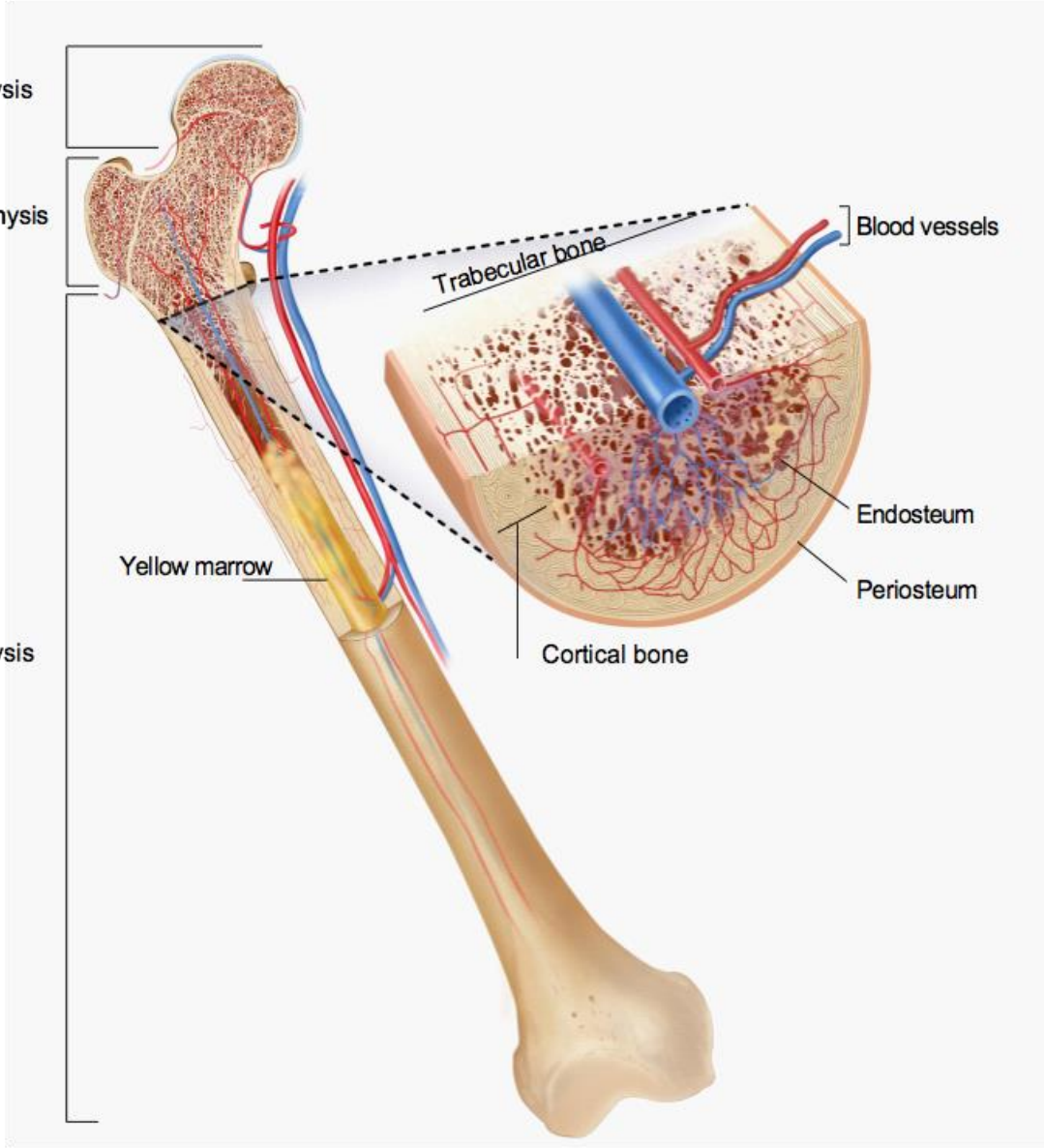


Figure 1. 1 The main anatomical features of a typical long bone
Illustration adapted from The National Cancer Institute visuals online, created by Terese Winslow (2014) Source: *https://visualsonline.cancer.gov/details.cfm?imageid=9687*

1.1.4 Bone Ossification

Bone formation can occur *via* either intramembranous or endochondral ossification (Yang, 2013). These two distinct processes have evolved to give rise to differentially shaped structures that, in turn, facilitate diverse skeletal functions; ranging from mobility to protection of internal organs.

Intramembranous ossification takes place during the formation of flat bones. It describes a process of skeletal development by direct differentiation of mesenchymal stem cells (MSCs) into functional, matrix secreting and mineralising osteoblasts – the cells responsible for bone formation. The progenitor cells that do not differentiate at this stage remain at the bone periphery, which later develops into the periosteum. The periosteum is critical for bone growth (Ochareon and Herring, 2011) and fracture healing, the latter of which occurs *via* the endochondral process (Maes et al., 2010).

Endochondral ossification is the developmental process by which the majority of long and short bones in the skeletal system are formed. It involves the initial generation of a cartilage template that is replaced by osteoid and subsequently mineralised (Kronenberg, 2003). MSCs expressing paired-related homeobox gene 1 (PRX1) condense and the central cells give rise to sex determining region Y box 9 (SOX9) positive chondrocytes (Akiyama et al., 2002, Akiyama et al., 2005) – the cells responsible for the production of cartilage. The remaining, undifferentiated, cells form the perichondrium at the periphery. As the cartilage grows, the chondrocytes in the central region stop proliferating and become hypertrophic. These hypertrophic chondrocytes induce mineralisation and promote vascularisation (Kronenberg, 2003) creating a microenvironment to recruit osteoblasts that subsequently induce the differentiation of perichondrial cells into osteoblasts, leading to the mineralisation of their surrounding environment, converting the perichondrium template into the periosteum.

1.2 CELLS OF THE SKELETAL SYSTEM

Anatomically, the bone and bone marrow are contiguous. In addition to being the site of haematopoiesis, generating blood and immune cells from haematopoietic stem cells (HSCs), it harbours well-established cell types of the bone; osteoclasts, osteoblasts, osteocytes, and bone lining cells (Takayanagi, 2007a) (**Fig. 1.2**). Skeletal diseases are attributable to an imbalance in the differentiation and/or activity of these cellular components (Pietschmann et al., 2016). Therefore, an understanding of the factors that influence their biology, and the signalling pathways that control their formation and function, is of therapeutic value.

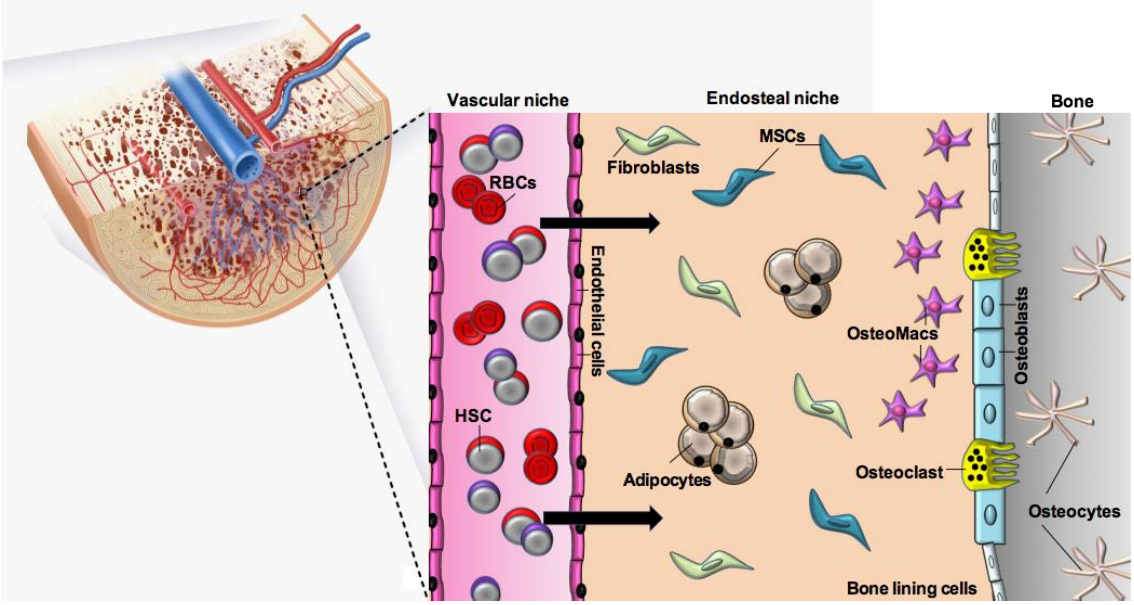


Figure 1. 2 Constituent cells of the bone/bone marrow
The niche consists of a heterogeneous population of cells. The immune and skeletal cells are formed in the bone marrow cavity from HSCs, placing these populations in close anatomical proximity. Image adapted from:
https://visualsonline.cancer.gov/details.cfm?imageid=9687
http://www.nature.com/nrendo/journal/v10/n12/pdf/nrendo.2014.169.pdf

1.2.1 Osteoclast Origin, Function and Characteristics

Despite the relatively short average lifespan [~12.5 days (Jaworski et al., 1981)] and small numbers [1-2 % of total adult bone cells (Conn, 2013)], osteoclasts are the only known cells capable of bone resorption (Hancox, 1972). They were first discovered by Albert Von Kolliker in 1873, and constitute a mobile, polarised, phagocytic population of cells characterised by their multicellular nature, positive for tartrate-resistant acid phosphatase (TRAP) enzyme (Hammarstrom et al., 1971, Minkin, 1982), and expression of calcitonin, and vitronectin receptors (Hemingway et al., 2011) as well as the presence of calcium channels and ruffled borders (Hollberg et al., 2005).

During the late 1970s, much controversy surrounded the origin of osteoclasts. It was already established that inherited osteopetrosis eventuated from an osteoclast deficiency – as opposed to a humoral defect (Marks and Walker, 1969). To this end, the transplantation of histocompatible haematopoietic cells, derived from the bone marrow/spleen, to the osteopetrotic murine model (*op/op*) corrected the pathological bone phenotype (Loutit and Sansom, 1976, Nisbet et al., 1978, Walker, 1975), and suggested that osteoclast progenitors are of haematopoietic origin. Subsequently, it was shown that osteoclasts belong to the macrophage/monocyte lineage (Ash et al., 1980, Marshall et al., 1983). In mice, F4/80 negative myeloid cells expressing the tyrosine kinase receptor; colony stimulating factor-1 (c-Fms) and the type I transmembrane receptor activator of nuclear factor kappa B (RANK) are proposed osteoclast precursors (Mizoguchi et al., 2009). In humans osteoclast precursors originate from the $CD14^{+}CD16^{-}$ population (Fujikawa et al., 1996, Hemingway et al., 2013).

1.2.2 Osteoblast Origin, Function and Characteristics

In contrast to osteoclasts, osteoblasts are bone forming mononuclear cells that make up 4-6% of the total population of adult bone cells (Conn, 2013). Pre-osteoblasts express parathyroid hormone (PTH)- receptor 1, alkaline phosphatase (ALP) and Collagen I and II, decorin, MCAM, MEPE, Osterix (OSX), runt-related transcription factor 2 (RUNX2)/CBFA1 and thrombopoietin, and originate from MSCs which express bone morphogenetic (BMP) receptors, CD29, CD44, CD51, CD73 CD90, CD105, CD166, integrinα1, platelet-derived growth factor receptor (PDGFR)-α, nestin, c-Kit STRO-1 and VCAM-1, and lack CD31, CD34, CD45. MSCs were first isolated by Friedenstein and colleagues in the 1970s from the bone marrow and described as adherent, replicative, fibroblasts-like clonogenic cells with multi-lineage properties when cultured *in vitro* (Friedenstein et al., 1970, Friedenstein et al., 1974). The differentiation of MSC down the osteoblast lineage involves the expression of temporally regulated genes. Thus, the differentiation state can be determined based on transcription factors (**see Figure 1.3**) and **table 1.1** for osteoblast markers and their associated functions.

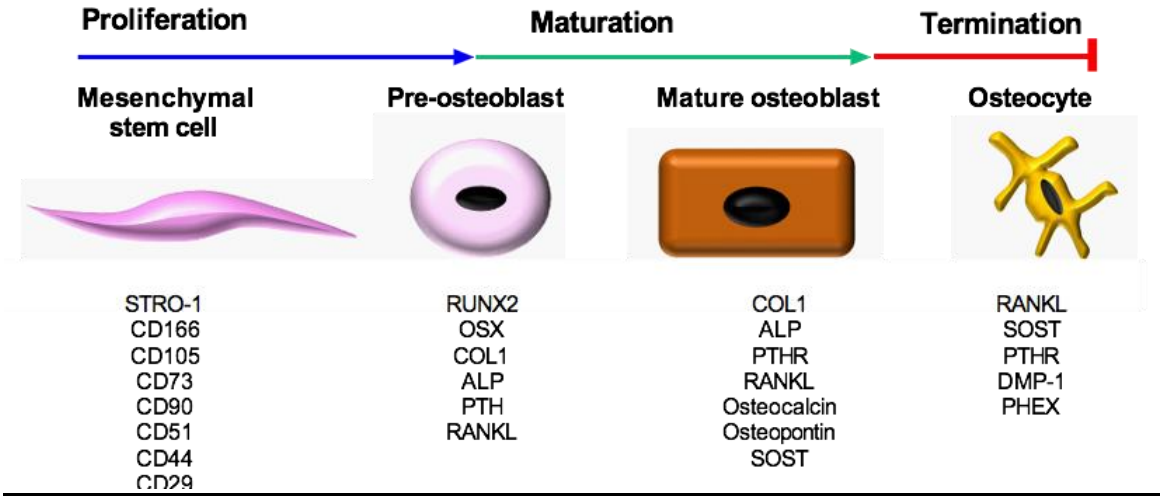


Figure 1. 3 Sequential gene expression during osteoblast differentiation.

Table 1. 1 Osteoblast markers and their associated functions

Marker	**Skeletal-related phenotype in deficient mouse models**
Bone ALP	□ Osteoporotic (Li et al., 2000) □ Defects in osteoblast maturation (Li et al., 2000) □ Hypophosphatasia, (Fedde et al., 1999) □ Impaired cartilage and matrix mineralisation (Fedde et al., 1999)
Fibronectin	□ Embryonically lethal (George et al., 1993)
M-CSF	□ Lack osteoclasts (Dai et al., 2002) (Yoshida et al., 1990) □ Osteopetrotic (Kodama et al., 1991, Wiktor-Jedrzejczak et al., 1990)
RANKL	□ Lack osteoclasts, therefore osteopetrotic (Dougall et al., 1999, Kong et al., 1999) □ Defect in secondary lymphoid organ development (Theill et al., 2002)
Osteocalcin/bone gamma-carboxyglutamate (gla) protein	□ Stimulates mineral maturation of bone (Boskey et al., 1998)
Osteonectin	□ Low bone turnover (Delany et al., 2000) □ Decreased bone mass (Delany et al., 2000) □ Defective osteoblast formation maturation and survival (Delany et al., 2003)
Osteopontin/bone sialoprotein I	□ Resistant to ovariectomy-induced bone loss (Yoshitake et al., 1999)

1.2.3 Osteocyte Origin, Function and Characteristics

Osteocytes make up 90-95% of the adult bone cell population and have a half-life of about 25 years (Knothe Tate et al., 2004). They develop from osteoblasts and express E11/gp38, dentin matrix protein 1 (DMP)-1, sclerostin, fibroblast growth factor (FGF)-23 and oxygen regulated protein-150 (**see Table 1.3 for associated functions**). They are stellate-shaped with cytoplasmic projections (canalicular processes) that allow communication with proximal cells through gap junctions. Their functions include the detection of mechanical stimuli, micro-damage and initiation of tissue repair (Bellido, 2014). This occurs by modulating the function of bone cells positioned on the surface through chemical signals. They are also involved in phosphate homeostasis (Feng et al., 2009). It is becoming increasingly clear that they play prominent roles in both arms of the remodelling process. They initiate remodelling by recruiting osteoclast precursors and also express pro-osteoclastogenic cytokines (Bellido, 2014).

Table 1. 2 Osteocyte markers and their associated functions

Factor	Role on the skeletal system	Reference(s)
DMP-1	promotes mineralisation	(Feng et al., 2006)
Sclerostin	- Inhibits osteoblast differentiation by disrupting Wnt signalling pathway - Antagonises members of the BMP protein family - Inhibits mineralisation	(Li et al., 2008, Li et al., 2005, van Bezooijen et al., 2004)
DKK-1	Inhibits the WNT signalling pathway	(Li et al., 2006)
FGF-23	Maintenance of physiological mineralisation	(Shimada et al., 2004)
ORP150	During the osteoblast to osteocyte transition, Hypoxia-induced stress protein that protects the cell from apoptosis	(Ozawa et al., 1999)
E11/gp38	Mechanical load Dendrite elongation	(Zhang et al., 2006)
OPG	A secreted decoy receptor of RANKL	(Bucay et al., 1998)
M-CSF	Promotes osteoclast differentiation, osteoclast cytoskeletal arrangement	(Asagiri and Takayanagi, 2007, Boyle et al., 2003)
RANKL	Promotes osteoclast differentiation and activity	Nakashima et al., 2011a

Osteocytes negatively regulate osteoblast formation and activity by expressing dickkopf (DKK)-1 and sclerostin. During physiology, the sclerostin gene (*SOST)* is upregulated by osteocytes in unloaded bone (Tu et al., 2012b) but downregulated under mechanical load (Robling and Turner, 2009). Sclerostin is a Wingless (Wnt) signalling pathway antagonist and of great therapeutic interest. These factors bind Frizzled (FZD) receptors and low density lipoprotein receptor-related protein (LRP)-5/6 thereby preventing activation of the Wnt signalling pathway (Bellido, 2014, Choi et al., 2009). Mice deficient in sclerostin exhibit increased bone mass and strength (Li et al., 2008). More recently, the deletion of LRP-4, which supports the function of sclerostin, has been found to increase bone mass and formation (Chang et al., 2014). Human patients with LRP-5 disrupting mutations have osteoporosis-pseudoglioma syndrome (OPPG) (Gong et al., 2001), and patients with *SOST* or *SOST*-associated gene mutations exhibit bone overgrowth such as that seen in sclerosteosis and Van Buchem's disease (Balemans et al., 2001, Balemans et al., 2002, Staehling-Hampton et al., 2002). The discovery of loss-of-function mutations to abnormal skeletal phenotype have resulted in the development of pro-anabolic agents, such as anti-sclerostin (Clarke, 2014).

1.2.4 Bone Lining Cells

Bone lining cells are post-mitotic and cover quiescent bone surfaces (Miller et al., 1989). They are distinguished from osteoblasts based on the expression of intercellular adhesion molecule (ICAM) – 1, as well as their long flattened morphology. Bone lining cells express also receptor activator of nuclear factor kappa-B ligand (RANKL) and macrophage-colony stimulating factor (M-CSF) and so can initiate osteoclastogenesis and bone resorption. They are responsive to hormones and growth factors such as PTH, FGF (Dobnig and Turner, 1995, Power et al., 2004). The role of bone lining cells includes; detecting osteoclast resorption of trabecular bone (Sims and Martin, 2014), linking resorption phase to formation (Everts et al., 2002), and protecting bone surfaces

from the osteoclasts attaching to the bone matrix in areas that are not required for resorption (Mosley, 2000). They also bridge the communication between the osteocytes and provide factors from the HSCs (Calvi et al., 2003, Zhang et al., 2003).

1.3 MOLECULAR CONTROL OF BONE CELLS

1.3.1 Osteoclastogenesis

In vitro experiments of mouse bone marrow or spleen cells co-cultured with a feeder layer of primary stromal cells or calvarial-derived osteoblasts helped shape our understanding of osteoclast development (Takahashi et al., 1988, Suda et al., 1992). These studies demonstrated, for the first time, that osteoclast differentiation is very much dependent on contact with stromal stem cells and the subsequent factors/cytokines derived from the osteolineage cells. M-CSF and transmembrane RANKL – a member of the tumour necrosis factor (TNF) superfamily, were later found to be the minimal requirements of *in vitro* osteoclastogenesis (Asagiri and Takayanagi, 2007, Boyle et al., 2003, Pixley and Stanley, 2004, Suda et al., 1999).

M-CSF is now a well-established survival and proliferative factor of RANK-expressing osteoclast precursors (Felix et al., 1994, Hodge et al., 2007) (**Fig. 1.6**); M-CSF-deficient mice lack osteoclasts (Yoshida et al., 1990, Dai et al., 2002), and point mutations in the *Csf1* gene leads to osteopetrosis (Kodama et al., 1991, Wiktor-Jedrzejczak et al., 1990). Equally, the administration of recombinant human (rh) M-CSF results in an expanded osteoclast pool, alleviating the osteopetrotic bone phonotype, in osteopetrotic (op/op) mutant mice model (Kodama et al., 1991). M-CSF also induces RANK upregulation on osteoclast precursors, rendering them responsive to RANKL (Yavropoulou and Yovos, 2008).

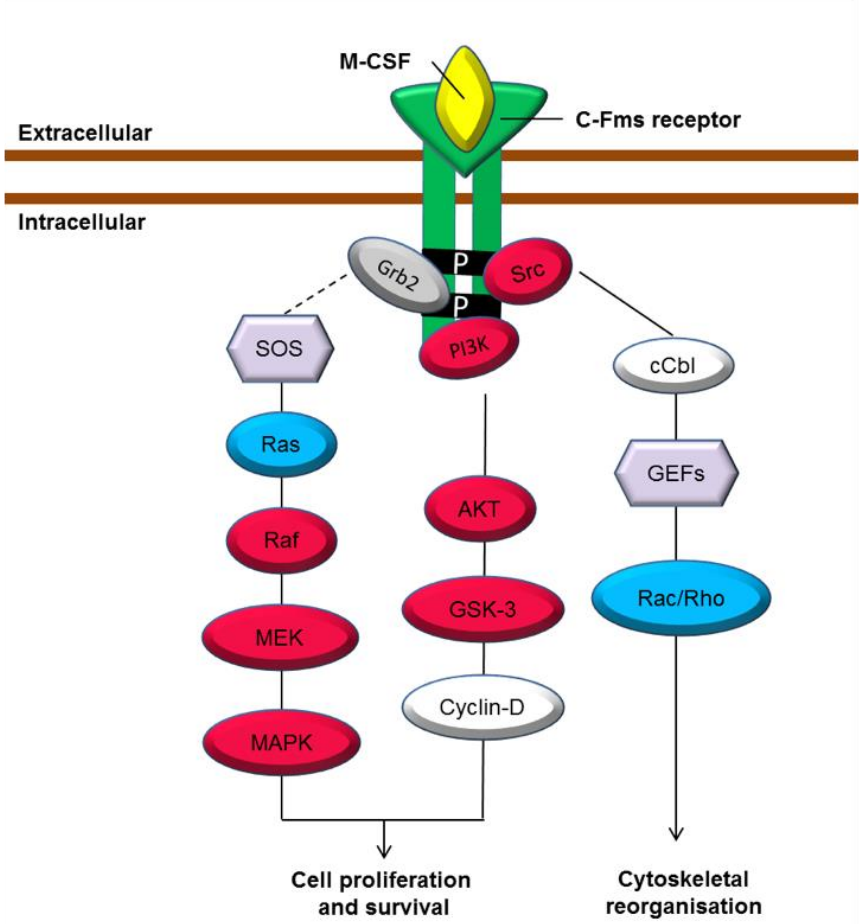


Figure 1. 4 M-CSF signaling pathway in osteoclast precursors.

Upon binding of M-CSF to the extracellular domain of the c-Fms receptor (Sherr et al., 1992, Stanley et al., 1997), the receptor tyrosine kinase phosphorylates its cytoplasmic domain. This attracts Src homology 2 (SH2) or phosphotyrosine-binding (PTB) domain containing protein which, in turn, amplify and transduce the signals by associating with other kinases/adaptors - leading to downstream signalling (Schlessinger, 2000). Key pathways of M-CSF signalling leading to cell proliferation and survival include the GRB2-ERK and PI3K/AKT. Rac/Rho signalling facilitates cytoskeletal reorganisation.

Colour key Red; kinases**|** Blue; GTPase**|** Purple; GAP/GEFs**|** Grey; accessory proteins **Abbreviations** GRB2; growth-factor-receptor-bound protein 2**|** SOS; sun of sevenless**|** MAPK; mitogen-activated protein kinase**|** MEK; MAPK extracellular signal-regulated kinase**|** PIK; Phosphoinositide 3-kinase**|** c-Cbl; casitas B-lineage lymphoma**|** GEFs; Guanine nucleotide exchange factors.

However, M-CSF is not sufficient to drive osteoclastogenesis. In 1972 Horton *et al.* found that supernatant from stimulated human peripheral blood leukocytes cultures can induce *in vitro* resorption (Horton et al., 1972). A significant advancement was made once the osteoclastogenic factor was identified as RANKL (Lacey et al., 1998, Yasuda et al., 1998b), allowing for pure osteoclast cultures to be generated (**Fig. 1.7**) and studied *in vitro*. RANKL exists in two forms; soluble and membrane bound, where the latter can be presented in its transmembrane form, by both marrow stromal and osteoblast cells, in response to systemic hormones such as 1, 25-dihydroxyvitamin D3 (1, 25(OH) 2D3) (Kostenuik and Shalhoub, 2001) prostaglandin E_2 (PGE_2) and PTH (Horwood et al., 1998).

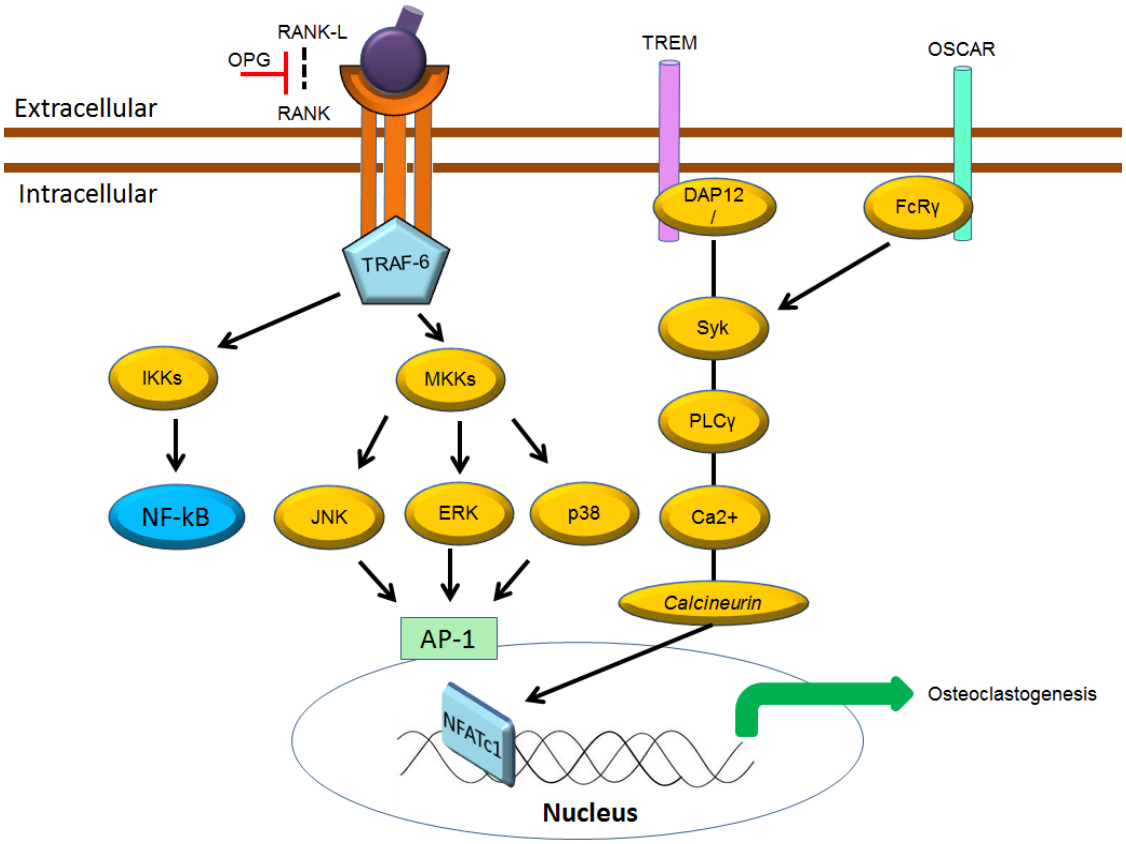


Figure 1. 5 RANKL-mediated signaling controlling osteoclast lineage commitment and activation

When RANK-L binds RANK on osteoclast precursors, several signalling pathways are activated such as; mitogen activated protein kinase (MAPK), NF-kB, c-Fos and calcium signalling (Takayanagi, 2007b). Binding of RANKL to RANK is competitively inhibited by OPG. The intracellular domain of RANK lacks intrinsic enzymatic activity (Takayanagi, 2007a); therefore adaptor proteins such as a TNF-receptor-associated factor (TRAF) activate intracellular kinase cascades (Galibert et al., 1998, Kim et al., 1999, Wong et al., 1998). TRAF-6 is a potent mediator of RANK signalling (Lomaga et al., 1999, Naito et al., 1999, Wong et al., 1999) which leads to downstream cascades including IKK kinase complexes (IKKα, IKKβ, IKKγ, and NIK-IKKα), and mitogen-activated protein kinases (MAPKs) (Erk1/2, p38 and JNK), which result in the activation of transcriptional factors. NF-kB degradation and NFATc1 activation together induce transcription of key factors for osteoclastogenesis (Aliprantis et al., 2008, Asagiri et al., 2005, Takayanagi et al., 2002). RANKL-driven osteoclastogenesis is facilitated by co-stimulatory signals mediated by immunereceptor tyrosine-based activation motif (ITAM) containing adaptor proteins such as DNAX-activating protein (DAP)-12 and Fc-receptor common γ-subunit (FcRγ) associated to immunoglobulin (Ig)-like receptors.

Figure adapted from http://www.nature.com/nm/journal/v13/n7/fig_tab/nm1593_F2.html

Abberviations DNAX-activating protein 12 (DAP12), JNK; Janus N-terminal kinase, MAPK kinase (MKK) Both Fc receptor common γ subunit (FcRγ) and NFATc1; Nuclear factor of activated T-cells 1.

Bone homeostasis depends on RANKL-mediated osteoclast activity, which is tightly regulated through cell-cell contact as well as soluble cytokines. Both RANK and RANKL deficient mice lack osteoclasts, and therefore exhibit an osteopetrotic phenotype (Dougall et al., 1999, Kong et al., 1999), highlighting its indispensable role in osteoclast development and bone homeostasis. However, phenotypic deformities of $RANKL^{-/-}$ mice are not only restricted to the skeletal system but also the immune system, as secondary lymphoid organ development (Theill et al., 2002), dendritic cell development (Loser et al., 2006), T-cell/dendritic cell interaction (Takayanagi, 2010), and peripheral tolerance (Loser et al., 2006) were disrupted. Therefore, genetic knockout models have been instrumental in unravelling the relationship between the skeletal and immune system, helping researchers identify common precursors, cytokines, receptors, adapter proteins, signalling molecules, and transcriptional factors (Terpos and Dimopoulos, 2011).

The functional relationship between the two systems is supported by earlier experiments that demonstrated cells of the immune system to regulate osteoclast differentiation and function, thereby modulating net skeletal mass (Dewhirst et al., 1985, Horowitz et al., 1984, Mundy et al., 1974), making it impossible to study the two systems in isolation. For example, although RANKL is a potent osteoclatogenic factor, it requires ITAM co-stimulation (Koga et al., 2004, Mocsai et al., 2004), generally provided by accessory immune cells. In addition, activation of the adaptive arm of the immune system leads to RANKL expression by B and T-cells (Kanematsu et al., 2000). T-cell derived RANKL (Kong et al., 1999) can stimulate dendritic cells (Anderson et al., 1997, Lacey et al., 1998, Yasuda et al., 1998b) and is also a well-known mediator of adjuvant-induced arthritis (Kong et al., 1999, Takayanagi et al., 2000a, Toraldo et al., 2003).

As RANK is expressed on osteoclast precursors, mature osteoclasts and osteocytes (Nakashima et al., 2011a) resorption can be modulated at various stages of bone de-

velopment and remodelling. Osteoprotegerin (OPG) – a non-signalling soluble peptide receptor antagonist of RANK, can modulate both the formation and activation of osteoclasts *in vivo* and *in vitro* by binding RANKL (Simonet et al., 1997, Yasuda et al., 1998a). It is an important contributor to the RANK-RANKL axis and believed that the balance between RANKL and OPG within the milieu ultimately dictates the extent of osteoclast formation and subsequent activity (Hofbauer et al., 2000). Transgenic mice overexpressing OPG have an osteopetrosis phenotype and its exogenous addition *in vitro* can inhibit osteoclastogenesis (Simonet et al., 1997, Yasuda et al., 1998a). Apart from OPG, osteoclasts differentiation and function can be influenced by cell-cell contact, hormones, matrix proteins, vitamins, as well as soluble cytokines - many of these cytokines are immune cell-derived, that modulate the RANK/RANKL/OPG axis (Boyle et al., 2003), one such factor is TNF stimulated gene (TSG)-6 (Mahoney et al., 2011), which also works in synergy with OPG. These factors can broadly be divided into osteoclastogenic/anti-osteoclatogenic (**see Tables 1.3 and 1.4**).

Table 1. 3 Stimulatory factors on osteoclastogenesis

Factor	Stimulator effect on osteoclastogenesis/activity	Reference
TNF-α	Increases RANKL expression on stromal cells and/or osteoblasts	(Abu-Amer et al., 2004)
	Inhibits osteoclast apoptosis	(Lee et al., 2001)
IL-1	Increases RANKL expression by stromal cells/osteoblasts	(Wei et al., 2005)
	Increases M-CSF, PGE2 by osteoblasts, while decreasing OPG production by osteoblasts	(Tanabe et al., 2005)
IL-6	Increases RANKL on stromal cells/osteoclasts	(Gao et al., 1998)
	Induces the secretion of IL-1	(Kurihara et al., 1990)
IL-11	Maintains/supports osteoclast progenitor cells	(McCoy et al., 2013)
IL-17	Increases RANKL on stromal cells/osteoblasts	(Kotake et al., 1999)
IL-23	Increases osteoclastogenesis by increases RANK expression on myeloid precursors	(Chen et al., 2008)
IL-32	Promotes differentiation	(Mabilleau and Sabokbar, 2009)
TGF-β	Increases survival, differentiation	(Gingery et al., 2008, Lovibond et al., 2003)
PGE_2	Stimulates formation through endogenous IL-1β expressed through protein kinase K	(Amano et al., 1996)

Table 1. 4 Inhibitory factors on osteoclastogenesis

Factor	Inhibitory effect on osteoclastogenesis/activity	Reference
IL-4	Inhibits STAT-6 mediated NF-κB signalling to inhibit differentiation	(Abu-Amer, 2001)
	Inhibits expression of RANKL by TNF-α stimulated stromal cells	(Fujii et al., 2012)
IL-6	Inhibits osteoclastogenesis by interfering with the NF-κB pathway	(Yoshitake et al., 2008)
IL-12	Acts in synergy with IL-18 or alone to inhibit osteoclastogenesis	(Horwood et al., 2001)
IL-23	Under physiology, IL-23, acts via T-cells to inhibit osteoclastogenesis	(Quinn et al., 2008)
IL-27	Disrupts RANKL-induced NFATc1 of RANK signalling	(Kalliolias et al., 2010)
	Induces INF-γ production which inhibits osteoclastogenesis	(Park et al., 2012)
IL-33	Induces the expression of Blimp-1 and IRF-8	(Kiyomiya et al., 2015)
	Induces the formation of alternatively activated macrophages	(Zaiss et al., 2011)
TSG-6	Binds RANKL to inhibit osteoclast activity, also works in synergy with OPG	(Mahoney et al., 2008, Mahoney et al., 2011)

It is clear from knockout studies that immune-derived pro-inflammatory cytokines can cause bone destruction. However, the same cytokines that facilitate bone damage are associated with enthesitis and excess bone formation, typical of diseases such as ankylosing spondylitis (Gorman et al., 2002). Such observations encouraged the study of osteoimmunology – a discipline first coined by Arron and Choi in 2000 (Arron and Choi, 2000), that seeks to address bone metabolism in the context of the functions of the immune system. A major finding in the field of osteoimmunology was in 2000, when Takayanagi *et al*. identified the bone protective role of IFN-γ – a soluble cytokine produced during innate immune responses; by natural killer cells, as well as the adaptive immune response; by NKT-cells $CD4^+$ Th1 $CD8^+$ cytotoxic T lymphocytes (CTL) effector T-cells

(Delves and Roitt, 2000), by binding to RANK on osteoclasts and disrupting RANKL signalling by degrading the RANK adaptor protein; TRAF6 (Takayanagi et al., 2000b).

1.3.2 Osteoblastogenesis

Osteoblast differentiation occurs through various complex signalling pathways: Wnt, IL-6, BMP, transforming growth factor (TGF)-β, insulin-like growth factor (IGF), Notch, and Hedgehog. These pathways are inter-related in that; there is a high degree of cross talk, where one signalling can control another, allowing for inter-pathway regulation. For example, FGF and Wnt signalling can control the duration of BMP signalling and the outcome depends on timing and environmental conditions of co-stimulation. TGF-β can inhibit BMP-induced osteoblast differentiation under certain conditions (Maeda et al., 2004, Spinella-Jaegle et al., 2001), whereas under others it can promote it (de Gorter et al., 2011, Matsaba et al., 2001). Different signalling pathways are under the control of various downstream transcription factors, where the activation of the transcriptional factor RUNX2 is the stage where most of these pathways converge, where the differentiation process can be either positively or negatively regulated. RUNX2 precedes the expression of another major transcriptional factor important for osteoblast differentiation – called osterix. Although not exclusive to osteoblasts, as chondrocytes also express it, RUNX2 is widely regarded as the master gene of osteoblast differentiation, because the absence of RUNX2/OSX specifically inhibits osteoblast differentiation (Komori et al., 1997, Nakashima et al., 2002). Evidence of this was provided by RUNX2-deficient mice which lack osteoblasts (Ducy et al., 1997, Komori et al., 1997). Subsequent studies showed that RUNX2 upregulates genes that typify osteoblastic cells, such as; *ColIA1, ALP, Bone sialoprotein, Osteonectin* and *osteocalcin* (Fakhry et al., 2013). Osteoblast progenitors that express RUNX2 and ColIA1 undergo a phase of proliferation (Zhang, 2010), during which ALP activity is upregulated and cells are considered to be pre-osteoblasts (Capulli et al., 2014) (**Figure 1.5**). Eventually, OSX expression differenti-

ates the pre-osteoblasts from more developed, mature osteoblasts. Cells adopt a cuboidal morphology with extensive endoplasmic reticulum, Golgi apparatus and secretory vesicles (Marks and Popoff, 1988). This is accompanied by the secretion of bone matrix proteins such as osteocalcin, BSP I/II and collagen type I [**see Table 1.1 (section 1.2.3) for their associated functions**]. However, mature, functional osteoblasts are not terminally differentiated cells and, can further differentiate into subpopulations of cells, namely; osteocytes and quiescent bone lining cells.

Wnt signalling is a well-established and well-characterised regulator of osteoblast differentiation, activity and survival (Baron and Kneissel, 2013). Wnt ligands bind the 7-transmembrane spanning receptor FZD and the low-density LRP-5/6. Patients with loss of function mutations in these co-receptors have decreased bone mass and higher incidence rates of fracture. In addition, mutation in *LRP-5* results in eye abnormality in patients, while mutation in *LRP-6* results in patients with coronary artery disease (Barros et al., 2008, Laine et al., 2011, Mani et al., 2007).

LRP5/6 can induce downstream signals *via* the β-catenin or canonical pathway. The former pathway involves the dissociation of β-catenin from the destruction complex[1], followed by its nuclear translocation and association with lymphoid enhancing factor (Lef)-1 transcription factor facilitates the transcription β-catenin target genes. This allows the conversion of $RUNX2^+$ cells to $RUNX2^+OSX^+$ (**see Fig. 1.8A**). The β-catenin LRP5/6-independent (canonical) pathway is less understood, but involves protein kinases C delta (PKCδ).

BMPs signalling have been shown to be able to promote bone formation and function *via* both endochondral and intramembranous ossification (Katagiri et al., 1994, Mundy,

[1] **adenomatous polyposis coli (APC) - glycogen synthase kinase 3 (GSK3) - casin kinase I (CKI) complex**

1996). BMP-2 binds as dimers to type-I and type-II serine/threonine receptor kinase. The binding of BMP-2/4 binding BMPR leads to Smad 1, 5 or 8 to be phosphorylated at the c-termini (Rahman et al., 2015). Phosphorylated Smad associate with the co-Smad (Smad 4) and translocate to the nucleus, with the help of other transcriptional factors they induce the expression of RUNX2 and OSX (Rahman et al., 2015). RUNX2 binds Smad 1&5 in BMP-induced osteoblast differentiation (**see Fig. 1.8B**).

The Indian Hedgehog signalling pathway is required for osteoblastogenesis during endochondral ossification (St-Jacques et al., 1999). Hedgehog binding to the tumour suppressor 12-transmembrane protein Patched (Ptch)-1 activates signalling through the 7-transmembrane receptor oncoprotein smoothened (Smo) to initiate intracellular signalling (Yang et al., 2015). This leads to the generation of three related zinc finger transcriptional factors glioma-associated oncogene homolog (GLI)-1, -2, and -3 while GLI-3 with different target genes. While GLI-3 is suppressive of osteogenesis, GLI-2 is activation leads to $RUNX2^{+}OSX^{+}$ cells (Yang et al., 2015) (**see Fig. 1.8C**).

The notch signalling pathway inhibits osteoblastogenesis (Hilton et al., 2008). Binding of Jagged (JAG) or Delta-liked (DLL) causes the notch receptor to be proteolytically cleaved by the γ-secretase complex. This generates a Notch intracellular domain (NICD) that forms a complex with recombining binding protein suppressor of hairless (RBPJ) to activate downstream **inhibitory** pathways involving transcriptional factors such Hairy and Enhancer of Split (HES) and HES-related with YRPW motif (HEY) (Tu et al., 2012a) (**see Fig. 1.8D**).

In regards to IL-6 signalling, soluble IL-6 acts through gp130. Gp130 has a cytoplasmic domain for signal transducer and activator of transcription (STAT) binding as well as regions to associate with Janus kinase (JAK) to transduce downstream signals (Itoh et al., 2006) (**see Fig. 1.8E**). FGF signalling plays multiple roles on osteoblast lineage. FGF

binding to the surface of tyrosine kinase FGF receptors activates multiple signalling pathways. This signalling is involved in pre-osteoblast proliferation and osteoblast differentiation and function (**see Fig. 1.8F**)

Although past works have directed most attention to the unravelling the relationship between the immune cells and that of the osteoclasts, increasing attention is being turned onto how the immune system can support the development of osteoblasts. Osteoblast differentiation is highly coordinated by various signalling pathways in temporally regulated manner. *In vitro* experiments demonstrated cells of the immune system can regulated osteoblast differentiation and function thereby modulating net skeletal mass (Dewhirst et al., 1985, Horowitz et al., 1984, Mundy et al., 1974). This is of high therapeutic value as the identification of novel bone anabolics is dependent on the disentanglement of such relationship.

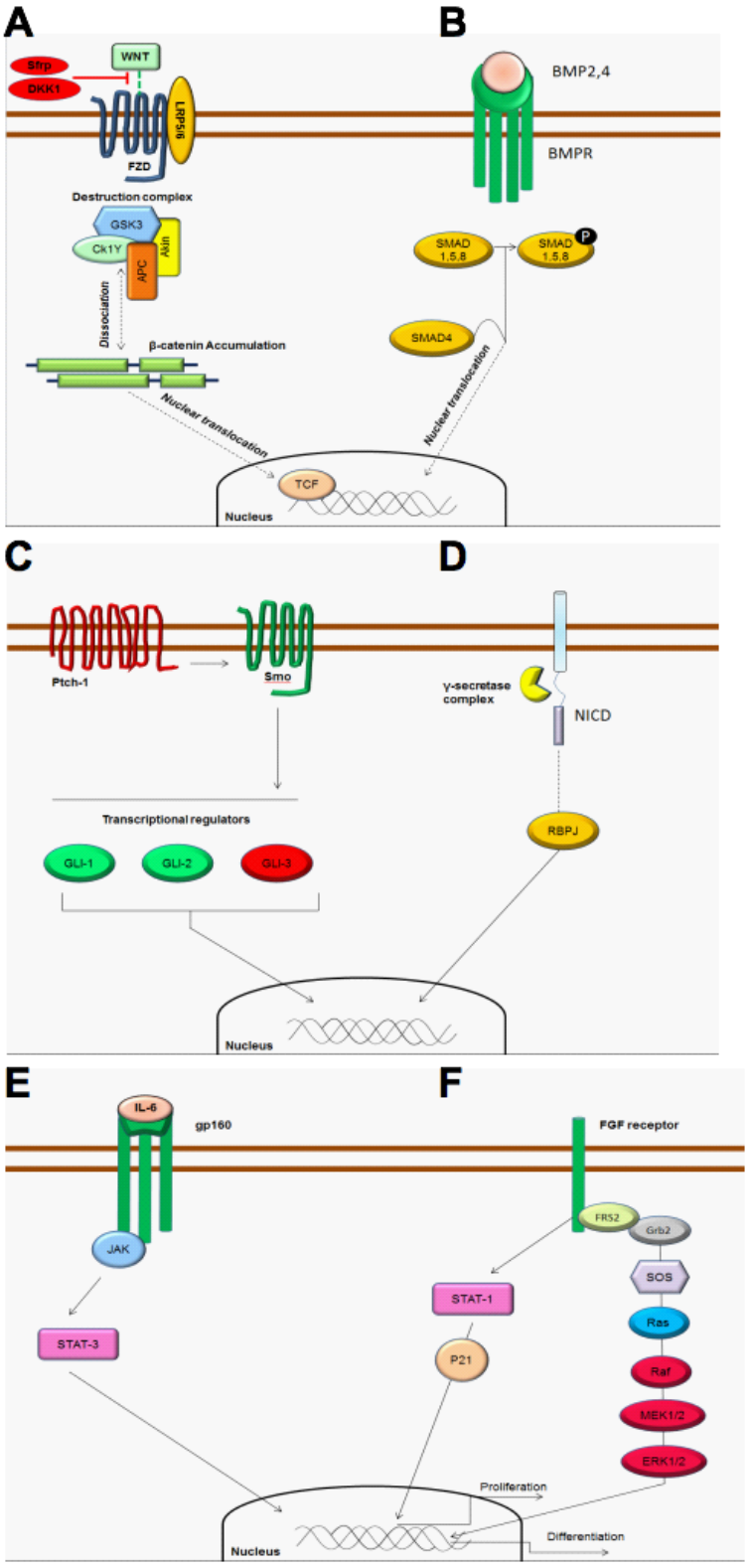


Figure 1. 6 Signalling pathways controlling osteoblastogensis.
The different signalling pathways that can be activated to regulate differentiation include (**A**) Wnt, (**B**) BMP, (**C**) Indian Hedgehog, (**D**) Notch, (**E**) STAT, and (**F**) FGF signalling.

1.3.3 Other Important Interactions Orchestrating Bone Remodelling

An emerging body of literature recognises a subtype of bone-resident macrophages, termed 'osteomacs' (Alexander et al., 2011, Chang et al., 2008, Pettit et al., 2008, Wu et al., 2013) which partake in tissue modelling and remodelling. In respect to their development, phenotype and function, macrophages are heterogeneous (Yona et al., 2013). To this end, most organs harbour a specific subpopulation of tissue-resident macrophages - for example the Kupffer cells found in the liver, or Langerhans and microglia found in the lungs and brain respectively. Bone is no different and in 1984 David Hume demonstrated that both the periosteal and endosteal membranes carry tissue-resident macrophage populations (Hume et al., 1984), during development (Cecchini et al., 1994) and in mature tissue. It was only in 2008 that the term 'osteomac' was coined by Allison Pettit and colleagues to describe these bone-resident macrophages (Chang et al., 2008, Pettit et al., 2008) - a subpopulation distinct to osteoclast precursors (Pettit et al., 2008), characterised as F4/80 positive (mouse macrophage marker), c-Fms (Chang et al., 2008), ALP and CD80 (Austyn and Gordon, 1981) expressing cells. They originate from the $CD68^{+}$ population of macrophages that are also found in other tissues (Gordon and Taylor, 2005), providing direct evidence of the relationship between immune cells and skeletal system.

Osteomacs line the endosteal surface separating mineralised bone from the bone marrow cavity and make up one-sixth of the total bone cells (Chang et al., 2008). This structural arrangement was reported earlier by Burkhardt *et al.* (1984). Using *in vivo* mouse models, it has been shown that osteomacs associate with osteoclasts, osteoblasts, as well as bone lining cells during steady-state remodelling (Chang et al., 2008, Pettit et al., 2008) and post-injury (Alexander et al., 2011). As such, they serve various functions; from supporting osteogenesis and mineralisation (Chang et al., 2008) to pro-

moting fracture healing (Alexander et al., 2011), and maintaining the HSC pool (Winkler et al., 2010).

Osteomacs support the mineralising activity of osteoblasts both *in vitro* and *in vivo*; whilst their isolation from osteoblasts was found to inhibit bone formation (Chang et al., 2008, Pettit et al., 2008). The ablation of the bone-resident macrophages in murine macrophage Fas-induced apoptosis (MAFIA) models compromised bone-modelling surfaces as indicated by a significant decreased ratio of the bone surface lined with osteoblasts to amount of new bone deposited (Chang et al., 2008). This also corresponded to a decrease in osteocalcin expression in the bone marrow (Chang et al., 2008) and endocortical bone thickness (Chang et al., 2008).

The interaction between the immune-derived macrophages and bone cells is not only important during steady-state, but also during injury - akin to the role of other organ-specific macrophages in tissue injuries. They detect bone damage and recruit osteoclasts to initiate remodelling (Jilka et al., 2007). In murine models of bone injury they have been associated with enhanced intramembranous matrix deposition and mineralisation (Alexander et al., 2011). Osteomacs involved in fracture repair are believed to be inflammatory in nature and produce significant amounts of TNF-α (Alexander et al., 2011, Chang et al., 2008). In support, cytokines released from activated macrophage/monocytes have shown to enhance osteoblast differentiation and matrix mineralisation from MSC precursors (Guihard et al., 2012).

Not only does depletion of macrophages disrupt physiological bone formation (Cho et al., 2014, Chang et al., 2008) and bone repair (Alexander et al., 2011), it is also critical for the maintenance of the hematopoietic niche (Winkler et al., 2010). *In vivo* ablation of osteomacs in MAFIA transgenic mouse model decreased osteoblast population - as determined by a reduction in osteoblast-derived cytokines such as; CXCL-12, KIT ligand

and KIT, as well as decreased ANG-1 and stem cell factor transcripts of whole bone marrow (Winkler et al., 2010). In addition to the changes in osteoblast populations, HSCs and their precursor population had homed to the bloodstream, rather than contained within their usual bone marrow niche (Winkler et al., 2010).

Currently, many studies report the immune's engagement in bone regeneration with one integral component being the monocyte/macrophage lineage and their possible interactions with MSCs (Nicolaidou et al., 2012, Guihard et al., 2012, Fernandes et al., 2013). As MSCs, lack major histocompatibility class II antigens as well as the costimulatory molecules; CD40, CD80, CD86 (Le Blanc et al., 2003), they are immunoevasive and immuosuppressive. Hence they are capable of regulating the immune response (Jones et al., 2007), these are properties essential from tissue repair and regeneration. MSCs regulate innate cells such as neutrophils (Khan et al., 2015), dendritic cells (Mohammadpour et al., 2015) and macrophages (Song et al., 2015, Zanier et al., 2015), as well as T and B-cells (Uccelli and de Rosbo, 2015), where HLA-G (major histocompatibility complex, class I, G) secretion by allogeneic MSCs has shown to suppress T-cell proliferation in mixed lymphocyte reactions (Montespan et al., 2014). Bone marrow derived human MSCs (BM-hMSCs) can regulate inflammation-induced through NF-κB signalling in colitis (Zuo et al., 2015), and been found to be therapeutic in IBD (Abdel Salam et al., 2014) and periodontitis (Racz et al., 2014), as well as in allogeneic immune cells responses (Aggarwal and Pittenger, 2005). These studies are significant because although it was thought that BM-MSCs replace cells in damaged tissues given their multipotency, emerging evidence suggest implanted MSCs provide paracrine signals (such as TGF-β, TNF-γ, TNF-α, IL-10, and PGE_2) which aid tissue repair through immune regulation (Lee et al., 2011).

1.4 BONE REMODELLING

Once bone has formed, it will need to adapt to mechanical changes and repair damage throughout life to maintain structural integrity. To do so, the tissue is continuously re-modelled through a complex inter-play of cells controlled by local, systemic and cell-bound factors (Eriksen, 2010, Sims and Martin, 2014).

1.4.1 Physiological Bone Remodelling

To ensure homeostatic bone mass is maintained throughout adulthood, the removal of old material, by the bone resorbing osteoclasts, is tightly '**coupled**' to the replacement of new bone matrix, by the osteoblast. The concept of 'coupling' was first proposed in the early 1980s, describing factors generated during the resorptive phase that stimulate bone formation (Howard et al., 1981) to temporally and spatially regulate the physiological remodelling (Delaisse, 2014).

Remodelling occurs at discrete sites along the skeleton called; 'basic multicellular units' (BMUs) in cortical bone (**Fig. 1.4**) or 'Howship's lacunae' in the trabeculae. These do not arise randomly, instead forming in response to stimuli that include changes in hormone levels (Khosla et al., 2012), mechanical loading (Bonewald, 2007, Tatsumi et al., 2007), and micro-damage (Verborgt et al., 2000). Within the BMUs coupling ensures that the recruitment, differentiation, activation and survival of bone cells is highly co-ordinated (Chambers, 1980, Rodan and Martin, 1981). Our understanding of BMUs have evolved from the one Frost and colleagues first described in 1966, and the one later refined by Parfitt 1979 (Frost, 1966, Parfitt, 1979), who both limited the concept of coupling, within the BMUs, to osteoclasts and osteoblasts. More recent works describe the importance of immune cells and precursor bone cell populations to this process (Wythe et al., 2014, Horwood, 2015, Sims and Martin, 2015)(**see Fig. 1.4**).

Because BMUs occur at multiple sites asynchronously, the local concentration of factors and cells required for each stage of the cycle must be tightly regulated within each individual BMU. This is achieved by the formation of structural canopies over the BMUs, creating bone remodelling compartments (Hauge et al., 2001). These canopies consist of cells and microvessels that cover the osteoblasts at the periosteum as well as BMUs (Wesseling-Perry, 2014, Jensen et al., 2015). In humans these structural canopies are believed to be created by bone lining cells and osteoblasts (Kristensen et al., 2013), while in mice they comprise mainly of bone resident macrophages; called osteomacs (Chang et al., 2008).

Although the exact link between the canopy and the BMU niche is not yet understood, the function of the canopy is not limited to maintaining optimal conditions/concentrations within the BMU. It also provides substrates and essential nutrients for the osteoclasts, osteoblasts, MSCs bone lining cells, and osteocytes contained within the BMU (Jensen et al., 2015), and facilitates all three phases of bone remodelling; resorption, reversal and formation (**Fig. 1.5**).

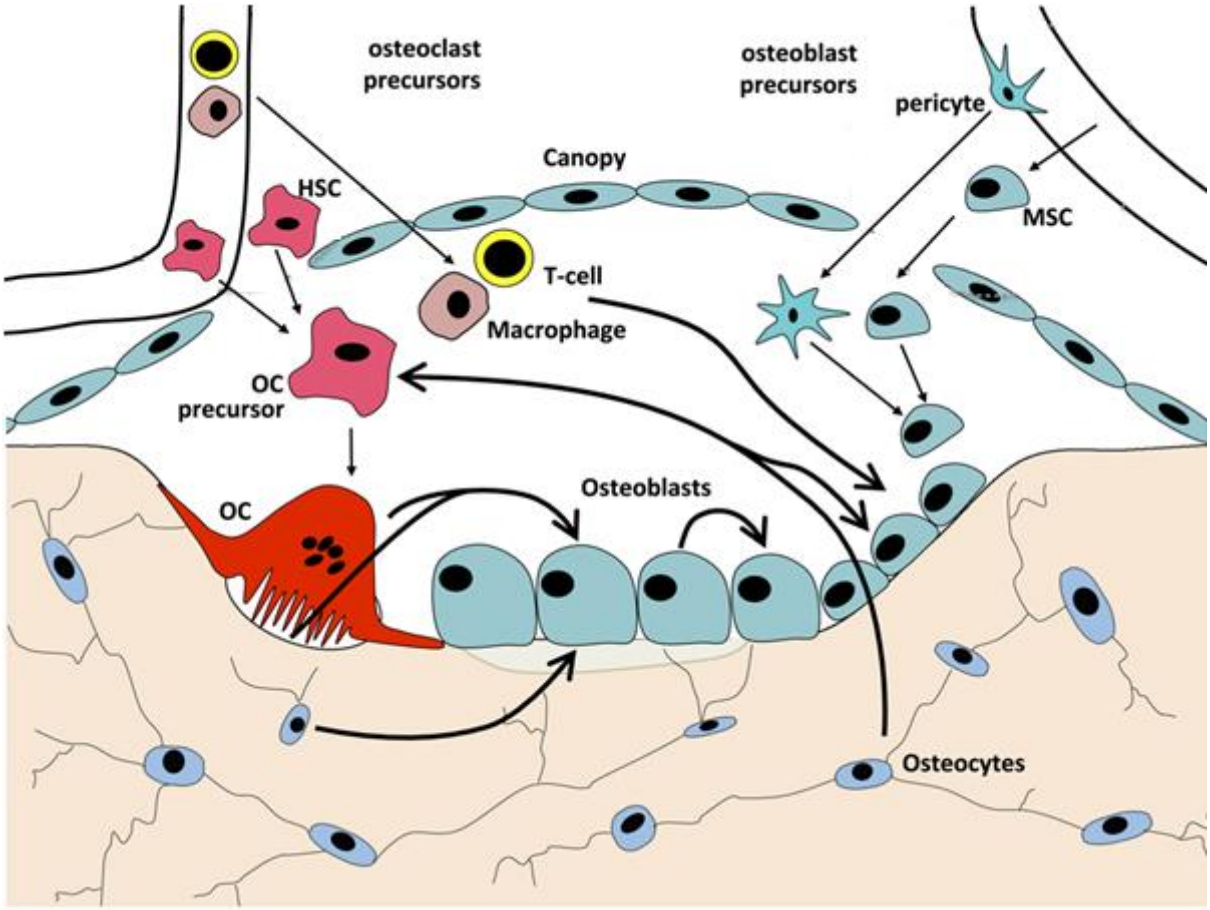


Figure 1. 7 Bone remodeling unit and its cellular components.
Image adapted from: (Sims and Martin, 2014)

During the resorptive phase, the interaction of RANKL with RANK (the latter being present on osteoclast surface), stimulates osteoclastic bone resorption - an event believed to initiate the remodelling cycle. Osteoclasts attach to bone matrix proteins *via* $\alpha_v\beta_3$ integrin's interaction with bone matrix proteins at the amino acid sequence; arginine-glycine-aspartic acid (R-G-D) (Flores et al., 1992). Cytoskeletal reorganisation, within the osteoclasts, gives rise to an actin-rich sealing zone, to define the surface area targeted for resorption (Aubin, 1992). Polarisation of the plasma membrane in contact with the bone surface creates a ruffled border (Hollberg et al., 2005). Hydrogen ions (H^+) and chloride ion (Cl^-) released through the V-adenosine triphosphatase (V-ATPase) proton and chloride ion-proton anti-porter ClC-7 pump respectively, to lower the pH of the lacunae to 4.5, (Blair et al., 1989, Kornak et al., 2001) and dissolve mineral contents of the matrix. Matrix-degrading enzymes such as lysosomal protease, cathapsin K, ma-

trix metalloprotease (MMP)-9 and MMP-13, which work optimally in these acid conditions are then released into the lacunae and cleave off the exposed proteins. Osteocalcin and COLI, liberated from the matrix, further recruit pre-osteoclast precursors (Malone et al., 1982). Molecular cues that terminate the resorption phase are still unidentified. However, following activity, some osteoclasts undergo apoptosis in either a Bim/caspase-3 (Wakeyama et al., 2007) or oestrogen-induced Fas ligand dependent manner (Nakamura et al., 2007). This may occur in response to the high calcium concentrations that ensue as a result of bone resorption (Lorget et al., 2000).

Following bone resorption, a lag phase occurs before bone formation takes place - called the reversal phase. This phase is orchestrated by osteoblast-like cells termed 'reversal cells'. Given the fact that it takes several weeks before osteoblasts start laying down new bone, following resorption (Eriksen et al., 1984), recent groups have hypothesised it is reversal cells that transmit osteogenic signals derived during the resorptive phase. This makes the reversal cells instrumental in mediating coupling (Abdelgawad et al., 2016). This is supported in models of post-menopausal and glucocorticoid-induced osteoporosis, in that, bone loss is exacerbated when these cells are disrupted (Andersen et al., 2013, Jensen et al., 2015).

To initiate bone formation, coupling factors released (during the resorptive phase) recruit pre-osteoblasts into the remodelling cavities. Matrix-released factors, such as; TGF-β (although context dependent), IGFs (Fuller et al., 2008, Martin and Sims, 2005, Tang et al., 2009) as well as osteoclast-derived factors, such as; BMP-2, -4, -5, -6, -7, -13, and -14 stimulate osteoblast development (Wozney et al., 1988).

An important interaction within the coupled process of osteoclasts-osteoblasts is the binding of membrane bound ephrin (Eph) B1 on osteoclasts and EphB4 on osteoblast precursors that triggers bidirectional signalling. Forward signalling promotes osteoblast

formation in human and inhibition in murine cultures (McBeath et al., 2004, Zhao et al., 2006), by inhibiting RhoA (Martin et al., 2010). Whereas reverse signalling, blocks the expression of the transcription factor c-Fos, hence osteoclast formation is inhibited. The c-Fos element of AP-1 has been shown to be a critical determinant of fate of haematopoietic precursors into macrophages or osteoclasts, as mice lacking c-Fos harbour enhanced populations of marrow macrophages (Grigoriadis et al., 1994). Other factors that regulate osteoblast differentiation do so through activation of different signalling pathways, such as Wnt, Hedgehog, Notch and BMP (**described in section 1.5.2**), under the control of various transcriptional factors, adding to the complexity of the regulation.

Mature osteoblasts latch onto the surface and lay down osteiod (Delaisse, 2014). Osteoid consists of COLI, hyaluronan (HA), decorin, biglycan, as well as proteins such as fibronectin and thrombospodin which consists of arginine, glycine, aspartic acid (RGD) sequence that is needed for integrin binding capabilities, crucial for cell-matrix interactions (Okamoto et al., 1998). Mineralisation occurs in two stages: the vesicular and the fibrillary. The former is achieved by osteoblasts releasing matrix vesicles that bind proteoglycan and other organic components. Negatively charged sulphated proteoglycans entrap calcium ions stored in the matrix vesicles (Yoshiko et al., 2007, Arana-Chavez et al., 1995). When osteoblasts secrete enzymes that degrade proteoglycans, calcium ions are liberated from the proteoglycan and cross the calcium channels presented in the matrix vesicles membrane. These channels are formed by proteins called annexins (Balcerzak et al., 2003). Once this is completed, mature osteoblasts undergo either apoptosis, become bone-lining cells or osteocytes.

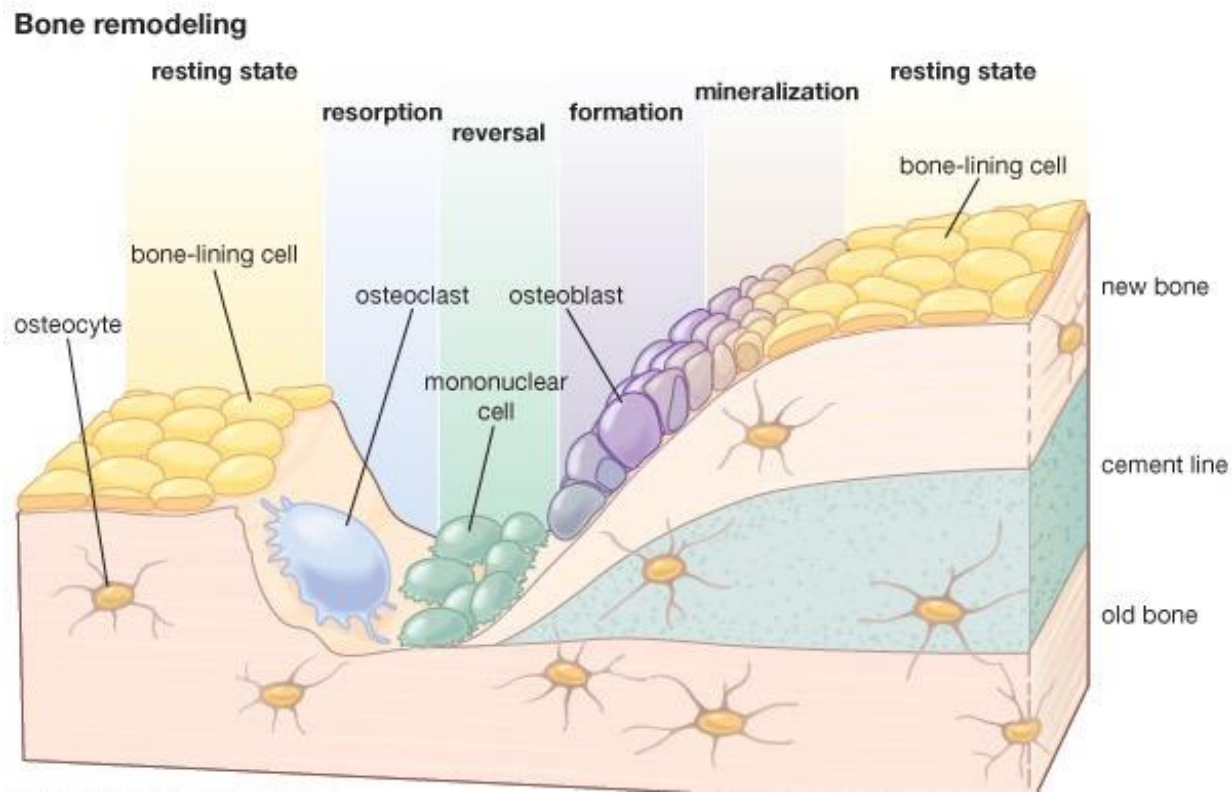


Figure 1. 8 The phases of bone remodelling

Osteoclasts secrete H^+ and proteolytic enzymes to degrade bone during the resorption phase. When osteoclast exit the resorption lacunae, osteoblast precursors are recruited into the cavity possibly in response to TGF-β and BMPs released from bone and differentiate to mature osteoblasts. osteoblasts replace bone material by producing bone matrix that is then mineralised. M-CSF, secreted by osteoblasts, induces osteoclasts to upregulate RANK and also serves as an osteoclast survival factor at later stages of the cycle. Osteoblasts, T-cells and dendritic cells express RANKL in response to prostaglandin-E_2, IL-1 and TNF-α. RANK/RANKL interaction is a key regulator of osteoclast differentiation through signalling pathways such as NF-κB. OPG, released by osteoblasts, is a soluble decoy receptor of RANKL and functions to inhibit osteoclast differentiation. Factors released from the bone following osteoclast activity, such as BMPs, TGF-β, IGF-I and II induce osteoblast differentiation from progenitor cells and act on osteoclast to limit their activity.

Image adapted from Encyclopaedia Britannica (2010)

1.4.2 Pathological Bone Remodelling

Acute inflammation encompasses a vital part of the body's defence to pathogens, but also plays an important role in tissue healing throughout the body. With regards to bone, early administration of anti-inflammatory compounds inhibit fracture healing (Barry, 2010), low concentrations of tumour necrosis factor (TNF)-α has been shown to promote MSC osteoblastogenesis in transient exposure (Lu et al., 2012), while TNF-α knockout mice have disrupted fracture healing (Gerstenfeld et al., 2003). However, chronic inflammation can cause a deregulation of bone metabolism leading to pathological changes of bone phenotype as seen in gout (Dalbeth et al., 2011, Dalbeth and So, 2010), systemic lupus erythematous (Bultink et al., 2012) and rheumatoid arthritis (RA).

The observation that bone erosion accompanies chronic inflammatory diseases such as RA had been known for some time, but it was only until the recognition of the high degree of cross-talk between immune cells and bone cells, termed osteoimmunology, that we started gaining an insight into the mechanisms. The chronic expression and abundance of inflammatory cytokines are documented and shown to play key roles in bone and cartilage erosion during RA (Choy and Panayi, 2001). During inflammatory derived pathology, RANKL-expressing activated T-cells promote bone resorption either directly (Horwood et al., 1999, Kong et al., 1999) or indirectly, *in vitro*. In RA, enhanced concentration of proinflammatory cytokines such as TNF-α, IL-6 and IL-17 (Brennan and McInnes, 2008) can directly augment osteoclastogenesis (Nakashima et al., 2011b) and promote osteoclast activity (Kotake et al., 1999) by stimulating production of RANKL from fibroblast-like cells and osteoblasts. As this is not counter-balanced by OPG, there is a net reduction in bone loss leading to the characteristic destruction of joints (Geusens, 2012). In RA, the systemic release of metalloproteinases and proinflammatory cytokines such as TNF-α and IL-1 can induce systemic bone loss as well (Saidenberg-Kermanac'h et al., 2004). Bone loss can be further augmented by the use of glucocorti-

coids administered therapeutically to reduce inflammation (Kaur et al., 2010). In other conditions, such as osteoporosis, the role of inflammation in driving systemic bone loss is beginning to be appreciated.

1.5 OSTEOPOROSIS

Osteoporosis is a systemic metabolic disease of the bone characterised by low mass, deterioration of the microstructure, and weakened strength (Leslie and Morin, 2014). There are various types of osteoporosis. Susceptibility to osteoporosis is multifactorial, and can be genetic resulting from molecular mutations involved in regulating the differentiation, activity, or interactions between osteoclasts and osteoblasts. Other factors include oxidative stress and menopause but age and lifestyle can also predispose individuals to subtypes of the disorder. Type I, also called postmenopausal osteoporosis, occurs following oestrogen reduction, and the concurrent increase in follicle stimulating hormone (FSH), at menstrual cessation. Type 2 (senile osteoporosis) is age-related and can therefore occur in both sexes, and type 3 (also called secondary osteoporosis) arises from side effects of drugs used to treat underlying disorders, for example glucocorticoids to treat chronic inflammatory conditions.

1.5.1 Glucocorticoid-Induced Osteoporosis

Glucocorticoid-induced osteoporosis is the most common type of secondary osteoporosis (Van Staa et al., 2000). Although glucocorticoids are immunosuppressive agents administered therapeutically to resolve inflammatory disorders, they can harm bone formation. Bone loss occurs through an increase in bone resorption (Chappard et al., 1996) as well as a decrease in bone formation (Weinstein et al., 1998), as glucocorticoids hinder replication, differentiation and maturation of osteoblasts (Canalis et al., 2007). It also affects osteocyte numbers (Sambrook et al., 2003). Suggested mechanisms of bone loss in GIO include; decreasing OPG in the circulation (Sasaki et al.,

2001), enhancing DKK-1 expression by osteoblasts (Ohnaka et al., 2004) as well as activating the local renin-angiotensin system (Yongtao et al., 2014).

1.5.2 Postmenopausal Osteoporosis

At menopause women face two stages of bone loss following a reduction in oestrogen levels. During its onset, a significant drop in oestrogen levels leads to enhanced bone resorption in comparison to formation, at the trabecular sites. Following a significant increase in osteoclast activity, what later follows is a slower but persistent loss of bone; effecting both the cortical and trabecular compartments, as a result of decreased bone formation.

Although, osteoporosis is not classically regarded as an inflammatory disorder (Bultink et al., 2005), TNF-α deficiency in bilateral ovariectomy - the gold standard animal model used to study post-menopausal osteoporosis has been shown to prevent bone loss. This has been shown through the use of both TNF-α deficient mice (Roggia et al., 2001) and through the use of TNF-α blocking antibodies (Kimble et al., 1997).

In the absence of oestrogen, pro-osteoclastogenic cytokines such as IL-6 are elevated significantly in the marrow space, which are otherwise shown to be inhibited *in vitro* by the synthetic oestrogen; 17β-estradiol *(Girasole et al., 1992, Jilka et al., 1992)*. The relevance of TNF-α in osteoporosis comes from T-cell transfer experiments where recipients of TNF-α deficient T-cells fail to develop bone loss (Roggia et al., 2001). TNF-α produced by T cells induces the co-expression of soluble RANKL, also significant in the pathogenesis of post-menopausal osteoporosis. Its expression is elevated on the surface of bone marrow derived cells, e.g. osteoblasts, lymphocytes, from postmenopausal women with osteoporosis compared with cells from postmenopausal controls (Eghbali-Fatourechi et al., 2003). Furthermore, both human and animal studies of post-menopausal bone loss have attributed systemic bone loss to the presence of elevated

levels of proinflammatory cytokines, such as TNF-α, IL-1 and IL-6 (Cenci et al., 2000, Eghbali-Fatourechi et al., 2003, Roggia et al., 2001). Moreover, osteoporosis is a natural part of the ageing process and immunosenescence, commonly associated with ageing, also positively correlates with the production of proinflammatory cytokines (Bruunsgaard, 2002, Franceschi et al., 2000).

The adaptive arm of the immune system plays a key role in post-menopausal osteoporosis, with T-cells being a critical component (Cenci et al., 2000). This has been shown in athymic mouse models, who exhibit protection against trabecular bone loss (Cenci et al., 2000, Roggia et al., 2001). In addition, in humans, oestrogen reduction has been found to expand RANK expressing T and B- cells (Eghbali-Fatourechi et al., 2003, Taxel et al., 2008). T-cells isolated from pre-menopausal women, which have undergone ovariectomy, display enhanced T-cell activity as indicated by T-cell markers and TNF-α production (Adeel et al., 2013). Oestrogen-deficiency causes the expansion of the T-cell population that harbour the CD40L surface receptor. These cells enhance osteoclastogenesis indirectly as they provide signals for stromal cells to upregulate M-CSF and RANKL and decrease OPG production – thereby promoting osteoclastogenesis (Yokoyama et al., 2011). Oestrogen-deficiency also leads to the expansion of the B-cells (Masuzawa et al., 1994), another population of cells implicated to play a role in post-menopausal bone loss (Weitzmann, 2014, Onoe et al., 2000). IL-7 administration can expand the B-cell pool *in vivo* and osteoclast-mediated bone resorption (Miyaura et al., 1997). More specifically, the RANKL expressed by B-cells promotes bone loss in ovariectomised mice, because when RANKL is specifically ablated from B-cells, it leads to protection from trabecular bone loss (Onal et al., 2012).

1.5.3 Treating Osteoporosis

The primary goal of treating osteoporotic patients is to reduce their risk of fragility fractures (Leslie and Morin, 2014). Current therapeutics are categorised based on their mode of action; the antiresorptives and anabolics. The former functions to slow down or inhibit bone loss, while the latter stimulates bone formation.

Antiresorptives work by targeting the osteoclast population and preventing their differentiation activity. There are three classes of drugs currently in clinical use: bisphosphonates, monoclonal antibodies such as denosumab, and selective oestrogen receptor modulators (SERM). Bisphosphonates have been commonly prescribed for disorders such as Paget's disease, myeloma, and osteoporosis. They are pyrophosphate analogues and have an affinity for hydroxyapatite; therefore they bind mineralised bone and prevent osteoclasts from forming ruffled borders inhibiting their ability to latch onto bone surfaces (Rodan and Fleisch, 1996). When embedded into bone, and internalised by osteoclasts, it targets their metabolic enzyme farnesyl pyrophosphate synthase (FPPS), disrupting modifications of internal proteins involved in osteoclast activity and survival (Russell, 2007, Russell et al., 2008). The fully human monoclonal antibody denosumab binds RANKL and inhibits the differentiation of pre-osteoclasts into mature osteoclasts and induces them to apoptose (Hanley et al., 2012). SERMs are synthetic compounds that bind oestrogen receptors (ER), with similar affinity to that of oestrdiol (Hendrix and McNeeley, 2001). They can be agonistic or antagonistic depending on the molecular structure and function of the target receptor and targeted organ. Raloxifene is the only SERMs listed for the treatment of osteoporosis, although its mechanism of action is not fully understood, it acts on osteoblasts through ERs and modulates the RANKL/OPG ratio (Rey et al., 2009). Although antiresorptive agents are effective at reducing further bone loss, they do not replace lost bone which is needed for patients suffering from severe bone loss.

Bone can be replaced by either enhancing the osteoblast number or activity using anabolic factors. Bone anabolics stimulate the formation of new bone material by targeting the osteoblast population. Currently, the only approved anabolic, for the treatment of osteoporosis is the intermittent administration of teriparatide – the recombinant N-terminal region of PTH (PTH_{1-34}) (Dempster et al., 2016), although strontium renelate is also approved in Europe, but not in the United States. PTH enhances osteoblast proliferation, differentiation by inhibiting the peroxisome proliferator activator (PPAR)-γ receptor. It also induces the expression of IGF-1 expression, to enhance osteoblast survival. Another amino acid fragment of PTH (1-84) is currently in phase III clinical trials where a 7% increase in bone mineral density (BMD) of the lumber spine in comparison to the controls has been observed (Rittmaster et al., 2000). PTH, however, is a pleiotropic molecule and its use has been associated with off-target effects such as osteosarcoma, and with long term usage leading to a net bone loss (Martin and Sims, 2005).

Strontium ranelate, currently in phase III clinical trials, consists of two atoms of strontium. The agent is of interest because animal studies have shown that it can uncouple bone formation, favouring bone formation while inhibiting resorption (Canalis et al., 1996). *In vitro,* it has been found to enhance bone nodules, and upregulate the expression of RUNX2 (Lymperi et al., 2008). *In vivo*, despite increasing osteoblast populations, the HSC population frequency was not affected (Lymperi et al., 2008). An issue is that the content of the calcium and phosphorous content of the tissue does not significantly change with treatment (Boivin et al., 1996). Another major limitation is that the strontium ranelate is heavier than calcium; hence the X-ray signal is weakened causing an overestimation bone density (Nielsen et al., 1999). In addition, its mode of action is still not clear and its molecular target remains a matter of debate.

The glycoprotein sclerostin has also been recognised as a molecular target, following the discovery that *SOST* gene mutations are associated with enhanced bone mass (Costa et al., 2014, Ke et al., 2012). Features of sclerostin that make it an attractive option to target therapeutically, include its extracellular nature and the fact that majority of its expression is by the osteocytes (Yavropoulou et al., 2014). Preclinical studies in rodents and primates that have been supported by clinical studies, where two distinct humanised sclerostin antibodies, namely, remosozumab (McClung et al., 2014, Padhi et al., 2014) and blosozumab have found promising results with respect to increases in bone mass in postmenopausal patients diagnosed with osteoporosis. Although targeting sclerostin has shown a good safety profile, the identification of sclerostin protein in calcifying tissues (*in vitro* studies) (McClung et al., 2014, Padhi et al., 2014), together with Wnt signalling's role on the vascular system has raised some concerns over its effect on the vasculature (Evenepoel et al., 2014). Therefore there is an unmet need for novel anabolic factors as those few that are currently available are associated with limitations (Axelrad and Einhorn, 2009, Baron and Hesse, 2012, Garrison et al., 2010, Papapoulos, 2015).

More recently TNF-stimulated gene (TSG)-6 has been recognised as a MSC-derived immunomodulatory factor that regulates macrophages (Choi et al., 2011a) as well as dampening down inflammation (Wang et al., 2015). $CD14^+$ peripheral monocytes have been shown to induce osteoblast differentiation from hMSC precursors via STAT3 activation (Guihard et al., 2012, Nicolaidou et al., 2012), partially attributable to oncostatin M (OSM) (Guihard et al., 2012, Nicolaidou et al., 2012). Other groups also found macrophages promote bone formation (Tu et al., 2015, Vi et al., 2015). To explore the soluble mediators responsible for osteogenic effect of monocytes, following interacting with MSCs, whole Illumina genome was performed and tumour necrosis factor alpha stimu-

lated gene (TSG)-6 was amongst one of the most up-regulated genes (PhD thesis Dr. Vicky Nicolaidou 2011) – This thesis will focus on the role of TSG-6 on bone formation.

1.6 TSG-6

During the early 1990s, it was of interest to further delineate how TNF exerts its downstream biological actions by studying the genes regulated or activated by TNF. In such attempt a screen of the cDNA library of TNF-α stimulated fibroblast identified eight distinct cDNA sequences. These were TSG-1, 6,8,12,14,21,27 and 37. Among these TSG-1 (IL-8 – a neutrophil and T-cell chemotactic factor), TSG-8 (monocyte chemotactic and activating factor of monocytes), TSG-21 (a collagenase), and TSG-27 (a stromelysin) were previously identified. However, TSG-6, 12, 14, and 37 were previously unreported. TSG-6 has since been described as a protein possessing immunomodulatory and chondroprotective properties with circumstantial evidence for its protective role on bone tissue. This therefore warranted therefore further investigation into its role on bone tissue.

1.6.1 The Structure of TSG-6 Protein

The human *tsg-6* gene is mapped to the 'q' arm of chromosome 2 (2q23.2) (Nentwich et al., 2002). Its product is a ~35 kilodalton (kDa) soluble secreted glycoprotein, 277 amino acids in length with the 17 amino acid residue signal peptide (Lee et al., 1992). It is evolutionary conserved across different species, sharing 93.8% sequence homology with that of mice (Lee et al., 1992) and 91.3% to that of rabbit homologue (Feng and Liau, 1993), although the functional homology is higher.

Structurally, the TSG-6 has two contiguous domains, namely; the Link and CUB (derived from: **C**omplement subcomponents C1r/C1s, **U**rchin embryonic growth factor, **B**mp-1) domain. The Link domain is located at amino acid residues 37-128 of the preprotein (Nentwich et al., 2002). NMR solution structure of this domain (Kohda et al.,

1996) shows α-helices and two anti-parallel β-sheets and stabilised by its hydrophobic core (Blundell et al., 2003, Higman et al., 2007, Kohda et al., 1996). The sequence of the Link domain of TSG-6 is highly homologous with CD44 (Lee et al., 1992).

The C-terminus CUB domain (Bork and Beckmann, 1993), located at amino acid residues 129-250 of the pre-protein (Lee et al., 1992), consists an aspartic acid rich region (Asp^{179}-Asp^{217}) (Lee et al., 1992) and two N-glycan modification sites (Asn^{118}-Arg-Ser and Asn^{258}-Thr-Ser) (Lee et al., 1992). The X-ray crystal structure of the TSG-6 CUB domain consists mostly of β-sheets and a calcium binding site (Briggs and Day, 2008). The CUB domain has high sequence homology to complement C1rα (Lee et al., 1992). However, allelic variation at nucleotide position 431 (Nentwich et al., 2002) gives rise to two distinct TSG-6 protein populations (Mukhopadhyay et al., 2001), switching a glycine residue located in the CUB functional domain to an alanine, raising possibilities of functional variations (Nentwich et al., 2002).

TSG-6 is a unique member of the Link module superfamily proteins that binds the glycosaminoglycan - HA, in that it has both the Link and CUB domain (Wisniewski and Vilcek, 1997).

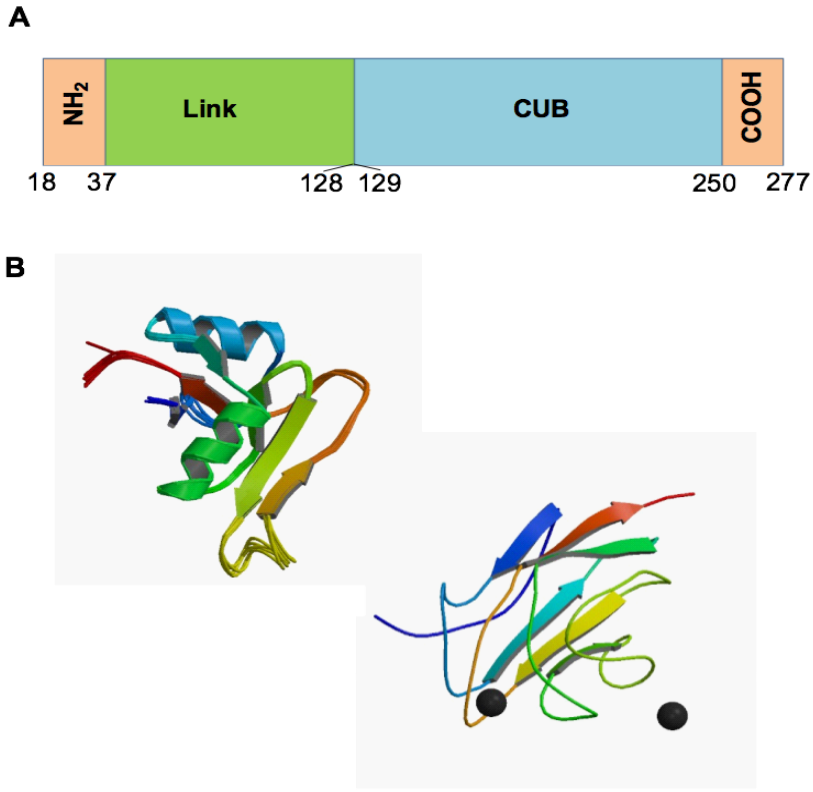


Figure 1. 9 The structure of TSG-6 protein
(A) Showing location of the domains of the protein corresponding to the amino acid residues. (**B**) Cartoon depiction of the macromolecular structure of the Link and CUB domain of TSG-6 obtained from Protein Data Bank (PDB). Link, PDB ID: 107B, obtained by solution NMR (Higman et al., 2014). CUB, PBD 2WNO, obtained by X-ray diffraction (Briggs et al., 2015).

1.6.2 TSG-6: Pattern of Expression

TSG-6 is expressed by a variety of cells, and associated with matrix remodelling. It is considered to be non-constitutively expressed, instead induced in response to a variety of proinflammatory cytokines (Lee et al., 1992, Wisniewski et al., 1993), growth factors (Maier et al., 1996) and/or double stranded RNA (Lee et al., 1992).

Proinflammatory cytokines, such as; TNF-α and IL-1, are inducers of TSG-6 (Milner and Day, 2003). To this end, the protein is regarded as an inflammatory-mediated protein (Lee et al., 1992, Wisniewski et al., 1993, Wisniewski and Vilcek, 1997). Studies using *in vitro* cultured fibroblasts have shown that the promoter site for TNF-α and IL-1 induced gene expression of TSG-6 is located at -165 and +78 (Klampfer et al., 1994).

This region contains three *cis*-acting elements; two adjacent nuclear factor IL-6 (NF-IL6) and one AP-1 sites (Klampfer et al., 1995). Therefore, factors that activate these transcription factors are likely to induce its expression.

In vitro, different cell populations have been shown to express TSG-6 to varying degrees. This is because different cell populations are differentially regulated to express TSG-6 by various cytokines and growth factors (Maier et al., 1996, Milner and Day, 2003). For example, TNF-α induces strong expression of TSG-6 from osteoclasts (Mahoney et al., 2011), whereas IL-1 and IL-6 do so to a lesser extent, albeit from osteoclast precursors (Maina et al., 2009). Articular chondrocytes express TSG-6 in response to TNF-α and IL-1 (Margerie et al., 1997, Stove et al., 2000) - TGF-β does so to a weaker extent (Maier et al., 1996). In human neutrophils, TSG-6 is stored in granules and only secreted in response to pro-inflammatory stimuli (Maina et al., 2009). Lipopolysaccharide (LPS) can cause both macrophages, and dendritic cells of monocytic origin, to express TSG-6 (Maina et al., 2009). This makes the TSG-6 expression pattern complex and highly context specific, with the protein found expressed in both non-pathological inflammatory-like settings as well as pathological-inflammatory settings.

1.6.3 TSG-6 Expression in Non-Pathological Processes

CUB domains are found in a variety of proteins, and involved in protein-protein as well as protein-carbohydrate interactions, which in turn are prerequisite for embryo and organ development (Bork and Beckmann, 1993). TSG-6 is also found to play a role in fertilisation. In humans, TSG-6 messenger RNA (mRNA) is up-regulated in the endometrium at specific stages of the menstrual cycle (Capp et al., 2014) and cervical ripening (Fujimoto et al., 2002). This is replicated in mice models where TSG-6 mRNA is upregulated during the cumulus-oocyte complex (COC) expansion (Fulop et al., 1997), and its protein product found specifically co-localised with matrix HA and the plasma protein inter-α-trypsin inhibitor (IαI) (Carrette et al., 2001). TSG-6 is believed to act as a co-

factor catalysing the transfer of IαI heavy chains (HC) onto individual HA chains, in a calcium ion dependent mechanism (Briggs et al., 2015), thereby enhancing crosslinking and facilitating the assembly of the cumulus-oocyte matrix required for cumulus expansion. The significance of TSG-6 in the fertilisation processes has also been studied *in vitro* using a COC culture system, where neutralising TSG-6 was found to inhibit COC expansion by disturbing the HC-HA complex (Ochsner et al., 2003). In addition to this, knockout TSG-6 mice are found to be semi-fertile due to their inability to produce intact matrix formation around the developing oocyte (Fulop et al., 2003). This shows the significant contribution of TSG-6 in tissue matrix stability.

1.6.4 TSG-6 Expression in Pathological Processes

TSG-6 has been detected in the synovial fluid of patients with characteristic joint diseases such as Sjögren's syndrome, polyarthritis gout (Mahoney et al., 2011), osteomyelitis, as well as joints of RA patients but not in that of controls with no history of joint disease (Wisniewski et al., 1993). Its production in the synovial fluid of RA patients is correlated with high levels of TNF-α and IL-1 (Yoshida et al., 1992), with higher levels detected in the joints compared to the serum, indicating that its effect may be local as opposed to systemic. Synovial fluid derived from RA patients is found to carry high levels of IαI coupled to HA; a process mediated by TSG-6 and calcium ions (Jessen and Odum, 2004).

In osteoarthritis patients, TSG-6 is detected (Bayliss et al., 2001) at higher levels in inflammatory forms of the disease compared to its non-inflammatory form (Mahoney et al., 2011). The basal levels of the protein have been described as an indicator of disease progression of osteoarthritis; where basal levels of TSG-6 can determine the extent of progression to end-stage pathology (Wisniewski et al., 2014), implying that TSG-6 is a potential biomarker of the osteoarthritis. More recently, TSG-6 was identified as a

molecule significantly expressed in the synovial fluid of patients following knee injury (Watt et al., 2016).

1.6.5 Understanding the Function of TSG-6 through its Ligands

One of the major ligands of TSG-6 is the glycosaminoglycan HA (Blundell et al., 2003, Parkar and Day, 1997, Parkar et al., 1998, Wisniewski et al., 2005). HA is a ubiquitous linear polymer, unbound to a core protein (Taylor and Gallo, 2006), composed of two repeating disaccharide unites of D-glucoronate and N-acetyl-D-glucosamine (Laurent and Fraser, 1992) present in all tissues and imperative for tissue integrity. It is different from other glycosaminoglycan (GAGs) in that it is synthesised at the inner plasma membrane rather than the Golgi apparatus, remaining unmodified until inflammation arises (Jiang et al., 2011, Gandhi and Mancera, 2008).

HA binds the serum proteoglycan IαI covalently. IαI is structurally composed of two HCs; HC1 and HC2, which are bound to chondroitin sulphate, which in turn is covalently attached to bikunin protein (Enghild et al., 1999). The binding of IαI to HA involves an intermediate step mediated by the Link module of TSG-6 (Baranova et al., 2011), where a covalent ester bond forms between the Asp α-carbon at the C-terminal end of the IαI HC and the Ser^{28} β-carbon of the TSG-6 pre-protein (Sanggaard et al., 2008). This gives rise to crosslinked HA polymers. The transfer of HCs onto different GAGs by TSG-6 is evolutionary conserved as seen in mammals, birds and reptiles. It is believed to have evolved before mammalian ovulation, as the covalent interaction between HC and TSG-6 is present mammals, birds and reptiles with varying forms of reproductive organs (Sanggaard et al., 2010). This highlights the importance of this intermediate.

In the synovial fluid of RA patients, HA levels are elevated (Dahl et al., 1985) and the HC-HA complex is found at high levels (Hutadilok et al., 1988), this is more aggregated structure than unmodified HA, with different mechanical the cell-adhesion properties

(Milner et al., 2007). The HC-HA complex is relevant in inflammation because it enhances leukocyte cell accumulation with enhanced association to HA-rich matrixes (Lauer et al., 2013, Petrey and de la Motte, 2014). This may also explain how TSG-6 is retained at inflammatory sites. Both osteoblasts and osteocytes produce HA (Aubin et al., 1982, Fedarko et al., 1990, Takagi et al., 1982) and involved in osteoclastogenesis (Chang et al., 2007).

TSG-6 binds a variety of other ligands, these include the sulphated GAGs heparin (Mahoney et al., 2005), and chondroitin-4-sulphate (Parkar and Day, 1997, Wisniewski et al., 2005), as well as aggrecan (Parkar et al., 1998), bikunin (Lamkin et al., 2015). These ligands orchestrate TSG-6's binding ability to HA.

The Link module of TSG-6 binds heparin (Mahoney et al., 2005); at a different binding site to that of HA (Higman et al., 2014, Wisniewski et al., 2005). Its binding to heparin has been shown to enhance its anti-plasmin activity of inter-α-inhibitor (IαI) (Mahoney et al., 2005). TSG-6 binds IαI non-covalently. IαI inhibits plasmin's serine protease activity (Getting et al., 2002, Wisniewski et al., 1996), which would otherwise activate MMPs, which degrade ECM. Inhibition of this protease cascade suppresses the inflammatory response.

TSG-6 binds most of the osteogenic BMPs through its Link and CUB modules (Mahoney et al., 2008). BMP-2, a growth factor, associated with ectopic bone formation (Wozney, 1995), binds type I and II serine/threonine kinase receptors inducing Smad phosphorylation. Phosphorylated Smad is translocated into the nucleus, activates osteoblast associated gene expression such as ALP, osteocalcin and RUNX2. *In vitro* experiments have shown TSG-6 to inhibit BMP-2 induced osteoblastogenesis on cell lines (Mahoney) as well as on primary cells (Tsukahara et al., 2006).

In the synovium of rheumatoid, TSG-6, HA and CD44 are upregulated (Balazs et al., 1967, Emlen et al., 1996, Wisniewski et al., 1993). HA interacts with the cell surface receptor CD44, this plays a role in mediating cell adhesion (Day and de la Motte, 2005) also cell proliferation and differentiation (Entwistle et al., 1996, Lee and Spicer, 2000). CD44 is expressed on the plasma membrane of osteoblasts and osteoclasts (Hughes et al., 1994), and involved in mediating the attachment of hematopoietic stem cells to stromal cells (Miyake et al., 1990).

1.6.6 The Significance of TSG-6 in Murine Models of Inflammatory Arthritis

Proteoglycan-induced arthritis (PGIA) is a model of polyarthritis disease, induced in response to antigenic fragments of aggrecan (Glant et al., 1998). It exhibits similar clinical and histological characteristics to that of human RA, including joint inflammation accompanied by bone and cartilage erosion, as well as destruction of the intervertebral discs (Glant et al., 1987).

In murine model of PGIA, systemic injection of rmTSG-6 found reduced oedema at the joints in short-term and in the long-term cartilage was protected against breakdown and periosteal bone erosion was prevented (Bardos et al., 2001). However, no effect was seen in terms of the onset, or disease severity; in that, the time and extent of paw swelling and redness were comparable between the rmTSG-6 treated and the phosphate-buffered saline (PBS) control group. Inflammatory cells had migrated into the tissues, and proinflammatory cytokines as well as IgG1 and IgG2a antibody were produced, characteristic feature of PGIA, were detected both locally and systemically (Bardos et al., 2001). This showed that during inflammation, TSG-6 exerts its tissue protective effect locally. In support of this, a single local intraarticular administration of rmTSG-6 found to be chondroprotective in antigen-induced arthritis (AIA) (Bardos et al., 2001), a monoarticular model of arthritis. In addition, site-specific overexpression of TSG-6 at the cartilage in AIA found to inhibited cartilage breakdown as indicated by aggrecan

loss (Glant et al., 2002). The protective mechanism of this has been attributed to the ability of the protein to bind IαI, thereby inhibiting plasmin activity which would otherwise lead to matrix breakdown. This is supported by two lines of evidence. Firstly, the MMP activity can be inhibited by treatment with rmTSG-6 (Bardos et al., 2001, Szanto et al., 2004). Secondly, plasmin activity is increased in PGIA mice that are globally deficient of TSG-6 (Szanto et al., 2004).

PGIA induced on TSG-6-deficient mice develop more severe disease symptoms in comparison to their wild-type littermates. They also exhibit faster rate of disease progression accompanied with significant higher numbers of neutrophil cells at the synovial joints (Szanto et al., 2004). This observation is consistent with groups that have reported the ability of TSG-6 to regulate the recruitment of inflammatory immune cells. For example, the Link module of the human TSG-6 protein has been shown to prevent neutrophil (Getting et al., 2002) and granulocyte (Wisniewski et al., 1996) infiltration in air pouch models of acute inflammation. TSG-6 Link module also inhibits leukocyte-endothelial interactions both *in vitro* and *in vivo* by impairing their rolling and migration between endothelial cells (Cao et al., 2004). The mechanism underlying this is starting to be elucidated and attributed to its ability to bind the chemokine CXCL-8 inhibiting chemotaxis (Dyer et al., 2014). TSG-6 has also been shown to prevent the recruitment of $CCR2^{+}$ monocytes (Kim et al., 2015). These observations imply that TSG-6 is anti-inflammatory in a classical sense.

Collagen-induced arthritis (CIA) is an alternative polyarthritis model of inflammatory autoimmune disorder, also showing similar histopathology to that of RA (Brand et al., 2007). The disease results in severe synovitis, pannus formation, and cartilage and bone erosion. Characteristic mechanisms of pathology include elevated levels of circulating arthritogenic antibodies IgG2a and IgG2b against type II collagen, elicited in re-

sponse to cytokines secreted by subsets of T-cells, that in turn can activate the complement system (Watson and Townes, 1985). The presence of both local and systemic TSG-6 within this model have been associated with improved disease symptoms, and a suppressed inflammatory response, preventing destruction of joint tissue (Mindrescu et al., 2002, Mindrescu et al., 2000). More specifically, systemic treatment of CIA mice with rmTSG-6 reduced antibodies against type II collagen, as histological analysis found cartilage and bone erosion to be mild in comparison to the PBS control (Mindrescu et al., 2000). In addition, restricted overexpression of TSG-6 to T-cells, found a delayed disease onset, reduced cellular infiltration and mild cartilage and bone damage (Mindrescu et al., 2002) In the overexpression study, antibodies against type II collagen were not decreased, nor were T-cells prevented from infiltrating into the joints, demonstrating that TSG-6 does not mediate bone and cartilage protection by inhibiting cellular and humoral compartments of the adaptive immune response to type II collagen, but rather through an alternative unknown mechanism. The mechanism of TSG-6 protection against bone damage in these models is not well understood to date.

1.6.7 TSG-6 and the Therapeutic Effects of MSCs

Currently, MSCs are in clinical trials for their use in a variety of diseases. In various models of injury where an inflammatory response is evoked, the therapeutic effects of MSCs have been attributed to the secretion of TSG-6 (Choi et al., 2011a, Lee et al., 2009, Oh et al., 2010, Prockop, 2013). This includes mice with traumatic cortical brain damage (Watanabe et al., 2013) and chronic periodontitis (Yang et al., 2014). In gingival inflammation following operation, TSG-6 is believed to modulate the inflammatory cascade by suppressing TNF-α expression (Beltran et al., 2015). TSG-6 has also been found to suppress inflammation in models of acute lung injury (ALI) induced by various agents such as the toxic paraquat (Xu et al., 2016), LPS (Danchuk et al., 2011), or oleic

acid (Abd-Allah et al., 2015), as well as bleomycin induced lung inflammation (Foskett et al., 2014).

TSG-6 is believed to promote proliferation of vascular smooth muscle cells (Ye et al., 1997). In murine model of zymosan-induced peritonitis TSG-6 secreted by MSCs regulates inflammation by downregulating the nuclear translocation of NF-kB *via* CD44 receptor (Choi et al., 2011a), silencing of TSG-6 in the hMSCs before injection into the mice did not find a suppressed inflammatory response (Choi et al., 2011a).

TSG-6 is protective towards bone erosion in the presence of inflammatory responses induced by proteoglycan, antigen and collagen induced arthritis (Bardos et al., 2001, Mindrescu et al., 2002, Mindrescu et al., 2000, Szanto et al., 2004) . However, the mechanism by which TSG-6 protects bone loss during these inflammatory diseases is not understood and its direct role on osteoblastogenesis has not been extensively studied.

1.7 THESIS AIMS AND HYPOTHESIS

Replacing bone once it has been lost, due to oestrogen deficiency, long term glucocorticoids or inflammation, is a currently an under met clinical need. In inflammatory disorders, the role of TSG-6 is described as protective to cells of mesenchyme origin, such as chondrocytes; bone producing osteoblasts form from the same lineage. Previous work in the lab has shown that the interaction between immune cells of the monocyte/macrophage lineage and MSCs results in osteoblast formation that is accompanied by a significant up-regulation of TSG-6. Therefore the hypothesis of this thesis is that TSG-6 possesses bone anabolic properties.

The objectives of this thesis are:

1. Mass express and purify biologically active, cell-culture grade rhTSG-6 using baculovirus-insect cell expression system.
2. To determine the role of TSG-6 on osteoblastogenesis of primary hMSCs, using endogenous monocyte-derived TSG-6 as well as exogenous recombinant TSG-6 protein.
3. To determine the pathophysiology effect of TSG-6 on bone phenotype using (i) global TSG-6 knockout, and (ii) wild-type mice treated with exogenous with recombinant TSG-6 protein, in a model of oestrogen-deficiency induced bone loss.

2

CHAPTER 2: EXPRESSION AND PURIFICATION OF BIOLOGICALLY ACTIVE FULL-LENGTH RECOMBINANT HUMAN TSG-6 PROTEIN

2.1 INTRODUCTION

The bone marrow provides a close anatomical niche for the development of skeletal (Hofmann et al., 2013) and immune cells (Ding et al., 2012). Identification of common precursors, cytokines, receptors, adaptor proteins, signalling molecules and transcriptional factors common to both systems (Terpos and Dimopoulos, 2011) highlighted their close functional relationship, in both physiological (Negishi-Koga et al., 2015) and pathological conditions.

The most well-established Link is the RANK/RANKL/OPG axis (Leibbrandt and Penninger, 2008) – a potent regulator of osteoclastogenesis that also modulates adaptive immunity through its involvement in secondary lymphoid organ development (Theill et al., 2002), immune cell interactions (Takayanagi, 2007a) and peripheral tolerance (Loser et al., 2006).

Our knowledge of molecular cues regulating the osteoimmune system is expanding. A factor expressed by both immune and bone cell lineages, in response to pro-inflammatory stimuli, is the 35 kDa multifunctional protein TSG-6 (Fulop et al., 1997, Lee et al., 1992, Milner et al., 2006, Szanto et al., 2004, Wisniewski and Vilcek, 2004). TSG-6 suppresses inflammation through various mechanisms, including, inhibiting immune cell recruitment, (Cao et al., 2004, Dyer et al., 2014, Getting et al., 2002) and reducing Toll-like receptor (TLR2)/NF-κB-driven pro-inflammatory response (Choi et al., 2011a, Oh et al., 2012, Oh et al., 2010, Prockop and Oh, 2012). The association of TSG-6 to the tissue-protective effects of MSCs (Choi et al., 2011a, Lee et al., 2009, Oh et al., 2012, Oh et al., 2010), as well as its protective effects on cartilage and bone in inflammatory arthritic mouse models (Bardos et al., 2001, Glant et al., 2002, Mindrescu et al., 2002, Mindrescu et al., 2000) has initiated interest in the protein as a potential therapeutic.

TSG-6 binds a variety of factors involved in maintaining and remodeling of the ECM, such as; HA (Baranova et al., 2011, Blundell et al., 2005), fibronectin (Kuznetsova et al., 2008), thrombospondin-1 (Kuznetsova et al., 2005), BMP-2 (Mahoney et al., 2005).

It synergises with OPG to inhibit osteoclast activity in an autocrine manner (Mahoney et al., 2011) and its global knockout leads to higher baseline bone mass (Mahoney et al., 2008). Given the coupled nature of bone remodeling, it is plausible to assume factors controlling resorption also modulate formation. However, the involvement of TSG-6 on the latter is under-studied and evidence on its bone protective properties remains circumstantial.

Commercially-available full-length rhTSG-6 has poor biological activity, as determined by its inconsistent ability to inhibit osteoclast activity (personal communications with Dr. David Mahoney). Studies exploring the role of TSG-6 on bone biology are limited due to the difficulties in purifying large amounts of the protein (Bardos et al., 2001, Mindrescu et al., 2000, Nentwich et al., 2002). Although relatively high yields of biologically active (Dyer et al., 2014, Getting et al., 2002, Kuznetsova et al., 2008, Mahoney et al., 2005) CUB/Link domains of TSG-6 have been generated in *Escherichia coli* (*E.coli*) systems (Day et al., 1996), and thus studied independently, in nature, the protein is expressed exclusively in its full-length form, therefore studies using the full-length protein is physiologically more relevant. Moreover, amino acid residues spanning the Link and CUB domain interact with well-characterised osteoinductive factors, such as BMP-2 (Mahoney et al., 2008), suggestive that both domains play a role on osteoblastogenesis.

As the pharmokinetic and pharmodynamic properties of TSG-6 have not been previously studied, the concentration of TSG-6 required for *in vitro* and *in vivo* osteogenic assays must be determined empirically. Given the relatively low molecular weight (MW) of

TSG-6 protein, a rapid serum clearance rate is expected *in vivo*. Therefore high amounts of the protein need to be administrated frequently to sustain high enough systemic concentrations to exert its effect.

The *E.coli* expression system does not have the glycosylation machinery of insect and mammalian cells, resulting in the generation of TSG-6 with a shorter half-life (Kim et al., 2016), as unglycosylated or mis-folded proteins result in higher clearance rates *in vivo* (Sinclair and Elliott, 2005). Therefore, proteins expressed in this system require extensive refolding steps (Day et al., 1996, Kahmann et al., 1997) to restore structural properties essential for the biological activity of the protein. Additionally, this approach increases in the likelihood of endotoxin contaminants from which are detrimental to any subsequent functional *in vitro* and *in vivo* studies (Guha and Mackman, 2001, Rossol et al., 2011).

This Chapter describes the mass expression, purification and biological activity of soluble cell-culture grade rhTSG-6 using baculovirus-*Spondoptera frugipedra* (Sf)-9 expression system, a modification from the *Drosophila* S2 cells and *Trichoplusia ni* (BTI-TN-5B-4) systems described previously (Mindrescu et al., 2000, Nentwich et al., 2002, Rugg et al., 2005, Wisniewski et al., 1994)

2.2 MATERIALS AND METHODS

All reagents purchased and used were biologically pure and certified LPS free. All buffers were made using ultrapure water and filter-sterilised prior use to minimise bacterial and mycoplasma contamination.

2.2.1 Expression, Purification, Quantification of Full-Length rhTSG-6 Protein

The full-length rhTSG-6 fusion protein was expressed using a baculovirus insect cell expression system of ovarian derived armyworms; *Spodoptera frugiperda* (Sf)-9 (Oker-Blom and Summers, 1989) (Invitrogen Corporation, California USA) **(See Fig. 2.1 and 2.2)**

The human TSG-6 gene (obtained from The Structural Genomics Consortium, University of Oxford, UK), excluding its native 17 amino acid N-terminal signal peptide (δ17N_TSG-6), was cloned into a commercially purchased p**F**AST**B**AC^{TM}HT secretory (pFB-Sec) vector (Invitrogen Corporation, California USA) using bacterial-derived restriction enzymes (Thermo Fisher Scientific). The replacement of the native signal peptide by that of the vector, greatly improved secretion efficiency of the protein. This vector contained an N-terminal FLAG-tag, hexa-histidine (His)-tag and a tobacco etch virus (TEV) digestion site. This made it possible to remove the immunogenic N-terminal tag from the recombinant protein using TEV protease (Carrington and Dougherty, 1988, Polayes et al., 1998) prior to *in vivo* studies.

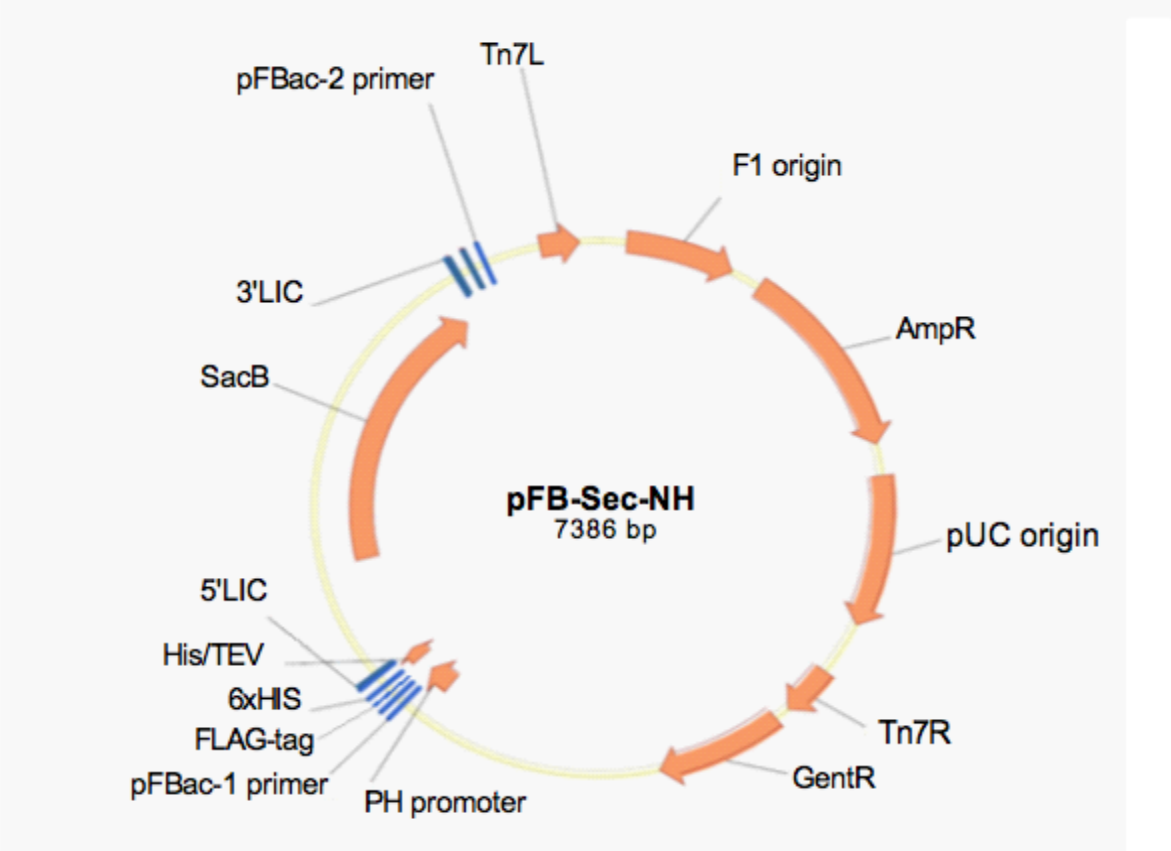


Figure 2. 1 Map of the baculovirus transfer vector showing the location of vector elements and annealing sites of primers
SacB is the location where the TSG-6 target gene is inserted. Image extracted from vector information sheet, (addgene)[2].

pBac1 primer 5'- TATTCATACCGTCCCACCA-3'

pBac2primer 3'-GGGAGGTTTTTTAAAGCAAGTAAA-5'

Following cloning, the resulting recombinant plasmid was amplified in XL-1 *E.coli* (Invitrogen Corporation, California USA) initiated at the plasmid's origin of replication and isolated using plasmid preparation kit (Fermentas; Fisher Scientific, Leicester, UK). Competent $DH10B_{AC}$ *E.coli* cells (Invitrogen Corporation, California USA), carrying a

[2] Biological resource centre, global plasmid repository.

(host) bacmid, were transduced with these recombinant (donor) plasmids and plated onto Luri-Bertani (LB) Agar (Fisher Scientific, Leicester, UK) containing gentamicin (MP Biomedicals, Fisher Scientific, Leicester, UK). Recombinant bacmid were generated through site specific transposition between mini-Tn7 site on the donor plasmid and the mini-*att*Tn7 on the host bacmid, aided by transposition protein elements from the helper plasmid. Colonies containing the recombinant bacmid were identified by blue white screening as well as antibiotic selection. This was made possible because transposition disrupts the *lacZα* gene, producing white colonies as opposed to blue. In addition, the pFB-Sec vector carried a gentamicin resistance gene allowing antibiotic selection. The recombinant bacmid were then purified using high MW mini-prep kit (Invitrogen). The nucleotide sequence was confirmed using the chain termination dideoxynucleotide [3]method, developed by Sanger *et. al* (Sanger et al., 1977). This was carried out at the FBAC-1 (5' to 3') and FBAC-2 (3' to 5') (**see section 2.3.1 of Results**). This was then used to infect Sf9 cells to generate passage 0 (P0) recombinant baculovirus. In order to obtain higher recombinant baculovirus titer, Sf9 cells were infected with P0 recombinant baculovirus over three rounds of viral amplification (see section 2.2.2 of Materials and Methods). Mass production of the full-length TSG-6 protein was carried out using P3 recombinant baculovirus (see section 2.3.1 of results). The purified protein was identified as TSG-6 by immunoblotting (**see section 2.3.5 of Results**).

[3] Sequencing was carried out at The Wellcome Trust Centre for Human Genetics, University of Oxford, UK

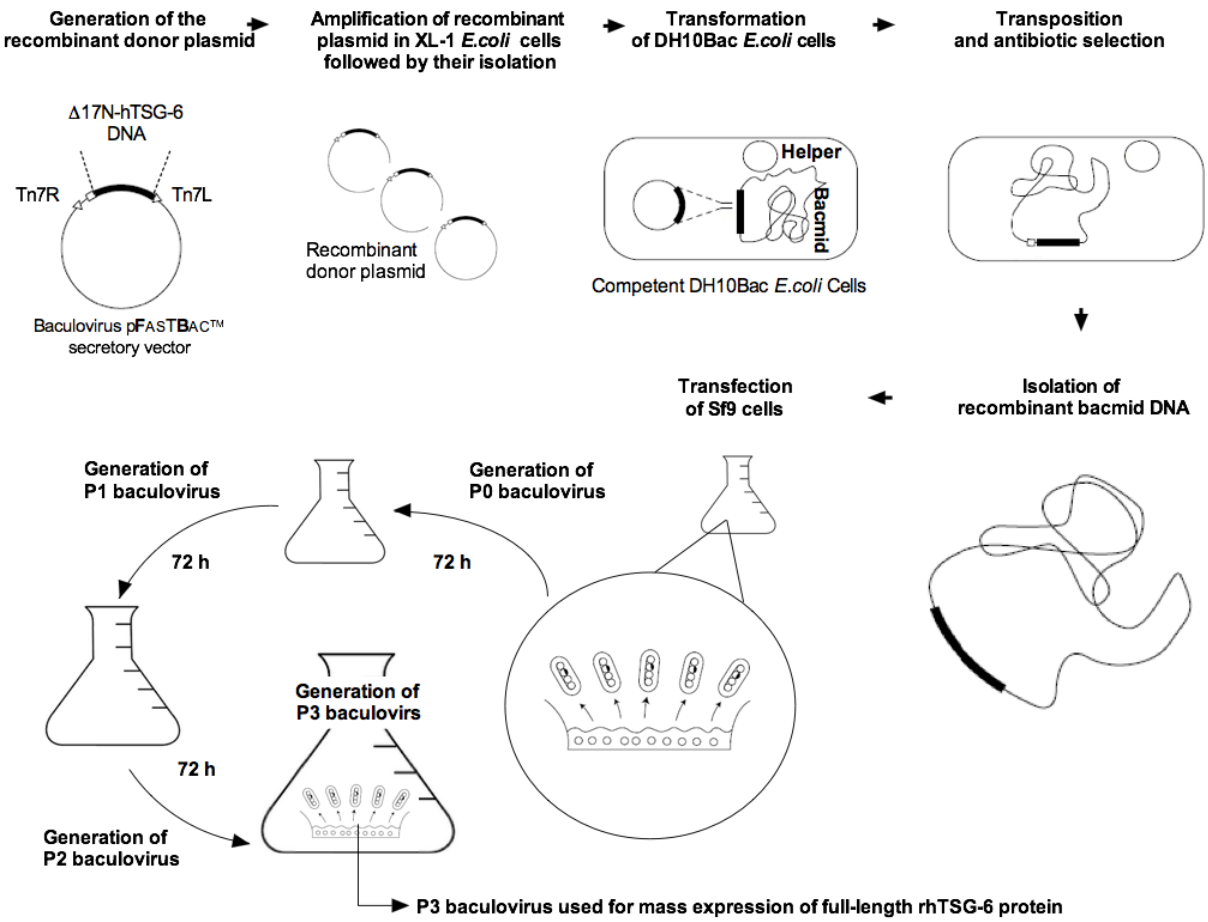


Figure 2. 2 Overview of steps taken to generate high titer P3 recombinant baculovirus for the expression of full-length rhTSG-6 protein

Figure adapted from Invitrogen life technologies, Instruction Manual: Guide to Baculovirus Expression Vector Systems (BEVS) and Insect Cell Culture Techniques. (https://tools.thermofisher.com/content/sfs/manuals/bevtest.pdf).

2.2.2 Preparation of High-Titer Passage 3 Viral Stock for Protein Expression

Passages (P) 1 were generated from P0 baculovirus stocks (gifted by Dr. David Mahoney) by transfecting 0.5 mL of Sf9 cells seeded at a density of $2x10^6$/mL, and incubated for 72 hours (h). Cells were harvested by centrifugation 3000 revolutions per minute (rpm) for 15 minute (min). One percent (1%) inactivated foetal bovine serum (FBS) was added and the baculovirus was filter sterilised with 45 µm filter. The stock was then aliquoted and stored at 4°C.

To generate high tire P2 viral stock, $1x10^8$ Sf9 cells suspended in 50 mL of protein free insect-XPRESS™ media (Life Technologies, Paisley, UK) infected with 0.5 mL of P1 baculovirus stock and incubated for 72 h in I26 New Brunswick incubator shaker (VWR, Leicestershire, UK) (225 rpm, 27°C). Cells were harvested in a Sorvall™ Legend™ RT Plus centrifuge (ThermoFisher Scientific, Hertfordshire, UK) using SLA1500 rotor (3000 rpm, 15 min, 4°C) and supernatant containing the P2 baculovirus was transferred into a fresh 50 mL tube and sterilised using a 45 micron filter (Sartorius Ltd., Surrey, UK). For long-term stability, the media was supplemented with 1% [volume per volume (v/v)] FBS (Life Technologies, Paisley, UK), and stored in the dark at 4°C. The higher titer P3 baculovirus stocks required for TSG-6 mass expression was generated from the P2 baculovirus stock by the same method, however, on a 10-fold larger volume scale.

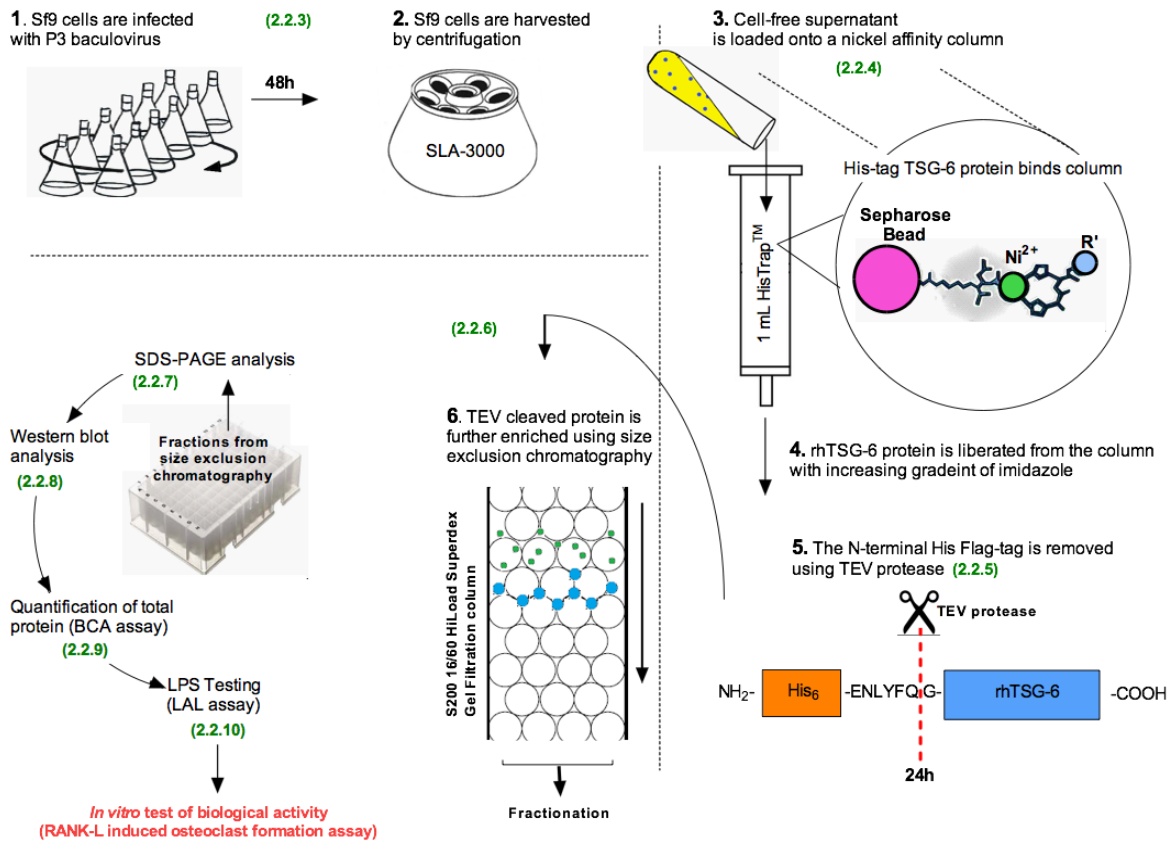


Figure 2. 3 Overview of workflow in expressing and purifying full-length rhTSG-6 protein.

As described in sections 2.2.3 to 2.2.10 of this Chapter's Materials and Methods.

N.B. Numbers in green refer to sections numbers in the text

2.2.3 Baculovirus-Sf9 Cell Expression System

To induce the expression of rhTSG-6 fusion protein, 5 mL of P3 baculovirus was added to $2x10^9$ Sf9 cells suspended in 500mL of SF-900™ serum and protein free insect culture media (Life Technologies, Paisley, UK) and incubated for 48 h in I26 New Brunswick incubator shaker (VWR, Leicestershire, UK) (225 rpm, 27°C). To separate the solubilised rhTSG-6 fusion protein from the Sf9 cultures, cells were harvested by centrifugation (15000 rpm, 15 min, 4°C) using Sorvall Evolution centrifuge RC and SLA-3000 fixed angle rotor (ThermoFisher Scientific, Hertfordshire, UK).

2.2.4 Affinity Chromatography4

The TSG-6 expression construct included an N-terminal $(His)_6$ tag, which allows for its positive selection from other solubilised factors by nickel affinity, as originally described by Hochuli *et al.* (Hochuli et al., 1987). To do so, the cell-free supernatant was loaded onto an ÄKTA™purifier (GE Healthcare Life Sciences, Buckinghamshire, UK) and passed through a 1 mL gel filtration buffer [0.5 M sodium chloride (NaCl), 20 mM HEPES, 5% glycerol] equilibrated HisTrap™ column (GE Healthcare Life Sciences, Buckinghamshire, UK) containing charged nickel ions in the matrix. Bound rhTSG-6-His tagged fusion proteins were liberated from the column by competitive elution using an increasing gradient (0-400mM) of imidazole with increasing increments of 40mM/mL, also contained within this buffer was 0.5 M NaCl, 20 mM HEPES, and 5% glycerol. Fractions were collected in sterile 96 deep-well plates (Greiner Bio-One, Gloucestershire, UK) at 1 mL elution volumes.

4 Carried out with the assistance of Dr. James Dunford (The Botnar Research Centre, University of Oxford)

2.2.5 TEV Digestion of His-FLAG Tag

To prevent immunogenic reactions in response to the N-terminal FLAG epitope of the rhTSG-6 protein during *in vivo* studies, the fractions containing the rhTSG-6-fusion protein were pooled and treated overnight at 4°C with 50 µL of 6 mg/mL TEV protease produced in-house[5]. Usage of TEV to cleave recombinant proteins was first described by Parks *et al.* (Parks et al., 1994).

2.2.6 Size Exclusion Chromatography[6]

To further purify the rhTSG-6 protein preparation, size exclusion chromatography was used, as described by Porath *et al.* (Porath and Flodin, 1959). This technique allowed for the separation of protein species based on their relative MW. The FLAG cleaved TSG-6 preparations were concentrated to a volume of 1-1.5 mL using Viva spin columns (Sartorius, Surrey, UK) of 10 kDa MW cut off. S200 16/60 HiLoad Superdex gel filtration column (GE Healthcare Life Sciences, Buckinghamshire, UK), connected to the ÄKTA™ purifier system (GE Healthcare Life Sciences, Buckinghamshire, UK), was equilibrated with 120 mL of gel filtration buffer (20 mM HEPES, 0.5 M NaCl, 5% glycerol). The concentrated protein sample was then manually injected into the system and run at a rate of 1 mL/min. The profile of the eluted protein material was monitored in real-time at a UV absorbance reading of 280 nm using UNICORN 5.11 software (GE Healthcare Life Sciences, Buckinghamshire, UK). Fractions were collected in 2 mL volumes in a sterile 96-deep-well plate (Greiner Bio-One, Gloucestershire, UK).

2.2.7 Sodium Dodecyl Sulphate Polyacrylamide Gel Electrophoresis Analysis

Polyacrylamide gel electrophoresis analysis (SDS-PAGE) was carried out by standard procedures, as previously described by Laemmli *et al*. (Laemmli, 1970) to identify elutes

[5] TEV Protease produced by Dr. James Dunford (Botnar Research Centre, University of Oxford)

6 Carried out with the assistance of Dr. James Dunford (Botnar Research Centre, University of Oxford)

containing the rhTSG-6 protein. Briefly, protein disulphide bonds were disrupted by suspending 20 µL of fraction elutes at a 1:1 volume ratio in protein sample buffer supplemented with 1x β-mercaptoethanol reducing agent (Life Technologies, Paisley, UK). The tertiary structure of the protein was linearised by heating the samples to 100°C for 5 min on a heat block. Next, 20 µL of the sample mixtures were loaded onto 1.0 mm thick BIS-TRIS 4-12% gradient gel (Life Technologies, Paisley, UK). The protein content was separated based on their relative MW using electrophoresis (150V, 80 min) in 3-Morpholinopropane-1-sulfonic acid (MOPS) SDS-PAGE running buffer (Life Technologies, Paisley, UK). To visualise protein bands, gels were stained with Coomassie Brilliant Blue (ThermoFischer Scientific Ltd., Leicestershire, UK) for 30 min at room temperature (RT), and then washed using deionised water and visualised under white light. The relative MW of the protein present in samples was determined in comparison to the protein ladder standard (Precision plus™ Bio-Rad).

2.2.8 Western Blot Analysis

Chemiluminescent Western blot procedures were carried out as previously described by Towbin *et al.* (Towbin et al., 1979). Briefly, following resolution of protein species by gel electrophoresis (detailed in Section **2.2.1.6**), proteins were wet transferred (100V, 1 h) onto a methanol treated PVDF nitrocellulose membrane (Millipore Ltd., Hertfordshire, UK) in transfer buffer (Life Technologies, Paisley, UK). Membranes were washed in PBS containing 0.002% (v/v) tween-20 and blocked with 1% [weight per volume (w/v)] milk reconstituted in PBS-Tween for 1h. Membranes were probed overnight with 1 µg/mL of primary anti-human/mouse monoclonal TSG-6 antibody (mAb 2104, R&D Systems Europe), on a shaking platform at 4°C. The following day, three quick washes were performed on the membrane, followed by three 10 min washes on a shaking platform. The membranes were next incubated with 1:1000 diluted polyclonal IgG goat anti-mouse horse-radish peroxidase (HRP) enzyme conjugated secondary antibody (Life

Technologies, Paisley, UK) for 90 min at RT on a shaking platform. Following three quick washes and three 10 min washes, protein bands were detected using Amersham enhanced chemiluminescence (ECL) blotting reagents (GE Healthcare Life Sciences, Buckinghamshire, UK) as per manufacturer's instructions.

2.2.9 Bicinchoninic Acid Assay: Quantification of Total Protein in Preparations

To determine the total protein concentration in preparations, the micro-plate Bicinchoninic acid (BCA) assay (Life Technologies, Paisley, UK) was carried out as per manufacturer's instructions. Colourimetric detection was performed at an absorbance reading of 563 nm using FLUOstar® Omega microplate reader (BMG LABTECH, Buckinghamshire, UK).

2.2.10 Chromogenic Limulus Amebocyte Lysate Assay: Quantification of LPS Endotoxin Contaminate in TSG-6 Protein Preparations

To detect the presence of contaminating LPS endotoxin molecules in rhTSG-6 protein preparations and its associated reagents, limulus amebocyte lysate (LAL) colourimetric assay (Lonza, Slough, UK) was carried out on all preparations as per manufacturer's instructions at an absorbance reading of 405 nm using FLUOstar® Omega microplate reader (BMG LABTECH, Buckinghamshire, UK).

2.2.11 Osteoclast Formation Assay[7]: *In Vitro* test of TSG-6 Biological Activity

To determine the biological activity of TSG-6 produced, its effect on RANKL-induced human osteoclast formation was investigated, as previously described by Sabokbar and Athanasou (Sabokbar and Athanasou, 2003). Briefly, whole blood was collected form healthy male human volunteers into ethylenediaminetetraacetic acid (EDTA)-treated tubes and diluted 1:1 in α-minimum essential medium (α-MEM) (ThermoFischer Scien-

7 Assay was carried out by Dr. David Mahoney (Botnar Research Centre, University of Oxford, UK)

tific Ltd., Leicestershire, UK). To isolate the peripheral blood mononuclear cells (PBMCs), the mixture was layered over Histopaque (Sigma-Aldrich, Dorset, UK) and centrifuged (693 x g), washed and re-suspended in α-MEM supplemented with 10% (v/v) heat-inactivated foetal calf serum (FCS) (ThermoFischer Scientific Ltd., Leicestershire, UK). 5% (v/v) of acetic acid was used to lyse the red blood cells before the PBMCs were counted and seeded at 5 $x10^5$ cells/wells into 96-well tissue culture plates containing coverslips.

Following 2h incubation, the non-adherent cells were removed, by washing the coverslips in α-MEM. The adherent cells were then cultured in 24-well tissue culture plates with 1 mL/well α-MEM supplemented with 10% (v/v) FCS, 10 mm L-glutamine, antibiotics (100 IU/ml penicillin and 10 µg/ml streptomycin), 25 ng/mL M-CSF (R&D Systems Europe, UK), and 50 ng/mL soluble RANKL (PeproTech Ltd., UK). Following the addition of rhTSG-6 (0-250 ng/mL), cultures were maintained for 21 days, with media changes every 2-3 days.

2.3 RESULTS

2.3.1 Determination of TSG-6 Vector Sequence and its Corresponding Peptide Sequence Using Bioinformatics Tools

To determine the match and mismatch frequency of the deoxyribonucleic (DNA) sequencing to that of human TSG-6 [National Center for Biotechnology Information (NCBI) accession number AJ419936.1], a pairwise alignment was carried out using Basic Local Alignment Search Tool (BLAST®). The sequence identity obtained was 100% identical to the human TSG-6 sequence retrieved from the database. With an expect value of '0' (probability rounded down) indicates that the alignment between the query and retrieved sequence did not occur by chance (**Fig. 2.4**). This indicated the presence of the human *tsg-6* gene with a low probability that the pair-wise match was random.



Score	Expect	Identities	Gaps	Strand
1445 bits(782)	0.0	782/782(100%)	0/782(0%)	Plus/Plus

```
Query  1    TGGGGATTCAAGGATGGAATTTTTCATAACTCCATATGGCTTGAACGAGCAGCCGGTGTG  60
            ||||||||||||||||||||||||||||||||||||||||||||||||||||||||||||
Sbjct  52   TGGGGATTCAAGGATGGAATTTTTCATAACTCCATATGGCTTGAACGAGCAGCCGGTGTG  111

Query  61   TACCACAGAGAAGCACGGTCTGGCAAATACAAGCTCACCTACGCAGAAGCTAAGGCGGTG  120
            ||||||||||||||||||||||||||||||||||||||||||||||||||||||||||||
Sbjct  112  TACCACAGAGAAGCACGGTCTGGCAAATACAAGCTCACCTACGCAGAAGCTAAGGCGGTG  171

Query  121  TGTGAATTTGAAGGCGGCCATCTCGCAACTTACAAGCAGCTAGAGGCAGCCAGAAAAATT  180
            ||||||||||||||||||||||||||||||||||||||||||||||||||||||||||||
Sbjct  172  TGTGAATTTGAAGGCGGCCATCTCGCAACTTACAAGCAGCTAGAGGCAGCCAGAAAAATT  231

Query  181  GGATTTCATGTCTGTGCTGCTGGATGGATGGCTAAGGGCAGAGTTGGATACCCCATTGTG  240
            ||||||||||||||||||||||||||||||||||||||||||||||||||||||||||||
Sbjct  232  GGATTTCATGTCTGTGCTGCTGGATGGATGGCTAAGGGCAGAGTTGGATACCCCATTGTG  291

Query  241  AAGCCAGGGCCCAACTGTGGATTTGGAAAAACTGGCATTATTGATTATGGAATCCGTCTC  300
            ||||||||||||||||||||||||||||||||||||||||||||||||||||||||||||
Sbjct  292  AAGCCAGGGCCCAACTGTGGATTTGGAAAAACTGGCATTATTGATTATGGAATCCGTCTC  351

Query  301  AATAGGAGTGAAAGATGGGATGCCTATTGCTACAACCCACACGCAAAGGAGTGTGGTGGC  360
            ||||||||||||||||||||||||||||||||||||||||||||||||||||||||||||
Sbjct  352  AATAGGAGTGAAAGATGGGATGCCTATTGCTACAACCCACACGCAAAGGAGTGTGGTGGC  411

Query  361  GTCTTTACAGATCCAAAGCAAATTTTTAAATCTCCAGGCTTCCCAAATGAGTACGAAGAT  420
            ||||||||||||||||||||||||||||||||||||||||||||||||||||||||||||
Sbjct  412  GTCTTTACAGATCCAAAGCAAATTTTTAAATCTCCAGGCTTCCCAAATGAGTACGAAGAT  471

Query  421  AACCAAATCTGCTACTGGCACATTAGACTCAAGTATGGTCAGCGTATTCACCTGAGTTTT  480
            ||||||||||||||||||||||||||||||||||||||||||||||||||||||||||||
Sbjct  472  AACCAAATCTGCTACTGGCACATTAGACTCAAGTATGGTCAGCGTATTCACCTGAGTTTT  531

Query  481  TTAGATTTTGACCTTGAAGATGACCCAGGTTGCTTGGCTGATTATGTTGAAATATATGAC  540
            ||||||||||||||||||||||||||||||||||||||||||||||||||||||||||||
Sbjct  532  TTAGATTTTGACCTTGAAGATGACCCAGGTTGCTTGGCTGATTATGTTGAAATATATGAC  591

Query  541  AGTTACGATGATGTCCATGGCTTTGTGGGAAGATACTGTGGAGATGAGCTTCCAGATGAC  600
            ||||||||||||||||||||||||||||||||||||||||||||||||||||||||||||
Sbjct  592  AGTTACGATGATGTCCATGGCTTTGTGGGAAGATACTGTGGAGATGAGCTTCCAGATGAC  651

Query  601  ATCATCAGTACAGGAAATGTCATGACCTTGAAGTTTCTAAGTGATGCTTCAGTGACAGCT  660
            ||||||||||||||||||||||||||||||||||||||||||||||||||||||||||||
Sbjct  652  ATCATCAGTACAGGAAATGTCATGACCTTGAAGTTTCTAAGTGATGCTTCAGTGACAGCT  711

Query  661  GGAGGTTTCCAAATCAAATATGTTGCAATGGATCCTGTATCCAAATCCAGTCAAGGAAAA  720
            ||||||||||||||||||||||||||||||||||||||||||||||||||||||||||||
Sbjct  712  GGAGGTTTCCAAATCAAATATGTTGCAATGGATCCTGTATCCAAATCCAGTCAAGGAAAA  771

Query  721  AATACAAGTACTACTTCTACTGGAAATAAAAACTTTTTAGCTGGAAGATTTAGCCACTTA  780
            ||||||||||||||||||||||||||||||||||||||||||||||||||||||||||||
Sbjct  772  AATACAAGTACTACTTCTACTGGAAATAAAAACTTTTTAGCTGGAAGATTTAGCCACTTA  831

Query  781  TA  782
            ||
Sbjct  832  TA  833
```

Figure 2. 4 BLAST® pairwise alignment of full-length rhTSG-6 sequencing results against existing full-length TSG-6 sequence on the NCBI database.

Base-call against the true human TSG-6 nucleotide sequence (NCBI accession number: AJ419936.1), where 'Query' denotes sequencing results and 'Sbjct' denotes true sequence retrieved from the database.

Using the bioinformatics program ‘EMBOSS Transeq’ (version 6.6.0), the nucleic acid sequence obtained from the sequencing result was translated to its protein sequence using all six forward (+) and reverse (-) open reading frames (ORFs). ORF +1 was the only reading frame that produced a continuous product without interrupted stop codons, whereas ORF +2, +3, -1, -2, and -3 were interrupted with multiple stop codons, as designated with a red asterisks (**Fig. 2.5**). This suggests that ORF+1 is the reading frame used to translate the TSG-6 protein product. In order to verify this, the amino acid sequence obtained using ORF+1 was aligned with the amino acid sequence of TSG-6 (excluding its 1-17 amino acid signal peptide) obtained from UniProt knowledge base (UniProtKB; P98066) using Clustal Omega (**Fig. 2.6**). With the exception of the last amino acid, which was previously denoted as unidentified (designated ‘**X**’), the sequence matched exactly that of the known TSG-6 sequence, indicating that the translated product would be TSG-6.

>ORF+1
WGFKDGIFHNSIWLERAAGVYHREARSGKYKLTYAEAKAVCEFEGGHLATYKQLEAARKI
GFHVCAAGWMAKGRVGYPIVKPGPNCGFGKTGIIDYGIRLNRSERWDAYCYNPHAKECGG
VFTDPKQIFKSPGFPNEYEDNQICYWHIRLKYGQRIHLSFLDFDLEDDPGCLADYVEIYD
SYDDVHGFVGRYCGDELPDDIISTGNVMTLKFLSDASVTAGGFQIKYVAMDPVSKSSQGK
NTSTTSTGNKNFLAGRFSHL**X**

>ORF+2
GDSRMEFFITPYGLNEQPVCTTEKHGLANTSSPTQKLRRCVNLKAAISQLTSS*RQPEKL
DFMSVLLDGWLRAELDTPL*SQGPTVDLEKLALLIMESVSIGVKDGMPIATTHTQRSVVA
SLQIQSKFLNLQASQMSTKITKSATGTLDSSMVSVFT*VF*ILTLKMTQVAWLIMLKYMT
VTMMSMALWEDTVEMSFQMTSSVQEMS*P*SF*VMLQ*QLEVSKSNMLQWILYPNPVKEK
IQVLLLLEIKTF*LEDLATYX

>ORF+3
GIQGWNFS*LHMA*TSSRCVPQRSTVWQIQAHLRRS*GGV*I*RRPSRNLQAARGSQKNW
ISCLCCWMDG*GQSWIPHCEARAQLWIWKNWHY*LWNPSQ*E*KMGCLLLQPTRKGVWWR
LYRSKANF*ISRLPK*VRR*PNLLLAH*TQVWSAYSPEFFRF*P*R*PRLLG*LC*NI*Q
LR*CPWLCGKILWR*ASR*HHQYRKCHDLEVSK*CFSDSWRFPNQICCNGSCIQIQSRKK
YKYYFYWK*KLFSWKI*PLI

>ORF-1
*VAKSSS*KVFISSRSSTCIFSLTGFGYRIHCNIFDLETSSCH*SIT*KLQGHDISCTDD
VIWKLISTVSSHKAMDIIVTVIYFNIISQATWVIFKVKI*KTQVNTLTILESNVPVADLV
IFVLIWEAWRFKNLLWICKDATTLLCVWVVAIGIPSFTPIETDSIINNASFSKSTVGPWL
HNGVSNSALSHPSSSTDMKSNFSGCL*LLVSCEMAAFKFTHRLSFCVGELVFARPCFSVV
HTGCSFKPYGVMKNSILESP

>ORF-2
ISG*IFQLKSFYFQ*K*YLYFFLDWIWIQDPLQHI*FGNLQLSLKHHLETSRS*HFLY**
CHLEAHLHSIFPQSHGHHRNCHIFQHNQPSNLGHLQGQNLKNSGEYADHT*V*CASSRFG
YLRTHLGSLEI*KFALDL*RRHHTPLRVGCSNRHPIFHSY*DGFHNQ*CQFFQIHSWALA
SQWGIQLCP*PSIQQHRHEIQFFWLPLAACKLRDGRLQIHTPP*LLRR*ACICQTVLLCG
THRLLVQAIWSYEKFHP*IPX

>ORF-3
YKWLNLPAKKFLFPVEVVLVFFP*LDLDTGSIATYLIWKPPAVTEASLRNFKVMTFPVLM
MSSGSSSPQYLPTKPWTSS*LSYIST*SAKQPGSSSRSKSKKLR*IR*PYLSLMCQ*QIW
LSSYSFGKPGDLKICFGSVKTPPHSFACGL*Q*ASHLSLLLRRIP*SIMPVFPNPQLGPG
FTMGYPTLPLAIHPAAQT*NPIFLAASSCL*VARWPPSNSHTALASA*VSLYLPDRASLW
YTPAARSSHMEL*KIPSLNPX

Figure 2. 5 EMBOSS Transeq translation of full-length TSG-6 nucleic acid into the corresponding peptide sequence in all six reading frames.
Translation of the nucleic acid sequence obtained from the DNA sequencing run at all six possible ORFs, using EMBOSS Transeq.



Figure 2. 6 TSG-6 protein sequence alignment using Clustal Omega program
Pairwise Sequence alignment of translated nucleotides from the DNA sequencing result (Query) against the known TSG-6 protein sequence (Sp|P98066|18-277) using Clustal Omega

2.3.2 Optimisation of Baculovirus-Mediated Expression of Full-length rhTSG-6 Protein

To determine the optimal Sf9 cell density for efficient rhTSG-6 expression, cells were seeded at varying densities (1, 2, 4, 6, and 8x10^6/mL) in 3 mL of insect cell culture media and infected with a fixed ratio of passage 3 (P3) baculovirus volume to cell density (15 µL of P3 baculovirus stock per 1x10^6 Sf9 cells/mL). Following 48 h of incubation in a shaker (224 rpm, 25°C) cells were harvested and Western blot was carried out on the cell-free supernatants to assess the relative rhTSG-6 expression levels (**Fig. 2.7A**). A visual assessment of relative band intensities found the strongest to correspond to the '2x10^6cells/mL' condition. This showed that 2x10^6 Sf9 cells/mL was the optimal cell density to maximise rhTSG-6 protein expression using the respective P3 baculovirus batch.

To determine the ratio of P3 baculovirus stock required to saturate 3 mL of 2x10^6/mL of Sf9 cells and the optimal incubation period required to obtain efficient rhTSG-6 expression, different volumes of P3 stock was titrated against 3 mL of cells at a fixed density of 2x10^6 cells/mL and incubated (224 rpm at 25°C) for 48 h and 72 h. Following incubation, the cells were harvested and the levels of secreted rhTSG-6 protein was visualised by Western blot (**Fig. 2.7B**). A visual evaluation of protein bands showed the signal intensity to level off at the '18 µL of P3 virus' condition at the 48 h time point (**Fig. 2.7B (i)**). In addition no protein was detected in the culture supernatants (determined by Western blot) at the 72 h time-point, when the matching baculovirus dose range was titrated against the cells (**Fig. 2.7 B (ii)**). This showed that 18 µL of the respective P3 baculovirus stock was sufficient to saturate 6x10^6 Sf9 cell infectivity, inducing maximal rhTSG-6 expression 48 h post-infection.

To investigate whether infecting Sf9 cells with a higher titer of P3 baculovirus increases the expression of rhTSG-6, a higher dose of P3 stock was titrated against 3 mL of Sf9 cells seeded at $2x10^6$ for 48 h (224 rpm, 25°C). The relative signal intensity was uniform across the different conditions as visualised by Western blot (**Fig. 2.7C**), confirming that 18 µL of the respective P3 baculovirus stock was sufficient to saturate $6x10^6$ Sf9 cells.

These small-scale (3 mL total volume per condition) optimisation experiments allowed extrapolation to predict the optimal conditions (Sf9 cell density, P3 baculovirus batch volume, and duration of incubation) to use for the efficient expression of rhTSG-6 protein on a larger scale. Accordingly, the results show that for a larger volume (500 mL per flask); 5 mL of the respective P3 baculovirus batch contains enough baculovirus particles to saturate $1000x10^6$ Sf9 host cells, 48 h post-infection. 72 h post-infection, the concentration of the rhTSG-6 protein drops below the lower detection limit of the Western blot.

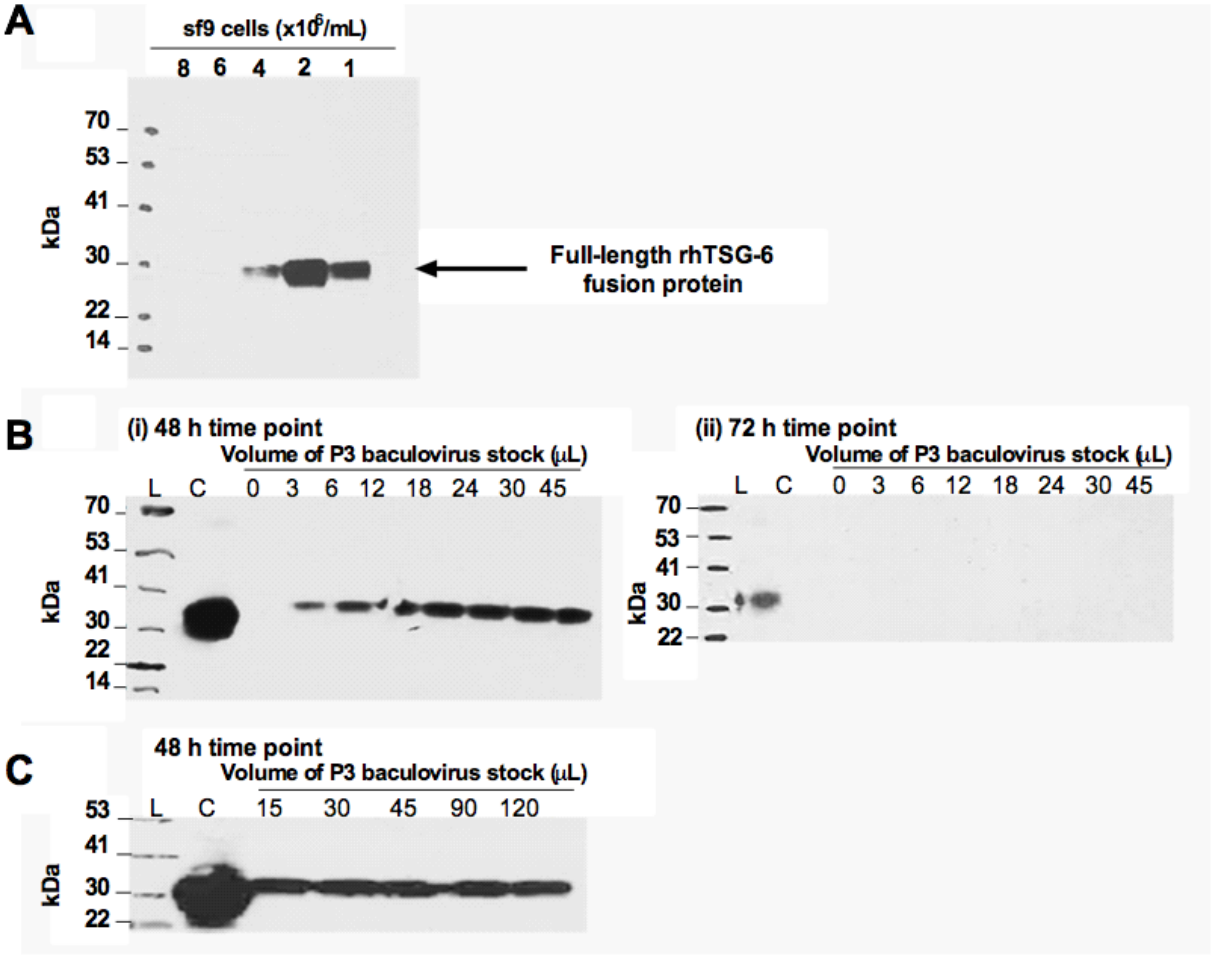


Figure 2. 7 Western blot showing optimisation of baculovirus-mediated expression of rhTSG-6 protein.

To visualise the level of rhTSG-6 expression at each optimisation step, 20 µL of cell-free supernatants per condition were electrophoretically resolved (150V, 85 min) on a 4-12% Bis-Tris protein gradient gel and electrotransfered onto a nitrocellulose membrane (100V, 60 min). The membranes were immunoblotted with 1 µg/mL of mouse anti-human TSG-6 primary antibody, clone mAb2104 (R&D Systems), followed by 1:1000 goat anti-mouse IgG HRP-conjugated secondary antibody (ThermoFisher Scientific). Blots were developed by ECL as per manufacturer's instructions. A fixed ratio of P3 volume to cell number was titrated against 3 mL Sf9 cells at decreasing densities (**A**). Varying volumes of P3 baculovirus stock was titrated against a fixed Sf9 cell density of $2x10^6$ cells/mL in 3 mL total media (**B**) for 48 h (**i**) and 72 h (**ii**). A relatively higher volume of P3 baculovirus stock was titrated against a fixed density Sf9 cells at $2x10^6$/mL in 3 mL total media, and incubated for 48 h (**C**).

2.3.3 Affinity Purification of Full-Length rhTSG-6 Fusion Protein

Both gravity-flow affinity purification and chromatography affinity purification was employed to determine the technique that resulted in optimal protein yield and purity.

2.3.3.1 Gravity-flow technique

Once the conditions of the baculovirus expression system were optimised, the system was scaled up to 500 mL volumes per culture flask to increase protein yield required for *in vivo* studies.

To separate the rhTSG-6-fusion protein from other components secreted within the culture media, cell-free supernatant was passed through 5 mL of pre-primed nickel-charged resin with specific affinity to the His-tag motif expressed on the N-terminal region of the rhTSG-6-fusion protein. Dissociation of the His-tag expressing rhTSG-6 fusion protein from the column ligand was achieved through competitive displacement by imidazole in the elution buffer.

To assess the MW of the protein constituents within the eluates and determine fraction purity, every other eluted fractions were resolved electrophoretically (**Fig. 2.8 A**). The MW of the species was ~31kDa as determined in comparison to the protein standard ladder, indicated 'L'. In order to identify the ~31 kDa protein species, Western blot was carried out on the fractions (**Fig. 2.8 B**). A positive reactivity to the mouse anti-human TSG-6 monoclonal antibody (R&D systems) confirmed the 31 kDa species to be hTSG-6. The protein bands seen at ~70 kDa are likely to be TSG-6-bikunin (the light chain of the IαI). Similarly, the bands visualised at ~130 kDa may be HC of IαI complexed to TSG-6 complexes, as their bands react positively to the TSG-6 antibody. IαI is likely to be sourced by the serum or the Sf9 cells. A steady decrease in band intensity was visualised over greater eluted volumes as a result of the protein being liberated in from the

column. Importantly, much of the rhTSG-6-fusion protein was lost from the column during the wash steps and detected in the flow through (F.T.).

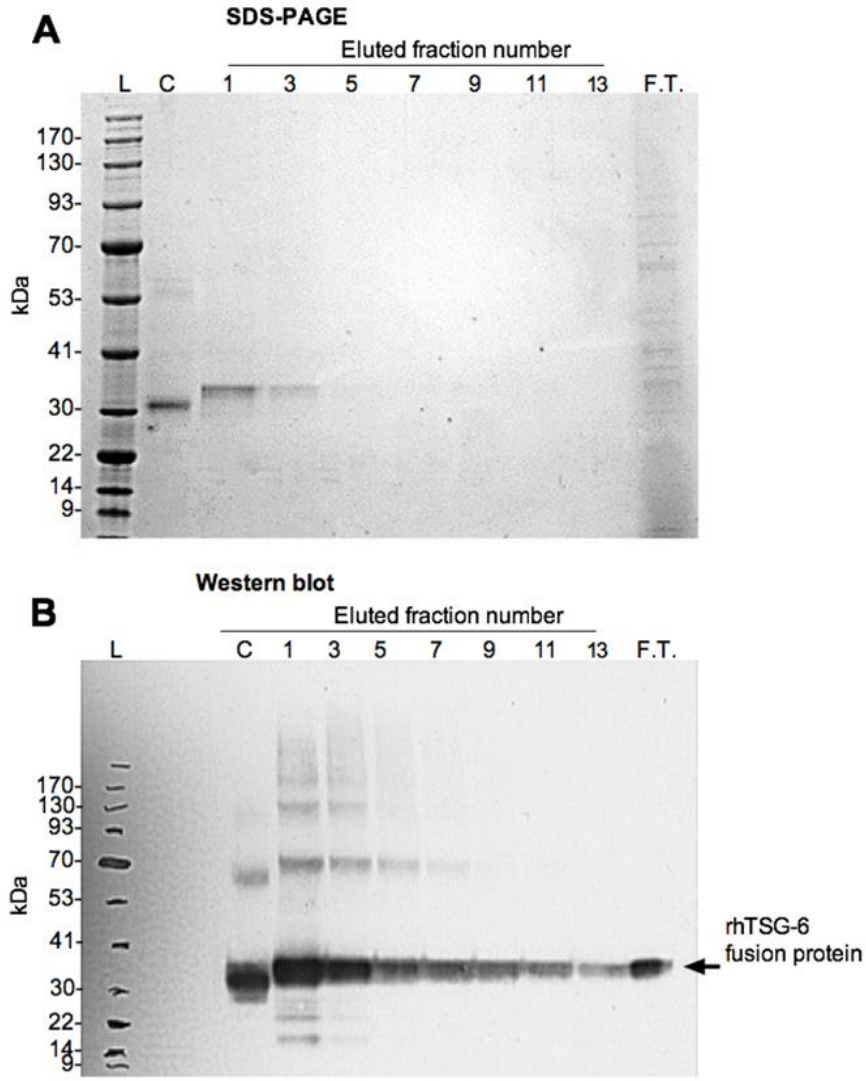


Figure 2. 8 Representative SDS-PAGE gel and its corresponding Western blot showing fractions containing the rhTSG-6 protein following gravity-flow affinity separation.

500 mL of 2x10^6/mL Sf9 cells in suspension culture were infected with 5 mL of P3 virus and incubated for 48 h (224 rpm, 24°C). Cell-free supernatant was passed through 5 mL of pre-equilibrated resin slurry. The rhTSG-6 fusion protein carrying the N-terminal $(His)_6$-affinity-tag were retained by the $Ni2^+$-NTA agarose beads. The bound proteins were released by passing elution buffer (20 mM HEPES, 400 mM imidazole, 0.5 M NaCl, 5% glycerol) down the column. The protein content of every other fraction were resolved electrophoretically (150V, 85 min) on a 4-12% Bis-Tris protein reducing gradient gel and visualised by Coomassie Brilliant Blue dye (**A**). The relative MW (kDa) of the bands were determined by comparison to the protein ladder, indicated 'L'. Five (5) µg of previously produced in-house full-length rhTSG-6 was added as the positive control, indicated 'C'. For Western blot, proteins were transferred onto a nitrocellulose membrane and then immunoblotted with 1 µg/mL of mouse anti-human TSG-6 primary antibody; mAb2104 (R&D Systems), followed by 1:1000 diluted goat anti-mouse IgG HRP-conjugated secondary antibody (ThermoFisher Scientific). Blots were developed by ECL as per manufacturer's instructions (**B**). 'F.T' denotes 'flow through'.

2.3.3.2 Affinity chromotography technique

To reduce protein loss, a different affinity purification method was employed following Sf9 cell harvest. Using an automated mode, 500 mL of cell-free supernatant was loaded onto the ÄKTA^{TM}purifier system and then passed through a 1 mL His-Trap^{TM} column, containing charged nickel ions. Elution of the His-tag rhTSG-6 protein from the column was achieved by competitive elution, using an increased linear gradient (40 mM/mL) of imidazole (0-400 mM). Proteins that did not carry the His-tag domain were washed off the column at the lower concentrations of imidazole (104 mM - 156 mM), in comparison to His-tag expressing rhTSG-6 fusion proteins that bound the column at a higher affinity. This allowed for the separation of contaminating protein from rhTSG-6 as indicated by the two distinctive peaks in the chromatogram trace (**Fig. 2.9 A)**

To confirm fraction purity and the presence of rhTSG-6 (indicated by a 31 kDa protein) at the chromatogram peaks, eluted fractions were resolved on an SDS-PAGE and visualised by Coomassie Brilliant Blue dye (**Fig. 2.9 B (i)**). The presence of a ~31 kDa protein band, in comparison to the protein standard, indicated the presence of rhTSG-6 protein within fraction eluates.

Western blot analysis of a preparation carried out following affinity chromatography purification (**Fig. 2.9 B (ii)**) showed a positive reactivity to the human TSG-6 antibody, confirming the identity of the 31 kDa species as hTSG-6**.** A faint band was visualised in the condition sampled from the supernatant 'S' prior to affinity chromatography, as the total rhTSG-6 protein had not yet been concentrated. More importantly, no band was detected in the flow-through; showing a lack of protein loss during the wash step using the affinity chromatography purification technique

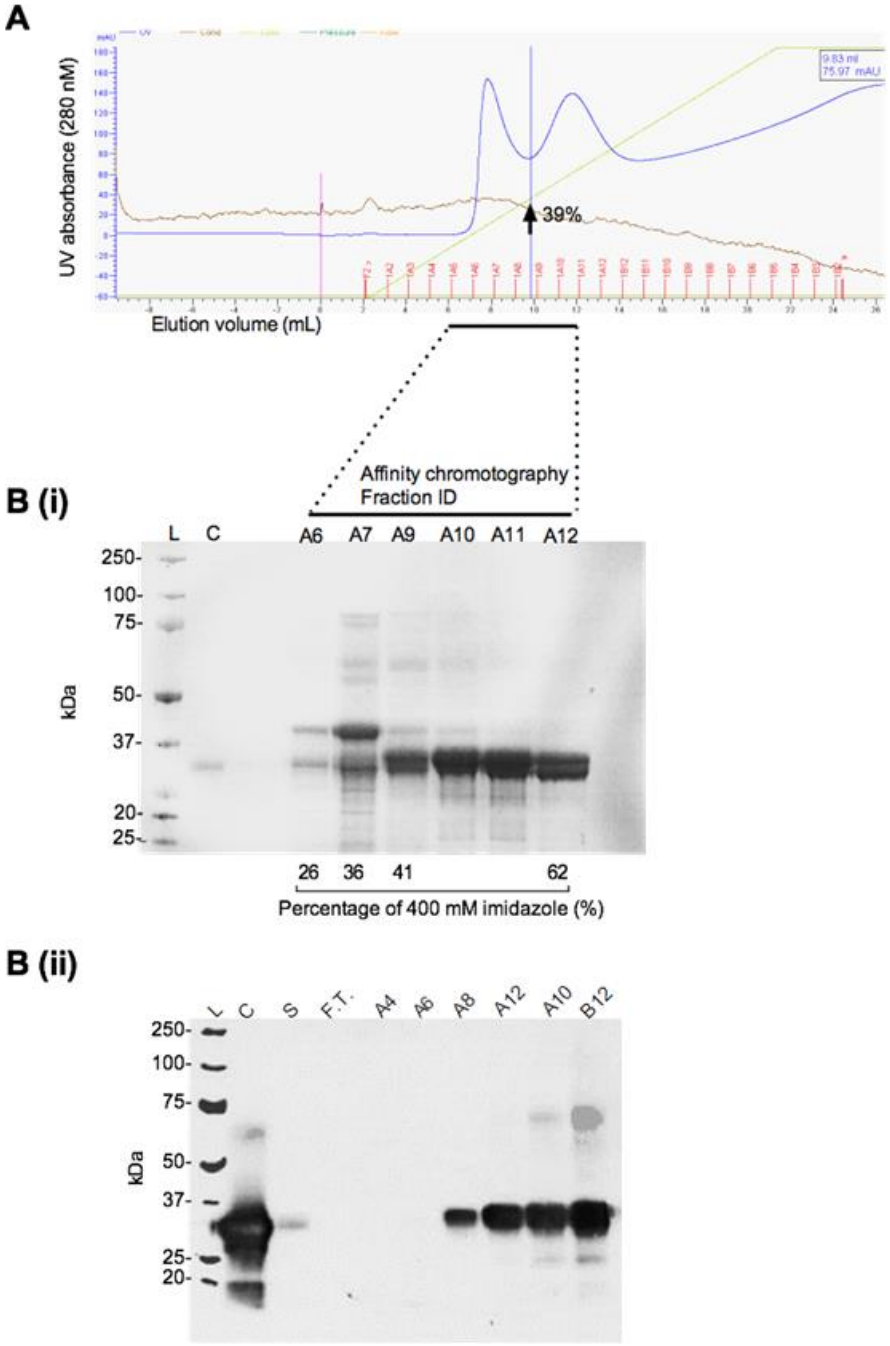


Figure 2. 9 Chromatography trace showing affinity purification of full-length rhTSG-6 protein and its corresponding fractions as visualised by SDS-PAGE and Western blot.

Protein profile obtained (at UV absorbance of 280) when cell-free supernatant, collected 48 h post P3 baculovirus infection of Sf9 cells, was passed through a 1 mL His-Trap^{TM} column and eluted using increased gradient (0-400 mM) of imidazole (**A**). 20 µL elutes corresponding to fractions below the peaks were resolved *electrophoretically* on a 4-12% Bis-Tris protein gradient gel and stained with Coomassie Brilliant Blue dye (**B**). For Western blot of affinity chromatography purified fractions, proteins were transferred onto a nitrocellulose membrane and then immunoblotted using 1 µg/mL mouse anti-human TSG-6 primary antibody; mAb2104 (R&D Systems), followed by treatment with 1:1000 goat anti-mouse IgG HRP-conjugated secondary antibody (1:1000). Blots were developed by ECL as per manufacturer's instructions (**B**). 'L' denotes ladder, 'C' denotes control, 'S' denotes supernatant, F.T. denotes flow through.

2.3.4 Cleavage of Full-Length rhTSG-6 Fusion Protein

To prevent immunogenicity in response to the FLAG-tag peptide sequence of the rhTSG-6-fusion protein during *in vivo* studies, the fusion protein was cleaved using the nuclear inclusion TEV protease. To do so, fractions containing the rhTSG-6 fusion protein were pooled and treated overnight with 50 µL of 6 mg/mL TEV protease at 4°C. Western blot was carried out on 20 µL of pre and post cleavage samples. TEV digestion liberated a ~29 kDa protein product, reactive to the human TSG-6 antibody, relative to the ~31 kDa product also reactive to the antibody (**Fig. 2.10**). This showed that the FLAG-tag had been removed from the protein.

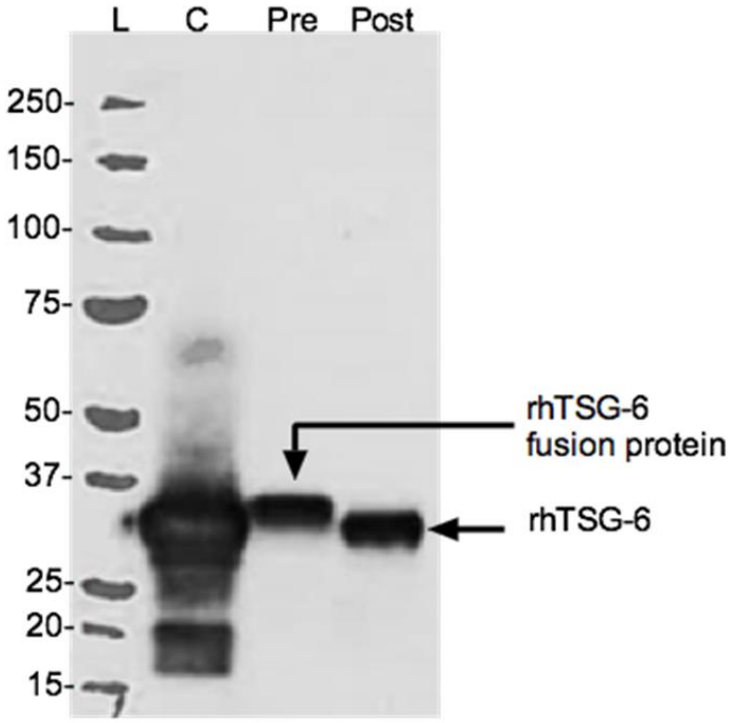
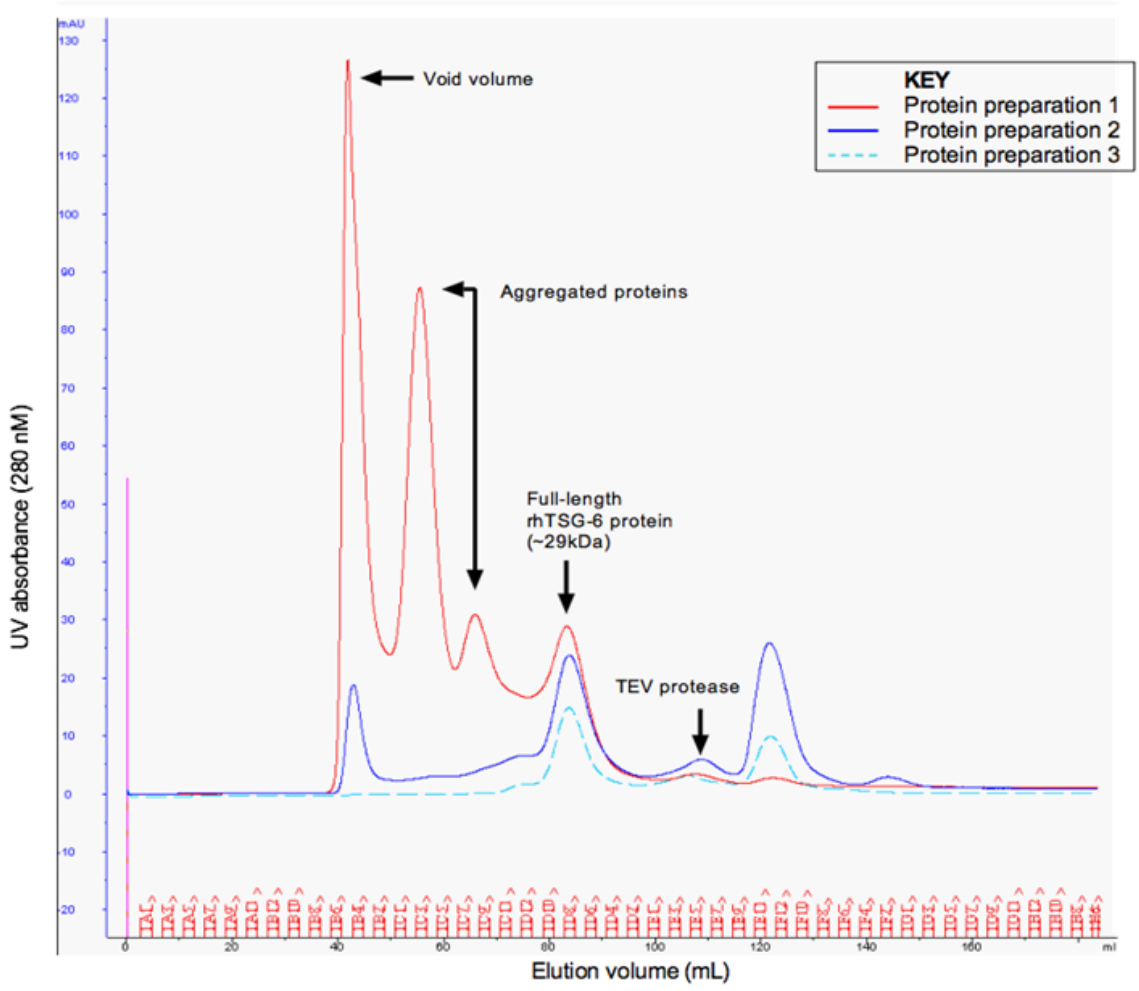


Figure 2. 10 Western blot showing TEV-mediated removal of the N-terminal FLAG-tag peptide sequence of the rhTSG-6 fusion protein.
Fractions were pooled and incubated with 50 µL of 6 mg/mL TEV protease at 4°C. Following overnight incubation, 20 µL sample of the TEV-treated and non-treated sample were electrophoretically resolved on a 4-12% Bis-Tris protein reducing gradient gel, and then transferred onto a nitrocellulose membrane. Membranes were immunoblotted with 1 µg/mL mouse anti-human TSG-6 primary antibody; mAb2104 (R&D Systems), followed by a goat anti-mouse IgG HRP-conjugated secondary antibody (1:1000). Blots were developed by ECL as per manufacturer's instructions. 'L' denotes protein ladder, 'C' denotes positive control, 'Pre' denotes pre-TEV digestion, 'Post' denotes post-TEV digestion.

2.3.5 Size Elusion Chromatography Purification of Full-Length rhTSG-6 Protein

To further purify the rhTSG-6 protein preparation, size exclusion chromatography was used to separate the remaining species based on their relative MW. The total volume of the FLAG-cleaved rhTSG-6 protein fractions was reduced to ~1-1.5 mL using a 10 kDa MW cut-off Viva spin column (Sartorius UK Ltd., Surrey, UK) and manually loaded onto the ÄKTA^{TM} purifier system. Samples were run onto a S200 16/60 HiLoad Super-dex gel filtration column at a rate of 1 mL/min. The protein elutes were monitored in re-al-time using UV detection at an absorbance of 280 nM. In different preparations, rhTSG-6 protein eluted at the same retention volume; running as a dimer (**Fig. 2.11 A**) through possible CUB-CUB domain interactions via disulphide bonds (Beveridge et al., 2012, Gaboriaud et al., 2011, Venkatraman Girija et al., 2013). This property proved useful during purification and was exploited to achieve size exclusion separation from the 30 kDa TEV protease monomers (Carrington and Dougherty, 1988) Fractions were analysed on a SDS-PAGE **(Fig. 2.11 B (i)**), and confirmed to be hTSG-6 by reactivity to the human TSG-6 antibody **(Fig. 2.11 B (ii)**.

A


mAU
130
120
110
100
90
80
70
60
50
40
30
20
10
0
-10
-20
UV absorbance (280 nM)
Void volume
Aggregated proteins
Full-length
rhTSG-6 protein
(~29kDa)
TEV protease
KEY
Protein preparation 1
Protein preparation 2
Protein preparation 3
0
20
40
60
80
100
120
140
160
ml
Elution volume (mL)

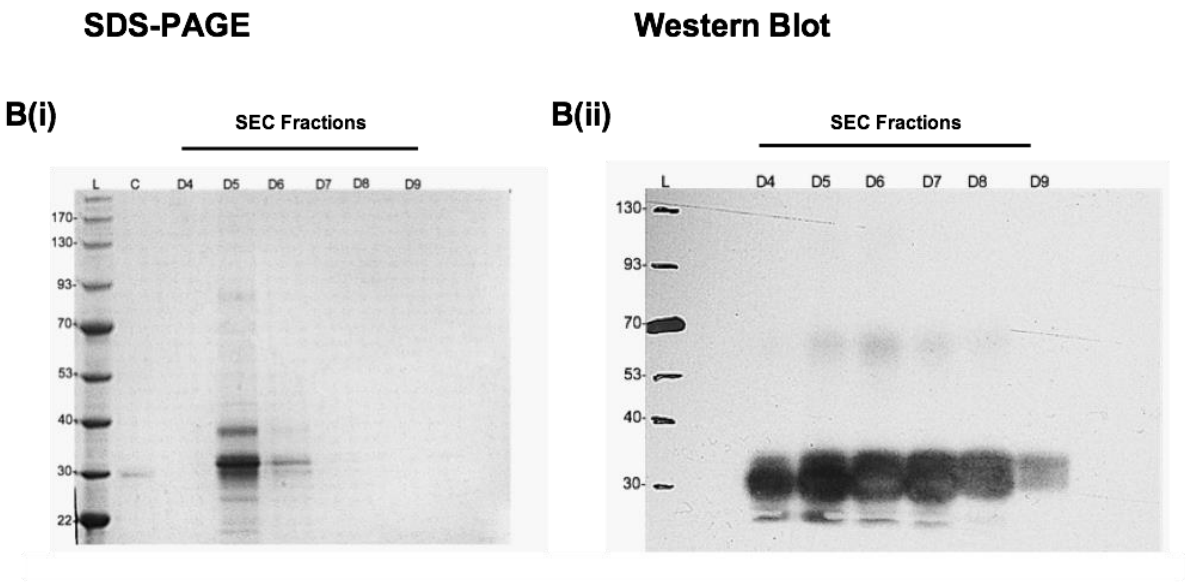


Figure 2. 11 Size exclusion chromatography trace showing purification of rhTSG-6 protein and its corresponding fractions on SDS-PAGE and Western blot.

The volume of the protein preparation was reduced to 1-1.5 mL using a spin column (10 kDa MW cut off). Size exclusion chromatography was performed using S200 16/60 HiLoad superdex gel filtration column pre-equilibrated with 120 mL of de-gassed gel filtration buffer (0.5 M NaCl, 20 mM HEPES, 5% glycerol). The elution profiles were monitored in real time using UV absorbance at 280 nM. (**A**) The trace shows the overlay of the size exclusion chromatography trace of three independent rhTSG-6 protein preparations, with the arrow indicating the elution position of the rhTSG-6 protein molecules (~30 kDa). Following size exclusion chromatography, the protein content of every other fraction were resolved electrophoretically on a 4-12% Bis-Tris protein reducing gradient gel and visualised using Coomassie Brilliant Blue dye. (**B (i)**) The relative MW (kDa) of the protein bands were determined by comparison to the protein ladder (designated 'L'), while 'C' designates 3 µg of rhTSG-6 protein as positive control. (**B (ii)**) For Western blot, protein were transferred onto nitrocellulose membranes and then immunoblotted using a mouse anti-human TSG-6 primary antibody (1 µg/mL), followed by a goat anti-mouse IgG HRP-conjugated secondary antibody (1:1000). Blots were developed by ECL as per manufacturer's instructions.

2.3.6 Quantification and Quality Control of Full-Length rhTSG-6 Protein Preparation

Fractions containing the purified full-length rhTSG-6 protein (as determined by gel and Western blot) were pooled and volume of each preparation was reduced using a spin column (10 kDa MW cut off). BCA assay (described in Section **2.2.1.8** of Materials and Methods) was used to determine the total protein content of the purified preparation. Using LAL colourimetric assay, samples were then tested at different concentrations (100 ng/mL and 500 ng/mL), for the presence of contaminating LPS, and preparations exhibited LPS levels below 10 pg/mL – suitable for cell culture use.

Table 2. 1 TSG-6 protein quantification values as determined by BCA assay, with levels of LPS contamination, as determined by LAL assay

'< D.L' denotes below detection level of LAL assay; meaning that the levels of LPS are below 10 pg/mL. 'Amt.' denotes amount and 'Conc.' Denotes concentration. Values are rounded to two decimal places.

	PROTEIN PREPARATION				VEHICLE CONTROL			
Prep. ID	**Full-length rhTSG-6**		**LPS**		**Gel filtration buffer**		**LPS**	
	Amt. (mg)	**Conc. (mg/mL)**	**Amt.**	**Conc.**	**Amt.**	**Conc.**	**Amt.**	**Conc.**
1	0.50	1.10	< D.L	<0.1 EU/mL	N/A	N/A	< D.L	<0.1 EU/mL
2	1.20	1.20	< D.L	<0.1 EU/mL	N/A	N/A	< D.L	<0.1 EU/mL
3	2.60	2.60	< D.L	<0.1 EU/mL	N/A	N/A	< D.L	<0.1 EU/mL
4	1.00	0.71	< D.L	<0.1 EU/mL	N/A	N/A	< D.L	<0.1 EU/mL

2.3.7 Full-length TSG-6 Inhibits Osteoclast Activity *In Vitro*[8]

TSG-6 is reported to inhibit osteoclast activity (Mahoney et al., 2008), therefore osteoclasts were assayed for their activity in the presence of TSG-6 as an indicator of the biological activity of the protein. To do so, different doses of full-length rhTSG-6 protein were exogenously added human monocytes derived from PBMCs, in the presence of pro-osteoclastogenic factors (RANKL and M-CSF). The addition of increasing doses of full-length rhTSG-6 found to inhibit of activity (**Fig. 2.12**) in a dose dependent manner, as determined Pit formation. This demonstrated that the full-length rhTSG-6 produced was biologically active.

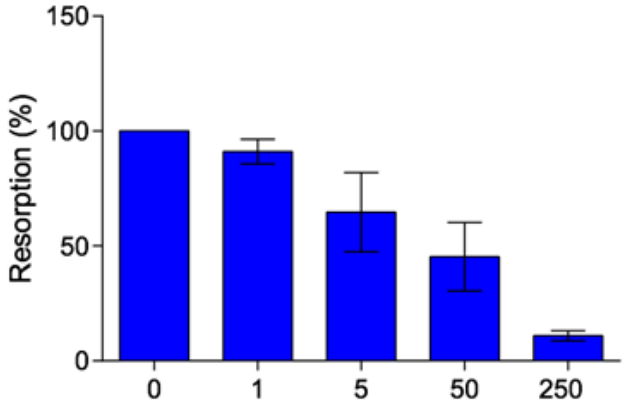


Figure 2. 12 Full-length rhTSG-6 inhibits RANKL induced osteoclast activity.
$5x10^6$ PBMCs per well were seeded onto 96-well tissue culture plates with dentine slices. The adherent cells were then cultured in 24-well tissue culture plates in 1 mL/well α-MEM (supplemented with 10 % FCS, 10 mm L-glutamine and antibiotics (10 IU/mL penicillin and 10 µg/mL streptomycin). Osteoclastogenesis was induced by the addition of 50 ng/mL of RANKL and 25 ng/mL of M-CSF (25 ng/mL). Full-length rhTSG-6 was added to wells at varying doses and cultured for 14 days, with media entirely replenished every 2-3 days. On day 21, dentine slices were removed from wells, washed in PBS. To remove the adhered cells, dentine were placed in 1 M NH_4OH, and then sonicated for 5-10 min. The slices were then washed in distilled water, stained with 0.5% (w/v) aqueous toluidine blue, pH 5.0, and examined by light microscopy. Data is expressed as mean ± SEM of percentage resorption compared to the 'RANKL and M-CSF only' condition. Each condition was carried out in quadruplicates.

[8] Experiments carried out by Dr. David Mahoney (Botnar Research Centre, University of Oxford). Image courtesy of Dr. David Mahoney.

2.4 DISCUSSION

The role of TSG-6 on osteoblast biology remains poorly characterised. Historically, the overexpression of full-length TSG-6 in cellular systems has been a challenge due to intrinsic properties of the protein. This experimental Chapter demonstrated the expression and purification of full-length rhTSG-6 from baculovirus-Sf9 insect cell expression system, using a two-step liquid chromatography approach, to achieve microgram amounts of highly purified protein per liter of culture media. The protein was confirmed to be biologically active and contained negligible amounts of LPS (Malyala and Singh, 2008), and was thus suitable for downstream *in vitro* and *in vivo* studies.

The mature, full-length TSG-6 protein consists of two functional units, namely the Link and CUB domains (Milner and Day, 2003). These are structurally contiguous in their arrangement (Milner and Day, 2003) and interact with a multitude of different ligands (Milner and Day, 2003, Milner et al., 2006), giving TSG-6 its multifunctional properties. TSG-6 is the only known protein to contain both the Link and CUB domains (protein sequence analysis & classification search). These are evolutionary conserved domains associated with structural components of connective tissues. Although the CUB domain has not been characterised to the same degree as the Link domain, it is known to be involved in many processes including tissue repair, cell signalling, angiogenesis and developmental patterning (Perry et al., 2007).

Previously, the Link and CUB domains have been expressed independently and therefore their functions tested separately (Mahoney et al., 2005, Kuznetsova et al., 2008, Getting et al., 2002, Dyer et al., 2014). However, as they are contiguously arranged in nature it may indicate a linked functionality of the domains. For example, amino acid residues spanning the Link and CUB domains interact with well-characterised osteoin-

ductive factors, such as BMP-2 (Mahoney et al., 2008), suggesting that both domains may be important for osteoblastogenesis. Similarly, the binding of the Link domain to a ligand, such as HA may have profound effect on the functional properties of the CUB domain, or vice-versa. Equally, the CUB domain also interacts with ECM components for example fibronectin (Kuznetsova et al., 2008). This is particularly significant in osteogenesis**,** as fibronectin is deposited by osteoblasts, and expressed around the newly formed nodules (Nefussi et al., 1997, Moursi et al., 1996, Evans et al., 2010). The interaction of fibronectin with integrin is a prerequisite for early osteogenesis (Moursi et al., 1996), where blocking integrinB1 (α5β1) disrupts osteogenesis and nodule formation (Moursi et al., 1997, Moursi et al., 1996, Hamidouche et al., 2009). This highlights the importance of studying the role of the protein on osteoblast biology in its full-length form.

Previous attempt to purifying full-length rhTSG-6 include work by Wisniewski *et al*. (1994) (Wisniewski et al., 1994), who used the insect cell expression system BTI-TN-5B1-4, derived from *Trichoplusia ni*, to successfully express TSG-6, reporting a yield of 1 µg/mL (Wisniewski et al., 1994). The amounts obtained in this Chapter, when using affinity chromatography - as opposed to the gravity-flow method, were comparable to that reported by Wisniewski *et al.* (Wisniewski et al., 1994). However, increasing cell culture volumes did not linearly correlate to an increased protein yield. This may be due to the fact that TSG-6 binds a diverse range of extracellular proteins making specific interactions of TSG-6 to other secreted material highly likely causing protein aggregation and precipitation.

Although Sf9 is a popular choice for protein expression, alternative insect cell lines are available for use in baculovirus-expression of recombinant protein, these include the Sf21 (Vaughn et al., 1977), and the relatively newer characterised BTI-Tnao 38 cell line

– also a derivative of *Trichoplusia ni* (Hashimoto et al., 2010). The baculovirus system has been compared in Sf9 insect cells and silkworms (Usami et al., 2011). Although the later has higher expression yields (Nagaya et al., 2008, Nagaya et al., 2004, Muneta et al., 2004), the polyhedrosis virus used to transfect Sf9 can be used in serum-free media, making a protein like TSG-6 less prone to aggregation and easier to purify (Altmann et al., 1999). Additionally, Sf9 cells are reported to express better yields of soluble proteins in comparison to silkworms (Usami et al., 2011).

Recently, Prockop and colleagues used the mammalian Chinese hamster ovary (CHO) cells to express scalable amounts of full-length rhTSG-6 (Kim et al., 2016). Using immunocytochemistry they found TSG-6 to aggregate to CHO host cells by binding HA present on the cell brush borders (Kim et al., 2016). The authors overcame these issues by inhibiting the synthesis of HA using 4-methylumbelliferone and out-competing this interaction using heparin (Kim et al., 2016), to obtain a significantly enhanced yield of 4.1 mg – 5.6 mg per liter of culture medium. The adhesion of TSG-6 to the brush borders of Sf9 cells is also highly likely, making it a viable reason for the low yields in relation to the volume of expression preparations.

The difference in MW between full-length TSG-6 purified in this work from insect cells (~29 kDa) and that expressed in humans (~35 kDa) has also been reported by Wisniewski *et al.* (Wisniewski et al., 1994). This may be due to differences in levels of glycosylation. More specifically, the amino acid sequence contains an asparagine residue which is a potential N-glycosylation site (predicted using NetNGlyc 1.0 server). The insect glycosyaltion machinery is different to that of mammals, where the former consists of high mannose type, non-fucosylated and core-fucosylated tri-mannose of N-glycans (Altmann et al., 1999). Modification in glycosyaltion often result in decreased protein efficacy (Wilde et al., 2014), and more recently unglycosyalted TSG-6 was found

to correspond to higher clearance rates when endogenously administerd *in vivo* (Kim et al., 2016)

Commercially, the biological activity of full-length rhTSG-6 protein has been determined by its ability to bind HA, using enzyme-linked immunosorbent assay (ELISA). Although their ability to bind HA may be an indicator of correct structural fold, it does not give any information on its biological activity. Apart from the cost of using commercially available TSG-6 for large scale in vivo experiments, its function has in the past highly varied in osteoclast activity assays (Personal communications with Dr. David Mahoney). A contributing factor of this may be the fact that these proteins are lyophilised, whereas our in-house protein was keep stored at -80 in liquid formulations. Although lyophilisation ensures protein stability over extended periods (Abdelwahed et al., 2006), as well as easier methods of distribution, the steps involved in the process impose stress on the protein which may hinder protein stability (Kasper et al., 2013) and therefore quality.

The *in vitro* biological test showed that the full-length rhTSG-6 make in-house inhibits bone resorption, consistent to that reported by Mahoney *et al.* Mahoney et al. (2008). However, a variety of activity tests both *in vivo* and *in vitro* were required to validate its anabolic activity, which will be addressed in the next two experimental Chapters.

3

CHAPTER 3: THE ROLE OF TSG-6 ON BONE MARROW-DERIVED MESENCHYMAL STEM CELLS' OSTEOGENESIS *IN VITRO*

3.1 INTRODUCTION

Accelerated bone loss, characteristic of osteoporosis, predisposes patients to skeletal fracture and breakage (Leslie et al., 2012, Kanis et al., 2013). Anabolic therapies increase bone mass by promoting osteoblast differentiation and/or function, allowing the replacement of lost bone (Pazianas, 2015). However, existing therapeutic options are few and those available have associated limitations creating an unmet clinical need for novel anabolic interventions (Axelrad and Einhorn, 2009, Baron and Hesse, 2012, Garrison et al., 2010, Papapoulos, 2015).

Like the liver and brain, the bone harbours an organ-specific subpopulation of macrophages (Hume et al., 1984) termed the “Osteomacs” (Chang et al., 2008). These are found at the periosteum and endosteum, in both murine and humans, and are distinct to tissue-resident bone resorbing osteoclasts (Chang et al., 2008, Pettit et al., 2008). They initiate tissue repair and bone formation (Chang et al., 2008, Pettit et al., 2008) where their systemic and local depletion delays fracture healing (Alexander et al., 2011). In addition, they modulate osteoblasts function in bone tissue (Chang et al., 2008), and maintain HSCs and their precursor populations within the bone marrow niche (Winkler et al., 2010).

It has been shown that macrophages produce soluble proteins that stimulate osteoblast differentiation of MSCs through direct and indirect activation of a number of receptors. For example, in *in vitro* human co-culture assays contact between peripheral $CD14^{+}$ monocytes and BM-hMSCs increases osteoblast the formation of functionally active osteoblasts (Nicolaidou et al., 2012). The coupling factor between monocytes/macrophage and MSC was partially attributable to the production of OSM, by monocyte/macrophages through a positive feedback loop of STAT-3 activation following OSM and leukaemia inhibitory factor (LIF) receptor signalling in the MSCs (Fernandes

et al., 2013, Guihard et al., 2012, Nicolaidou et al., 2012). These seminal studies demonstrated that, under certain conditions, monocyte/macrophages have bone anabolic activities - a property that can be exploited to identify novel bone anabolic factors.

One of the top fifty most up-regulated transcripts within the human monocyte population, when co-cultured with BM-hMSCs in a 10:1 ratio in osteogenic media, was determined to be TSG-6. Within the first 2-8 h of direct contact between monocytes and MSCs, TSG-6 mRNA was up-regulated 23-fold in the monocytes (PhD thesis of Dr. Vicky Nicolaidou 2011) - a time frame at which osteoinductive genes are up-regulated within this system (Nicolaidou et al., 2012). TSG-6 protein (also known as TNF-alpha inducing protein 6; TNFAIP-6) is expressed by many immune cells including macrophages, dendritic cells and neutrophils (Maina et al., 2009), as well as within the bone marrow of healthy mice (Mahoney et al., 2008).

There is some evidence of the importance of TSG-6 in bone and cartilage development (Bardos et al., 2001). For example, the presence of TSG-6 has been shown to be associated with delayed bone erosion in murine models of inflammation (Mindrescu et al., 2002, Mindrescu et al., 2000). On the other hand, TSG-6 binds potent pro-osteogenic BMPs, such as BMP-2 through its CUB and Link domains indicating roles of osteoblast population (Mahoney et al., 2008). Although TSG-6 has been demonstrated to initiate repair and regeneration of various tissues (Kim et al., 2016, Lee et al., 2009, Oh et al., 2010, Prockop, 2013), to date no evidence of anabolic properties within bone has been reported.

The aim of this *in vitro* experimental Chapter is to ascertain the role of monocyte-derived TSG-6, as well as exogenous full-length rhTSG-6 on osteoblast formation using primary BM-hMSCs as precursor cells. Thus, experiments were designed to answer the following two research questions:

1. Does endogenous monocyte-derived TSG-6 promote early osteoblast differentiation of primary BM-hMSCs
2. Does exogenous addition of full-length rhTSG-6 promote early osteoblast differentiation of primary BM-hMSCs?

3.2 MATERIALS AND METHODS

All cell cultures were incubated at 37°C in 5% CO_2 humidified atmosphere and all reagents used were tissue culture grade, unless otherwise stated. All cell culture procedures were carried out under aseptic conditions in a laminar flow cabinet, class II microbiological safety (ESCO Technologies Inc., Yorkshire, UK).

3.2.1 Chromogenic LAL Assay: Quantification of LPS Endotoxin Contaminant in Reagents

To exclude the potential bacterial contamination within the reagents, endpoint chromogenic LAL assay (Lonza, Slough, UK), was employed to determine the presence of endotoxin molecules in reagents, as per manufacturer's instructions. Briefly, the samples were made up at the concentration used in cell culture assays as well as a 10-fold greater concentration, while the endotoxin reference standards were prepared to the concentrations of 0.1, 0.25, 0.5 and 1 endotoxin unit per mL (EU/mL) using reference endotoxin provided in the LAL kit; *E. coli* 0111:B4. 50 µL of standard, blank (LAL reagent water, provided in the kit) and samples were added in a sterile 96-well microplate in duplicates. 50 µL of LAL was then added to each well and incubated at 37°C for 10 minutes. 100 µL of substrate solution was added to the microplate and incubated for 6 minutes before 100 µL of 25% v/v glacial acetic acid was added to stop the reaction. Absorbance was read at 405 nm using FLUOstar® Omega microplate reader (BMG LABTECH, Buckinghamshire, UK). Absorbance readings from blank controls were subtracted from the test samples and the concentration of LPS was determined relative to the standard curve. Data were expressed as EU/mL, where 1 EU is equivalent to 100 picogram of endotoxin per microgram of protein.

3.2.2 *In Vitro* Expansion and Maintenance of BM-hMSCs

Commercially purchased primary BM-hMSCs (Lonza, Slough, UK) were suspended in 30-40 mL of Dulbecco's Modified Eagle Medium (DMEM)-GlutaMAX (Life Technologies,

Paisley, UK) supplemented with 10% (v/v) heat inactivated FBS (Life Technologies, Paisley, UK) and 100 units/mL of penicillin with 100 µg/mL streptomycin (Life Technologies, Paisley, UK). Cells were grown and maintained as adherent monolayers in 175 cm^2 culture flasks (Greiner bio-one, Gloucestershire, UK), and fed weekly. Once flasks were ~80% confluent, cells were dissociated with 0.05% Trypsin-EDTA (GE Healthcare Life Sciences, Buckinghamshire, UK) and split in a 1:2 ratio. Cells were maintained and used for experiments only up to eight passages.

3.2.3 Isolation of Human Monocytes from Peripheral Blood Mononuclear Cells

The isolation of monocytes from whole blood was achieved by density gradient centrifugation followed by centrifugal elutriation.

3.2.3.1 Density gradient separation

Twenty five mL of blood obtained from healthy donors (NHS Blood and Transplantation Unit) was diluted at a 1:1 volume ratio in Hank's balanced salt solution (HBSS) (Lonza, Slough, UK) then gently layered over 20 mL of Cederlane® Lympholyte® human cell separation media (VH Bio Ltd., Durham, UK). Following centrifugation using Sorvall™ Legend™ RT Plus centrifuge (ThermoFisher Scientific, Hertfordshire, UK) at a speed of 2500 rpm for 30 min (10ºC, slowest acceleration and deceleration), PBMCs were collected from the buffy coat fraction and washed twice with HBSS (1800 rpm, 10 min, 10ºC; followed by 1500 rpm, 5 min, 10 ºC).

3.2.3.2 Elutriation

To separate monocytes from other peripheral blood cells, cell populations were fractionated based on their size and granularity using Avanti® J-20XP centrifugal elutriation system (Beckman Coulter, Ltd., High Wycombe, UK), as described by Foxwell and colleagues (Conron et al., 2001) . The rotor speed was set to constant speed of 2600 rpm

and cells were loaded at a rate of 15 mL/min using a Masterflex^{TM} peristaltic pump (Cole-Parmer Instrument Co. Ltd., London, UK). To elute off cell fractions, the pump speed was incrementally increased and population composition analysed using Beckton-Dickinson (BD) FACScan flow cytometry (Beckton Dickinson Ltd., Oxford, UK). Fractions consisting of ≥80% monocytes, determined by the forward and side scatter profile as previously described by Salzman *et al.* (Salzman et al., 1975), were pooled counted and their viability determined using trypan blue solution prior to downstream processing.

3.2.4 *In Vitro* Osteogenic Differentiation of BM-hMSCs

Primary BM-hMSCs were validated for their basal osteogenic potential *in vitro*. To do so, bone-marrow derived hMSCs (passages 4-8), were seeded in DMEM supplement with 10% FBS and 1% penicillin/streptomycin, overnight to allow adherence to culture plates. To begin the osteogenic differentiation assay (day 0), cultures were treated with test conditions in the presence and absence of osteogenic media for seven days, constituting of complete DMEM-GlutaMAX supplemented 10% FBS and 1% penicillin/streptomycin, with 10 mM β-glycerolphosphate (Sigma-Aldrich, Dorset, UK), 50 µg/mL ascorbate-2 phosphate (Sigma-Aldrich, Dorset, UK) and 100 nM dexamethasone (Sigma-Aldrich, Dorset, UK).

3.2.4.1 ALP assay: An indicator of early osteoblast formation

ALP enzyme activity was measured as one of the early markers of osteoblast differentiation based on the technique, previously described by King and Armstrong (King and Armstrong, 1934). Briefly, BM-hMSCs were seeded at $1x10^4$/well onto 96-well flat-bottomed culture plates and treated with 200 µL of test condition in the presence/absence of osteogenic media. ALP activity was measured on day 7 using colourmetric-enzymatic LabAssay ALP Kit (Alpha Laboratories Ltd., Hampshire, UK) as per

manufacturer's instructions. Mean absorbance reading per experimental condition was calculated from triplicate wells and used to determine ALP levels by comparison to the standard curve (standard curve range: 0-0.5 mmol/L. As the levels of ALP enzyme activity varied greatly between biological donors of passages 4-8, the data are represented as fold change relative to control conditions, i.e. BM-hMSCs treated with osteogenic media only.

3.2.4.2 Bone nodule assay: determination of functional mature osteoblast formation

To assess the formation of mature functional osteoblasts *in vitro*, the ECM was examined for the presence of nodules containing calcium deposits (Orriss et al., 2014, Bhargava et al., 1988) on day 28. BM-hMSCs were seeded onto 24-well culture plates at a density of $2x10^4$ per 400 µL of test condition media in the presence of osteogenic stimuli and the media was replenished once a week. To detect calcium deposits, cells were fixed with 70% ice-cold ethanol for 1 h at $4^{\circ}C$ and then stained with 400 µL of 40 nM alizarin red (Sigma-Aldrich, Dorset, UK) at pH 4.2, for 20 min at RT, as previously described by Gregory and colleagues (2004) (Gregory et al., 2004). Finally, cells were washed three times (5 min/wash) with deionised water on a shaking platform and calcium deposits were visualised under low magnification using a light microscope.

3.2.5 Human TSG-6 ELISA

To quantify TSG-6 protein expression levels in culture supernatants, in-house[9] sandwich ELISA, with a linear working range of 1-40 ng/mL, was used. NUNC Maxisorp ELISA plates (VWR International, Leicestershire, UK) were coated overnight at RT with 100 µL of 1.25 µg/mL TSG-6 (A38.1.20) mouse anti-human monoclonal capture antibody (Santa Cruz Biotechnology Inc., Heidelberg, Germany) diluted in 20 nM sodium

[9] Botnar Research Centre- Oxford University – ELISA was established by Dr. David Mahoney prior to the start of this DPhil.

carbonate (VWR International, Leicestershire, UK) coating buffer, pH 9.6. The following day, the plates were washed 3 times with wash buffer [PBS with 0.002% (v/v) tween-20 (Sigma-Aldrich, Dorset, UK)] and each well was blocked with 200 µL of 1% (w/v) bovine serum albumin (Sigma-Aldrich, Dorset, UK) for 90 min at 37°C. Wells were then washed in PBS-tween and 100 µL of standard/samples was added per well and incubated for 2 h at RT. Following another wash, 200 µL/well of 1:10,000 extra-avidin-ALP detection enzyme (Sigma-Aldrich, Dorset, UK) was added and the plates were incubated for a further 30 mins. To detect the level of ALP enzyme, which correlated to the amount of bound TSG-6 in the samples. Plates were washed as before, and 200 µL of 5 mg/mL soluble nitrophenyl (*p*NPP) substrate solution (Sigma-Aldrich, Dorset, UK) was added per well. Plates were incubated in the dark for 60 min at RT and the absorbance was read at 405 nm using FLUOstar® Omega microplate reader (BMG LABTECH, Buckinghamshire, UK). Mean absorbance values of samples within the linear range of the standard curve were calculated from triplicate wells and used to determine the TSG-6 concentration in samples by comparison to the standard curve.

3.2.6 Knockdown of tsg-6 Gene in Primary Human Monocytes

3.2.6.1 Experimental set up

To silence TSG-6 expression in human monocytes prior to their co-culture with BM-hMSCs, human monocytes obtained by elutriation (**see Section 3.2.2.2**) were transfected with small interfering (si) RNA targeting human TSG-6 mRNA (Santa Cruz Biotechnology, Inc., Heidelberg, Germany) using the Human Monocyte Nucleofector® kit (Lonza, Slough, UK) as per manufacturer's instructions.

Briefly, cells were washed with Opti-MEM® reduced serum media (Life Technologies, Paisley, UK) and re-suspended in 200 µL of electroporation buffer. 200 nM of siRNA TSG-6 target (Sc-39819A, Santa Cruz, Biotechnology); sense:

CAGGUUGCUUGGCUGAUUAtt, Antisense: UAAUCAGCCAAGCAACCUGtt and scramble control[10] was added to the cell suspensions, and mixtures were then added to 0.2 cm plastic cuvettes (provided in the Lonza kit). Electroporation was performed using nucleofector™II/2b (Lonza, Slough, UK) device on programme Y001. Once electroporated, cell suspension was added to 1.5 mL Opti-MEM® media supplemented with 10% (v/v) FBS and 100 ng/mL rhM-CSF (PeproTech EC Ltd., London, UK) - required for long-term culture and survival of mononuclear cells (Conron et al., 2001). Viable mononuclear monocytes (as determined by trypan blue exclusion test) were co-cultured at $1x10^5$ with $1x10^4$ BM-hMSCs (10:1 ratio) in replicates of 5 per treatment condition. $5x10^6$ monocytes/well were added onto 24-well culture plates to assess *tsg-6* gene knockdown efficiency 72 h post transfection.

3.2.6.2 Total RNA extraction from human monocytes

Qiagen RNeasy mini Kit (Qiagen, Manchester, UK) was used to extract total RNA from human monocytes. Briefly, cells were lysed on culture plates at day 3 using RLT buffer (provided by Qiagen, proprietary blend) supplemented with 0.01% (v/v) 2-mercapthoethanol (VWR International, Leicestershire, UK) to inactivate RNAses present in the lysate. Lysates were homogenised using QIAshredder columns before carrying out downstream purification steps as per manufacturer's instructions. NanoDrop™ 1000 Spectrophotometer (ThermoFisher Scientific, Hertfordshire, UK) at an absorbance of 260 nm was used to quantify total RNA purified. The 260/280 nm absorbance ratio was used to assess purity of the samples and all RNA preparations were stored at −80°C for future real-time polymerase chain reaction (PCR) analysis.

[10] The scramble sequence is proprietary information and was not provided by Santa Cruz Biotechnology.

3.2.6.3 Real time-PCR detection of TSG-6 mRNA expression levels in human monocytes

To quantify relative TSG-6 transcript levels between treatment conditions, one step Real-Time-PCR master-mix (Eurogentec Ltd., Hampshire, UK) was used in combination with TaqMan® gene expression assay (Life Technologies, Paisley, UK)- this allowed for both the reverse transcription and the PCR amplification steps to be performed within the same reaction well. Each reaction volume of 10 µL constituted the components listed in **Table 3.1**. No template control conditions were included in runs to detect background/non-specific fluorescent signal. All conditions were run in duplicates in optical 386-well plates (Life Technologies, Paisley, UK) protected with an optical adhesive cover (Life Technologies, Paisley, UK) to avoid evaporation during the run. Quantitative PCR was performed using an Applied Biosystems ViiA7 instrument (Life Technologies, Paisley, UK), cycle programme: 48°C for 30 min, 95°C for 10 min, 40 cycles (95°C for 15s, 60°C for 1 min).

Table 3. 1 Constituents of the RT-PCR reaction mix

Reagent	Constituents	Final concentration per reaction well	Volume added per 10 µL reaction mix
2X Reaction buffer	Deoxynucleotides	1X	5 µL
	HotGoldStar DNA polymerase		
	$MgCl_2$		
EuroScript RT	Reverse transcriptase (Moloney murine leukaemia virus)	0.25 U/mL	0.05 µL
	RNase inhibitor	0.1 U/mL	
20X TaqMan® probe	Unlabelled primer pair	900 nM	0.5 µL
	FAM labelled probe	250 nM	
Sample	RNA template	50 ng/µL	2 µL
RNase-free water	-	-	2.45 µL

3.2.6.4 Real time-PCR calculations and data analysis

To compare TSG-6 transcript levels between different treatment conditions, the average cycle threshold (Ct) values per condition was determined, and delta △Ct value obtained by calculating the difference between *tsg-6* target gene and *gapdh* housekeeping gene. Delta-delta Ct values were then obtained by determining the difference between △Ct of the treated subtracted from the △Ct of the untreated 'control' condition. Finally the data was represented as fold change ($2^{-\triangle\triangle Ct}$) in TSG-6 mRNA relative to the 'no treatment' control.

3.2.7 Statistical analysis

All experiments were carried out on three independent biological donors, and data is represented as mean ± the standard error of the mean (SEM) and each treatment was run in replicates of 2-3 where mean values were calculated. The statistical analysis chosen was dependent on the experimental design, and is stated in figure legends. All statistical tests were carried out using GraphPad Prism 6 (Version 6.03).

3.3 RESULTS

3.3.1 *In Vitro* Osteogenic Differentiation of BM-hMSCs

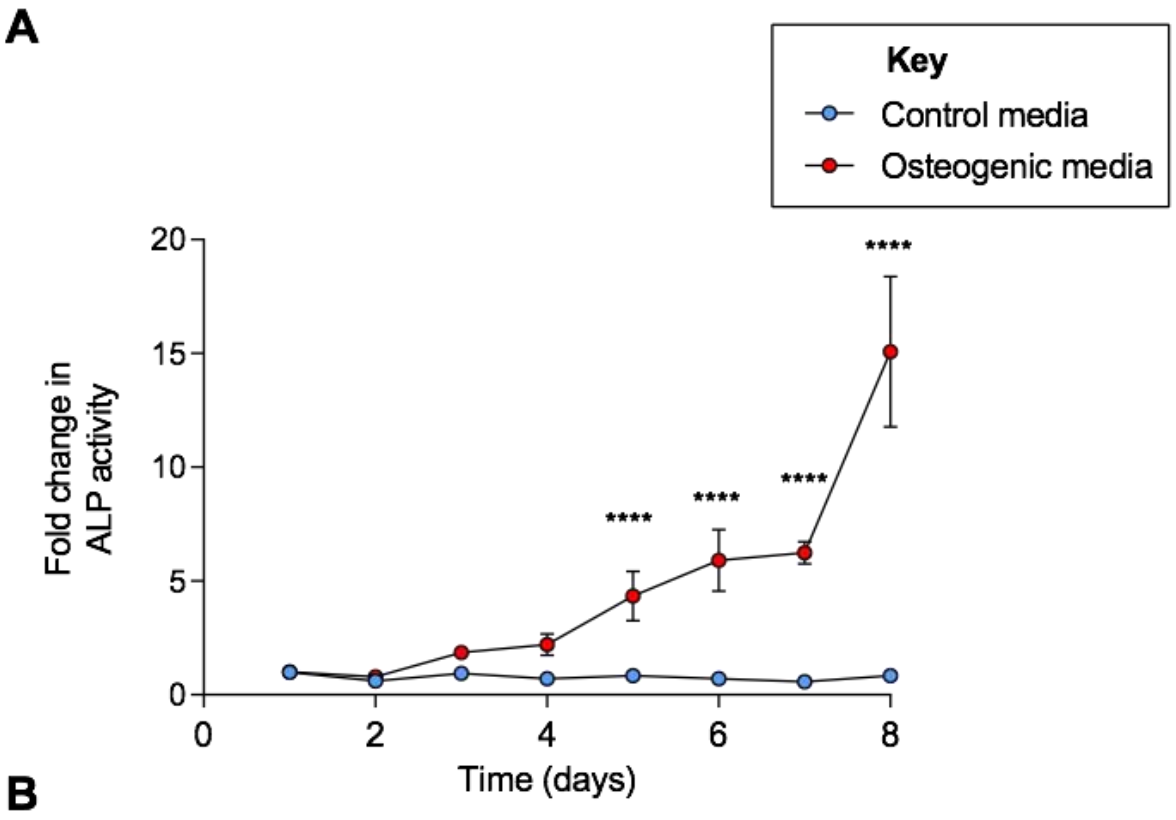
To confirm the osteogenic potential of primary BM-hMSCs *in vitro* and the optimal incubation period, three independent 8-day time-course assays were set up by culturing incubating BM-hMSCs in control media and osteogenic media, based on pre-established conditions[11]. At each designated time point, ALP enzyme activity was quantified as an indicator of early osteoblast formation. A significant level of ALP activity was noted in the osteogenic media treated group at days 5-8 in comparison to the control media treated group at each corresponding time point **(Fig 3.1A)**. This indicated that the optimal time point to measure significant levels of early baseline osteoblast differentiation in response to osteogenic stimuli was between days 5-8.

To confirm the formation of functional osteoblasts using pre-established osteogenic conditions, BM-hMSC cultures treated with control media and osteogenic media were assessed for bone nodule formation. As matrix mineralisation is the final stage of osteoblast differentiation (Aronow et al., 1990, Bellows et al., 1986), calcium deposition was visualised following alizarin red S staining in cultures treated with osteogenic media. By day 28, substantial calcium deposition was visualised in the osteogenic media-treated group compared to the control media group **(Fig. 3.1B**) indicating the formation of functional osteoblasts, that had in turn mineralised the ECM.

Nicolaidou *et al.* (2012) demonstrated that BM-hMSC-monocyte contact promotes a significant enhancement of primary BM-hMSC differentiation into functional osteoblasts in the presence of osteogenic media (Nicolaidou et al., 2012). To confirm this observation, BM-hMSC-monocyte co-culture assays, previously established and described in

[11] PhD thesis of Dr. Vicky Nicolaidou (2011)- Imperial College London, UK

the PhD thesis of Dr. Vicky Nicolaidou (2011) where; $1x10^4$ BM-hMSCs were co-cultured with $1x10^5$ human monocytes in the presence/absence of controls/osteogenic media (1:10 ratio), were set up. The finding of this thesis verified of that published by Nicolaidou *et al.* (Nicolaidou et al., 2012) - ALP protein activity was found to be significantly higher in the osteogenic media treated co-cultures, relative to osteogenic media treated BM-hMSC cultures alone **(Fig. 3.1C**).



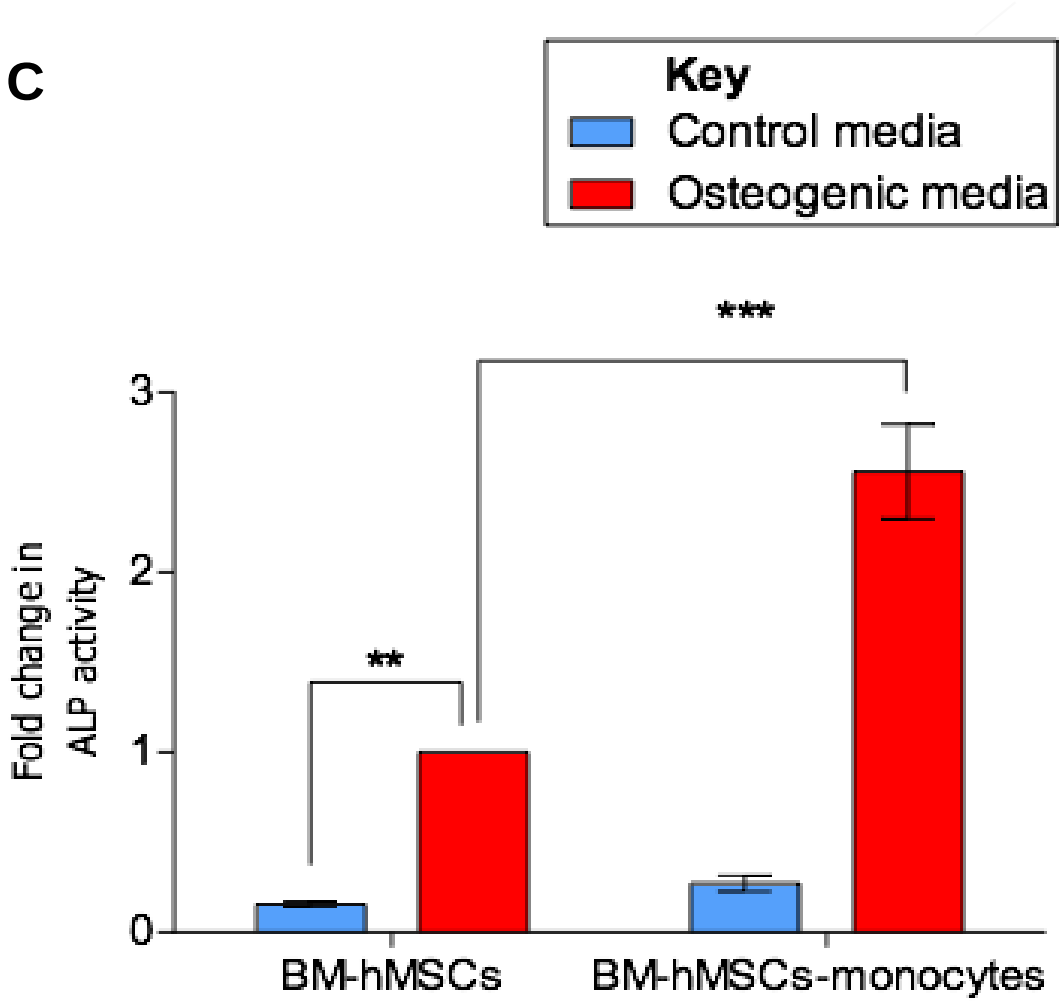


Figure 3. 1 Monocytes significantly enhances ALP activity of primary BM-hMSCs
(**A**) BM-hMSCs were seeded at a density of $1x10^4$ cells per well onto flat-bottomed 96-well plates with control or osteogenic media. Cells were lysed at each time point and ALP activity was measured. (**B**) BM-hMSCs, seeded at a density of $2x10^4$ cells per well onto 24 well plates, were treated with 400 µL of control/osteogenic media. Bone nodules were identified by staining with 40 nM alizarin red, and visualised under a light microscope (arrows). (**C**) BM-hMSCs-monocyte co-cultures, seeded at a density of $1x10^4$ to $1x10^5$ (1:10 ratio) per well onto 96-well flat-bottomed tissue culture plates, were treated with control or osteogenic media and incubated for 7 days before ALP activity was measured using a colorimetric-enzymatic ALP kit (Alpha Laboratories), as per manufacturer's instructions. Graphs (**A**) and (**C**) show fold change in ALP activity, relative to BM-hMSCs treated with osteogenic media, ± SEM of three independent experiments, where each condition was carried out in triplicates. BM-hMSCs were used between passages 4-8. Statistical differences were determined by Two-way ANOVA, followed by Tukey's post-*hoc* test where, **P*≤0.05 and *****P*≤0.0001.

3.3.2 TSG-6 Protein is Significantly Upregulated in Human Monocytes Following Contact with BM-hMSCs *In Vitro*

3.3.2.1 Microarray data

Nicolaidou *et al.* showed that BM-hMSC-monocyte contact led to the expression of cyclooxygenase (COX)-2 in both cell populations and the subsequent release of PGE_2 which in turn induced the gene expression of OSM. One of the top-fifty transcripts up-regulated in the monocyte population post-contact with BM-hMSCs (**Table 3.2**), OSM was subsequently found to promote the osteogenic differentiation of BM-hMSCs *via* STAT3 signalling (Nicolaidou et al., 2012). However blocking OSM activity in the co-culture assay using neutralising monoclonal antibody inhibited ALP activity only by a maximal of 50% relative to the isotype control (Nicolaidou et al., 2012). This suggested the presence of other unidentified osteoinductive factors within this system.

Table 3. 2 Top fifty most up-regulated gene transcripts within the human monocyte population 2 and 8 h post contact with BM-hMSCs

*This table has been extracted from the PhD thesis of Dr. Vicky Nicolaidou (2011) (Chapter 5, page 250). Illumina microarray data showing fold change in mRNA transcripts of the top 50 most up-regulated genes in human monocytes eluted from co-culture with primary BM-hMSCs following 2 or 8 h contact. Fold change was determined relative to monocytes that had not been in contact with BM-hMSCs. Note: Some genes are listed twice as their DNA sequences were targets of more than one probe on the chip. TNFAIP6/TSG-6 (highlighted in yellow), showing its position in relation to OSM (highlighted in green).

Symbol	Name	Fold change 2h	Fold change 8h
IL-6	Interleukin 6 (interferon, beta 2)	52.47	96.41
CCL20	Chemokine (C-C motif) ligand 20	47.99	36.31
PTGS2	Prostaglandin-endoperoxide synthase 2 (COX2)	47.14	39.04
IL-1A	Interleukin 1 alpha	47.00	42.72
F3	Coagulation factor III (thromboplastin tissue factor)	39.70	30.10
CXCL2	Chemokine (C-X-C motif) ligand 2	37.31	25.23
G0S2	G0/G1 switch 2	36.56	23.55
GJB2	Gap junction protein beta 2 26kDa	35.89	53.45
CCL3L1	Chemokine (C-C motif) ligand 3-like 1	35.64	32.25
LOC730249	PREDICTED: similar to immune-responsive protein 1	33.75	16.05
TNF	Tumour necrosis factor	31.82	30.24
CCL3L1	Chemokine (C-C motif) ligand 3-like 1	31.52	27.42
CCL4L2	Chemokine (C-C motif) ligand 4-like 2	27.32	22.27
CCL3L1	Chemokine (C-C motif) ligand 3-like 1	25.87	23.94
SERPINE2	Serpin peptidase inhibitor, clade E	25.65	26.02
CXCL1	Chemokine (C-C motif) ligand 1	23.49	22.03
TNFAIP6	**Tumour necrosis factor alpha-induced protein 6**	**23.20**	**29.44**
F3	Coagulation factor III (thromboplastin tissue factor)	21.56	16.41
PTGS2	Prostaglandin-endoperoxide synthase 2 (COX2)	21.28	21.05
IL-23A	Interleukin 23 alpha subunit p19	21.12	48.78
TNFAIP6	**Tumour necrosis factor alpha-induced protein 6**	**20.68**	**25.78**
CCL4	Chemokine (C-C motif) ligand 4	20.11	18.29
CCL4L2	Chemokine (C-C motif) ligand 4-like 2	19.99	20.32
CSF2	Colony stimulating factor 2 (granulocyte-macrophage)	19.12	18.34

EREG	Epiregulin	17.87	4.45
IL24	Interleukin 24	17.16	63.76
CCL3	Chemokine (C-C motif) ligand 3	16.86	16.72
PLAUR	Plasminogen activator, urokinase receptor	16.35	9.79
CXCL5	Chemokine (C-X-C motif) ligand 5	15.55	51.54
NLRP3	NLR family pyrin domain containing 3	15.36	3.72
LOC387763	PREDICTED: hypothetical LOC387763	14.98	12.83
IL1RN	Interleukin 1 receptor antagonist	14.77	16.91
EDN1	Endothelin 1	14.21	11.86
LRRC50	Leucine rich repeat containing 50	14.05	18.46
PLAUR	Plasminogen activator, urokinase receptor	13.33	8.81
HEY1	Hairy/enhancer-of-split related with YRPW motif 1	13.10	16.50
CCL4L1	Chemokine (C-C motif) ligand 4-like 1	12.85	12.99
NLRP3	NLR family pyrin domain containing 3	12.71	4.17
SOCS3	Suppressor of cytokine signalling 3	12.68	13.59
CDC2	Cell division cycle 2, G1/s and G2/M	12.22	2.22
PDE4B	Phosphodiesterase 4B, cAMP specific	11.91	9.63
IL1RN	Interleukin 1 receptor antagonist	11.91	13.26
OSM	Oncostatin M	11.89	6.97
LOC644943	Similar to peptidylglycine alpha-amidating monoxygenase COOH-terminal interactor	11.66	10.83
CXCL5	Chemokine (C-X-C motif) ligand 5	11.35	63.91
PDE4B	Phosphodiesterase 4B, cAMP specific	10.79	8.64
ARL5B	ADP-ribosylation factor-like 5B	10.45	8.29
NLRP3	NLR family pyrin domain containing 3	10.41	3.86
CTGF	Connective tissue growth factor	9.92	4.81
IL1B	Interleukin 1 beta	9.42	9.80

3.3.2.2 Real time PCR validation of microarray data and protein expression profile in co-culture supernatant

To validate the microarray data and confirm that TSG-6 mRNA is upregulated within the monocyte population following contact with BM-hMSCs, RT-PCR was used as an alternative gene expression profiling method. RT-PCR was run on RNA from monocytes that had been in contact with BM-hMSCs for 2 h (**Fig. 3.2A**), where a ~13-fold increase in TSG-6 mRNA was noted relative to monocytes plated in the absence of BM-hMSCs. To assess the protein expression profile of TSG-6 in hMSC-monocyte co-cultures compared to monocytes cultured on their own, supernatants were collected from 24 h post-contact – this time point was chosen because a preliminary time-course experiment had shown that TSG-6 was elevated between 16-24 h post-contact (data not shown). In addition, based on work by Nicolaidou *et al* (2012), it was clear that within this system of study, the osteogenic factor was released within the first 24 h of contact. Pre-established in-house sandwich ELISA was used to measure amount of TSG-6 protein secreted - 24 h post-contact 22.62 ± 2.227 ng/mL and 24.02 ± 2.866 ng/mL of TSG-6 protein was detected in the control and osteogenic co-culture conditions, respectively, compared to a concentration of 10.25 ± 1.610 ng/mL and 8.607 ± 3.110 ng/mL from monocytes cultured alone in control and osteogenic media, respectively (**Fig. 3.2B**).

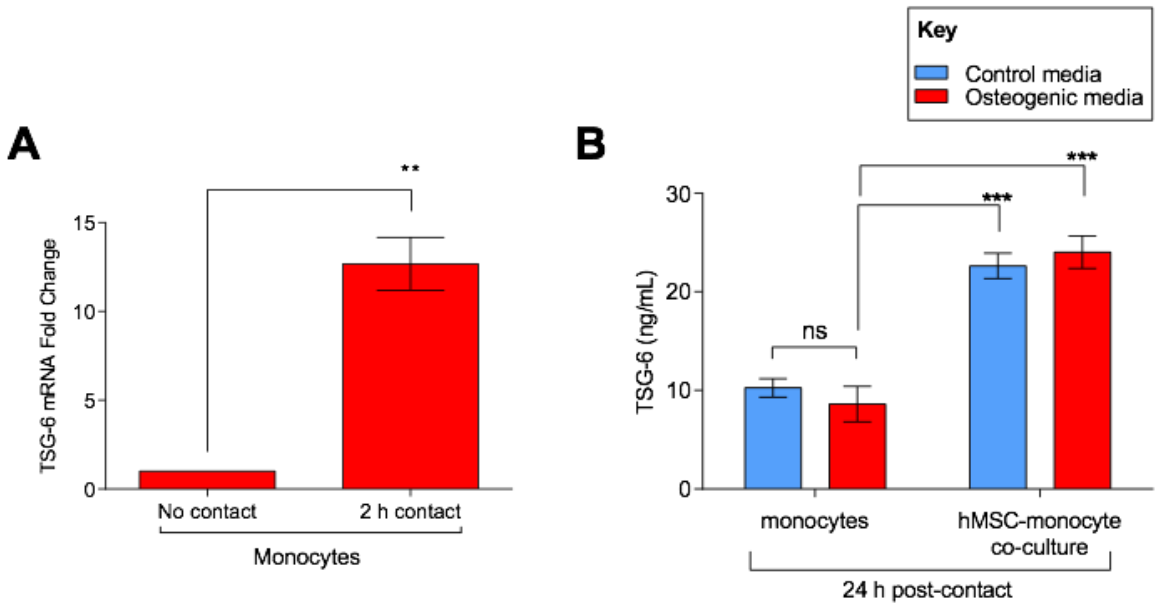


Figure 3. 2 TSG-6 protein expression is significantly upregulated following monocyte contact with BM-hMSCs

(A) $1x10^6$ Monocytes were seeded onto 6-well plates in the presence/absence of pre-adhered $1x10^5$ BM-hMSCs and treated with osteogenic media. 2 h post-culture, the monocytes were washed off using cell culture grade PBS and their RNA was extracted for RT-PCR. **(B)** $1x10^5$ human monocytes were seeded onto 96-well plates in the presence/absence of $1x10^4$ BM-hMSCs in control and osteogenic media. Following 24 h of culture, cell-free supernatant was collected. TSG-6 protein concentration in culture supernatant was measured using a sandwich ELISA. Samples for RT-PCR and ELISA were run in duplicates per each of the three individual biological replicates. Graph **'A'** shows mean ± SEM of three independent experiments, statistical difference was determined by Student's t-Test, where $^{**}P \leq 0.01$. Data in '**B**' are represented as mean ± SEM of three independent experiments, where statistical differences were determined by One-Way ANOVA, where $^{***}P \leq 0.001$ and ns denotes $P > 0.05$.

3.3.3 Addition of the Monoclonal Antibody against TSG-6 (A38.1.20) into BM-hMSC-Monocyte Co-Culture does not Influence ALP activity of primary BM-hMSCs

As shown in Table 3.2 and validated by RT-PCR (**Fig. 3.2A**), TSG-6 mRNA was upregulated, in the human monocyte population, 2 h post contact with BM-hMSCs. In addition, TGS-6 protein was upregulated in the BM-hMSC-monocyte co-culture supernatant in both control media and osteogenic media conditions 24 h post contact, compared to the supernatant of monocytes alone (**Fig. 3.2B**). Commercially-purchased monoclonal rat anti-human TSG-6 antibody (clone A38.1.20; Santa Cruz, sc-65866) was used to investigate whether TSG-6 was an essential factor in driving monocyte mediated osteoblastogenesis of BM-hMSCs.

The antibody was titrated against BM-hMSC-monocyte co-cultures and a dose-dependent decrease in ALP activity was measured in response to increasing doses of the monoclonal antibody, relative to those treated with rat IgG2a isotype control. However, LPS testing of the antibody revealed that the antibody contained 400 pg/mL of LPS. Therefore the same conditions were repeated where the antibody was pre-incubated with polymyxin B (Pm.B) prior to its addition onto co-cultures and the dose-dependent decrease in ALP was ablated (**Fig. 3.3A**).

To further confirm that the decrease in ALP in co-culture assays was due to contaminating LPS derived from the antibody, 0-4000 pg/mL of LPS with/without pre-incubation with Pm.B was titrated against the co-cultures. A dose-dependent decrease in ALP activity was seen in response to increasing doses of LPS, which was ablated on pre-incubation with Pm.B. This therefore showed that the decrease in ALP activity (**Fig. 3.3A**) was due to the effects of contaminating LPS, rather than the monoclonal antibody against TSG-6. In conclusion, the commercially-purchased antibody could not be used

due to LPS contamination; therefore RNA interference method was employed instead to address whether monocyte-derived TSG-6 plays an osteoinductive role in the co-culture system.

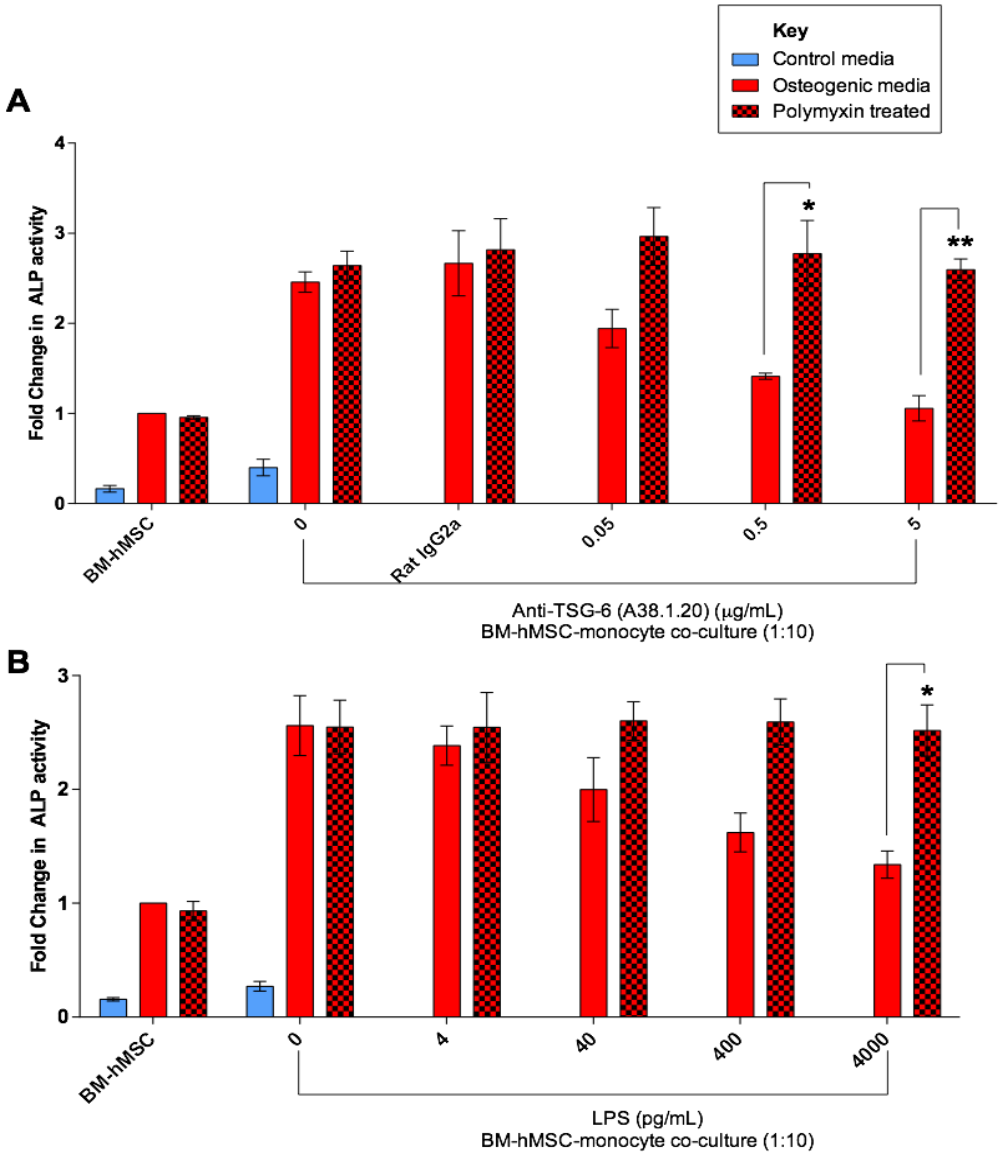


Figure 3. 3 Monoclonal antibody to TSG-6 (A38.1.20) in BM-hMSC-monocyte co-cultures does not inhibit ALP activity of primary BM-hMSCs.

(**A**) Commercially-purchased anti-TSG-6 monoclonal antibody; clone A38.1.20 (Sc-65866) and (**B**) LPS derived from *E.coli* serotype EH100 (Ra) were titrated onto $1x10^4$ BM-hMSCs co-cultured with $1x10^5$ monocytes co-cultures with or without prior incubation with 20 µg/mL of polymyxin B. Mean absorbance reading per experimental condition was calculated from triplicate wells and used to determine ALP levels by comparison to the standard curve. Graphs show the fold change in ALP activity, relative to BM-hMSC in osteogenic media, ± SEM of three independent biological experiments, where each treatment was carried out in triplicates. BM-hMSCs were used between passages 4-8. Statistical differences were determined by Two-Way ANOVA, followed by Tukey's post-*hoc* test where, **P*≤0.05 and ***P*≤0.01.

3.3.4 Silencing *tsg-6* Gene in Human Monocytes Prior to their *In Vitro* Co-Culture with BM-hMSCs does not Affect ALP Activity of Primary BM-hMSCs

A more specific approach of inhibiting the effect of monocyte-derived TSG-6 is by inhibiting its expression. This was achieved using silencing interference (si)-based method targeted at a post-transcriptional stage. This method was employed to address the role of monocyte-derived TSG-6 on early osteogenesis of BM-hMSCs.

To begin with, it was necessary to establish a positive control for the assay to ensure gene knockdown efficiency in response to siRNA. As human monocytes do not transcribe TSG-6 mRNA constitutively (Wisniewski et al., 1993, Lee et al., 1992), it was necessary to induce its transcription by rhTNF-α stimulation. To determine the length of stimulation required to detect TSG-6 mRNA above basal levels, 10 ng/mL of rhTNF-α was titrated against human monocyte cultures and incubated for varying lengths of time (2, 4, 8 and 16 h). An 8-fold increase in TSG-6 mRNA was seen at 2 h post-stimulation time point which was found to have degraded by the 4 h time point (**Fig. 3.4A**). To optimise the dose of TNF-α required to induce a significant level of TSG-6 mRNA by 2 h stimulation with rhTNF-α, the latter was titrated against human monocyte cultures and incubated for 2 h. A 2.5-fold increase of TSG-6 mRNA was found with 10 ng/mL of rhTNF-α (**Fig. 3.4B**), sufficient for the assessment of gene knockdown.

Determining the optimal conditions to induce TSG-6 mRNA transcription within monocytes allowed for the optimisation of the dose of siRNA required for its maximal knockdown. Human monocytes were transfected with 200 nM and 400 nM of TSG-6 siRNA and left for 72 h prior stimulation with 10 ng/mL of rhTNF-α. To distinguish between the effects of the transfection process to that of the siRNA as well as to assess the specificity of the siRNA, monocytes were also transfected with matching doses of siRNA unspecific to TSG-6 gene as a control (si-Scramble). At the 400 nM dose, the levels of TSG-6

gene knockdown were comparable and not significantly different to that of 200 nM (**Fig.3.4C**). Hence the latter dose was used for all subsequent experiments.

Once these conditions were predetermined TSG-6 in human monocytes was knocked-down using 200 nM of siTSG-6 prior to co-culturing them with BM-hMSCs. After 72 h post-silencing, monocytes were added onto BM-hMSCs and ALP was quantified at day 7. No significant difference in ALP activity was found in monocytes that had been treated with TSG-6 siRNA, relative to the group that received the control siRNA **(Fig. 3.5A)**. To ensure TSG-6 gene knockdown in the monocyte population was biologically effective, parallel assays were set up where 72 h post-transfection cells were stimulated with 10 ng/mL of TNF-α and RT-PCR was run to determine knockdown efficiency. A 3 fold-reduction in TSG-6 mRNA was achieved in the TSG-6 siRNA group compared to the scramble control group **(Fig. 3.5B).** Although an incomplete knock-down was achieved, these findings may suggest that knockdown of the TSG-6 mRNA does not affect ALP activity within the co-culture system; thus TSG-6 may not directly responsible for monocyte mediated osteoblastogenesis of BM-hMSCs.

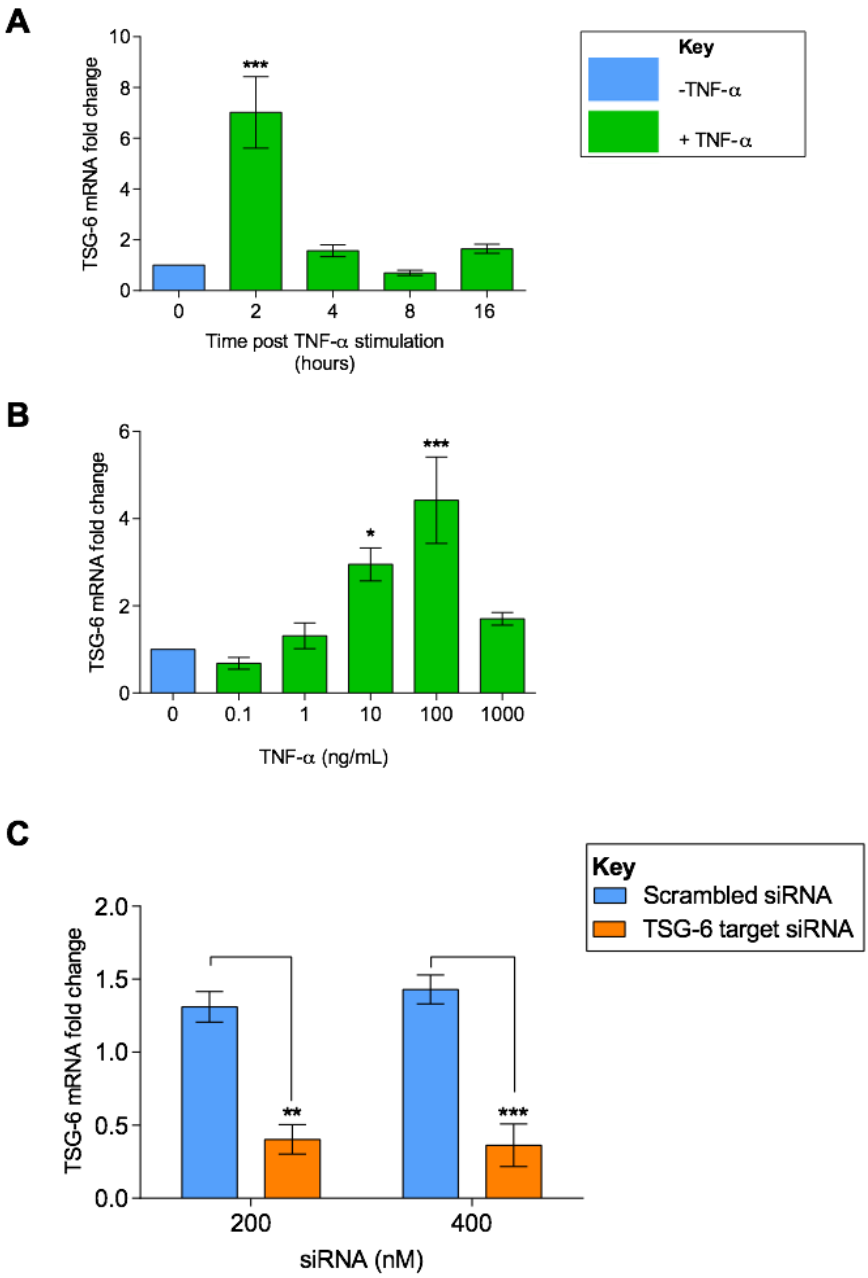


Figure 3. 4 Optimising TSG-6 target siRNA

(**A**) Human monocytes ($2x10^6$) seeded onto 24-well tissue cultures plates were stimulated with 10 ng/mL of TNF-α for 0-16 h, or (**B**) treated with 0-1000 ng/mL of rhTNF-α for 2 h. (**C**) $5x10^6$ Monocytes were electroporated and transfected with control or TSG-6 siRNA was introduced into the cells. 72 h post-transfection monocytes were stimulated with 10 ng/mL of rhTNF-α. Cells were lysed and RT-PCR was run on mRNA using GAPDH as a housekeeping gene. Each condition was run in duplicate. Fold change in mRNA is calculated relative to no TNF-α stimulation (**A**) and (**B**), or relative to electroporated monocytes treated with TNF-α. Graphs '**A**' and '**B**' show mean ± SEM, statistical differences were determined using One-Way ANOVA where *P≤0.05, ***P≤0.001. Graph '**C**' represent mean ± SEM, statistical differences were determined using Two-Way ANOVA where **P≤0.01.

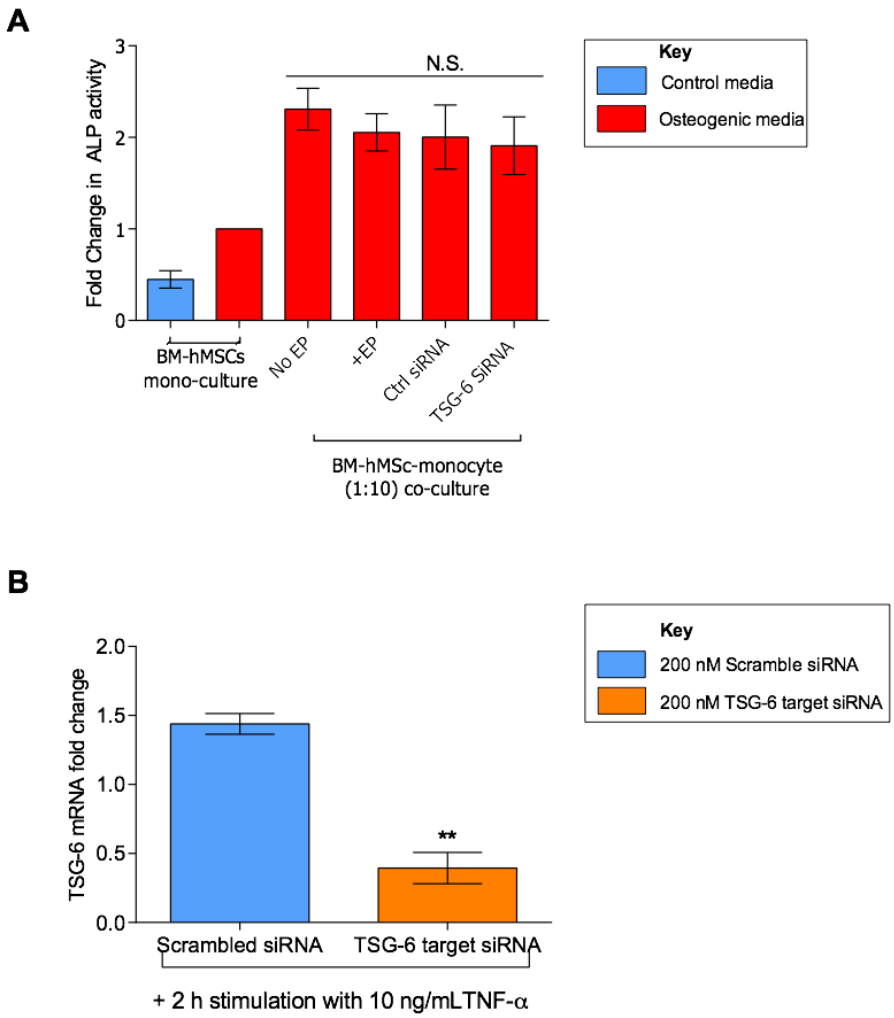


Figure 3. 5 Silencing *tsg-6* gene in monocytes does not affect early BM-hMSC osteogenesis in co-culture assays.

(**A**) 5x10^6 Human monocytes were transfected with siRNA targeting the TSG-6 mRNA using the Monocyte Nucleofector kit (Lonza, UK). Cell viability was determined following transfection by trypan blue exclusion before 1x10^5 monocytes were co-cultured with 1x10^4 of pre-adhered BM-hMSCs. Each condition was carried out in replicates of 5. On day 7 of the assay, ALP activity was quantified using ALP kit (Alpha Labs) as per manufacturer's instructions. (**B**) Human monocytes transfected with scramble siRNA for control or TSG-6 target siRNA were seeded in parallel onto 24 well plates, and 72 h post-transfection monocytes were stimulated with 10 ng/mL of rhTNF-α for 2 h. Fold change in mRNA was determined by RT-PCR relative to electroporated (EP) TNFα-stimulated monocytes. Graphs show mean ± SEM of three independent experiments, statistical analysis carried out was One-way ANOVA, followed by Dunnett's *post-hoc* test, where ns P>0.05 for graph A. Student's t-test was carried out on graph 'B', where $P \leq 0.01$.

3.3.5 TSG-6 does not Directly Enhance ALP Activity of Primary BM-hMSCs *In Vitro*

To investigate whether TSG-6 can directly enhance early osteoblast differentiation of primary BM-hMSCs, rhTSG-6 protein was exogenously added onto *in vitro* BM-hMSCs cultures. ALP protein activity was quantified at day 7 as an early marker of osteoblast formation. A significant increase in ALP activity was measured in the osteogenic media treated BM-hMSC conditions compared to those treated with control media. This demonstrated that the BM-hMSCs were capable of undergoing osteogenic differentiation under the established culture conditions. In the positive control condition, ALP activity was further enhanced by the exogenous addition of rhOSM – previously identified a direct mediator of early BM-hMSC osteogenesis (Nicolaidou et al., 2012, Guihard et al., 2012). However, no significant increase in ALP activity was measured in hMSCs treated with either commercially-purchased rhTSG-6 (R&D) (**Fig 3.6A**) or in-house[12] produced full-length rhTSG-6 (**Fig. 3.6B**), in the presence of osteogenic media compared to BM-hMSCs treated with osteogenic media only. These findings suggested three possibilities; (i) TSG-6 may not be a direct mediator of early BM-hMSC osteogenesis, (ii) the culture conditions for the protein, to function as an anabolic factor, were not optimal, and/or (iii) factors required to mediate its effects as an anabolic were absent in the milieu.

[12]In house rhTSG-6 protein was produced at the Botnar Research Centre [NDORMS], University of Oxford- see Chapter 2

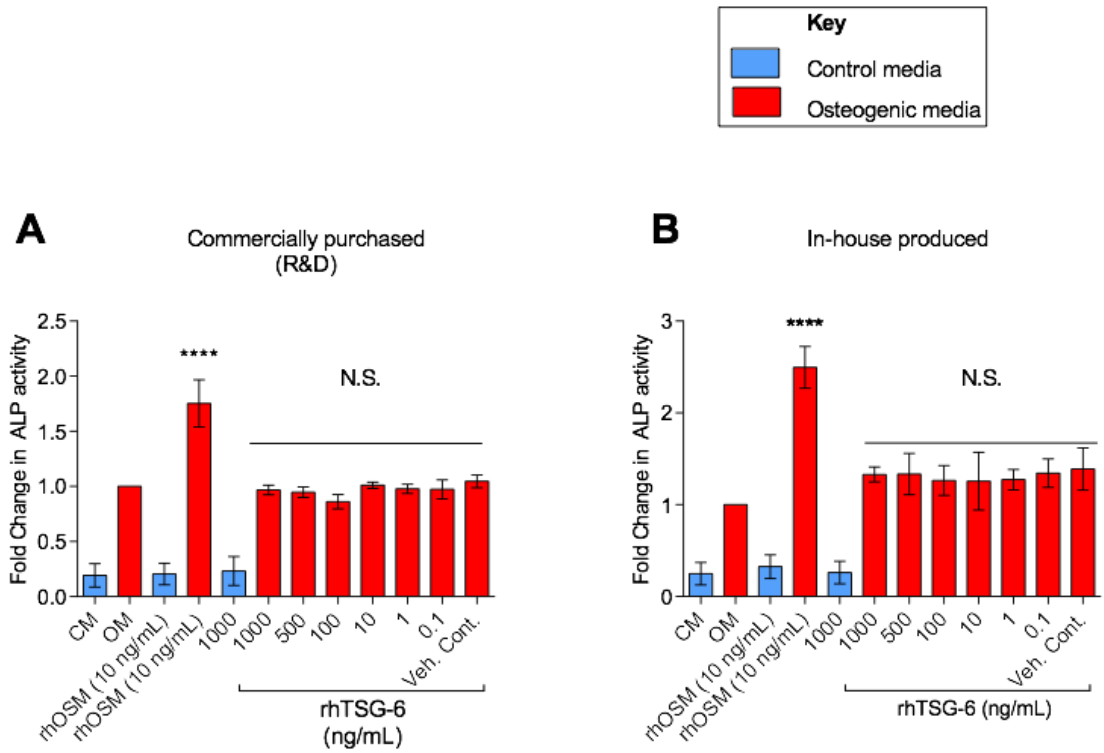


Figure 3. 6 TSG-6 does not directly enhance ALP activity of primary BM-hMSCs. $1x10^4$ BM-hMSCs were seeded onto flat-bottomed 96-well plates in control or osteogenic media were treated with increasing doses of commercially purchased; (**A**) R&D systems or (**B**) in-house produced full-length rhTSG6 protein. 10 ng/mL of rhOSM was used as a positive control, while as the vehicle control either tissue-culture grade water or (**A**) or gel filtration buffer (**B**) was employed. Graphs show fold change in ALP activity ± SEM of three independent biological experiments, where each condition was carried out in triplicates. BM-hMSCs were used between passages 4-8. Statistical differences were assessed by One-Way ANOVA, followed by Dunnett's *post-hoc* test where ****$P \leq 0.0001$ and N.S $P > 0.05$

3.3.6 TSG-6 displays additive effects on BMP-2 mediated enhancement of ALP Activity of Primary BM-hMSCs *In Vitro*

Other studies have investigated the role of TSG-6 on osteoblast differentiation in combination with BMP-2, and reported an inhibitory effect on MBA-15.4, MC3T3-E1 and C2C12 cell-lines (Mahoney et al., 2008, Tsukahara et al., 2006). To investigate this further, TSG-6 was cultured in the presence of BMP-2 in osteoblast differentiation of BM-hMSCs.

In vitro osteogenic differentiation of primary BM-hMSCs is frequently induced by osteogenic media (β-glycerolphosphate, ascorbate-2 phosphate and dexamethasone) (Nicolaidou et al., 2012). However, the signalling pathway of BMP-induced osteogenesis is better characterised than that of osteogenic media induce osteogenesis. In addition, it has been reported that simultaneous osteogenic induction with BMP-2 in the presence of osteogenic media further enhances osteogenic potential of hMSC (Jager et al., 2008); a factor also shown to be anabolic during fracture repair (Cheng et al., 2015, Li et al., 2015).

To determine the role of BMP-2 on early osteoblast differentiation of primary BM-hMSCs, rhBMP-2 was titrated against BM-hMSC cultures in the presence of control media (**Fig. 3.7A**) and osteogenic media (**Fig. 3.7B**). In control media, ALP activity on day 7 showed no significant enhancement at any of the tested doses compared to osteogenic media-only treated BM-hMSCs. However, in the presence of osteogenic media, a significant increase in ALP activity was measured when treated with 500ng/mL of rhBMP-2 relative to BM-hMSCs treated with osteogenic media only. This demonstrated that rhBMP-2 can induce early osteogenesis of primary BM-hMSCs *in vitro* in the presence of osteogenic stimuli; findings in agreement with the previous reported data (Jager et al., 2008).

To investigate whether TSG-6 is involved in osteoblast differentiation of primary BM-hMSCs through a BMP-2-dependent synergistic mechanism, rhTSG-6 was titrated in *in vitro* BM-hMSC cultures in the presence of 500ng/mL of rhBMP-2 in the presence of control media (**Fig. 3.7C**) or osteogenic media (**Fig. 3.7D**). A significant increase in ALP activity was measured at day 7 in hMSCs treated with 100ng/mL of rhTSG-6 in the presence of osteogenic media and rhBMP-2, compared to hMSCs treated with osteogenic media and rhBMP-2 only. This together Fig. 3.6B, which showed the lack of TSG-6 mediated BM-hMSC osteogenesis in the presence of osteogenic media only, demonstrated that TSG-6 has additive effects on BMP-2-mediated ALP enhancement of primary BM-hMSCs.

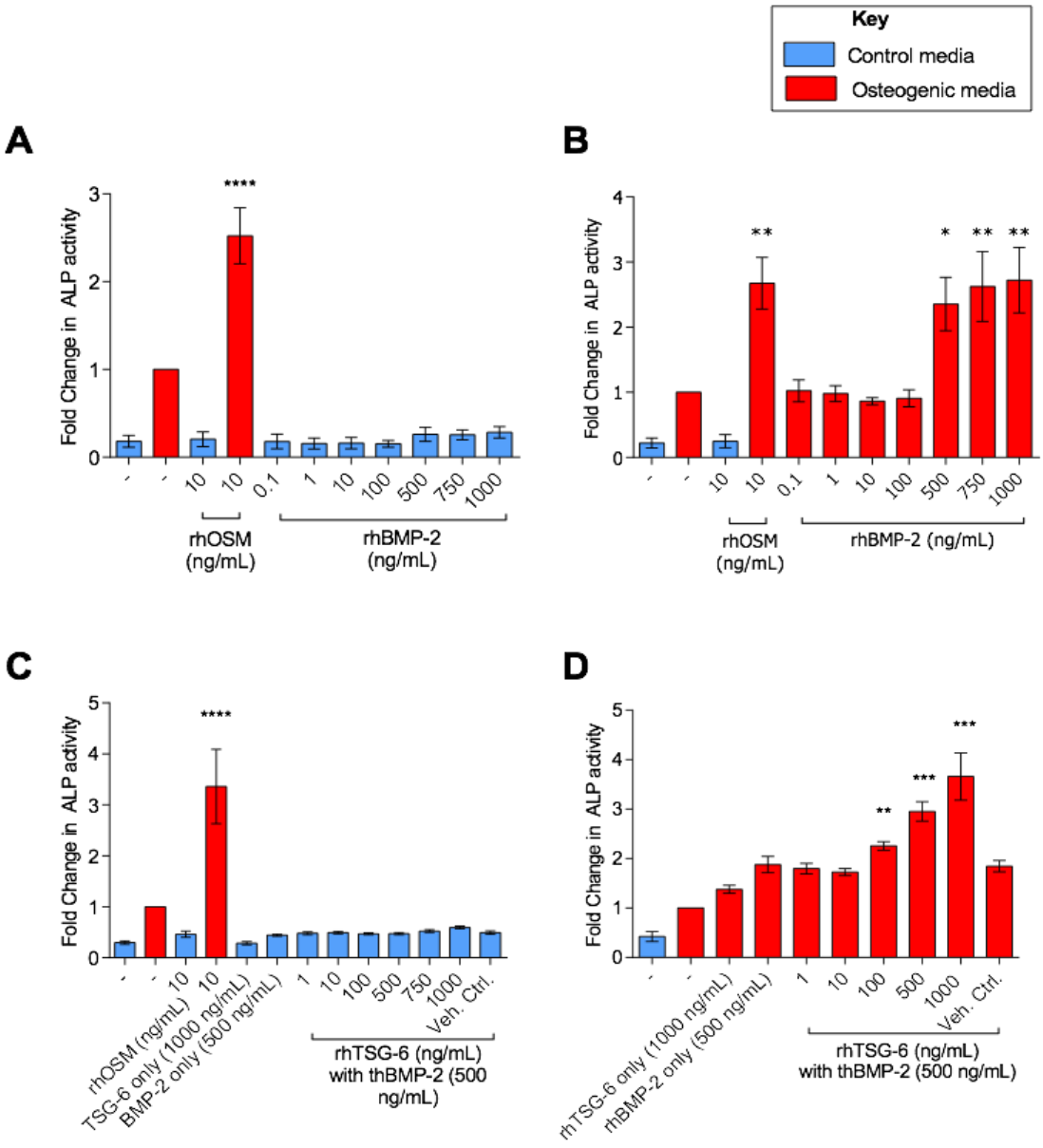


Figure 3. 7 TSG-6 enhances ALP activity of primary BM-hMSCs in the presence of BMP-2.

1x10^4 BM-hMSCs were seeded onto flat-bottomed 96-well plates in control media. 24 h later, media was changed for treatment condition containing increasing doses of rhBMP-2 in (**A**) control or (**B**) osteogenic media. Increasing doses of in-house produced full-length rhTSG-6 protein was also added onto BM-hMSCs in the presence of 500 ng/mL of rhBMP-2 in (**C**) control or (**D**) osteogenic media. Graphs represent the mean ± SEM fold change of three independent biological experiments, each condition carried out in triplicates. BM-hMSCs were used between passages 4-8. Statistical differences were assessed by One-Way ANOVA, followed by Dunnett's *post-hoc* test where *P≤0.05, **P≤0.01, ***P≤0.001, ****P≤0.0001.

3.4 DISCUSSION

Although TSG-6 is present in bone marrow tissue during physiology (Mahoney et al., 2008) and expressed by osteolineage cells in response to proinflammatory cytokines (Mahoney et al., 2011), its function on osteoblast differentiation and activity is poorly understood. This *in vitro* experimental Chapter sought to address the role of TSG-6 on osteoblastogenesis based on previous microarray data generated by high-throughput screens of monocytes transcripts following contact with BM-derived hMSCs (PhD thesis of Dr. Nicolaidou 2011)[13].

RNA-interference studies, within this Chapter, found monocyte-derived TSG-6 not to be osteoinductive in the context of bone marrow hMSC co-cultures (**see Result section 3.3.3**), instead found to work in synergy with BMP-2 to enhance early osteoblastogenesis of primary BM-hMSCs (**see Result section 3.3.6**).

The signalling pathway that monocytes use to exert osteoinduction on BM-hMSCs has been shown to be STAT3. Yet, constitutive overexpression of STAT3 in BM-hMSCs does not alter TSG-6 transcript (Nicolaidou et al., 2012). This, together with a literature search that failed to associate TSG-6 with the IL-6/STAT3 signalling pathway, hints at the redundancy of TSG-6 as an osteogenic factor within the co-culture system.

Given that the treatment of BM-hMSCs with full-length rhTSG-6 and rhBMP-2, in the presence of osteogenic media, significantly enhanced ALP – beyond that of BMP-2 treatment alone (**Fig. 3.7D**); suggested a possible pathway of TSG-6 mediated osteoinduction to be *via* the BMP/Smad pathway.

Osteoinductive BMPs, such as BMP-2 and BMP-7 have well characterised signalling pathways. Their binding to type I and II serine/threonine kinase receptors activates type

[13] Imperial College, London, UK

I receptor, which in turn, phosphorylates the receptor-associated R-Smad 1,5 and 8 leading to their translocation into the nucleus, in complex with Smad4 to initiate the transcription of osteogenic genes (Heldin et al., 1997). To gain mechanistic insights into how TSG-6 exerts osteogenic effects on BM-hMSCs in the presence of BMP-2, phosphorylation levels or nuclear accumulation of Smad 1/5/8 could be studied. Furthermore, the expression of transcription factors such as RUNX2 and OSX as well as genes that typify the osteoblast lineage such as osteocalcin and osteonectin could be examined.

In the co-culture system, the concentration of BMP-2 and BMP-7 were not increased in the BM-hMSC-monocyte co-culture condition in comparison to BM-hMSCs cultured on their own (Nicolaidou et al., 2012), nor did neutralising their activity in the co-culture assay inhibit ALP induction (Nicolaidou et al., 2012). This may indicate that the BMP/Smad pathway is not utilized within this system to mediate monocyte-mediated osteogenesis of BM-hMSCs.

Tsukahara *et al*. (Tsukahara et al., 2006) and Mahoney *et al*. (Mahoney et al., 2008) previously found an inhibitory effect of TSG-6 on BMP-2 mediated osteogenesis in both primary cells and cell lines (MBA-15.4, MC3T3.E1 and C2C12). However, the former study used partially purified rhTSG-6 and neither groups reported on LPS levels for their in-house purified protein. This is relevant because LPS has been shown to inhibit BMP-2-induced osteogenesis of hMSCs *via* the TLR-4/MyD88/NF-′B and BMP-Smad pathway (Huang et al., 2014). The conflicting results following the treatment with full-length TSG-6 observed in this study may also stem from the use of different cellular systems (Kaur and Dufour, 2012), which are indicative of different stage of the developmental pathway. It is not uncommon for primary hMSCs to respond differently to pre-osteoblast cell-lines in response to treatment with the same factor (Kaur and Dufour, 2012). For example MC3T3-E1 cell lines respond differentially to primary MSCs when

treated with inositol hexakiphosphate (Arriero Mdel et al., 2012). Cell-lines are normally selected for specific sub-clones that express certain characteristics (Wang et al., 1999), therefore genetic differences exist in addition to differences in cell origin, therefore the gold standard primary cells should be studied. Although the MC3T3-E1 cell lines is well studied (Sudo et al., 1983), passage numbers must also be reported as their biology shifts at higher passages (Chung et al., 1999).

Using an adenovirus delivery system in primary MSCs, Tsukahara *et al.* found the over-expression of TSG-6 in hMSCs to inhibit ALP activity (Tsukahara et al., 2006). However, a limitation of this study is that excessive expression of TSG-6 could have interfered with cellular processes, such as differentiation and survival. Therefore an indicator of the metabolic cell activity, such as an MTT assay, would have been informative to ensure that the noted decrease in ALP was in fact due to any potential adverse effects of the adenovirus. This is particularly relevant as, the authors do not show basal levels of hMSC ALP in the absence of the adenovirus (Tsukahara et al., 2006). Other factors contributing to differences in the findings include the possibility of fibroblast contamination in our BM-hMSC cultures, which secrete fibronectin with which TSG-6 can bind to *via* its CUB domain increasing matrix assembly (Kuznetsova et al., 2008).

Regardless of the presence or absence of osteogenic media (**Fig. 3.2B**), TSG-6 was upregulated in the co-culture supernatants within 24 h of contact. This signified other potential roles within the system, or possibly a by-product of proinflammatory cytokines – independent to osteogenesis. Yet another potential role of TSG-6 includes down-regulating pro-inflammatory cytokines - a function that is repeatedly associated with TSG-6 (Nagyeri et al., 2011, Milner et al., 2006, Lin et al., 2013, Getting et al., 2002), where TSG-6/CD44 interaction on macrophages been shown to limit TLR-2-driven NF-κB signalling thereby suppressing the expression of proinflammatory cytokines (Choi et al., 2011a). TSG-6 is known to bind HA (Blundell et al., 2005, Blundell et al., 2003,

Kong et al., 1999) and interact with CD44 indirectly through a TSG-6-HA-CD44 complex (Choi et al., 2011a). CD44 is a transmembrane glycoprotein that can modulate the BMP signalling cascade (Peterson et al., 2004).

Proinflammatory cytokines, such as TNF-α, are highly upregulated within 24 h of co-culture, and can inhibit osteogenesis of bone marrow-derived hMSCs (PhD thesis of Dr. Vicky Nicolaidou 2011). Attenuating proinflammatory signals also promotes the development of alternatively activated macrophages (M2) – a phenotype necessary for osteogenesis to ensue (Loi et al., 2016). In support of this, $CD16^{+/-}$ monocyte subsets, have been reported to differentially regulated MSC osteogenesis, upon activation (PhD thesis of Dr. Vicky Nicolaidou 2011).

A key limitation of *in vitro* studies, whether using primary cells or cell lines, is the absence of their native environment. The cellular response of MSCs may vary between 2-D and 3-D spatial (Kabiri et al., 2012) geometry as the complex cellular interactions are absent. BMP-2 has been reported to induce osteogenic differentiation of MSCs in both 2-D and 3-D culture systems, which may explain the lack of osteo-induction when the full-length rhTSG-6 was added onto bone marrow-derived MSC cultures in the absence of BMP-2.

If TSG-6 inhibits bone formation – as currently reported in the literature, it does not account for its protective effects on bone tissue in murine models of inflammation (Bardos et al., 2001, Mindrescu et al., 2002, Mindrescu et al., 2000, Szanto et al., 2004). Therefore, our novel findings require further investigation using *in vivo* models, where a complex network of cells, cytokines and receptors are present within a 3-D geometry to fully elucidate the protective role of TSG-6 on bone tissue. Therefore, the next Chapter will address whether the increase in ALP measured *in vitro*, in response to full-length

rhTSG-6 treatment, correlates with enhanced bone formation *in vivo*, using empirical, bone-specific readouts.

4

CHAPTER 4: THE *IN VIVO* ROLE OF TSG-6 ON OESTROGEN DEFICIENCY-INDUCED OSTEOPOROSIS

4.1 INTRODUCTION

In Chapter 3, TSG-6 was found to act in synergy with BMP-2 to enhance early osteoblast differentiation of BM-hMSCs *in vitro*. As this was a novel observation, we questioned whether this would correspond to enhanced bone formation *in vivo.* To test this, *in vivo* physiological (calvaria) as well as a pathological model of oestrogen-deficient induced bone loss were employed.

TSG-6 is expressed at high levels during ECM remodelling (Milner and Day, 2003), and shown to interact with a variety of matrix components, such as; glycosaminoglycans, HA (Blundell et al., 2003, Kohda et al., 1996, Lee et al., 1992) and aggrecan (Parkar et al., 1998). These components support the physiological functioning of the vertebra – the skeletal site most prone to fracture during osteoporosis (Kim et al., 2014a). In addition, TSG-6 has been shown to down-regulate the activity of MMPs (Getting et al., 2002, Wang et al., 2015) – an ECM protease found at high levels in osteoporotic patients, which degrade NCPs of the bone matrix (Logar et al., 2007).

Contrary to the finding that unchallenged mice globally deficient for TSG-6 show enhanced bone mass in comparison to their wild-type littermates (Mahoney et al., 2008), in murine arthritic studies, systemic administration of TSG-6 was found to protect both subchondral and periosteal bone against damage following exposure to a milieu of pro-inflammatory cytokines (Bardos et al., 2001). TSG-6 has been regarded as a negative regulator of inflammation in complex inflammatory diseases (Getting et al., 2002, Wisniewski et al., 1996). However, its exact role on the inflammatory signalling cascade is not yet fully understood. More so, the mechanism of bone protection associated with TSG-6 during inflammation is not known.

Although osteoporosis is not widely regarded as an inflammatory disease (Bultink et al., 2005), both human and animal studies of post-menopausal model of bone loss of have

attributed systemic bone destruction to the presence of elevated levels of proinflammatory cytokines such as TNF-α, IL-1 and IL-6 (Bertolini et al., 1986, Pfeilschifter et al., 2002, Terauchi, 2011). A consequence of this includes enhanced osteoclast formation and activity (Gowen et al., 1983, Lorenzo et al., 1987) which could decouple homeostatic bone turnover; leading to global destruction of trabecular plates and loss of tissue connectivity. This predisposes individuals to osteoporosis, fragility fractures and inefficient bone healing rates (Jemtland et al., 2011). The advent of osteoimmunology, gave prevalence to understanding the role of soluble factors on the pathogenesis of bone disorders that have not classically been regarded inflammatory, such as osteoporosis and osteoarthritis (Bondeson et al., 2010, Lencel and Magne, 2011). In this Chapter standard quantitative 2-D and 3-D bone-specific parametric readouts were used to assess the effect of TSG-6 on bone variables, the main objectives of this experimental Chapter are to:

1. Confirm the effect of global TSG-6 knockout on the baseline bone phenotype using purebred C57BL/6J mice.

2. Ascertain the ability of TSG-6 to stimulate local calvarial bone formation *in vivo*

3. Determine the role of TSG-6 on the bone phenotype of oestrogen-deficient induced bone loss using global TSG-6 knockout and TSG-6 transgenic models.

4. Elucidate the role of TSG-6 on bone remodelling during oestrogen-deficient induced bone loss by systemic exogenous administration of full-length TSG-6.

4.2 MATERIALS AND METHODS

4.2.1 Breeding and Maintenance of TSG-6 Knockout and Transgenic Murine Colonies

All mice breeding, maintenance and experimental procedures were performed at the Biomedical Services Unit (BSU) of the Kennedy Institute of Rheumatology, University of Oxford, in accordance to the UK Home Office guidelines[14]

BALB/c constitutively overexpressing TSG-6 in the cartilage under the COL2A promoter and global TSG-6 C57Black/6J (C57BL/6J) knockout mice were housed as two distinct mouse lines. Although the TSG-6 global knockout colony was received on a mixed background (Rush University, Chicago, Illinois, USA), prior to the commencement of experiments the mice were backcrossed onto a C57BL/6J background for a minimum of nine generations. This was done to minimise genetic variation between littermates and generate mice of closer genetic composition to the parent C57BL/6J.

At 6-8 weeks of age, monogamous breeding pairs were set up and their resulting offspring were weaned at 3 weeks of age, in sex-matched groups of 2-5 per each ventilated cage (Techniplast, Leicester, UK). The maintenance room was kept on a 12 h light (06:00-18:00) and 12 h dark (18:00-06:00) cycle at a constant temperature of 21 ± 1^{o}C. Special Diets Services (SDS) rat and mouse No. 3 breeding food pellets (LBS Serving Biotechnology, Ltd., Surrey, UK) and water supply were monitored daily, with weekly cage changes carried out by the BSU technicians.

[14] Guidance on the Operation of the Animals (Scientific Procedures) Act 1986 https://www.gov.uk/government/uploads/system/uploads/attachment_data/file/228831/0107.pdf

4.2.2 TSG-6 Knockout Colony Genotyping

To determine the genotype of the litters derived from the heterozygous crosses of TSG-6 global knockout mice colony, PCR was used to amplify selected nucleotide sequences from genomic DNA extracted from ear biopsies, as detailed below.

4.2.2.1 Preparation of genomic DNA

Genomic DNA were extracted from ear biopsies of the mice and incubated with 100 µL of lysis buffer (50nM Trish-hydrochloric acid (HCL), pH 8.0, 0.1 M NaCl, 1% SDS, and 20 mM EDTA) and 10 µL proteinase K at 20 mg/mL (Promega Ltd, Hampshire, UK) at 55°C on a heat block (Sigma Aldrich Ltd, Dorset, UK) for a minimum of 16 h. Following tissue lysis, samples were cooled to RT and 100 µL of 3.75 M ammonium acetate (Sigma-Aldrich, Dorset, UK) was added to the samples, then vortexed and centrifuged (14,000 rpm, 10 min, 4°C). 100 µL of chloroform was added to isolate the DNA from other organic constituents based on their differences in solubility following centrifugation (14,000 rpm, 5 min, 4°C). The upper aqueous phase, containing the nucleic acids, were transferred into a fresh 1.5 mL tube (Eppendorf Ltd., Stevenage, UK) containing 500 µL of 100% ethanol (Sigma Aldrich, Dorset, UK) to precipitate the DNA molecule. The samples were then vortexed, centrifuged (ThermoFisher Scientific, Hertfordshire, UK) (14,000 rpm, 5 min, 4°C), supernatants discarded and the residual liquid evaporated using a heat block (Sigma Aldrich Ltd, Dorset, UK). Genomic DNA Samples were then re-dissolved in 50 µL of TE (i.e. 10 mM **T**ris; pH 8.0, 1 mM **E**DTA) then stored at -20°C until downstream PCR amplification.

4.2.2.2 PCR amplification

The PCR reaction was performed using two different primers pairs (MWG-Biotech Ltd., Milton Keynes, UK). To detect the wild-type TSG-6 allele the primer pairs were; Forward 5' CCG CTG CTC TGA GAA TTT C 3' (In exon 1) and Reverse 5' TCA CTC CTT CCA TTC AGT CC3' (In intron 1)), with the following PCR cycle programme detailed below:

Table 4. 1 Cycling conditions used to amplify the TSG-6 wild-type allele.

Temperature	Duration	Number of cycles
94	5 min	
94	10 s	15
55	30 s	
72	5 min	
94	10 s	15
55	30 s	
72	20	
72	10 min	

To detect the neomycin-disrupted, TSG-6 target (knockout) allele the primer pairs used were; Forward 5' GGA TCG GCC ATT GAA CAA GC 3' and Reverse 5' CAC CAT GAT ATT CGG CAA GC 3' (Fulop et al., 2003), with the following PCR cycle program detailed below:

Table 4. 2 Cycling conditions used to amplify the target TSG-6 (knockout) allele

Temperature	Duration	Number of Cycles
94	2 min	
94	15 s	30
56	1 min	
72	1 min	
74	4 min	

For each PCR run, a pre-identified heterozygous DNA template was run as the positive control, while molecular grade water (Sigma-Aldrich, Dorset, UK) was used for the 'non-template', negative control, to assess false positive bands. Each 25 µL of total reaction mixture contained the following:

Table 4. 3 Constituents of the PCR reaction mix

Reaction components	Volume added (µL)
DNA template	1.0
H_2O	15.25
5x buffer	5
25 mM Mg^{2+}	1.0
dNTP	0.25
Forward primer	1.0
Reverse primer	1.0
Taq polymerase	0.5

4.2.2.3 Gel Electrophoresis of PCR Products

The products of the PCR were run on a 1.7% agarose gel (New England BioLabs Ltd., Hertfordshire, UK) produced in-house (3.4 g in 200 mL of 5x TAE). The mixture was heated in a microwave (high power) until the agarose was dissolved. To stain the nucleic acid, 20 µL of 1x gel red (Bioscience Ltd, Cambridge, UK) was added to the liquid mixture before it was poured onto a comb and gel mould and placed at 4°C to set. Each sample was mixed with 3 µL of 1x loading dye (New England BioLabs Ltd., Hertfordshire, UK) then loaded onto the solidified gel. Electrophoretic separation of the products was carried out at 100 volts for 60 min, in parallel with 5µL of Fermentas Mass ruler DNA ladder (New England BioLabs Ltd., Hertfordshire, UK) to determine the relative MW of the PCR products [range: 80 – 10,000 base pair (bp)]. PCR was used to amplify regions of the genomic DNA extracted from ear biopsies, the products of the reaction were then loaded onto a 1.7% agarose gel and resolved electrophoretically against a DNA ladder to determine the size of the products. Each genomic DNA template was subjected to two different cycle conditions pre-optimised per set of primers (**Tables 4.1 and 4.2)**, also described by Szanto *et al.* (Szanto et al., 2004)

4.2.3 Murine Calvarial Model: An In Vivo Test of Full-length TSG-6 Bone Anabolic Activity

To investigate the *in vivo* effect of full-length rhTSG-6 protein on local bone turnover, the left parietal calvarial bone **(2015, Nicolaidou et al., 2012)** of 5-week old C57BL/6J male mice (Charles River Laboratories) were treated subcutaneously (s.c.) daily with 50 µL of protein (at specified concentrations of: 0.0633, 0.633, and 6.33 µg/day) subcutaneously, for five consecutive days (**see Fig. 4.1A**). In parallel, the baseline control group received 50 µL of PBS, while the positive and negative control groups received 50 µL of 0.2µg/day recombinant mouse OSM (R&D Systems, Oxford, UK) [as used previously by Nicolaidou *et al.* (2012) (Nicolaidou et al., 2012)] and 50 µL gel filtration buffer respectively, for five consecutive days. To determine any newly formed bone in response to the treatments, all groups received 200 µL intraperitoneal injections (i.p.) of 20 mg/kg calcein dye (Sigma-Aldrich Ltd., Dorset, UK), at the start (day 0) and 24 h prior cull (day 15), as previously described by Nicolaidou *et al.* (2012) (Nicolaidou et al., 2012). Once all calvaria were harvested and fixed for 48 h in 10% neutral buffered formalin (NBF) (Sigma-Aldrich, Dorset, UK), the parietal bone was dissected along the coronal plane (**see Fig. 4.1B**) using a victor razor saw (Axminster, Buckinghamshire, UK).

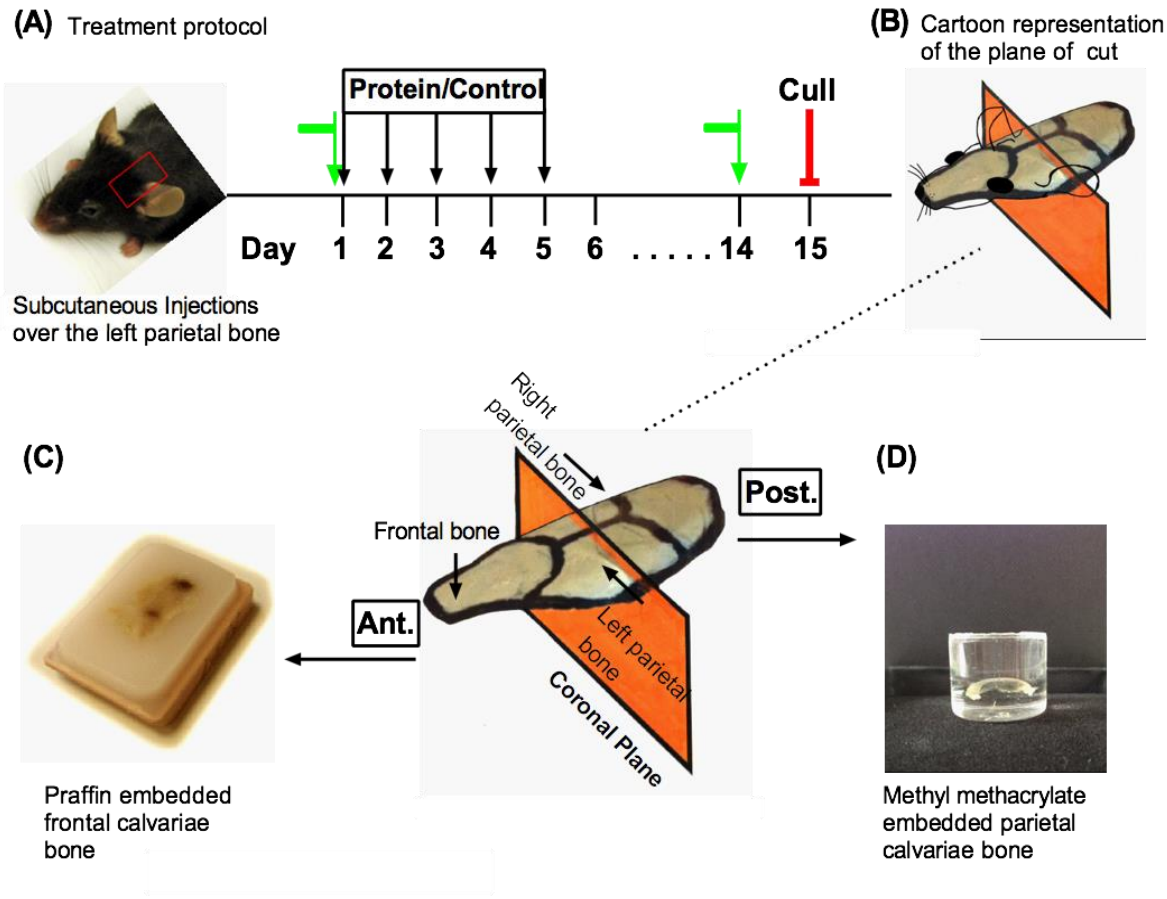


Figure 4. 1 Schematic of the *in vivo* calvarial assay used to test the local anabolic activity of TSG-6.

(**A**) Calvaria experiment treatment protocol, where green arrows indicates intraperitoneal injection of calcein, black arrows indicate protein/control treatment, red bar indicates cull. (**B**) The Plane of calvarial cut where 'Ant.' designates anterior and 'Post.' designates posterior. An example of (**C**) paraffin and (**D**) methyl methacrylate embedded calvariae tissue.

4.2.4 Surgical Bilateral Removal of Mouse Ovaries: Bilateral Ovariectomy – A Murine Model of Postmenopausal Osteoporosis

Bilateral ovariectomised BALB/c and C57BL/6J mice were used as models of oestrogen deficient-induced bone loss to mimic post-menopausal osteoporosis, as previously described by Ding *et al.* (Ding et al., 2010).

In preparation for the bilateral ablation of the ovaries, the fur around the surgical area of the subjects was shaved off using pet clippers and then sterilised using 1:10 iodine surgical scrub (Centaur Services, Somerset, UK). Mice received vetergesic (bupremorphine – 1:10) (Centaur Services, Somerset UK) subcutaneously (1:20 dilution in sterile water), prior to the start of the operations, and then anesthetised using isoflurane (Centaur Services, Somerset, UK), at 3% for induction and 1.5% for maintenance. Oxygen was supplied at a flow rate of 200 mL/min for induction and 100 mL/min for maintenance.

The surgical procedure began with a skin incision over the dorsal, middle lower vertebrae using sterile scissors. To disjoin the subcutaneous connective tissue from the underlying muscle, blunt dissection was carried out on either side of the incision. Smaller incisions were then created in the muscle on the left and right side to gain access into the peritoneal cavity, where the ovarian fat pads are located. Once the ovaries were located, the uterine horns, distal to the oviduct, were double ligated using absorbable Vicryl (Bunzl Healthcare, London, UK) and then the ovaries were excised as a whole using sterile scissors. The muscle incisions were sutured using absorbable Vicryl thread (6-0, P-3, 13 mm needle) (Bunzl Healthcare, London, UK), while the skin incision was stitched using non-absorbable monofilament polyamide Ethilon® nylon suture (5-0, P-6, 8 mm needle) (Bunzl Healthcare, London, UK). Following each operation, the mice were placed in an incubator pre-set to 37°C and monitored until they recovered from the general anaesthesia. Mice were assessed on movement and behaviour before placed

back into their cages. Following the surgery, the surgical wound, feeding, and physical activity of the mice were monitored daily.

4.2.5 Phenotypic Characterisation of Bone Tissue

The phenotypic parameters evaluated were the 3D microarchitecture (Micro-CT), bio-mechanical (3-point bend testing), 2D microarchitecture (histomorphometry) and the cellular components (histology).

4.2.5.1 Micro-computed tomography analysis

To assess micro-architectural changes in the tibial trabecular tissue in response to genotype, micro-computed tomography (micro-CT) analyses[15].

Briefly, samples were stripped of soft tissues before being placed in the X-ray chamber of the Sky Scanner. A 50 Kv, 800 µA electrical current was passed and images were acquired at a resolution of 8.30 µm/pixel. The raw images were then reconstructed and analysed using the CT Analyser software (version 1.132.1). Thresholding at 65 grey-scale units, (equivalent to a BMD of 0.442 g/cm^3) gave good morphological distinction between trabecular bone and bone marrow.

4.2.5.2 Three-point bend testing

To determine the biomechanical effect on long bones in response to the Link module of the TSG-6 protein, during ovariectomy-induced bone loss, three-point bend testing was carried out on the right femurs. Femurs that had been fixed in 70% ethanol, were rehydrated by incubating the tissues in PBS for 2 h. Each femur was then placed with its anterior surface positioned upwards. Load was applied vertically directed towards the

[15] Micro-CT analyses were performed by Dr. Andrew Freidin at the Kennedy Institute of Rheumatology, University of Oxford.

mid-shaft at a rate of 2 mm/sec, until complete failure. Load-deformation curves were plotted by Bluehill 3 software (Instron® Limited).

4.2.5.3 Histomorphometric analysis

The overall tissue (calvaria) thickness and bone mineralisation was quantified by histomorphometry on sections cut from calcified frontal halves of the parietal tissue. To prevent the detachment of denser components of the tissue from the softer ones during sectioning, calcified specimens were embedded in methyl methacrylate (MMA) resin (**Fig. 4.1C**) to complement the hardness of calcified tissue, as previously described by Erben *et al.* (Erben, 1997). To do so, specimens were first dehydrated by an hour's incubation at each increasing concentration of acetone solution (70%, 90%, and 100%) at 4°C. The specimens were then permeated with infiltrate composed of: 90% destabilised MMA (dMMA), 10% dibutyl-phthalate (DBP), and 0.05% benzyl peroxide (BPO) for 72h at 4°C. Once tissues were infiltrated, pre-polymerised bases (90% dMMA, 10% DBP, 3% BPO), within glass vial moulds, were treated with 7 mL of embedding mixture (85% dMMA, 15% DBP and 3% BPO) to soften the polymer. Once softened, the specimens were orientated flat onto the bases and left overnight at 37°C for the embedding mixture to polymerise. The embedded calvaria were sectioned at 4 μm thick using an automated *Leica RM2255* rotary *microtome* and histomorphometric analysis was carried out using the Osteomeasure™ software (Osteomeasure™, Osteometrics, Georgia, USA). The parameters measured were: overall calvaria thickness (**Fig. 4.2A**), and inter-label width (**Fig. 4.2B**). The latter was used to derive the mineral apposition rate (MAR) by diving the distance between the double calcein label by the time (days) elapsed between each administration (**Fig. 4.2C**).

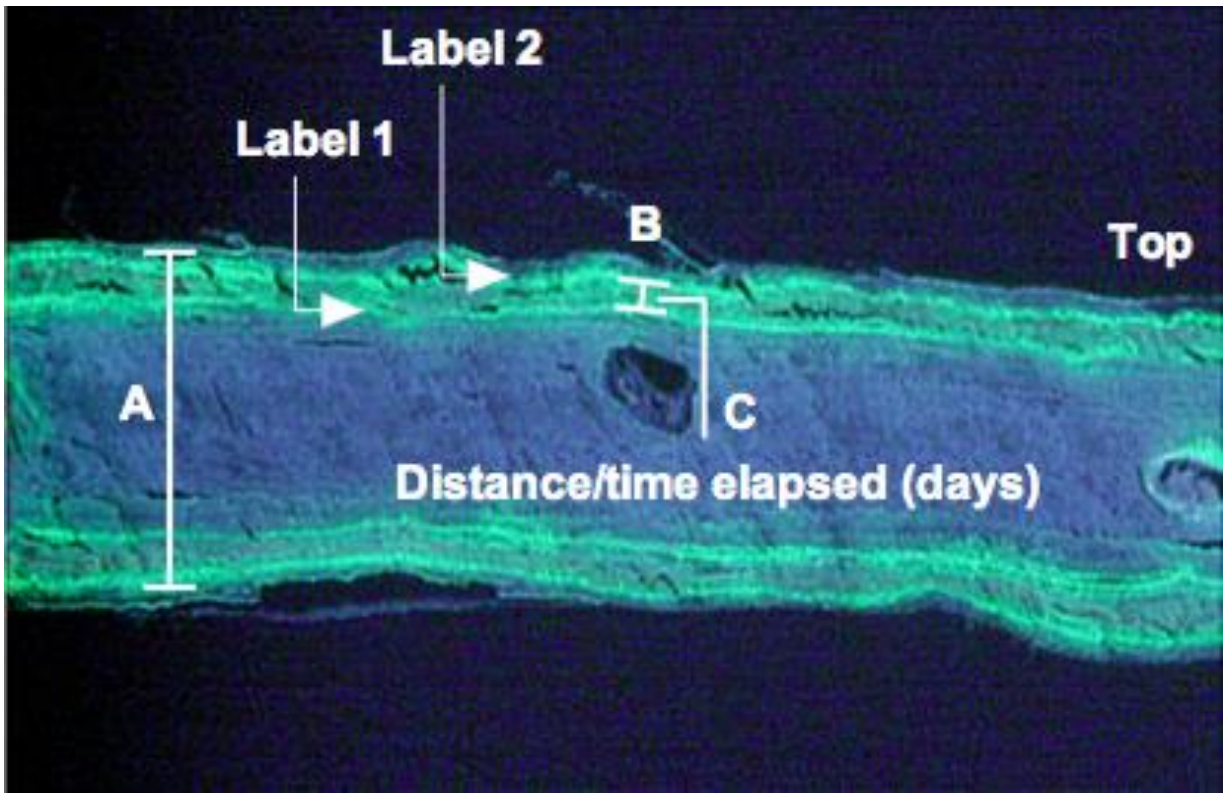


Figure 4. 2 Representative fluorescent micrograph of a calvaria section showing how 2-D quantification of calvariae were carried out using bone histomorphometry.

The green labels represent calcium-bound calcein. '**A**' shows measurement of overall thickness; '**B**' shows measurement of the distance between the double calcein labels (inter-label width). **'C'** The MAR is derived by dividing the average distance between the double labels between the time elapsed between label 1 and label 2. Magnification: x40.

4.2.5.4 Histological analysis

Histological examinations of cellular and structural differences between treatment groups were carried out on decalcified inter-parietal halves of the calvaria. Specimens were decalcified by treatment with 10% EDTA disodium salt dehydrate (Sigma-Aldrich, Dorset, UK) for three weeks, with solution changes every three days. Tissues were then washed, dehydrated, cleared, infiltrated and paraffin embedded Using Tissue-Tek® VIP™ Sakura (Sakura Finetek Ltd., Berkshire, UK) tissue processor with the automated program listed in **Table 4.4**.

Table 4. 4 Processing decalcified tissues within paraffin blocks.

Procedure	Treatment	Duration (min)	Temperature (ºC)
Wash	Saline	90	40
Dehydrate	70% ethanol	90	40
	90% ethanol	90	40
	100% ethanol 1	90	40
	100% ethanol 2	90	40
	100% ethanol 3	90	40
	100% ethanol 4	90	40
Clear	Xylene 1	90	40
	Xylene 2	90	40
	Xylene 3	90	40
Infiltrate	Paraffin 1	90	63
	Paraffin 2	90	63
	Paraffin 3	90	63
	Paraffin 4	90	63

4.2.5.4.1 Histological Staining - Toluidine Blue stain

Plastic embedded calcified sections were treated with Toluidine blue stain to distinguish cellular components of the tissues, using the protocol summary in the table below (**Table 4.5**). Dark blue-purple stain indicated the areas of dense nucleic acid, indicating the presence of cells.

Table 4. 5 Steps taken to stain tissue sections with toluidine blue stain.

Toluidine blue buffer constituted of 8.2 mM citric acid and 4.9 mM disodium phosphate (pH 3.7). Toluidine blue stain was made by reconstituting Toluidine blue O stain (Sigma, Aldrich Ltd., Dorset, UK) at 65.4 mM in Toluidine buffer (pH 3.7).

Procedure	Treatment	Duration	Temperature (°C)
De-plasticise	Cellulose solution1	25 min	RT
	Cellulose solution 2	25 min	
Rehydrate	100% ethanol 1	3 min	RT
	100% ethanol 2	3 min	
	80% ethanol	3 min	
	60% ethanol	3 min	
	Distil water	3 min	
Stain	Toluidine blue stain	60 min	RT
Rinse	Toluidine blue buffer 1	-	RT
	Toluidine blue buffer 2	-	
Blot	*With filter paper*	-	RT
Clearing	Butanol 1		RT
	Butanol 2		
	50:50Butanol: Toluidine		
	Toluidine 1		
	Toluidine 2		
Coverslip	DPX	---	RT

4.2.5.4.2 TRAP stain with methyl green counter stain

To determine the local *in vivo* effect of TSG-6 treatment on osteoclast number and distribution, decalcified, paraffin-embedded sections from the inter-parietal halves of mouse calvaria were examined for tartrate-resistant acid phosphatase (TRAP) activity.

Slides were first de-waxed by two 5 min treatments with xylene and then, rehydrated by 2 min treatments per decreasing concentration of ethanol (100%, 90%, and 75%) then deionised water. Prior to staining, sections were primed for 20min at RT in TRAP buffer composed of 50 mM sodium acetate anhydrous (Sigma-Aldrich, Dorset, UK) and 40 mM potassium sodium tartrate tetrahydrate (Sigma-Aldrich, Dorset, UK), pH 5.0.

To stain the sections, slides were incubated in TRAP staining solution composed of 0.5 mM of Naphthol AS-MX phosphate (Sigma-Aldrich, Dorset, UK), 1% (v/v) N,N-Dimethylformamide (Sigma-Aldrich, Dorset, UK) and 0.5 mg/mL of Fast Red Violet LB salt (Sigma-Aldrich, Dorset, UK) for 2 h at 37^{o}C. Sections were counterstained with 0.2 % methyl Green (dissolved in dH_2O) for 20 min. Sections were then air-dried before coverslips mounted using DPX. Quantitative assessment was performed using the the Osteomeasure^{TM} (Osteomeasure^{TM}, Osteometrics, Georgia, USA), bone histomorphology analysis system. TRAP reactivity was indicated by bright red staining.

4.2.5.4.3 Immunohistochemistry

Osteocalcin immunodetection

To investigate the local *in vivo* effect of TSG-6 treatment conditions on osteoblast numbers and distribution, in-direct immunohistochemistry (IHC) was performed by Dr. Ida Parisi (The Histology Department, The Kennedy Institute of Rheumatology, University of Oxford). 4 µm-thick sections were deparaffinised manually, as detailed in the table below (**Table 4.6**), in preparation for IHC.

Table 4. 6 Summary of the steps taken to process tissue sections in preparation for immunohistochemistry.

Procedure	Treatment	Duration (min)	Temperature (ºC)
Dewax	Xylene 1	5	RT
	Xylene 2	5	RT
Rehydrate	100% ethanol 1	2	RT
	100% ethanol 2	2	RT
	95% ethanol	5	RT
	85% ethanol	5	RT
	70% ethanol	5	RT
Wash	PBS	5	RT

To recover antigenic epitopes masked as a result of formalin fixing, sections were treated with trypsin enzymatic antigen retrieval solution (Abcam®, Cambridge, UK) as per manufacturer's instructions then washed with PBS for 5 min. To minimise non-specific binding, sections were incubated with serum block composed of PBS supplemented

with 10% (v/v) FBS and 10% (v/v) normal goat serum (Sigma-Aldrich Ltd., Dorset, UK). In addition, endogenous avidin-biotin binding sites were also blocked using Avidin/Biotin blocking kit (Life Technologies Ltd., Paisley, UK) as per manufacturer's instructions. Sections were then incubated overnight, at 4°C; with a rabbit anti-mouse polyclonal primary antibody (Enzo Life Sciences Ltd., Exeter, UK) at a final concentration of 1 µg/mL diluted in blocking buffer. The specificity of the primary antibody was assessed in comparison to a rabbit IgG polyclonal isotype control (Abcam®, Cambridge, UK) at matching dilution of 1:1000 in blocking buffer.

The following day slides were washed, as described before, and endogenous hydrogen peroxidase activity was blocked by incubating the sections with 3% hydrogen peroxidise solution (Benchmark Scientific Inc., New Jersey, UK) for 30min at RT. Sections were washed as previously described, and probed with the secondary biotinylated goat anti-rabbit IgG antibody (Abcam®, Cambridge, UK) for 1h at RT in the dark. Sections were washed and incubated with 1:300 diluted streptavidin-horseradish peroxidases (DAKO, P0397) for 30min at RT and then washed again. In order to detect the immunoreactivity, the chromogen substrate 3, 3'-diaminobenzidine (K3468, DAKO) was added to the tissue sections. Sections were inspected regularly to check colour development (with a minimum incubation period of 5 min to a maximum of 40 min) and later washed with running tap water for 5 min to mature the staining.

To counterstain, sections were treated with Mayer's haematoxylin solution (Sigma-Aldrich Ltd., Dorset, UK) for 1min then washed with water for 5min. Sections were dehydrated by 2 min treatment with 100% ethanol followed by 2min treatment with xylene. Finally, coverslips were applied using DPX mounting media (Sigma-Aldrich Ltd., Dorset, UK).

4.2.6 Statistical Analysis

All data are represented as mean ± the standard error of the mean (SEM) and each treatment was run in replicates of 2-3 where mean values were calculated. Selected statistical analyses were carried out using GraphPad Prism 6 (Version 6.03), and the choice (included in the Figure legends) was dependent on the experimental design.

4.3 RESULTS

4.3.1 Determination of Mice Genotypes Derived from the TSG-6 Heterozygous Colony

To determine the genotype of mice litters derived from a heterozygote crosses, the wild-type and target gene were detected by PCR using primers (**see Materials and Methods section 4.2.2**). A product size of 250 bp indicated the presence of the wild-type allele, while a product size of 600 bp indicated the presence of the TSG-6 mutant (target) allele (**Fig. 4.3**). Accordingly, wild-type mice were identified by the presence of a single 250 bp band; the TSG-6 knockout mice demonstrated a single 600 bp band, while the heterozygotes displayed two bands at both locations.

4.3.2 Twelve and Twenty Week-Old TSG-6 Deficient Female Mice Exhibit Lower Bone Mass Relative to their Wild-Type Littermates

To confirm whether the TSG-6 deficient mice backcrossed onto a pure C57BL/6J strain have a baseline bone phenotype, as reported by Mahoney *et al.* (Mahoney et al., 2008), fixed lumbar vertebrates of 12 and 20 weeks mice were assessed by micro-CT. Females at 12 to 20 weeks of age were chosen as these age groups were suitable for later ovareictomy studies, where 12 weeks was proximal to the start of ovariectomy and 20 week was proximal to the age of cull and subsequent analysis. 3-D bone morphology measurements showed that the lumbar vertebrae of TSG-6 deficient female mice of 12 and 20 weeks have lower bone mass compared to their heterozygous and wild-type counterparts (**Fig. 4.4 and 4.5**). Due to variations in the wild-type and the heterozygous, larger group sizes would be needed to determine if there are any statistical differences.

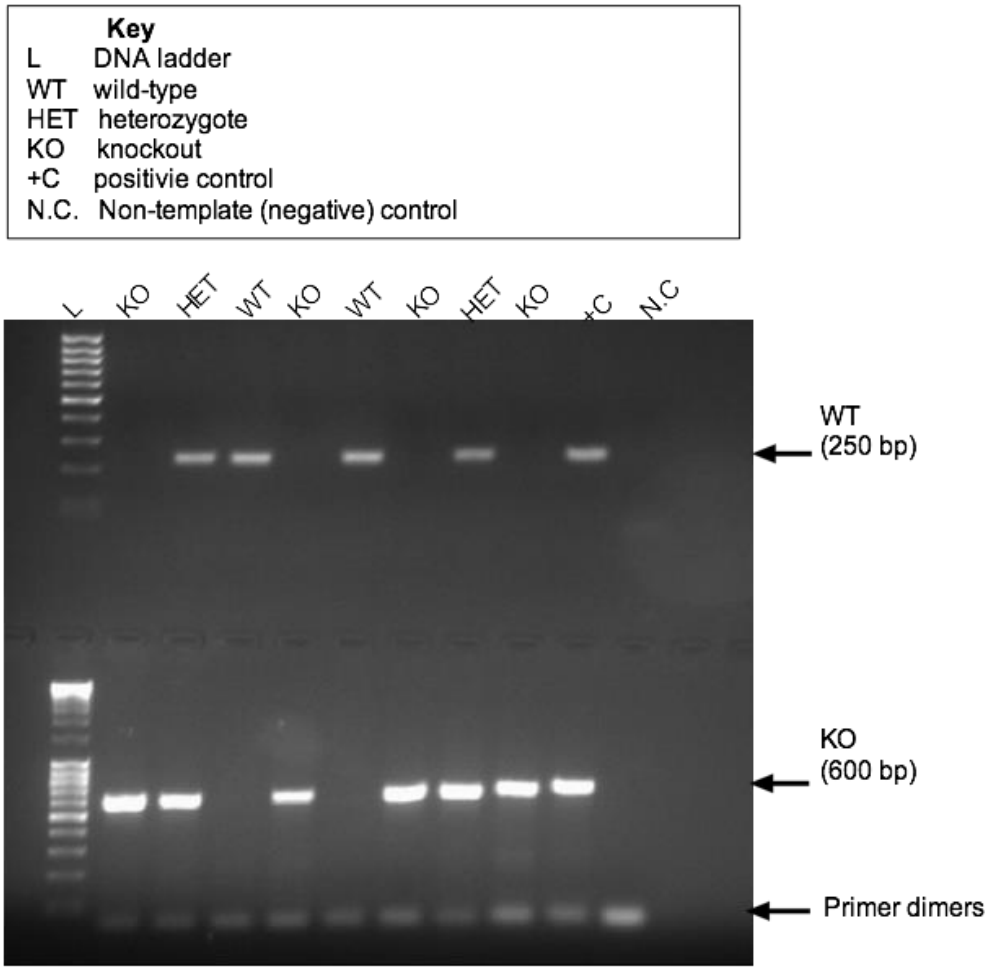


Figure 4. 3 Agarose gel electrophoresis showing PCR products used to determine the genotype of offspring derived from heterozygous TSG-6 crosses.
Ear biopsies were disrupted with lysis buffer at 55°C for a minimum of 16 h, and then the genomic DNA was extracted using chloroform. Each genomic sample underwent two different cycle conditions pre-optimised to two different sets of primers. The products of the PCR reactions were resolved electrophoretically on a 1.7% agarose gel and were run at 100 volts (V) for 60 min.

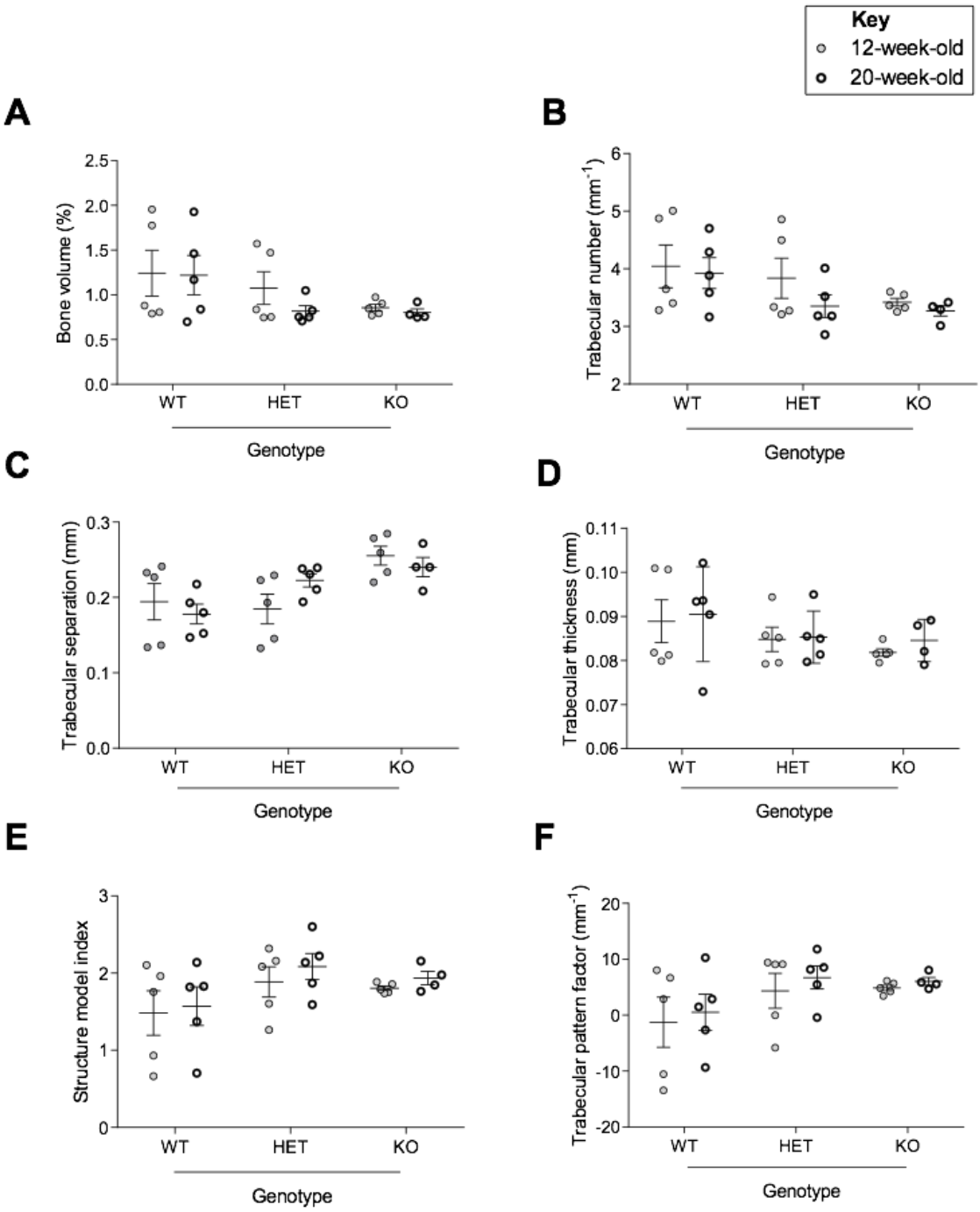


Figure 4. 4 Micro-CT derived morphological parameters from the lumbar vertebrae of wild-type and TSG-6 gene-targeted mice at 12 and 20 weeks of age.
Three dimensional structural parameters of ex-vivo micro-CT examinations of trabecular bone from the lumbar vertebrae of 12 and 20 week-old *tsg-6* gene targeted and wild-type female C57BL/6. Data is represented as mean ± SEM of 4-5 mice per group. Statistical differences were determined using Two-way ANOVA, followed by Tukey's *post-hoc* test.

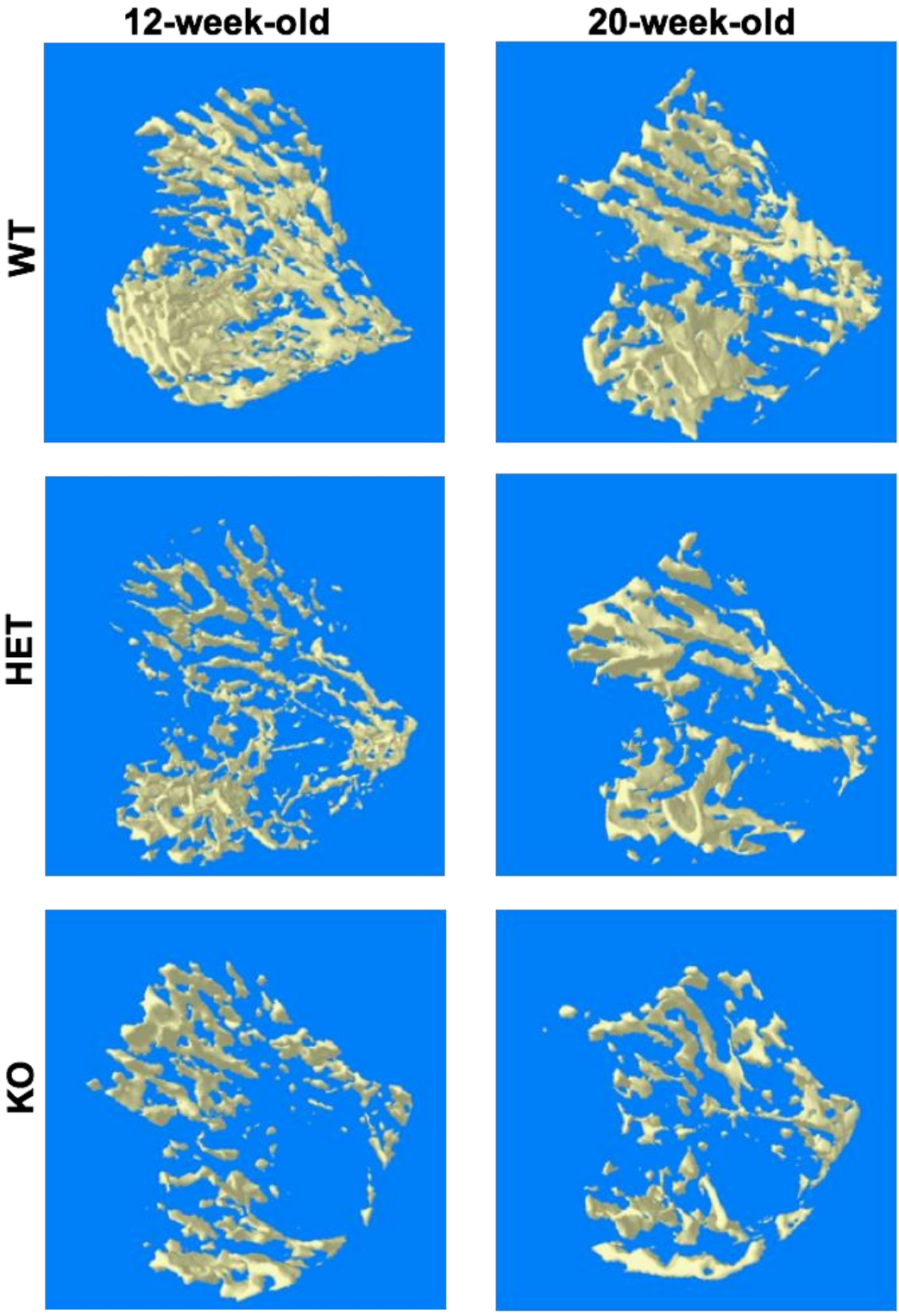


Figure 4. 5 Micro-CT generated images showing baseline bone morphology of the lumbar vertebrae of wild-type and TSG-6 gene targeted mice at 12 and 20 weeks of age.

Representative 3-D baseline trabecular architecture of the lumbar vertebrae of female C57BL/6 from the respective genotypes at 12 and 20-weeks of age**.**

4.3.3 TSG-6 Significantly Increases Local MAR in a Dose-Dependent Manner During Physiological Bone Modelling

In order to investigate the effect of TSG-6 on local bone formation *in vivo*, for five consecutive days, 6.33 µg/day of full-length rhTSG-6 protein was administered subcutaneously over the left parietal bone of five-week-old C57BL/6J male mice, while the control group received sterile PBS. A significant increase in the mean total calvaria thickness was found in the full-length rhTSG-6 treated mice relative to the PBS treated control group, as determined by the Student's t-test (**Fig. 4.6A**). This demonstrated that local TSG-6 treatment can enhance local calvarial thickness.

In support of the thickened phenotype a second parameter, the distance between the two distinct layers of fluorescent calcein labels was found to be significantly greater in the full-length rhTSG-6 treated mice relative to the PBS control (**Fig. 4.6B**). This showed that TSG-6 can enhance the inter-label width thereby increasing mineralisation of *de novo* local osteoid *in vivo*. Next, MAR was calculated as an indicator of bone formation in response to treatment. This parameter was derived by dividing the distance measured between the double calcein labels by the time elapsed (12 days) between their respective administrations. A significant increase in MAR was calculated in the full-length rhTSG-6 treated group, compared to the PBS control group (**Fig. 4.6C**). These data together suggest that TSG-6 can significantly enhance the rate of local membranous bone formation during physiological conditions.

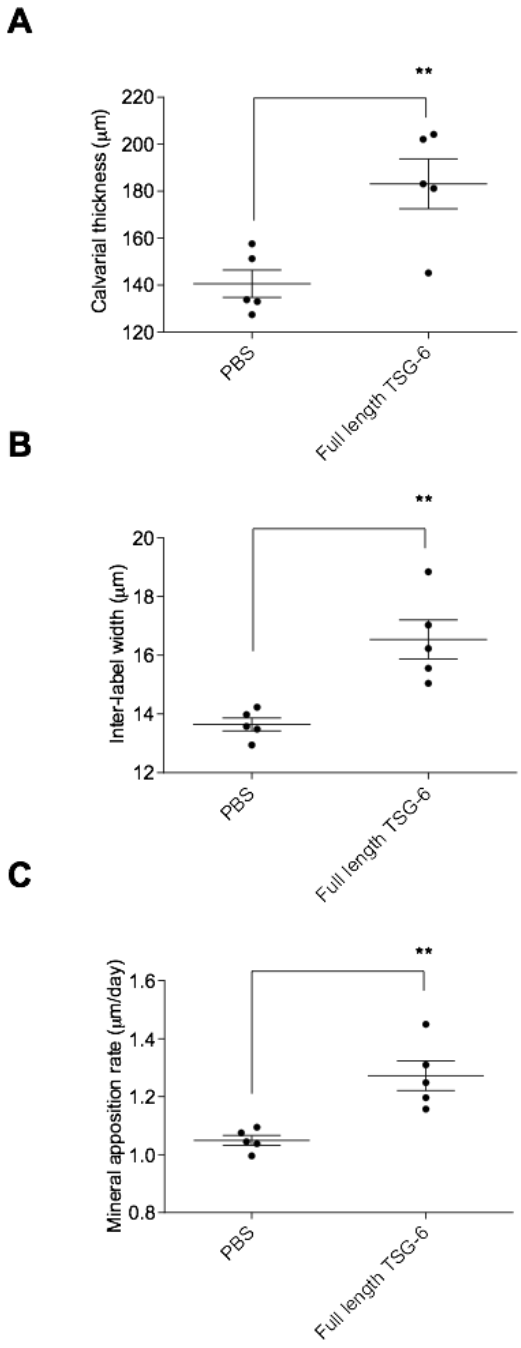


Figure 4. 6 Histomorphometry-derived parameters showing local administration of full-length rhTSG-6 significantly increases local calvarial MAR.

5-week-old C57BL/6 mice received full-length rhTSG-6 protein at a dose of 6.33 µg/day, for five consecutive days. 20mg/kg of calcein was injected on the day on which treatment commenced and 24 h prior cull to label new bone formation. Using Osteomeasure^{TM} software bone histomorphometry, the overall calvaria thickness (**A**), inter-label width (**B**) and MAR (**C**) were determined; the latter was calculated by dividing the inter-label width by the number of days (12) elapsed between labels. Six sections were analysed per mouse and the mean ± SEM values were noted. Statistical differences were determined using Student's t-test, where ***P*< 0.01.

4.3.3.1 Role of TSG-6 on local osteoblast and osteoclast numbers

A net increase in mineral apposition could either be due to an inhibition in osteoclast formation or function, or an increase in osteoblast formation and function. Therefore to examine the cellular reason behind the enhanced mineral apposition in response to full-length rhTSG-6, the calvarial sections were stained with the general stain toluidine blue to visualise the cellular components. Cells carrying high nucleic acid content were stained blue-purple (Sridharan and Shankar, 2012). The osteoblast (**Fig. 4.7A**) and osteoclast (**Fig. 4.7B**) populations were distinguished and counted based on size, morphology and position within the calvaria tissue. The mean number of osteoblasts counted in the TSG-6 treated group was found to be markedly higher than that of the control groups (90 to 29 respectively) (**Fig. 4.7C**). Meanwhile, the mean number of osteoclasts in the rhTSG-6 treated group were found to be 15 cells, compared to the mean 5 cells counted in the PBS control group (**Fig 4.7D**). However, these changes were not found to be significant.

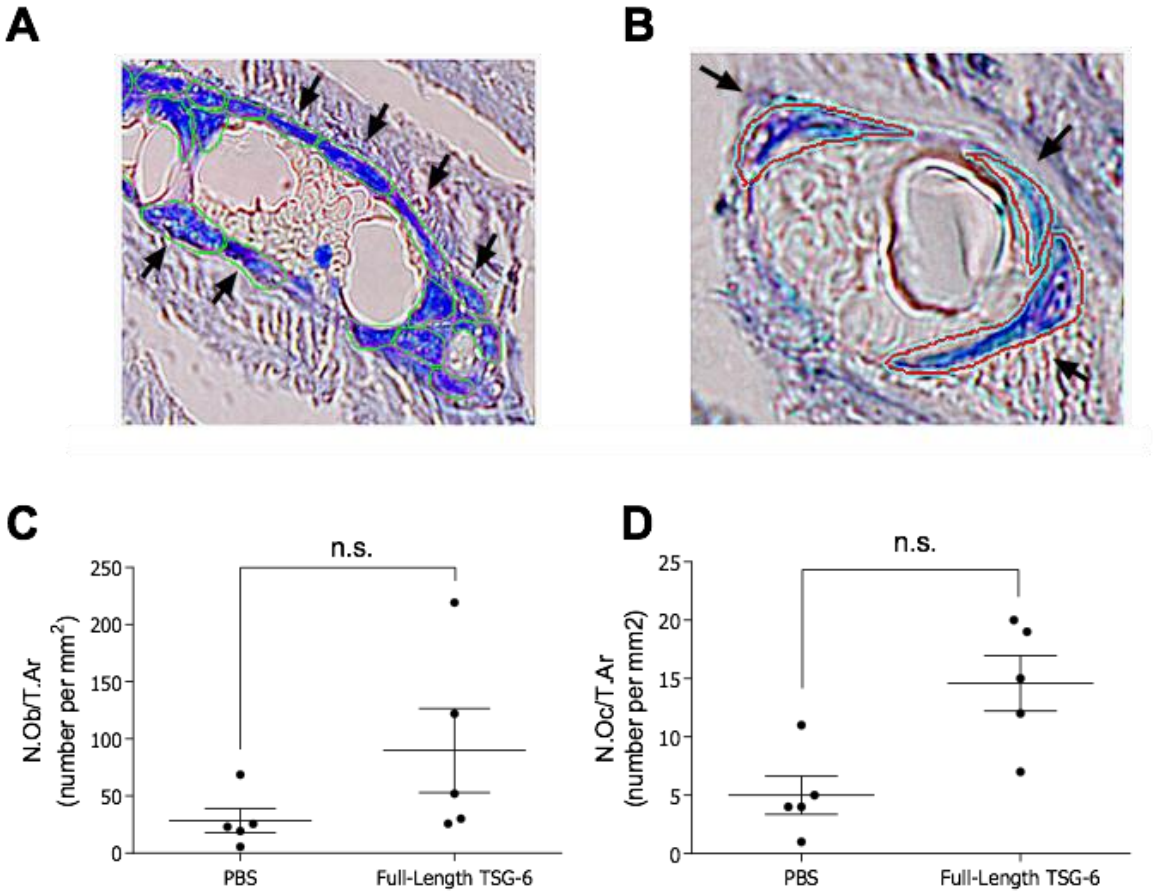


Figure 4. 7 Enumerating local calvaria osteoblasts and osteoclasts following local treatment with full-length rhTSG-6.

Osteoblasts (**A**) and osteoclasts (**B**) were distinguished based on size, position and morphology following Toluidine blue stain on calvaria sections and enumerated. The data is expressed as mean of three sections per mouse ± SEM in (**C**) and (**D**). There were no significant statistical differences between the treatments as determined using Student's t-test. Magnification x40

4.3.3.2 TSG-6 significantly increases the local MAR in a dose-dependent manner

In order to determine whether the increase in local MAR, following local full-length rhTSG-6 treatment, was a true biological effect, a dose-response study was carried out. Briefly, 5-6 C57BL/6J mice per group at five-weeks of age were treated with different doses of full-length rhTSG-6 (0.0633, 6.33, 0.633 µg/day) for five consecutive days. Initially, micro-CT analysis was carried out to investigate changes in bone volume (**Fig. 4.8**). However, no significant differences were found between the control groups; PBS (negative) and OSM (positive), or any other treatment groups. This indicated that the method was not sensitive enough – possibly due to scanner resolution- to distinguish changes in calvaria volume, or that there were not changes between treatment groups.

Therefore 2-D histomorphometry method was pursued to analyse the tissues on a micro-meter scale - resolving the issue of scanner resolution. The results found a dose-dependent increase in the inter-label width (**Fig. 4.9A**) and MAR (**Fig. 4.9B**), in response to increasing doses of full-length rhTSG-6 protein. This demonstrated that full-length rhTSG-6 protein can enhance bone acquisition during physiological modelling (**see Fig. 4.10 for representative images**).

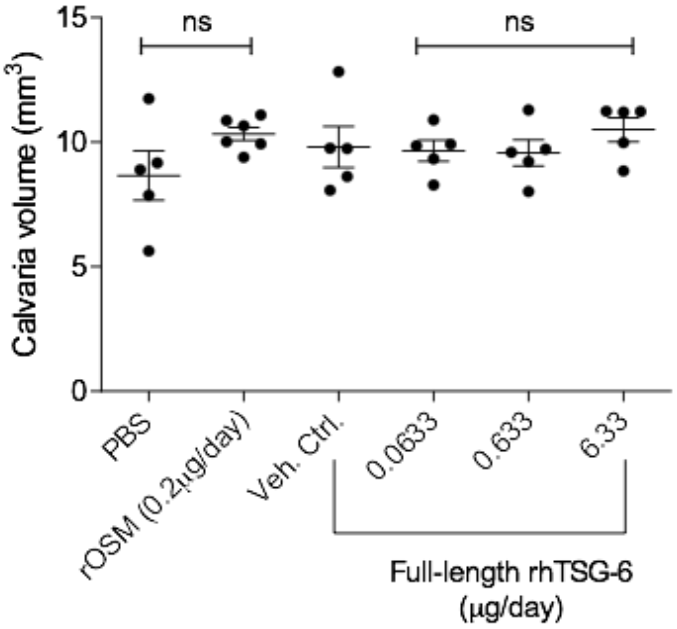


Figure 4. 8 Micro-CT quantification of calvarial bone volume following treatment with different doses of full-length rhTSG-6.

Five-week-old C57BL/6J mice were treated with doses of full-length rhTSG-6 for 5 consecutive days. Scatter graphs show the 3-D morphological parameter of calvarial volume as mean ± SEM of 5-6 mice per group. Statistical differences were determined using One-way ANOVA, followed by Dunnett's *post-hoc* test, where; N.S.*P*>0.05.

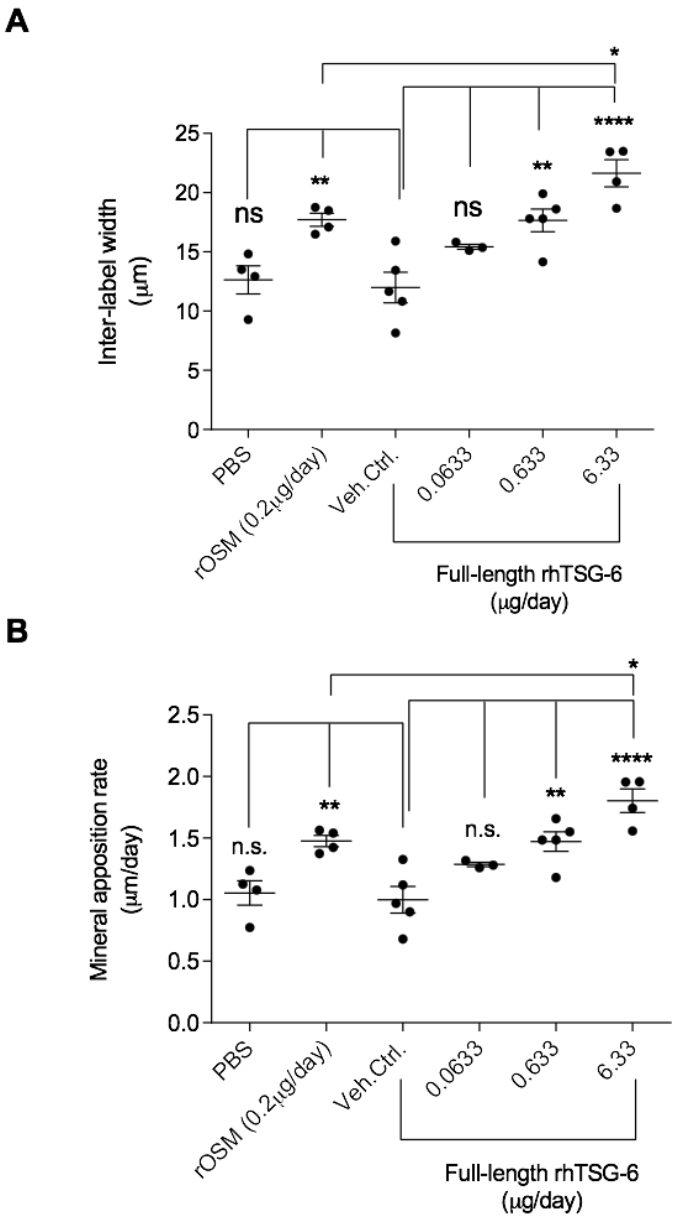


Figure 4. 9 Histomorphometry parameters showing local administration of full-length rhTSG-6 increases local MAR significantly in a dose-dependent manner.
Five week-old C57BL/6 mice received full-length rhTSG-6 protein at a dose of 0.0633, 0.633 and 6.33 µg/day, for five consecutive days. 20mg/kg of calcein was injected on the day on which treatment commenced and 24 h prior cull to label new bone formation. Using Osteo-measure™ software bone histomorphometry the (**A**) inter-label width was measured. The MAR (**B**) was derived by dividing the inter-label width by the number of days (12) elapsed between labels. Six sections were analysed per mice and averaged. Statistical differences determined using One-Way ANOVA, followed by Dunnett's *post-hoc* test where; n.s. $P>0.05$, *$P\leq0.05$ **$P\leq 0.01$, ****$P\leq0.0001$

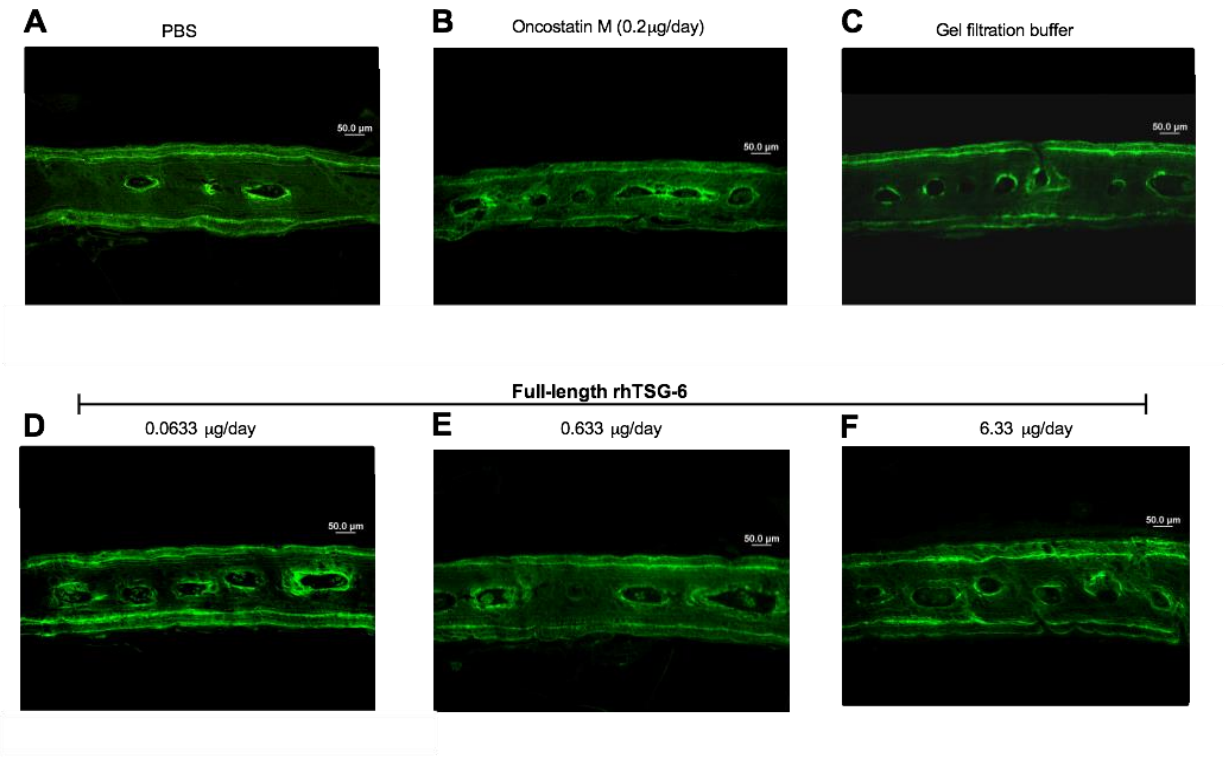


Figure 4. 10 Representative fluorescent micrograph of calvarial sections following treatment with different doses of full-length rhTSG-6.

The fluorescent labels show calcium-bound calcein in response to various treatments. (x20 magnification).

4.3.4 Global TSG-6 Deficiency does not Influence Bone Loss during Oestrogen-Deficiency-Induced Osteoporosis

To investigate the role of TSG-6 during osteoporosis-induced bone loss, a global TSG-6 deficient C57BL/6J female mouse line was used. This study began by confirming the genotype of mice litters derived from TSG-6 heterozygote crosses, followed by the induction of systemic bone loss on the different genotypic groups. Systemic bone loss was induced by bilateral removal of the ovaries in-house at 8-9 weeks of age. As a control, each genotypic group had sex and age matched non-ovariectomized littermate controls. All mice were culled at 18 ± 1 week(s) of age; the vertebrae were harvested and fixed, prior to downstream micro-CT analysis. Mice belonging to the different genotypic groups were found to respond in a similar manner to ovariectomy-induced bone loss as determined by 3-D bone morphological parameters generated through micro-CT analysis (**Fig 4.13**).

There was a significant drop in percentage BV/TV in response to ovariectomy in all three genotypes (**Fig. 4.13A**). This shows that global genetic manipulation of the TSG-6 gene does not significantly affect the magnitude of mineralised tissue lost at the vertebrae of C57BL/6J female mice. All genotypic groups showed a significant loss of trabecular number eight weeks post-ovariectomy (**Fig. 4.13B**). Consistent with this, the spatial separations between individual trabecular of all genotypic groups were significantly increased following ovariectomy (**Fig. 4.13C**). The same effect was seen for all other parameters including trabecular thickness (**Fig. 4.13D**), structure model index (SMI) (**Fig. 4.13E**) and trabecular pattern factor (**Fig. 4.13F**) (**see Table 4.7 for remaining parameters**).

In summary, TSG-6 does not seem to be involved in the formation of mineralised tissue following oestrogen withdrawal. The global knockout of the TSG-6 gene was also found

to decrease porous volume of the bone, characteristic of osteoporosis. In addition the manipulation of TSG-6 had no effect on the degree of anisotropy in response to mechanical load under osteoporosis. These findings show that TSG-6 on its own is not sufficient to influence bone morphological parameters *in vivo*, in response to oestrogen-deficient induced bone loss.

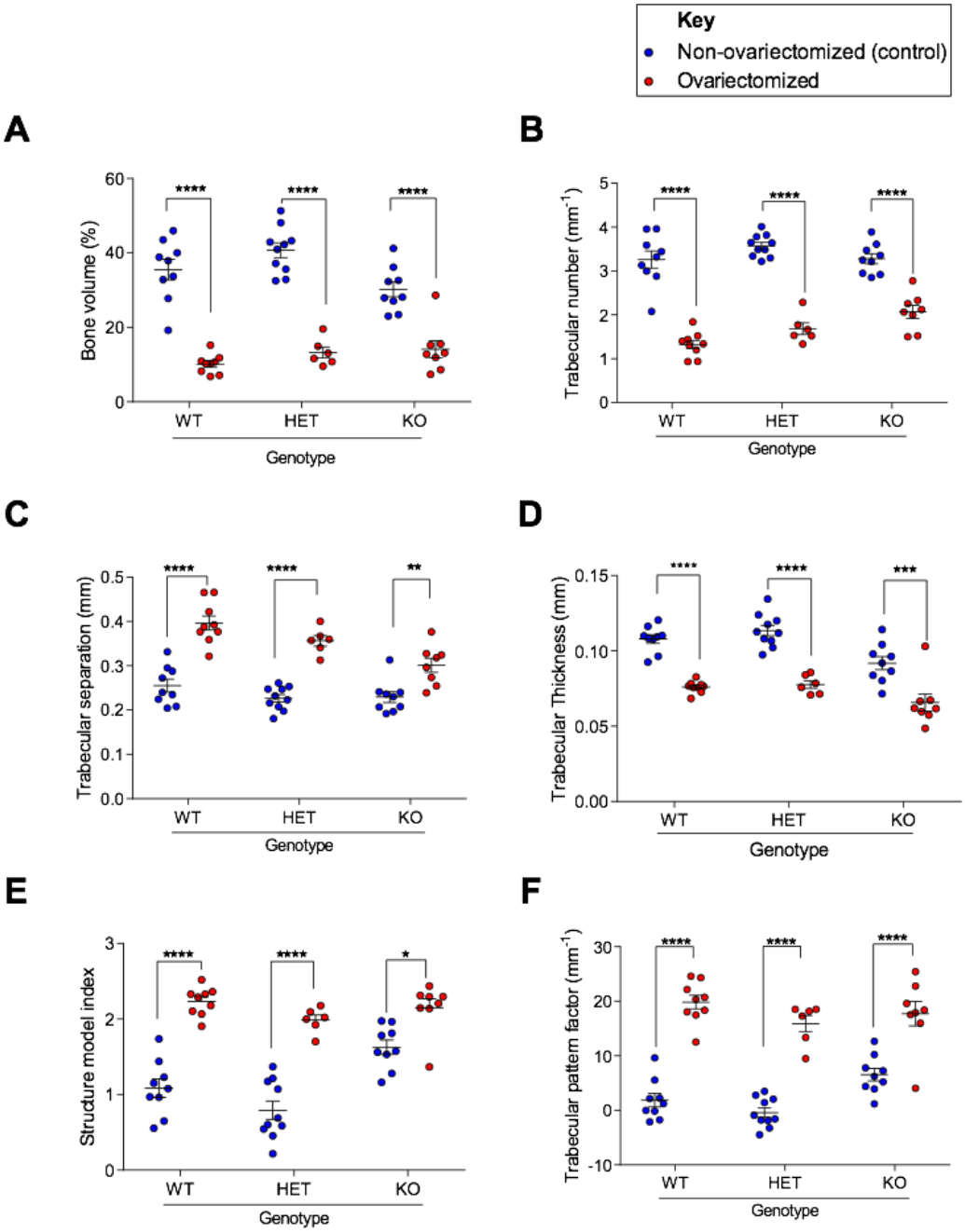


Figure 4. 11 Micro-CT derived parameters from the lumbar vertebrae of global TSG-6 targeted and wild-type mice following bilateral ovareictomy.

Mice wild-type, heterozygote and knockout for the TSG-6 gene were ovariectomised at 8-9 weeks of age and culled at 18 ± 1 weeks of age. The vertebrae were harvested, fixed in 10% NBF and stored in 70% ethanol prior to scanning. Micro-CT 3-D parameters show percentage bone volume (**A**), trabecular number (**B**), trabecular separation (**C**), and trabecular thickness (**D**) compared to the age and sex-matched non-ovariectomised littermate controls. Data are shown as the mean ± SEM (n = 9-10), statistical differences were determined by One-Way ANOVA followed by Dunnett's *post-test* (GraphPad Prism®), where * $P \leq 0.05$; ** $P \leq 0.01$; *** $P \leq 0.001$.

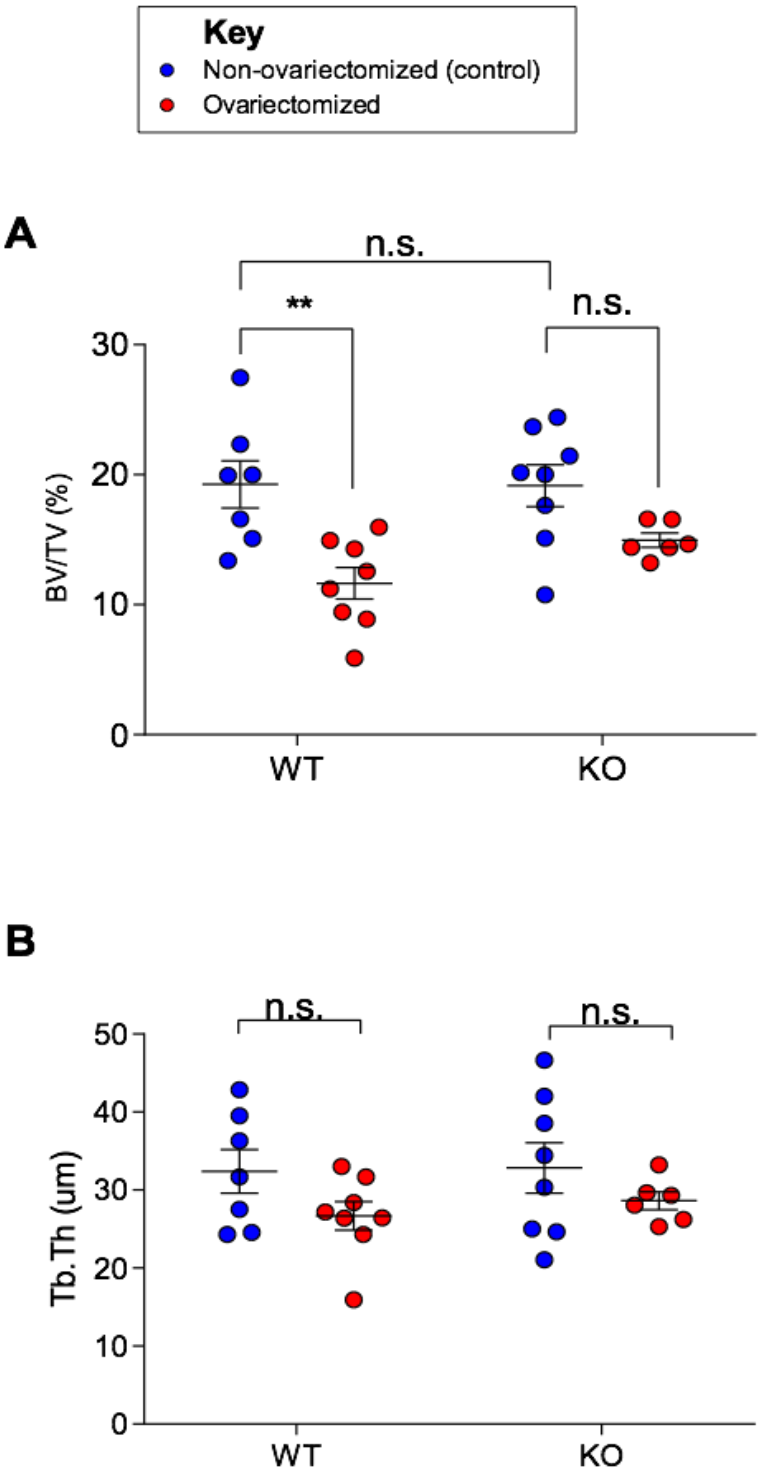
Table 4. 7 Quantitative micro-CT parameters from the lumbar vertebrae of 17 week-old TSG-6 global knockout, heterozygote, and wild-type with and without bilateral ovariectomy.

The table shows the mean ± SEM of 8-10 mice per group. Statistical differences, between sub-groups ($^{+}$OVX vs. $^{-}$OVX) of wild-type, heterozygote and knockout C57BL/6 mice were determined using Two-Way ANOVA followed by Tukey's *post-hoc* test (GraphPad Prism®).

		Wild-type		Heterozygous		Knockout	
Structural parameter	**Units**	**Non-ovariectomised**	**Ovariectomised**	**Non-ovariectomised**	**Ovariectomised**	**Non-ovariectomised**	**Ovariectomised**
Bone surface density	mm^{-1}	13.442±0.524	7.566±0.561	14.224 ± 0.170	8.468 ± 0.478	12.839 ± 0.343	8.777 ± 0.595
BS/BV	mm^{-1}	39.067 ± 2.086	67.961 ± 4.128	35.614 ± 1.636	61.438 ± 5.271	43.522 ± 2.164	64.637 ± 4.635
Degree of Anisotropy	N/A	2.959± 0.111	3.850 ± 0.280	2.957 ± 0.065	3.210 ± 0.228	2.274 ± 0.045	2.689 ± 0.104
Total volume of pore space	mm^3	1.531 ± 0.084	2.287 ± 0.082	1.405 ± 0.059	2.199 ± 0.063	1.570 ±0.074	2.131 ± 0.080
Total porosity	%	64.452 ± 2.758	87.577 ± 2.405	59.284 ± 1.969	85.075 ± 1.666	69.785 ± 1.986	85.316 ± 2.103
Volume of open pore space	mm^3	1.531 ± 0.084	2.287 ± 0.082	1.404 ± 0.059	2.199 ± 0.063	1.570 ± 0.074	2.131 ± 0.080
Open porosity	%	64.419 ±2.763	87.576 ± 2.405	59.252 ± 1.976	85.074 ± 1.667	69.777± 1.989	85.316 ± 2.103
Number of closed pores	N/A	27.778 ± 4.421	8.800 ± 3.788	29.500 ± 4.651	8.100± 1.958	16.444± 3.424	9.333 ± 1.936
Closed porosity	%	0.087 ± 0.028	0.005 ± 0.001	0.071 ± 0.026	0.003 ± 0.001	0.023 ± 0.010	0.006± 0.003
Surface of closed pore	mm^2	0.092 ± 0.023	0.008 ± 0.004	0.089 ± 0.026	0.006 ± 0.006	0.030 ± 0.009	0.008 ± 0.002
Volume of closed pore	mm^3	0.0008 ± 0.0002	0.00002 ± 0.000009	0.0007 ± 0.0003	0.00001 ± 0.000004	0.0002 ± 0.0001	0.00002 ± 0.000008
Number of objects	N/A	164.889± 17.135	486.700 ± 25.950	128.200 ± 20.850	428.700 ± 34.193	270.778 ± 26.347	481.333 ± 39.630
Fractual dimension		2.271 ± 0.019	1.991 ± 0.028	2.299 ± 0.007	2.037 ± 0.024	2.395 ± 0.022	2.142 ± 0.032

Confirming bone phenotype generated by micro-CT using 2-D bone histomorphomtery

Bone architectural parameters generated by the Osteomeasure^{TM} confirmed no significant difference in the baseline trabecular BV/TV of wild-type and TSG-6 deficient mice (**Fig.4.12**), confirming the micro-CT results (**Figure 4.11**). However, in response to ovariectomy, the wild-type group lost significantly more trabeculae in comparison to the non-ovareictomised control, whereas TSG-6 knockout mice did not. This suggests that the globally deficient TSG-6 mice may be **partially** protective against the effects of estrogen deficient-induced bone loss.


Key
Non-ovariectomized (control)
Ovariectomized
A
n.s.
**
n.s.
BV/TV (%)
30
20
10
0
WT
KO
B
n.s.
n.s.
Tb.Th (um)
50
40
30
20
10
0
WT
KO

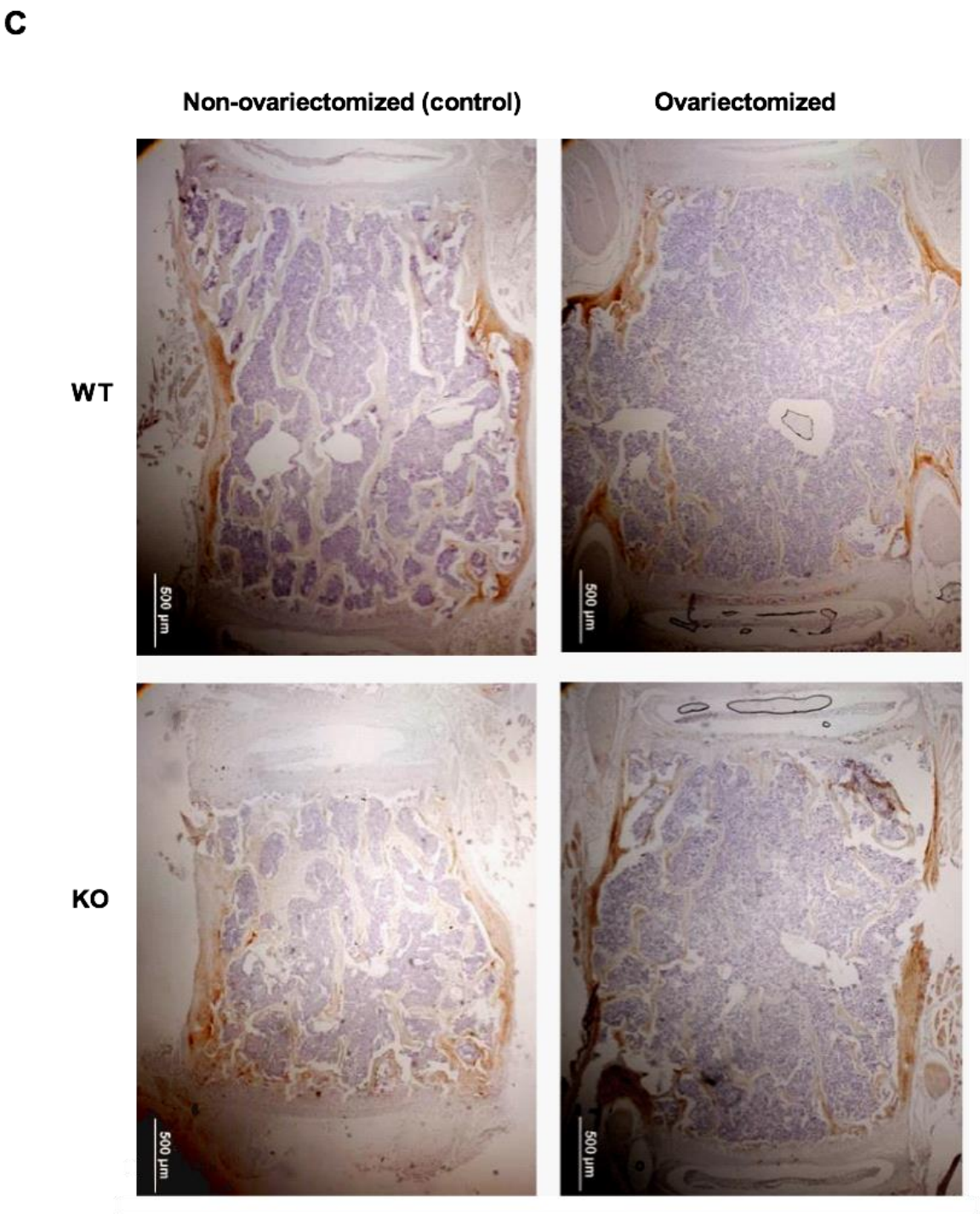


Figure 4. 12 Representative images of vertebral sections from 17 week old wild-type and TSG-6 knockout female mice, with and without ovariectomy.
Mice wild-type and global knockout for TSG-6 gene were ovariectomised at 8-9 weeks of age. The vertebrae were harvested four weeks later, fixed in 10% NBF and stored in 70% ethanol prior to decalcification, paraffin embedding and sectioning.

4.3.5 Global TSG-6 deficiency does not influence osteoblast or osteoclast numbers at four weeks post oestrogen-deficiency induced osteoporosis

Given that in response to ovariectomy the wild-type group lost significantly more trabeculae in comparison to the non-ovareictomised control and the TSG-6 knockout mice did not, it was of interest to investigate how these mice responded at a cellular level. To do so, the cellular distribution of osteoblasts and osteoclasts of the same TSG-6 knockout and wild-type mice shown in **Fig. 4.11** and **4.12** were assessed by 2-D bone histomorphometery (Osteomeasure^{TM}). Cellular distribution of osteoblasts and osteoclasts were counted following osteocalcin (**Fig. 4.13A**) and TRAP (**Fig. 4.13B**) staining, respectively.

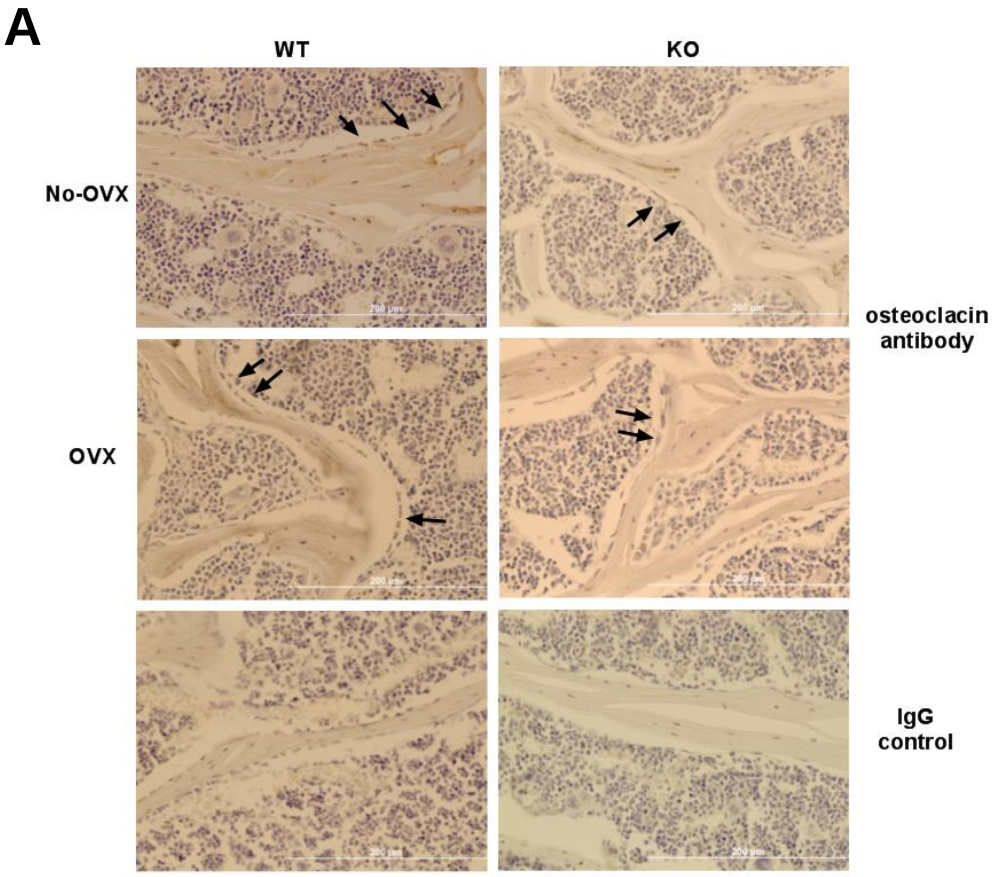


Figure 4. 13 Histology sections showing osteoblast and osteoclasts on lumbar vertebrae of TSG-6 deficint mice four weeks post-ovariectomy.

(A) Osteocalcin and **(B)** TRAP stained sections of TSG-6 deficient mice and wildtype littermates with and without ovareictomy; X40 magniication.

No significant change in **(A)** osteoblasts or **(B)** osteoclasts **(i)** number per tissue area nor **(ii)** size per bone perimeter were found between baseline bone (wild-type, and knockout), nor in response to ovariectomy per respective genotype. These results do not allow conclusions to be drawn on the systemic endogenous role of TSG-6 on osteoblast and osteoclast population during oestrogen deficiency with the reduction in bone mass.

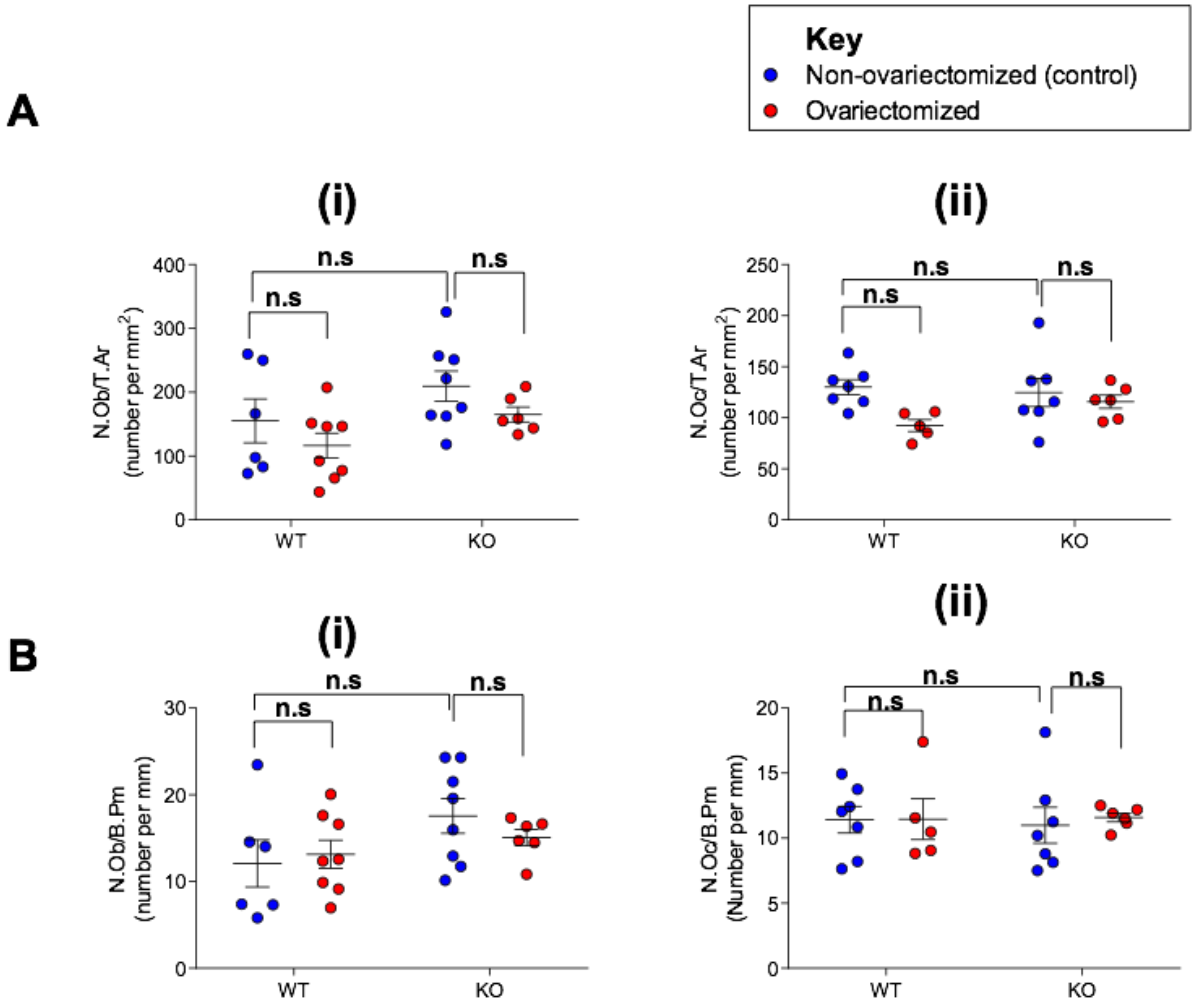


Figure 4. 14 Osteoblast and osteoclast counts from the lumbar vertebrae of TSG-6 deficient mice four weeks post ovariectomy.

(A) osteoblast and osteoclast **(i)** number per tissue area and **(ii)** bone perimeter in 18±1 week old TSG-6 knockout and wild-type mice 4 weeks post-ovariectomy.

The vertebrae were harvested, fixed in 10% NBF and stored in 70% ethanol prior to decalcification, paraffin embedding and sectioning. Following osteocalcin or TRAP staining Osteomeasure™ was used to count the number os osteoblast or osteoclasts respectively. Data are shown as the mean±SEM (n=6-8), statistical differences were determined by Two-Way ANOVA followed by Tukey's post-test (Graph Pad, Prism®), where **P<0.01 and ns; P>0.05

4.3.6 Systemic Administration of the Link domain of TSG-6 does not Influence Bone Loss during Oestrogen-Deficiency Induced Osteoporosis

Although knockout mice have been vital tools in aiding our understanding of genes/proteins function(s), compensatory pathways may influence the skeletal traits. Therefore, the systemic administration of the protein under investigation into wild-type mice models may be more informative and also exclude knock-on effects of other factors.

Previous works have attributed the tissue protective properties of TSG-6 to its Link domain (Dyer et al., 2014, Getting et al., 2002, Milner et al., 2006) (see Chapter 1, Fig. 1.10). The Link module has also been shown to possess partial inhibitory effects on osteoclast activity, with no effects on inhibiting osteoblast formation (Mahoney et al., 2008).

To investigate the role of the Link domain of the TSG-6 protein on osteoporosis-induced bone loss, 8-9 week old BALB/c mice that had undergone bilateral ovariectomy at Charles Rivers Laboratories, were systemically administered 3 times a week with two different doses of rhLink_TSG-6, at 11 week of age, for 4 consecutive weeks. The two doses were 2.75 mg/kg/week (22.9 µg/injection) and a relatively lower dose of 0.275 mg/kg/week (2.29 µg/injection). The groups consisted of a non-ovariectomised naïve group, the ovariectomised – PBS treated negative control, and the 17β-estradiol pellets (Innovative Research America, Florida, USA) receiving positive control group (**see table 4.8 below**).

Table 4. 8 Experimental groups and treatment conditions within the Link_TSG-6 ovariectomy study.

	Group	Condition	Treatment	Dosage	Route of administration	Number at harvest
1	Naïve	Non-ovariectomised	————	2.75 mg/kg/wk	N/A	10
2	Negative control	Ovariectomised	PBS	1X	Intra-peritoneal	10
3	Positive control	Ovariectomised	17-β-estradiol pellet	2.92 µg/wk	Subcutaneous implanted	9
4	Test group 1	Ovariectomised	rhLink_TSG-6	2.75 mg/kg/wk	Intra-peritoneal	9
5	Test group 2	Ovariectomised	rhLink_TSG-6	0.275 mg/kg/wk	Intra-peritoneal	10

4.3.6.1 Link_TSG-6 treatment does not have adverse effect on body mass

To ensure that the treatments had no adverse effect on the mice subjects, their total body mass was monitored by determining their body mass at the start and end of treatment. No significant differences in mean total body mass was found between treatment groups as well as within treatment groups (start and end) (**Fig. 4.14**), as determined by Two-Way ANOVA (GraphPad, Prism®).

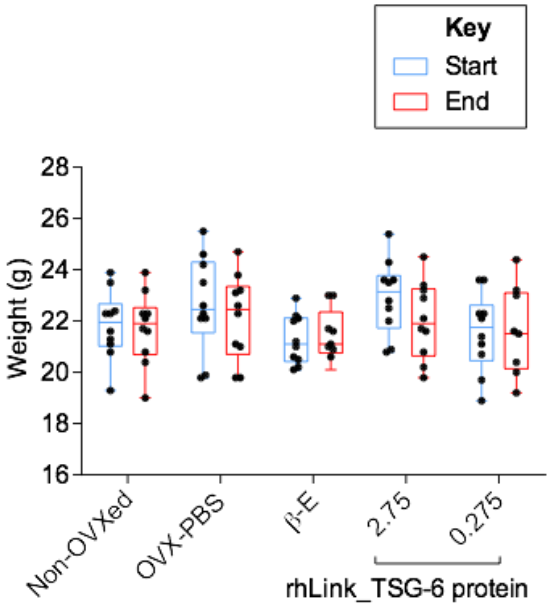


Figure 4. 15 Total body mass before and after treatment with the Link module of TSG-6.
BALB/c mice were weighed (g) using a top-loader scale at the start of treatment and at cull. Statistical test was carried out using Two-way ANOVA (GraphPad, Prism Software).

4.3.6.2 The Link domain of TSG-6 does not alter the biomechanical properties of the femurs during oestrogen-deficient induced bone loss.

In order to investigate the effect of rhLink_TSG-6, on the biomechanical strength of cortical bones, following osteoporosis induction, the right femurs, were stored in 70% ethanol prior to three-point bend testing to failure. The peak force was used to indicate the hardness, whilst the slope determined by the Young's modulus indicated brittleness.

No significant difference was found between the non-ovariectomised naïve group and the ovariectomised-PBS treated group for any of the parameters measured (**Fig. 4.15**). This suggested two possibilities; that either systemic depletion of oestrogen (over the course of six weeks) did not significantly affect the biomechanical properties of the femurs of BALB/c female mice, or that the technique was not sensitive enough to evaluate this property.

A significantly higher fracture load (**Fig. 4.15B**) and elastic modulus (**Fig. 4.15C**) was found in the 17β-estradiol treated ovariectomised group relative to all other treatment groups, suggesting increased femur strength and stiffness, respectively, in response to 17β-estradiol. Moreover, the 17β-estradiol treated group had a significantly lower displacement at fracture (**Fig. 4.15D**) relative to all other groups, which is indicative of an increased brittle phenotype. No significant difference was found in the ovariectomised-Link_TSG-6 treated (low and high dose) groups relative to the ovariectomised-PBS treated control group, suggesting the absence of an altered/recovered bone phenotype in response to rhLink_TSG-6 protein.

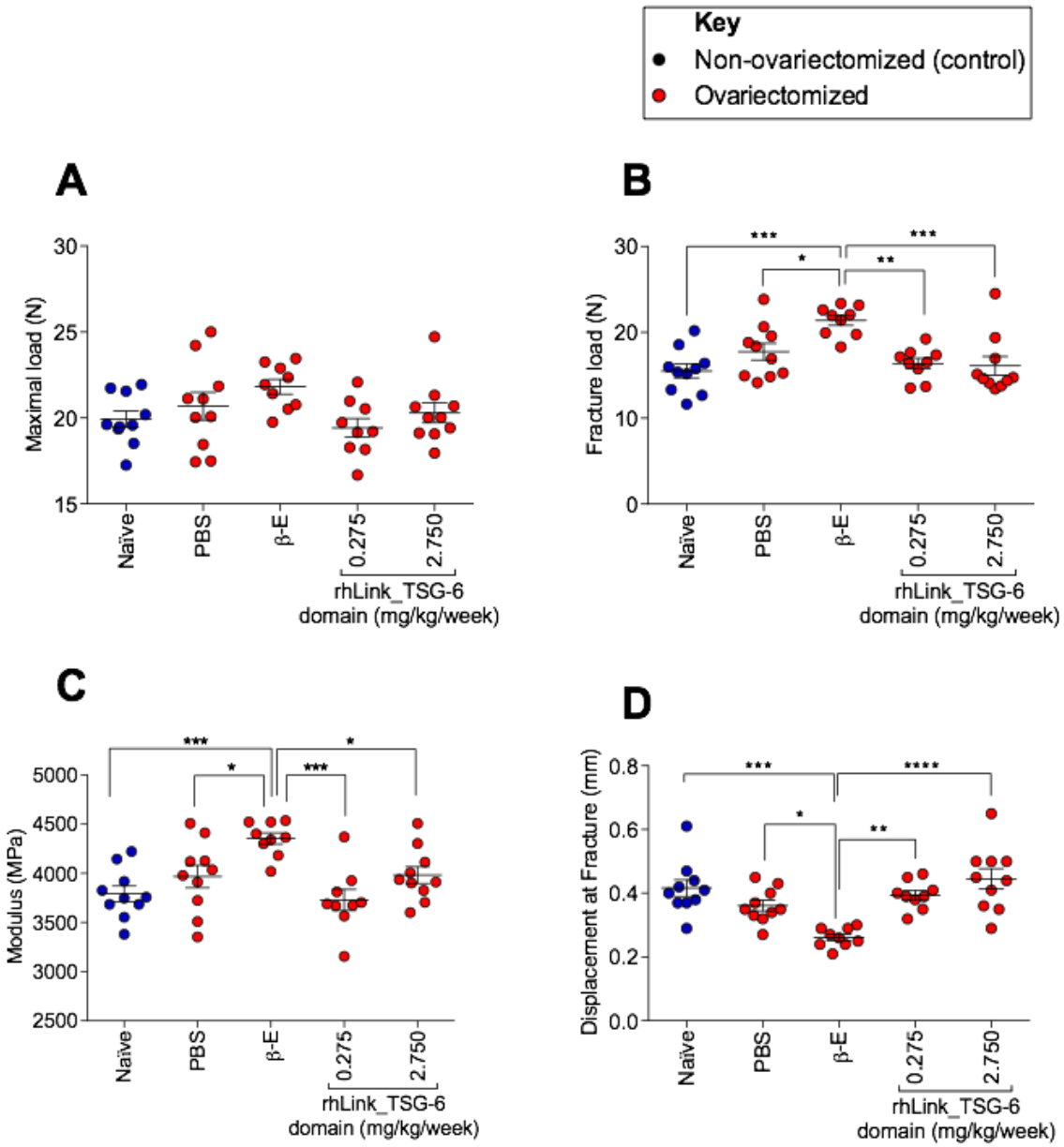


Figure 4. 16 Three-point bend testing showing the Link module of TSG-6 does not influence mechanical properties of the femoral diaphysis following ovareictomy.
The femurs preserved in 70% ethanol after harvest were individually subjected to three-point bending to failure, to assess the (**A**) maximal load, (**B**) fracture load, (**C**) Young's modulus, and (**D**) displacement at fracture. Data are shown as the mean ± SEM (n = 9-10), statistical differences were determined by One-Way ANOVA followed by Dunnett's *post-test* (GraphPad Prism®), where * $P \leq 0.05$; ** $P \leq 0.01$; *** $P \leq 0.001$

4.3.6.3 The Link domain of TSG-6 does not affect the 3-dimensional morphology of cortical and trabecular bone during oestrogen-deficient induced bone loss

As the three-point bend testing was either not sensitive enough to differentiate biomechanical differences in the model of study (i.e. non-ovariectomised vs. ovariectomised), or that there were no differences between treatment groups, the microarchitecture of the pre-fixed left tibiae were analysed by micro-CT (**Fig. 4.16 and table 4.9**).

Six weeks post-ovariectomy, a significant mean decrease in percentage BV/TV (**Fig. 4.16A**), Tb.N (**Fig. 4.16B**) with an increase in Tb.Pf (**Fig. 4.16C**) was found between the PBS-treated ovariectomised mice, compared to the non-ovariectomised naïve group. This indicated an osteoporotic bone phenotype in response to ovariectomy. Furthermore, the osteoporotic bone phenotype was counteracted by subcutaneous implantation of 17β-estradiol pellets, albeit that the dose used resulted in significantly higher bone parameters than the non-OVX mice.

No statistical differences were found in any parameters between the ovariectomised-PBS treated mice and the ovariectomised mice that received the relatively higher dose of rhLink_TSG-6 protein, neither in the tibiae (**Fig. 4.16 and Table 4.9**) nor the vertebral body (**Fig. 4.17**). This shows that rhLink_TSG-6 cannot prevent bone loss following bilateral ovariectomy of BALB/c female mice.

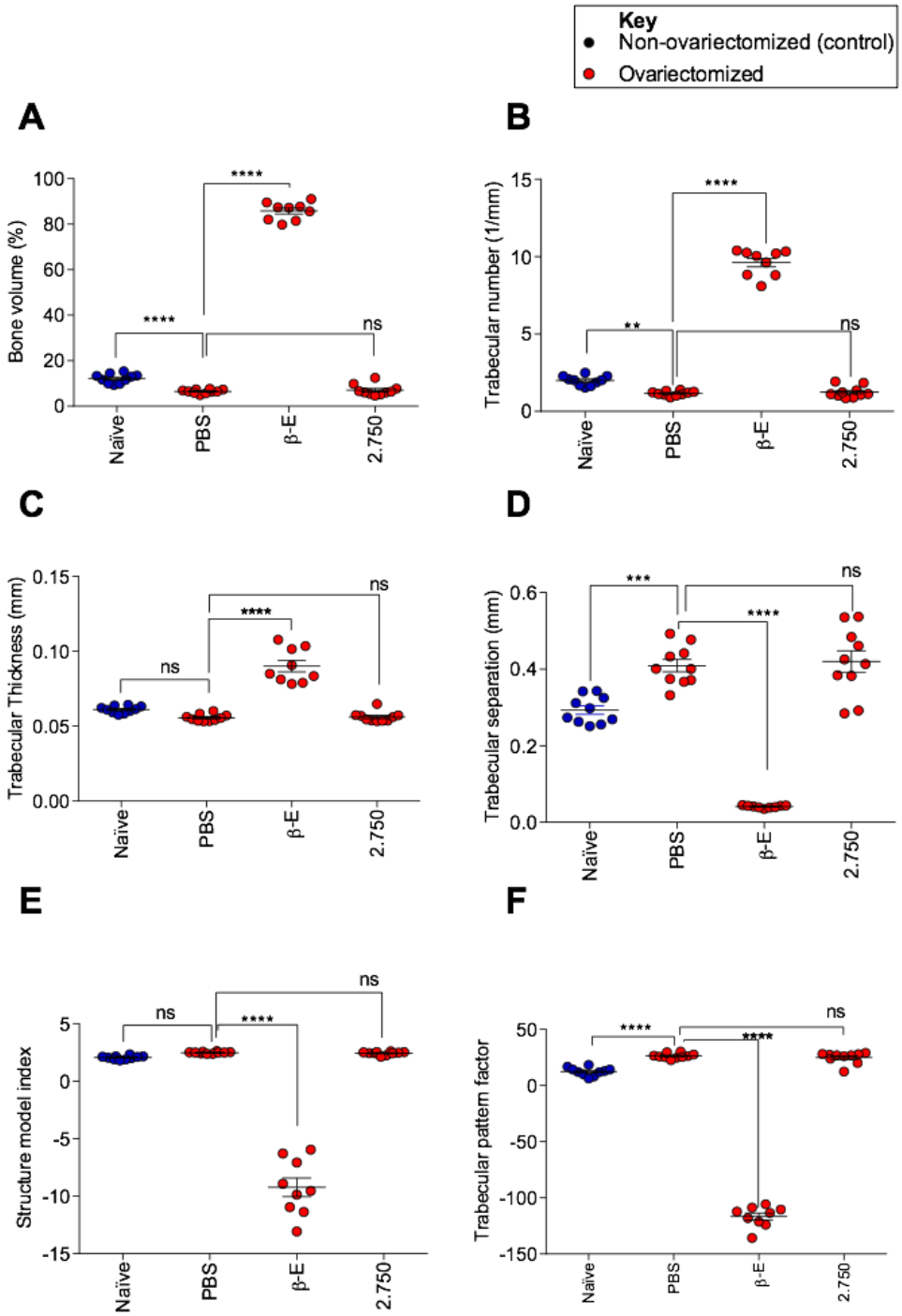


Figure 4. 17 Micro-CT data showing the Link module of TSG-6 does not protect cortical bone against ovariectomy-induced bone loss.

Female BALB/c mice ovariectomised at 8-9 weeks of age received 2.750 mg/kg/week of rhLink_TSG-6 treatment at 11 weeks of age for the duration of 4 weeks. Scatter graphs show the 3-D morphological parameters of the left tibiae as mean ± SEM of 9-10 mice per group. Statistical differences were determined using One-Way ANOVA, followed by Dunnett's *post-hoc* test, where; n.s. $P>0.05$, $^{*}P\leq0.05$ $^{**}P\leq0.01$, $^{***}P\leq0.001$, $^{****}P\leq0.0001$.

Table 4. 9 Quantitative micro-CT parameters from the left tibia of mice systemically treated with Link module of the TSG-6 protein following bilateral ovariectomy.

The table shows the mean ± SEM of 9-10 mice per group.

Structural parameter	Units	Naive	PBS	17β-estradiol	rhLink_TSG-6 domain
Bone surface density	mm^{-1}	9.877 ± 0.5061	6.009 ± 0.2561	27.99 ± 1.254	6.394 ± 0.5952
BS/BV	mm^{-1}	82.00 ± 1.475	93.94 ±1.216	32.87 ±1.963	91.99 ± 2.117
Degree of Antrisopy	N/A	1.9411 ±0.05790	2.025 ± 0.06980	1.268 ± 0.04175	2.030 ±0.07855
Connectivity	mm^3	2916 ± 248.6	1697 ±133.4	9295 ± 986.1	1784 ±269.0
Connectivity density	%	926.9 + 57.96	538.6 + 35.51	3575+ 340.4	560.4 + 78.73
Total volume of pore space	mm^3	2.731 ±0.07747	2.939 ± 0.09316	0.3695 ±0.03708	2.941 ± 0.08886
Total porosity	%	87.83 ±0.6488	93.52 ± 0.2682	14.25 ± 1.283	92.97 ± 0.7620
Volume of open pore space	N/A	2.730 ±0.07746	2.939 ±0.09316	0.3239 ± 0.03746	2.941±0.08886
Open porosity	%	87.83± 0.6493	93.52± 0.2683	12.48 ±1.338	92.97 ± 0.7625
Number of closed pores	N/A	427.4 ± 44.78	130.2 ± 13.63	15211±922.0	160.3 ±40.16
Closed porosity	%	0.06249 ±0.004382	0.03386 ± 0.002728	2.012 ± 0.1017	0.0344 ± 0.004539
Surface of closed pore	mm^2	0.1627 ± 0.01729	0.04789 ± 0.005006	14.97 ± 1.015	0.05741 ± 0.01409
Volume of closed pore	mm^3	0.000241 ±2.618 e-005	6.900 e-005 ±7.667e-00	0.04563 ±0.003539	8.500 e-005 ± 1.996 e-005
Number of objects	N/A	1982 ± 123.0	1583 ±105.0	1655 ± 213.5	1553 ± 1840
Fractal dimension	N/A	2.115 ±0.01147	1.980 ±0.006347	2.570 ± 0.01940	1.992 ± 0.01611

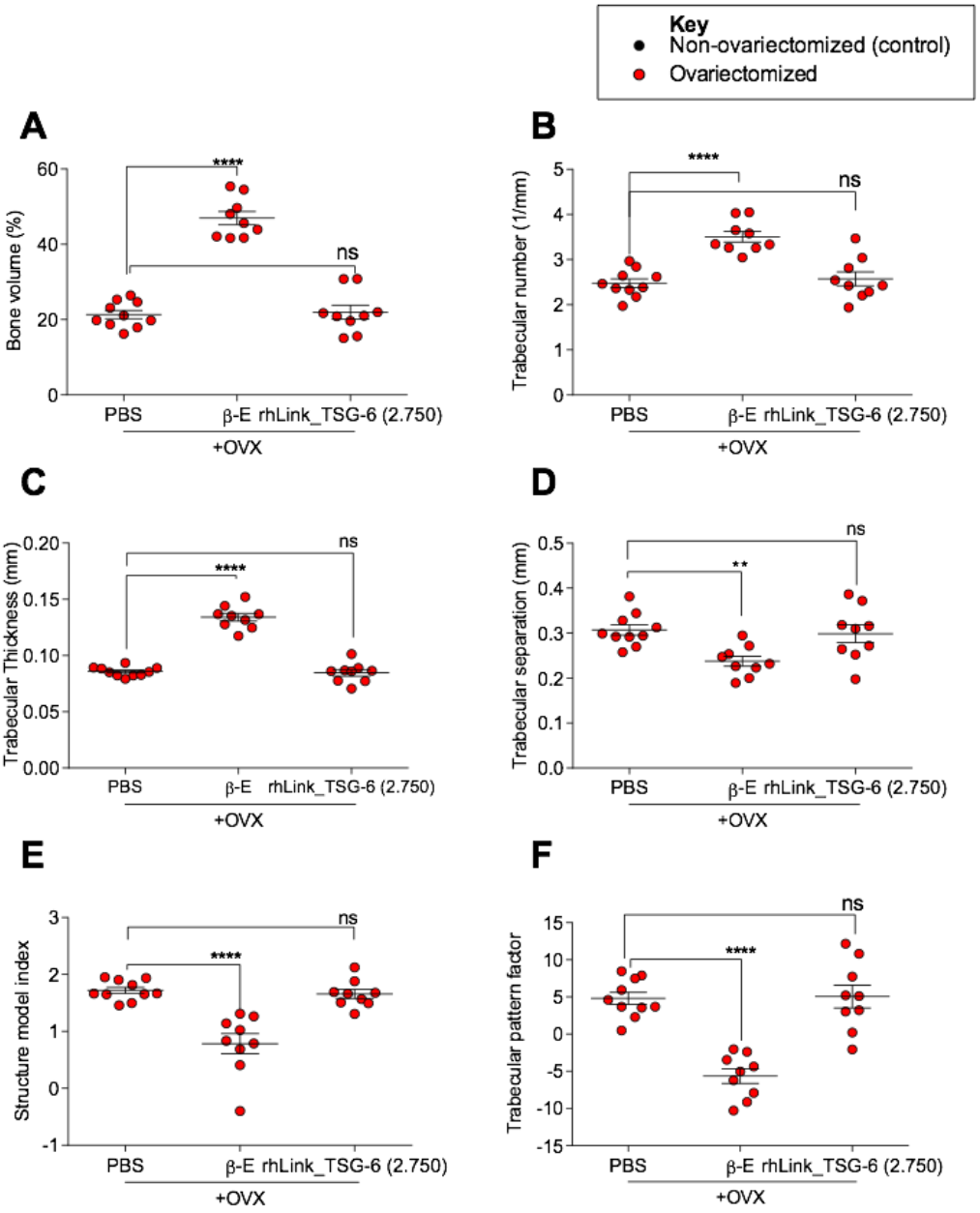


Figure 4. 18 Micro-CT data showing the Link module of TSG-6 does not protect trabecular bone from ovariectomy-induced bone loss.

BALB/c mice were ovariectomised at 8-9 weeks of age and culled at 17 weeks of age. The vertebrae were harvested, fixed in 10% NBF and stored in 70% ethanol prior to scanning. Micro-CT 3-D parameters show (**A**) percentage bone volume, (**B**) trabecular number, (**C**) trabecular thickness, and **(D)** trabecular separation of rhLink_TSG-6 and 17β-estradiol control compared to the age and sex-matched ovariectomised PBS-treated mice. Statistical differences were determined using One-Way ANOVA (GraphPad Prism®), followed by Dunnett's *post-hoc* test where $^{**}P \leq 0.01$.

4.3.7 The Link Domain of TSG-6 does not Enhance Local MAR

As the full-length TSG-6 protein increased MAR *in vivo*, we next ascertained whether the Link module could also directly promote bone formation. To address this, the murine calvaria model was used, where 2.29 µg/day of rhLink_TSG-6 protein, at a molar equivalent of the full-length rhTSG-6 was administered subcutaneously over the calvarial of 5 week old male mice, for five consecutive days. No significant increase in calvarial thickness (**Fig. 4.18A**), intra-label width (**Fig. 4.18B**) or mineral apposition (**Fig. 4.18C**) was detected as determined by 2-D bone histomorphometry, in the Link module treated group, whereas a significant increase in all parameters were found with treatment of the full-length TSG-6. This suggests; that either the Link_TSG-6 protein was functionally inactive, or that the Link module of the TSG-6 protein cannot promote intramembranous *de novo* bone formation. As this model measures osteoblast activity primarily, and given that the Link_TSG-6 model is thought to act on osteoclasts, changes in bone thickness may not be seen.

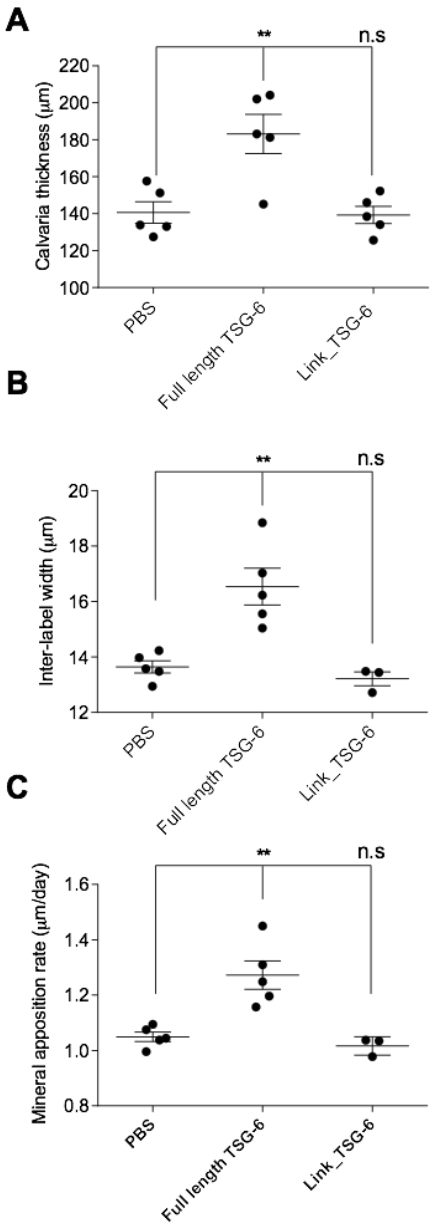


Figure 4. 19 Link module of TSG-6 does not enhance local calvarial MAR.
6.33 µg/day or 2.29 µg/day of the full-length rhSTG-6 or the rhLink domain respectively was injected subcutaneously over the calvaria of 5-week old male C57BL/6J mice, daily for 5 consecutive days. Intra-peritoneal injection of calcein (20 mg/kg) was administered at the start and 24h prior cull to label new bone formation during the course of the assay. Calvaria were harvest on day 14, fixed in 10% NBF for 48h and then stored in 70% ethanol until embedded in methyl methacrylate. Plastic blocks were sectioned and then analysed using by 2-D histomorphometry using the OsteoMeasure™ software to determine calvaria thickness (**A**), inter-label width (**B**) and MAR (**C**). Data shows Mean ± SEM of 3-5 mice. Statistical differences were determined by One-Way ANOVA, followed by Dunnett's post-hoc test where ***P*<0.01, and n.s denotes no significant difference (GraphPad, Prism®).

4.3.8 Systemic Administration of Full-Length rhTSG-6 Protein does not Influence Bone Loss during Oestrogen-Deficiency Induced Osteoporosis

Given that the rhLink_TSG-6 protein did not increase MAR over the calvaria, but the full-length rhTSG-6 did, it was next investigated whether the systemic administration of the full-length rhTSG-6 could prevent bone loss, following oestrogen-deficient-induced bone loss.

A pilot study was carried out to test the efficiency of the route of administration. Mice, ovariectomised at Charles Rivers Laboratories (Surrey, UK), received full-length rhTSG-6 protein, produced in-house, via two different modes of administration (intra-peritoneal and subcutaneous) for 4 week at a dose of 1mg/kg/week.

A significant difference was found between the non-ovariectomised naïve controls compared to the PBS treated ovariectomised mice, for bone volume (**Fig. 4.19A**), trabecular number (**Fig. 4.19B**), and trabecular separation (**Fig. 4.19C**) as measured by micro-CT, indicating that the model of study worked. This may be due to the low number of subjects per group, or the administration of sub-optimal dose.

No significant change in any of the bone parameters were found between intraperitoneal/subcutaneous and the ovariectomised group that received PBS only (**Fig.4.18**). This indicated that the full-length rhTSG-6 protein did not significantly increase bone parameters when given systemically, as opposed to its local effects over the calvaria.

To complete the study, the full-length rhTSG-6 protein will need to be administered subcutaneously (due to the slight difference, albeit not significant), or perhaps test the subcutaneous administration against intravenous administration. Then carry a dose-response study using a range of 10-fold higher and lower of what was used *via* the optimal mode of administration. In addition the number of mice per treatment group must be increase - 10 would be ideal.

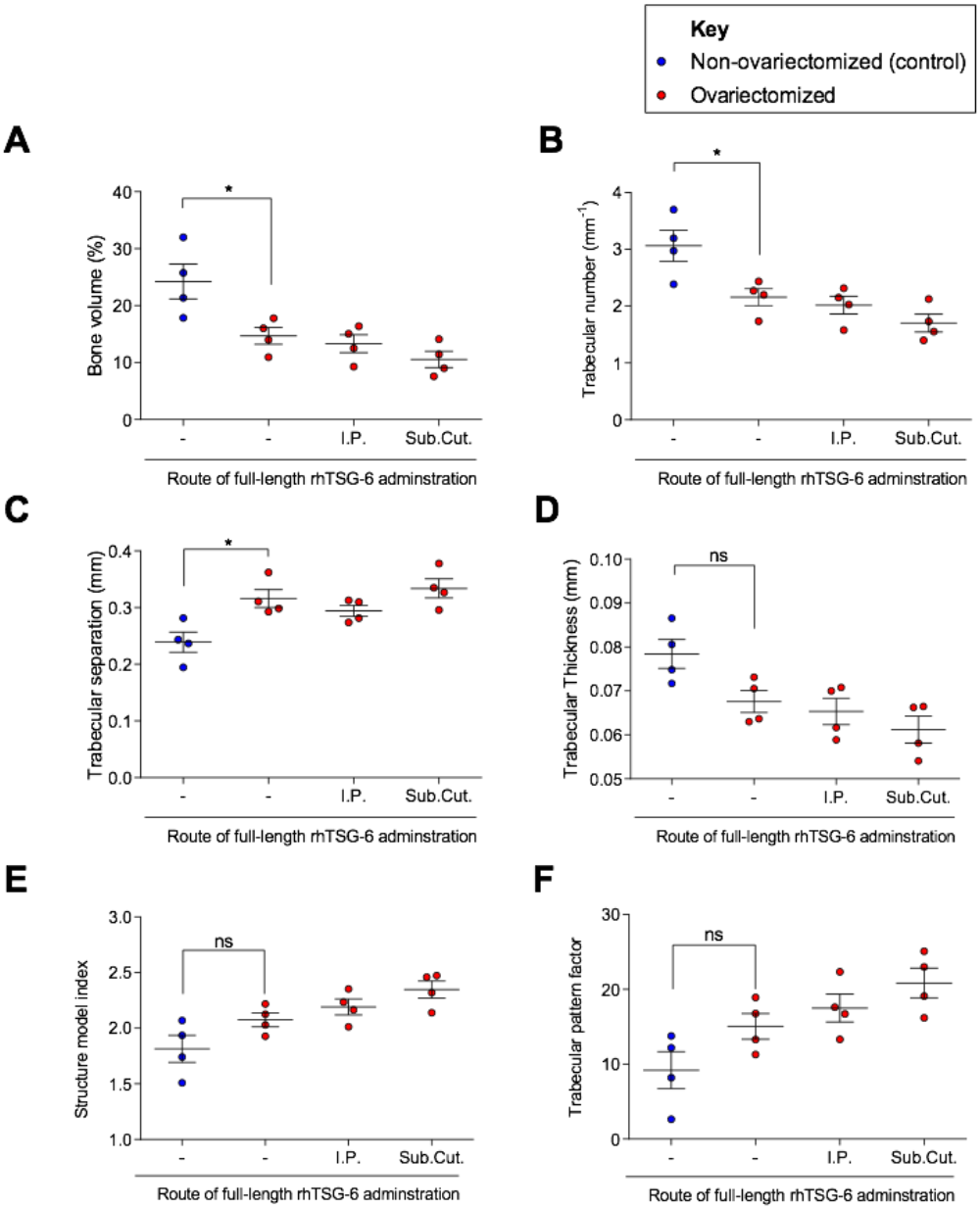


Figure 4. 20 Micro-CT data showing systemic administration of full-length TSG-6 does not protect lumbar vertebrae from ovariectomy-induced bone loss.

Wild-type mice C57BL/6J mice were ovariectomised at Charles Rivers at 8-9 weeks of age, at 11 weeks of age; the mice were treated with full-length rhTSG-6 *via* two different routes of administration. Vertebrae harvested fixed in 10% NBF and stored in 70% ethanol prior to scanning. Micro-CT 3-D parameters show (**A**) percentage bone volume, (**B**) trabecular number, (**C**) trabecular thickness, (**D**) trabecular separation, (**E**) SMI, (**F**) and trabecular pattern factor. Statistical differences were determined using One-Way ANOVA followed by Dunnett's *post-hoc* test (GraphPad Prism®), where; n.s. $P>0.05$, $^{*}P\leq0.05$.

4.4 DISCUSSION

Identification of novel bone anabolics is driven by the clinical need to treat fragility disorders, like osteoporosis (Ferrari, 2012, Harvey et al., 2010). Such conditions ideally require a treatment that can promote bone formation whilst simultaneously inhibiting bone resorption (Lewiecki, 2011). Although TSG-6 has been shown to prevent osteoclast differentiation and activity (Mahoney et al., 2008, Mahoney et al., 2011)(also see Chapter 3 section x), its role in osteoblastogenesis remains unclear. Early studies associated TSG-6 with delayed bone erosion in murine models of inflammation (Bardos et al., 2001, Mindrescu et al., 2002, Mindrescu et al., 2000, Szanto et al., 2004); however, later studies found TSG-6 to inhibit osteoblastogenesis *in vitro* (Mahoney et al., 2008, Tsukahara et al., 2006). The investigation of the role of TSG-6 on bone *in vivo* is presented in this chapter, using both physiological and pathological models in an effort to delineate which of the two biological functions prevails within a complex biological setting.

In this work, it was found that, the baseline bone mass of TSG-6 deficient female mice on a purebred C57BL/6J background was lower than their wild-type littermate controls. This finding was not in agreement with previous findings reported by Mahoney *et al*. who used purebred BALB/c background reported by Mahoney *et al.* (2008) and found TSG-6 deficient male mice to have higher bone mass than their wild-type littermates (Mahoney et al., 2008). As our baseline bone phenotype were conducted on female mice, whereas Mahoney *et al.* conducted the study on male mice, a contributing factor to the lack of similarities in results may stem from gender differences.

This may be further supported by another piece of information reported by the Mahoney *et al.* (2008) studies. The authors report that while the baseline phenotype of TSG-6 deficient mice demonstrated higher bone phenotype, compared to the wild-type litterma-

tes, osteoclasts generated from female TSG-6 deficient bone marrow-flushed HSCs demonstrated enhanced bone erosion. The effect of gender-specific differences on skeletal phenotype has previously been reported in markers such as for CD59 - a surface glycoprotein that inhibits the activity of the complement membrane attack complex. A deficiency in CD59 has been associated with increased femur length and cortical volume of male mice, with no changes to femur length or cortical volume observed in female mice (Bloom et al., 2016). Similarly, haplodeficiency of Lef-1 – a transcription factor that mediates Wnt signalling involved in the modulation of bone mass, significantly decreased bone mass of female but not male mice (Noh et al., 2009). However, to address whether TSG-6 has a gender-specific function on bone architecture, the baseline bone phenotype of age-matched male and female littermates should be studied and compared.

The impact of embryonic gene deletion of TSG-6 on bone architecture of mature skeletal mice must be interpreted with caution because the global knock-out of TSG-6 at an embryonic level may have other subsequent effects and could influence bone development. This further complicates the model of study, and results obtained cannot be generalised. Perhaps a model where wild-type, skeletally mature, C57BL/6J mice are treated with TSG-6 neutralising antibody for a period of time may be more conclusive, albeit antibody administration does have its own challenges such as immunogenicity of the antibody fragments.

It is tempting to assume the baseline bone phenotype obtained from both our and Mahoney *et al.* (Mahoney et al., 2008) TSG-6 knockout study was due to the absence of TSG-6. However, there is a possibility that the phenotype observed may also be due to tightly-linked loci proximal to the gene of target (Eisener-Dorman et al., 2009). To test whether the observed phenotype is indeed due to the absence of TSG-6, rhTSG-6

could be administered to TSG-6 knockout mice to address whether the phenotype can be reversed. However, a better understanding of endogenous TSG-6 expression levels, spatial and temporal expression patterns are required.

The systemic administration of TSG-6 did not protect against bone loss from the effects of ovareictomy **(Fig. 4.19)**. This may be due to insufficient protein being administered given its recently reported in vivo half-life of ~28 min (Kim et al., 2016). Other possible explanations include inefficient mode of protein delivery, or that TSG-6 may not play a role on oestrogen-deficient induced bone loss. Although ovariectomy is considered 'gold-standard' model of post-menopausal osteoporosis the relative impact of oestrogen deficiency and inflammation in bone loss during post-menopausal osteoporosis is not yet established, therefore, further experiments will be required to delineate the role of TSG-6 during *in vivo* bone pathology.

Although the local administration of TSG-6 promoted bone formation, the systemic administration did not. This may be due to insufficient protein administered, or its mode of administration which makes its crucial to determine its *in vivo* half-life. Well-established bone anabolic factors such as BMP-2 and PTH have been reported to exhibit differing effects (anabolic/catabolic) depending on the mode of administration. Moreover, the anti-inflammatory role of TSG-6 is noticeable *via* the intravenous route in contrast to intra-peritoneal (Bardos et al., 2001). Previous protective functions of TSG-6 on bone erosion in murine models of arthritis used intravenous delivery (Szanto et al., 2004) and used established inflammatory models. Therefore further studies must be carried out to delineate the mechanism of TSG-6 action, the optimal route of administration and dosing regiments.

Contrary to the belief that TGS-6 inhibits bone formation (Mahoney et al., 2008, Tsukahara et al., 2006), TSG-6 has exhibited anabolic properties when delivered locally

in developing mice (**Fig. 4.6**), the biological significance of which has been confirmed in a dose-relation study (**Fig. 4.9**). This is the first study to show full-length rhTSG-6 to significantly increase MAR. Although most functions of TSG-6 have been attributed to its Link domain (Kim et al., 2016), rhLink_TSG-6 did not enhance MAR over the calvaria, whereas the full-length rhTSG-6 did, when used at equimolar quantities to one another (**Fig. 4.17**). However in Chapter 3 (**section 3.3.6**), we have shown that the anabolic effects of full-length TSG-6 *in vitro* are mediated by BMP-2 (**Fig.3.7D**), and Mahoney *et al*. have previously shown that TSG-6 binds BMP-2 *via* residues spanning both the Link and CUB domains (Mahoney et al., 2008). This is significant because the function of the CUB domain is not very well understood, with fibronectin as its only known ligand (Kuznetsova et al., 2008). Fibronectin is an ECM glycoprotein that enhances osteoblast survival and differentiation in rat calvaria (Globus et al., 1998, Moursi et al., 1996). It has also been shown that expression of fibronectin can be enhanced with BMP-2 (Shah et al., 1999), this may imply that the CUB domain alone or both domains are essential for TSG-6 anabolic function in a fibronectin dependent mechanism.

These findings have implications in developing synthetic osteoinductive scaffold especially ones coated with BMP-2 in order to augment its anabolic activity. Other possibilities include local usage for at sites of bone fracture to enhance tissue healing.

5

CHAPTER 5: DISCUSSION

Osteoporosis is progressive, systemic skeletal disorder caused by a deregulation of bone metabolism (Rivadeneira and Makitie, 2016). Currently affecting 200 million people worldwide (Riancho and Hernandez, 2012), the disease is characterised by low BMD, predisposing individuals to increased risk of bone fractures (Troy and Morse, 2015). The primary aim of clinical intervention is to strengthen or heal bone, ideally, through tissue regenerative strategies. Despite the availability of various therapies, such as; bisphosphonates, SERMs, denosumab, hormone therapy and PTH, this objective remains largely unmet due to limitations associated with each option and, at times, the lack of translatability from laboratory experiments to human patients (Black et al., 2006, Martino et al., 2004, Rizzoli et al., 2011). This has created a demand for the discovery of novel bone anabolics.

Recently, much attention is given to the immune system's engagement in bone regeneration (Chang et al., 2008, Pettit et al., 2008), with one integral interaction being that of monocytes/macrophages and osteoblast precursors – the MSCs (Fernandes et al., 2013, Guihard et al., 2012, Nicolaidou et al., 2012). TSG-6 mRNA is upregulated during this interaction (PhD thesis of Dr. Nicolaidou, 2011), and independent studies have shown its protective roles, in disease models, on tissues of mesenchyme origin, such as cartilage (Glant et al., 2002) and corneal epithelium (Kim et al., 2014b). This thesis therefore hypothesised TSG-6 to be anabolic in relation to bone remodelling. The project began with the expression and purification of biologically active cell-culture grade full-length rhTSG-6 for downstream *in vitro* and *in vivo* studies. Exogenous treatment of BM-hMSCs with full-length rhTSG-6 was found to significantly enhance early osteoblast differentiation *in vitro*, in a dose-dependent manner, when BMP-2 was present. This also translated to a dose-dependent increase in MAR *in vivo* when administered, locally, over the calvaria of developing mice. However, the protein did not protect trabecular bone from the effects of oestrogen-deficiency induced bone loss. Therefore under dis-

ease settings the hypothesis was disproved. These findings imply that although TSG-6 does have anabolic properties, this property may prevail in a context-specific manner.

Although many groups have associated TSG-6 with tissue protective functions in animal models of arthritis (Choi et al., 2011a, Danchuk et al., 2011, Glant et al., 2002, Lee et al., 2009, Mindrescu et al., 2002, Mindrescu et al., 2000, Oh et al., 2010, Roddy et al., 2011) myocardial infarction (Lee et al., 2009) and lung injury induced by exposure to LPS (Danchuk et al., 2011) as well as eye injury (Oh et al., 2010), these models shared a common feature of an inflammatory response. Whether oestrogen-deficient induced osteoporosis could be, adequately, 'labelled' as an inflammatory model is debatable (D'Amelio et al., 2008, Ganesan et al., 2005, Ginaldi et al., 2005, Pacifici, 2010, Yousefzadeh et al., 2006, Yun and Lee, 2004). Therefore, the ligands/cells/conditions required for the protective functional properties of TSG-6 may be absent in a non-inflammatory milieu.

If time had permitted, perhaps a model such as the 'fracture healing model' would have been more appropriate. This model consists of four distinct phases: (i) inflammation, (ii) soft callus formation, (iii) hard callus formation, and (iv) remodelling (Pivonka and Dunstan, 2012). The inflammatory phase is essential for optimal healing (Barry, 2010, Lu et al., 2012). During this phase, proinflammatory factors such as TNF-α, IL-1β as well as BMP-2,4 and 6, that bind TSG-6, are released early on (Chan et al., 2015, Cho et al., 2002, Einhorn, 1998, Glass et al., 2011). Similarly, in rat models of chemically-injured cornea, TSG-6 was only found to be protective when administered at the start of the inflammatory response (Oh et al., 2010). Other inflammatory murine models of bone disease to consider include; chronic recurrent multifocal osteomyelitis (Hentunen et al., 2000), collagen type II-induced arthritis (Choi et al., 2011b), or perhaps even the LPS murine model of acute bone loss (Orcel et al., 1993), as TSG-6 has been shown to be protective against the LPS challenge in other disease models (Liu et al., 2014).

Perhaps the best characterised protective function of TSG-6 is largely down to its ability to inhibit the recruitment and homing of neutrophils to the inflammatory sites (Wisniewski et al., 1996, Szanto et al., 2004, Roddy et al., 2011, Lee et al., 2009, Getting et al., 2002, Danchuk et al., 2011, Choi et al., 2011a, Cao et al., 2004), by interacting with the GAG binding site of CXCL-8 (Dyer et al., 2014). Although insufficient recruitment of neutrophils may be damaging to the host, in that, infection cannot be dealt with properly (Zarbock et al., 2012), excessive infiltration, a characteristic feature of chronic inflammation (Medzhitov, 2010), leads to the abundance of MMP, proinflammatory cytokines, and also chemokines that further recruit inflammatory cells (Watanabe et al., 2013, Szanto et al., 2004, Oh et al., 2010, Lee et al., 2009, Danchuk et al., 2011), causing tissue damage. However, given that in AIA, the chondroprotective effect of TSG-6 was not mediated through anti-inflammatory events (Glant et al., 2002) suggests that the mechanism of tissue protection does not wholly rely on inhibiting inflammatory cells. Other protective functions of TSG-6 include ability to inhibit the protease network (Wisniewski et al., 1996, Mahoney et al., 2005), as well as its catalytic ability to cross-links HA (Baranova et al., 2011) – an essential component of the reparative phase of callus formation (Maurer and Hudack, 1952, Ayanoglu et al., 2015), signifying a role in matrix stability and integrity essential for tissue morphogenesis. Moreover, in Chapter 3, we found TSG-6 to enhance BMP-2 mediated osteogenesis, indicating its role on bone protection may be down to its anabolic properties.

The diverse range of ligands that TSG-6 can bind to and the fact that some of them, such as; heparin and HA, are ubiquitously expressed presents the possibility that the lack of bone protection in the osteoporosis model may have been due to the mode of administration. The intra-peritoneal mode of administration proved unsuccessful, possibly due to the ligands present in the abdomen that retain TGS-6 and prevent it from getting to other sites. Most studies that have shown TSG-6 to be tissue protective

(Yang et al., 2014, Lee et al., 2009, Bardos et al., 2001), have done so using the intravenous mode of administration; delivering the protein directly into the blood circulation for systemic distribution, or have delivered TSG-6 locally (e.g. to the cornea), with respect to the spatial proximity of the site of delivery to the site of tissue analysis (Oh et al., 2010, Lee et al., 2009, Kim et al., 2014b). Local delivery of TSG-6 used in the calvaria study, unveiled the *in vivo* anabolic properties of TSG-6 on bone tissue for the first time. Therefore delivery methods may be a significant contributing factor to the outcome. The advantage of using the calvarial model was the feasibility of delivering a designated amount of TSG-6 protein locally and in close proximity to bone cells and determine quantitative changes in MAR. In systemic delivery however, TSG-6 targets a wider population of cells as well as the lymphoid organs, increasing the chances of the protein being 'cleared up', or binding soluble ligands or receptors on cells, decreasing the chances of it reaching the skeletal site. In addition exposure to various cells types means more complex remodelling pathways are influenced.

In contrast, subcutaneous administration delivers TSG-6 to the hypodermis of the skin, a site consisting of GAGs, such as HA within the extracellular space (Richter and Jacobsen, 2014). This therefore presents the possibility that much of the protein administered was retained at the hypodermis and not immediately transported into the bloodstream and to the site of interest. In addition, given the relative MW of the TSG-6 protein (~29 KDa), a more likely route to circulation would be *via* the lymphatics (Supersaxo et al., 1990).

A method to resolve the issue of protein retention, at unwanted sites, may include bioengineering the full-length TSG-6 protein in such a way to mutate the amino acid that encourage excessive interaction with GAGs and other ubiquitously express factors. Given that most studies have attributed the effects of TSG-6 on stem cells and macrophages to HA-mediated CD44 signalling (Choi et al., 2011a, Day and de la Motte, 2005,

Lesley et al., 2004, Petrey and de la Motte, 2014) suggest the HA binding site to be crucial for TSG-6 activity. However, given that heparin sulphate can 'switch-off' HA binding (Mahoney et al., 2005), this might suggest a target site for mutation. Although using mutants would require a prior knowledge of which fragment of TSG-6 is essential for its osteogenic properties – an aspect currently undetermined. If TSG-6 mediates its osteogenic effects *in vivo* through BMP-2, as it does *in vitro*, then affinities of individual mutants must be compared to its full-length form as Mahoney *et al.* (2008) demonstrated the full-length to bind BMP-2 with greater affinity than individual domains (Mahoney et al., 2008). In addition, anabolic properties of TSG-6 mutants generated to decrease retention and at unwanted sites must be tested *in vitro* prior to their *in vivo* test of efficacy.

Drug exposure time and absorption rates, a function of the mode of administration, are also of high relevance in the context of skeletal metabolism. The subcutaneous route of protein delivery results in a relatively slow absorption rate, extending the duration of exposure (Mager and Jusko, 2002). Other well-established anabolic drugs, such as PTH (Collinge and Favela, 2016), have been shown to have differing metabolic activities on bone based on the duration of exposure. Daily administration at a low dosage leads to anabolic effects (Greenspan et al., 2007, Neer et al., 2001), whereas a sustained exposure leads to bone loss, as seen clinically in primary hyperparathyroidism (Majid et al., 2016). PTH-mediated bone formation is partially attributed to a decrease of sclerostin expression by osteocytes, and its catabolic properties occur by enhancing osteoblast-derived RANKL and concomitantly decreasing OPG (Ishtiaq et al., 2015). The gene profile of intermittent to continuous administration in both *in vivo* and *in vitro* is different, where the former was associated with genes that regulate bone formation and the latter with genes that regulate resorption (Locklin et al., 2003). This may also explain why the outcome of TSG-6 on calvarial bone model was different to that of the oestrogen-

deficient induced osteoporosis model. In the former study, acute exposure at the start of the assay was given, whereas a sustained exposure was achieved over a longer period of four weeks in the latter study by frequent administrations throughout the course of the assay. However, despite the frequent administration of the protein, we cannot be certain whether the protein was in the system long enough to take effect as the half-life of TSG-6 *in vivo* was not known. In an effort to study the half-life of the protein *in vivo*, TSG-6 was intraperitoneally injected in mice and cardiac punctures were carried out, at set intervals, to obtain blood. Failure of TSG-6 recovery from the plasma using ELISA, even when rhTSG-6 was directly spiked into plasma of varying dilutions, hindered our ability to study the half-life of the protein *in vivo* following systemic delivery. Although recently the half-life of the protein was reported *in vivo* who reported a half-life of 0.47h (~28 min) for the protein (Kim et al., 2016). Unlike us, they used the intravenous route of administration followed by cardiac puncture and, to eliminate the chances of false positive as a result of co-purified blood coagulation, blood was collected using heparin coated tubes. This information could now be used to determine the dosing regiments of future *in vivo* studies. It also indicates that suboptimal TSG-6 dosing regime was employed in the ovariectomy-induced osteoporosis model, as each mice received 25 µg/injection every 48 h.

Various studies have described the use of osteo-conductive scaffolds that carry BM-MSCs as well as scaffolds loaded with osteoinductive growth factors (Boden, 2000, Boden et al., 2002, Jaiswal et al., 1997, Jiang et al., 2002, Khashan et al., 2013, Kruyt et al., 2004, Pittenger et al., 1999). Synthetic scaffolds have also been coated with osteoinductive factors, growth factors, and peptides with the aim of creating a pro-osteogenic local environment to favour bone regeneration. One factor that has been at the forefront of this is BMP-2 (Wang et al., 2016). Milligram amounts need to be used in humans to induce osteogenic effects, such supra-physiological levels can lead to com-

plications, such as; ectopic bone formation (Wong et al., 2008), formation of cyst-like bone void formation, as well as osteoclast activation and its associated resorptive phase that could arise both directly, due to the presence of BMP receptors on osteoclasts (Itoh et al., 2001, Kanatani et al., 1995, Kaneko et al., 2000), and/or indirectly *via* osteoblasts and/or stromal cells that respond by expressing pro-osteoclastogenic factors (Kanatani et al., 1995, Koide et al., 1999). The finding that TSG-6 improves the osteogenic ability of BMP-2 could potentially be exploited to improve the osteoinductive properties of BMP-2 at a lower dose and prevent off-target effects. Past studies have used BMP subtypes, namely; BMP-2 and BMP-7, in isolation. Perhaps multiple factors to tailor a cellular response would achieve a more physiological dosing regimen. However, further understanding of the signalling pathways may be necessary to ensure correct targeting and understand potential off-target effects.

Through the course of this project, the major challenge was that the TGS-6 protein yield was quite low. Recently the scalable production of high yield TSG-6 (5 mg per mL of media) has been reported (Kim et al., 2016) using CHO as host cells, and bioreactors. This protein was found to exhibit a longer half-life than that of commercially available TSG-6. This allows different avenues of investigation. For example, as structural studies require protein amounts on milligram per mL scale, the crystal structure of TSG-6 can be elucidated from the full-length rhTSG-6 protein to obtain information in regards to the structure of the protein and elucidate structure-function relationships to understand molecular dynamics and used to make a pharmacophore models should it prove a valuable anabolic.

Future works looking at the *in vivo* effect of TSG-6 on bone tissue could use inflammatory models, such as the bone fracture healing, with specific attention to the initial phase of inflammation. As monocyte/macrophages are early players of this phase it would be

interesting to investigate whether TSG-6 can influence their phenotypic polarisation, and contribute to anti-inflammatory events and bone repair. These studies could be accompanied by histological examination to look at tissue quality, as opposed to morphological changes only.

In summary, this is the first study that demonstrates a bone anabolic role of TSG-6 both *in vitro* as well as *in vivo*. However, its anabolic property was found to be context specific, influenced by the model of study, route of administration, and possibly dose. Understanding the signalling pathway TSG-6 utilizes could potentially pave way for the discovery of other potential bone regulatory factors, within this pathway, with clinical application for treating local bone injuries. However, to ensure successful translation of TSG-6 from murine models to human patients, pharamcokinetics, mode of delivery, frequency and timing must be compared.

6

CHAPTER 6: BIBLIOGRAPHY

REFERENCES

ABD-ALLAH, S. H., SHALABY, S. M., ABD-ELBARY, E., SALEH, A. A. & EL-MAGD, M. A. 2015. Human peripheral blood CD34+ cells attenuate oleic acid-induced acute lung injury in rats. *Cytotherapy,* 17**,** 443-53.

ABDEL SALAM, A. G., ATA, H. M., SALMAN, T. M., RASHED, L. A., SABRY, D. & SCHAALAN, M. F. 2014. Potential therapeutic utility of mesenchymal stem cells in inflammatory bowel disease in mice. *Int Immunopharmacol,* 22**,** 515-21.

ABDELGAWAD, M. E., DELAISSE, J. M., HINGE, M., JENSEN, P. R., ALNAIMI, R. W., ROLIGHED, L., ENGELHOLM, L. H., MARCUSSEN, N. & ANDERSEN, T. L. 2016. Early reversal cells in adult human bone remodeling: osteoblastic nature, catabolic functions and interactions with osteoclasts. *Histochem Cell Biol*.

ABDELWAHED, W., DEGOBERT, G., STAINMESSE, S. & FESSI, H. 2006. Freeze-drying of nanoparticles: formulation, process and storage considerations. *Adv Drug Deliv Rev,* 58**,** 1688-713.

ABU-AMER, Y. 2001. IL-4 abrogates osteoclastogenesis through STAT6-dependent inhibition of NF-kappaB. *J Clin Invest,* 107**,** 1375-85.

ABU-AMER, Y., ABBAS, S. & HIRAYAMA, T. 2004. TNF receptor type 1 regulates RANK ligand expression by stromal cells and modulates osteoclastogenesis. *J Cell Biochem,* 93**,** 980-9.

ADEEL, S., SINGH, K., VYDARENY, K. H., KUMARI, M., SHAH, E., WEITZMANN, M. N. & TANGPRICHA, V. 2013. Bone loss in surgically ovariectomized premenopausal women is associated with T lymphocyte activation and thymic hypertrophy. *J Investig Med,* 61**,** 1178-83.

AGGARWAL, S. & PITTENGER, M. F. 2005. Human mesenchymal stem cells modulate allogeneic immune cell responses. *Blood,* 105**,** 1815-22.

AKIYAMA, H., CHABOISSIER, M. C., MARTIN, J. F., SCHEDL, A. & DE CROMBRUGGHE, B. 2002. The transcription factor Sox9 has essential roles in successive steps of the chondrocyte differentiation pathway and is required for expression of Sox5 and Sox6. *Genes Dev,* 16**,** 2813-28.

AKIYAMA, H., KIM, J. E., NAKASHIMA, K., BALMES, G., IWAI, N., DENG, J. M., ZHANG, Z., MARTIN, J. F., BEHRINGER, R. R., NAKAMURA, T. & DE CROMBRUGGHE, B. 2005. Osteo-chondroprogenitor cells are derived from Sox9 expressing precursors. *Proc Natl Acad Sci U S A,* 102**,** 14665-70.

ALEXANDER, K. A., CHANG, M. K., MAYLIN, E. R., KOHLER, T., MULLER, R., WU, A. C., VAN ROOIJEN, N., SWEET, M. J., HUME, D. A., RAGGATT, L. J. & PETTIT, A. R. 2011. Osteal macrophages promote in vivo intramembranous bone healing in a mouse tibial injury model. *J Bone Miner Res,* 26**,** 1517-32.

ALIPRANTIS, A. O., UEKI, Y., SULYANTO, R., PARK, A., SIGRIST, K. S., SHARMA, S. M., OSTROWSKI, M. C., OLSEN, B. R. & GLIMCHER, L. H. 2008. NFATc1 in mice represses osteoprotegerin during osteoclastogenesis and dissociates systemic osteopenia from inflammation in cherubism. *J Clin Invest,* 118**,** 3775-89.

ALTMANN, F., STAUDACHER, E., WILSON, I. B. & MARZ, L. 1999. Insect cells as hosts for the expression of recombinant glycoproteins. *Glycoconj J,* 16**,** 109-23.

AMANO, S., NAGANUMA, K., KAWATA, Y., KAWAKAMI, K., KITANO, S. & HANAZAWA, S. 1996. Prostaglandin E2 stimulates osteoclast formation via endogenous IL-1 beta expressed through protein kinase A. *J Immunol,* 156**,** 1931-6.

ANDERSEN, T. L., ABDELGAWAD, M. E., KRISTENSEN, H. B., HAUGE, E. M., ROLIGHED, L., BOLLERSLEV, J., KJAERSGAARD-ANDERSEN, P. & DE-

LAISSE, J. M. 2013. Understanding coupling between bone resorption and formation: are reversal cells the missing link? *Am J Pathol,* 183**,** 235-46.

ANDERSON, D. M., MARASKOVSKY, E., BILLINGSLEY, W. L., DOUGALL, W. C., TOMETSKO, M. E., ROUX, E. R., TEEPE, M. C., DUBOSE, R. F., COSMAN, D. & GALIBERT, L. 1997. A homologue of the TNF receptor and its ligand enhance T-cell growth and dendritic-cell function. *Nature,* 390**,** 175-9.

ARANA-CHAVEZ, V. E., SOARES, A. M. & KATCHBURIAN, E. 1995. Junctions between early developing osteoblasts of rat calvaria as revealed by freeze-fracture and ultrathin section electron microscopy. *Arch Histol Cytol,* 58**,** 285-92.

ARONOW, M. A., GERSTENFELD, L. C., OWEN, T. A., TASSINARI, M. S., STEIN, G. S. & LIAN, J. B. 1990. Factors that promote progressive development of the osteoblast phenotype in cultured fetal rat calvaria cells. *J Cell Physiol,* 143**,** 213-21.

ARRIERO MDEL, M., RAMIS, J. M., PERELLO, J. & MONJO, M. 2012. Inositol hexakisphosphate inhibits osteoclastogenesis on RAW 264.7 cells and human primary osteoclasts. *PLoS One,* 7**,** e43187.

ARRON, J. R. & CHOI, Y. 2000. Bone versus immune system. *Nature,* 408**,** 535-6.

ASAGIRI, M., SATO, K., USAMI, T., OCHI, S., NISHINA, H., YOSHIDA, H., MORITA, I., WAGNER, E. F., MAK, T. W., SERFLING, E. & TAKAYANAGI, H. 2005. Autoamplification of NFATc1 expression determines its essential role in bone homeostasis. *J Exp Med,* 202**,** 1261-9.

ASAGIRI, M. & TAKAYANAGI, H. 2007. The molecular understanding of osteoclast differentiation. *Bone,* 40**,** 251-64.

ASH, P., LOUTIT, J. F. & TOWNSEND, K. M. 1980. Osteoclasts derived from haematopoietic stem cells. *Nature,* 283**,** 669-70.

AUBIN, J. E. 1992. Osteoclast adhesion and resorption: the role of podosomes. *J Bone Miner Res,* 7**,** 365-8.

AUBIN, J. E., HEERSCHE, J. N., MERRILEES, M. J. & SODEK, J. 1982. Isolation of bone cell clones with differences in growth, hormone responses, and extracellular matrix production. *J Cell Biol,* 92**,** 452-61.

AUSTYN, J. M. & GORDON, S. 1981. F4/80, a monoclonal antibody directed specifically against the mouse macrophage. *Eur J Immunol,* 11**,** 805-15.

AXELRAD, T. W. & EINHORN, T. A. 2009. Bone morphogenetic proteins in orthopaedic surgery. *Cytokine Growth Factor Rev,* 20**,** 481-8.

AYANOGLU, S., ESENYEL, C. Z., ADANIR, O., DEDEOGLU, S., IMREN, Y. & ESEN, T. 2015. Effects of hyaluronic acid (Hyalonect) on callus formation in rabbits. *Acta Orthop Traumatol Turc,* 49**,** 319-25.

BALAZS, E. A., WATSON, D., DUFF, I. F. & ROSEMAN, S. 1967. Hyaluronic acid in synovial fluid. I. Molecular parameters of hyaluronic acid in normal and arthritis human fluids. *Arthritis Rheum,* 10**,** 357-76.

BALCERZAK, M., HAMADE, E., ZHANG, L., PIKULA, S., AZZAR, G., RADISSON, J., BANDOROWICZ-PIKULA, J. & BUCHET, R. 2003. The roles of annexins and alkaline phosphatase in mineralization process. *Acta Biochim Pol,* 50**,** 1019-38.

BALEMANS, W., EBELING, M., PATEL, N., VAN HUL, E., OLSON, P., DIOSZEGI, M., LACZA, C., WUYTS, W., VAN DEN ENDE, J., WILLEMS, P., PAES-ALVES, A. F., HILL, S., BUENO, M., RAMOS, F. J., TACCONI, P., DIKKERS, F. G., STRATAKIS, C., LINDPAINTNER, K., VICKERY, B., FOERNZLER, D. & VAN HUL, W. 2001. Increased bone density in sclerosteosis is due to the deficiency of a novel secreted protein (SOST). *Hum Mol Genet,* 10**,** 537-43.

BALEMANS, W., PATEL, N., EBELING, M., VAN HUL, E., WUYTS, W., LACZA, C., DIOSZEGI, M., DIKKERS, F. G., HILDERING, P., WILLEMS, P. J., VERHEIJ, J. B., LINDPAINTNER, K., VICKERY, B., FOERNZLER, D. & VAN HUL, W. 2002.

Identification of a 52 kb deletion downstream of the SOST gene in patients with van Buchem disease. *J Med Genet,* 39**,** 91-7.

BARANOVA, N. S., NILEBACK, E., HALLER, F. M., BRIGGS, D. C., SVEDHEM, S., DAY, A. J. & RICHTER, R. P. 2011. The inflammation-associated protein TSG-6 cross-links hyaluronan via hyaluronan-induced TSG-6 oligomers. *J Biol Chem,* 286**,** 25675-86.

BARDOS, T., KAMATH, R. V., MIKECZ, K. & GLANT, T. T. 2001. Anti-inflammatory and chondroprotective effect of TSG-6 (tumor necrosis factor-alpha-stimulated gene-6) in murine models of experimental arthritis. *Am J Pathol,* 159**,** 1711-21.

BARON, R. & HESSE, E. 2012. Update on bone anabolics in osteoporosis treatment: rationale, current status, and perspectives. *J Clin Endocrinol Metab,* 97**,** 311-25.

BARON, R. & KNEISSEL, M. 2013. WNT signaling in bone homeostasis and disease: from human mutations to treatments. *Nat Med,* 19**,** 179-92.

BARROS, E. R., DIAS DA SILVA, M. R., KUNII, I. S. & LAZARETTI-CASTRO, M. 2008. Three years follow-up of pamidronate therapy in two brothers with osteoporosis-pseudoglioma syndrome (OPPG) carrying an LRP5 mutation. *J Pediatr Endocrinol Metab,* 21**,** 811-8.

BARRY, S. 2010. Non-steroidal anti-inflammatory drugs inhibit bone healing: a review. *Vet Comp Orthop Traumatol,* 23**,** 385-92.

BAYLISS, M. T., HOWAT, S. L., DUDHIA, J., MURPHY, J. M., BARRY, F. P., EDWARDS, J. C. & DAY, A. J. 2001. Up-regulation and differential expression of the hyaluronan-binding protein TSG-6 in cartilage and synovium in rheumatoid arthritis and osteoarthritis. *Osteoarthritis Cartilage,* 9**,** 42-8.

BELLIDO, T. 2014. Osteocyte-driven bone remodeling. *Calcif Tissue Int,* 94**,** 25-34.

BELLOWS, C. G., AUBIN, J. E., HEERSCHE, J. N. & ANTOSZ, M. E. 1986. Mineralized bone nodules formed in vitro from enzymatically released rat calvaria cell populations. *Calcif Tissue Int,* 38**,** 143-54.

BELTRAN, S. R., SVOBODA, K. K., KERNS, D. G., SHETH, A. & PROCKOP, D. J. 2015. Anti-inflammatory protein tumor necrosis factor-alpha-stimulated protein 6 (TSG-6) promotes early gingival wound healing: an in vivo study. *J Periodontol,* 86**,** 62-71.

BERTOLINI, D. R., NEDWIN, G. E., BRINGMAN, T. S., SMITH, D. D. & MUNDY, G. R. 1986. Stimulation of bone resorption and inhibition of bone formation in vitro by human tumour necrosis factors. *Nature,* 319**,** 516-8.

BEVERIDGE, A. J., WALLIS, R. & SAMANI, N. J. 2012. A molecular dynamics study of C1r and C1s dimers: implications for the structure of the C1 complex. *Proteins,* 80**,** 1987-97.

BHARGAVA, U., BAR-LEV, M., BELLOWS, C. G. & AUBIN, J. E. 1988. Ultrastructural analysis of bone nodules formed in vitro by isolated fetal rat calvaria cells. *Bone,* 9**,** 155-63.

BLACK, D. M., SCHWARTZ, A. V., ENSRUD, K. E., CAULEY, J. A., LEVIS, S., QUANDT, S. A., SATTERFIELD, S., WALLACE, R. B., BAUER, D. C., PALERMO, L., WEHREN, L. E., LOMBARDI, A., SANTORA, A. C., CUMMINGS, S. R. & GROUP, F. R. 2006. Effects of continuing or stopping alendronate after 5 years of treatment: the Fracture Intervention Trial Long-term Extension (FLEX): a randomized trial. *JAMA,* 296**,** 2927-38.

BLAIR, H. C., TEITELBAUM, S. L., GHISELLI, R. & GLUCK, S. 1989. Osteoclastic bone resorption by a polarized vacuolar proton pump. *Science,* 245**,** 855-7.

BLOOM, A. C., COLLINS, F. L., VAN'T HOF, R. J., RYAN, E. S., JONES, E., HUGHES, T. R., MORGAN, B. P., ERLANDSSON, M., BOKAREWA, M., AESCHLIMANN,

D., EVANS, B. A. & WILLIAMS, A. S. 2016. Deletion of the membrane complement inhibitor CD59a drives age and gender-dependent alterations to bone phenotype in mice. *Bone,* 84**,** 253-61.

BLUNDELL, C. D., ALMOND, A., MAHONEY, D. J., DEANGELIS, P. L., CAMPBELL, I. D. & DAY, A. J. 2005. Towards a structure for a TSG-6.hyaluronan complex by modeling and NMR spectroscopy: insights into other members of the link module superfamily. *J Biol Chem,* 280**,** 18189-201.

BLUNDELL, C. D., MAHONEY, D. J., ALMOND, A., DEANGELIS, P. L., KAHMANN, J. D., TERIETE, P., PICKFORD, A. R., CAMPBELL, I. D. & DAY, A. J. 2003. The link module from ovulation- and inflammation-associated protein TSG-6 changes conformation on hyaluronan binding. *J Biol Chem,* 278**,** 49261-70.

BODEN, S. D. 2000. Biology of lumbar spine fusion and use of bone graft substitutes: present, future, and next generation. *Tissue Eng,* 6**,** 383-99.

BODEN, S. D., KANG, J., SANDHU, H. & HELLER, J. G. 2002. Use of recombinant human bone morphogenetic protein-2 to achieve posterolateral lumbar spine fusion in humans: a prospective, randomized clinical pilot trial: 2002 Volvo Award in clinical studies. *Spine (Phila Pa 1976),* 27**,** 2662-73.

BOIVIN, G., DELOFFRE, P., PERRAT, B., PANCZER, G., BOUDEULLE, M., MAURAS, Y., ALLAIN, P., TSOUDEROS, Y. & MEUNIER, P. J. 1996. Strontium distribution and interactions with bone mineral in monkey iliac bone after strontium salt (S 12911) administration. *J Bone Miner Res,* 11**,** 1302-11.

BONDESON, J., BLOM, A. B., WAINWRIGHT, S., HUGHES, C., CATERSON, B. & VAN DEN BERG, W. B. 2010. The role of synovial macrophages and macrophage-produced mediators in driving inflammatory and destructive responses in osteoarthritis. *Arthritis Rheum,* 62**,** 647-57.

BONEWALD, L. F. 2007. Osteocytes as dynamic multifunctional cells. *Ann N Y Acad Sci,* 1116**,** 281-90.

BORK, P. & BECKMANN, G. 1993. The CUB domain. A widespread module in developmentally regulated proteins. *J Mol Biol,* 231**,** 539-45.

BOSKEY, A. L., GADALETA, S., GUNDBERG, C., DOTY, S. B., DUCY, P. & KARSENTY, G. 1998. Fourier transform infrared microspectroscopic analysis of bones of osteocalcin-deficient mice provides insight into the function of osteocalcin. *Bone,* 23**,** 187-96.

BOULEFTOUR, W., BOUET, G., GRANITO, R. N., THOMAS, M., LINOSSIER, M. T., VANDEN-BOSSCHE, A., AUBIN, J. E., LAFAGE-PROUST, M. H., VICO, L. & MALAVAL, L. 2015. Blocking the expression of both bone sialoprotein (BSP) and osteopontin (OPN) impairs the anabolic action of PTH in mouse calvaria bone. *J Cell Physiol,* 230**,** 568-77.

BOYLE, W. J., SIMONET, W. S. & LACEY, D. L. 2003. Osteoclast differentiation and activation. *Nature,* 423**,** 337-42.

BRAND, D. D., LATHAM, K. A. & ROSLONIEC, E. F. 2007. Collagen-induced arthritis. *Nat Protoc,* 2**,** 1269-75.

BRENNAN, F. M. & MCINNES, I. B. 2008. Evidence that cytokines play a role in rheumatoid arthritis. *J Clin Invest,* 118**,** 3537-45.

BRIGGS, D. C., BIRCHENOUGH, H. L., ALI, T., RUGG, M. S., WALTHO, J. P., IEVOLI, E., JOWITT, T. A., ENGHILD, J. J., RICHTER, R. P., SALUSTRI, A., MILNER, C. M. & DAY, A. J. 2015. Metal Ion-dependent Heavy Chain Transfer Activity of TSG-6 Mediates Assembly of the Cumulus-Oocyte Matrix. *J Biol Chem,* 290**,** 28708-23.

BRIGGS, D. C. & DAY, A. J. 2008. A bug in CUB's clothing: similarity between clostridial CBMs and complement CUBs. *Trends Microbiol,* 16**,** 407-8.

BRUUNSGAARD, H. 2002. Effects of tumor necrosis factor-alpha and interleukin-6 in elderly populations. *Eur Cytokine Netw,* 13**,** 389-91.

BUCAY, N., SAROSI, I., DUNSTAN, C. R., MORONY, S., TARPLEY, J., CAPPARELLI, C., SCULLY, S., TAN, H. L., XU, W., LACEY, D. L., BOYLE, W. J. & SIMONET, W. S. 1998. osteoprotegerin-deficient mice develop early onset osteoporosis and arterial calcification. *Genes Dev,* 12**,** 1260-8.

BULTINK, I. E., LEMS, W. F., KOSTENSE, P. J., DIJKMANS, B. A. & VOSKUYL, A. E. 2005. Prevalence of and risk factors for low bone mineral density and vertebral fractures in patients with systemic lupus erythematosus. *Arthritis Rheum,* 52**,** 2044-50.

BULTINK, I. E., VIS, M., VAN DER HORST-BRUINSMA, I. E. & LEMS, W. F. 2012. Inflammatory rheumatic disorders and bone. *Curr Rheumatol Rep,* 14**,** 224-30.

CALVI, L. M., ADAMS, G. B., WEIBRECHT, K. W., WEBER, J. M., OLSON, D. P., KNIGHT, M. C., MARTIN, R. P., SCHIPANI, E., DIVIETI, P., BRINGHURST, F. R., MILNER, L. A., KRONENBERG, H. M. & SCADDEN, D. T. 2003. Osteoblastic cells regulate the haematopoietic stem cell niche. *Nature,* 425**,** 841-6.

CANALIS, E., HOTT, M., DELOFFRE, P., TSOUDEROS, Y. & MARIE, P. J. 1996. The divalent strontium salt S12911 enhances bone cell replication and bone formation in vitro. *Bone,* 18**,** 517-23.

CANALIS, E., MAZZIOTTI, G., GIUSTINA, A. & BILEZIKIAN, J. P. 2007. Glucocorticoid-induced osteoporosis: pathophysiology and therapy. *Osteoporos Int,* 18**,** 1319-28.

CAO, T. V., LA, M., GETTING, S. J., DAY, A. J. & PERRETTI, M. 2004. Inhibitory effects of TSG-6 Link module on leukocyte-endothelial cell interactions in vitro and in vivo. *Microcirculation,* 11**,** 615-24.

CAPP, E., MILNER, C. M., WILLIAMS, J., HAUCK, L., JAUCKUS, J., STROWITZKI, T. & GERMEYER, A. 2014. Modulation of tumor necrosis factor-stimulated gene-6 (TSG-6) expression in human endometrium. *Arch Gynecol Obstet,* 289**,** 893-901.

CAPULLI, M., PAONE, R. & RUCCI, N. 2014. Osteoblast and osteocyte: games without frontiers. *Arch Biochem Biophys,* 561**,** 3-12.

CARRETTE, O., NEMADE, R. V., DAY, A. J., BRICKNER, A. & LARSEN, W. J. 2001. TSG-6 is concentrated in the extracellular matrix of mouse cumulus oocyte complexes through hyaluronan and inter-alpha-inhibitor binding. *Biol Reprod,* 65**,** 301-8.

CARRINGTON, J. C. & DOUGHERTY, W. G. 1988. A viral cleavage site cassette: identification of amino acid sequences required for tobacco etch virus polyprotein processing. *Proc Natl Acad Sci U S A,* 85**,** 3391-5.

CARTER, D. R. & BEAUPRÉ, G. S. 2001. *Skeletal function and form : mechanobiology of skeletal development, aging, and regeneration, Chapter 2, p 31-52,* Cambridge, Cambridge University Press.

CECCHINI, M. G., DOMINGUEZ, M. G., MOCCI, S., WETTERWALD, A., FELIX, R., FLEISCH, H., CHISHOLM, O., HOFSTETTER, W., POLLARD, J. W. & STANLEY, E. R. 1994. Role of colony stimulating factor-1 in the establishment and regulation of tissue macrophages during postnatal development of the mouse. *Development,* 120**,** 1357-72.

CENCI, S., WEITZMANN, M. N., ROGGIA, C., NAMBA, N., NOVACK, D., WOODRING, J. & PACIFICI, R. 2000. Estrogen deficiency induces bone loss by enhancing T-cell production of TNF-alpha. *J Clin Invest,* 106**,** 1229-37.

CHAMBERS, T. J. 1980. The cellular basis of bone resorption. *Clin Orthop Relat Res***,** 283-93.

CHAN, J. K., GLASS, G. E., ERSEK, A., FREIDIN, A., WILLIAMS, G. A., GOWERS, K., ESPIRITO SANTO, A. I., JEFFERY, R., OTTO, W. R., POULSOM, R., FELDMANN, M., RANKIN, S. M., HORWOOD, N. J. & NANCHAHAL, J. 2015. Low-dose TNF augments fracture healing in normal and osteoporotic bone by up-regulating the innate immune response. *EMBO Mol Med,* 7**,** 547-61.

CHANG, E. J., KIM, H. J., HA, J., KIM, H. J., RYU, J., PARK, K. H., KIM, U. H., LEE, Z. H., KIM, H. M., FISHER, D. E. & KIM, H. H. 2007. Hyaluronan inhibits osteoclast differentiation via Toll-like receptor 4. *J Cell Sci,* 120**,** 166-76.

CHANG, M. K., KRAMER, I., HUBER, T., KINZEL, B., GUTH-GUNDEL, S., LEUPIN, O. & KNEISSEL, M. 2014. Disruption of Lrp4 function by genetic deletion or pharmacological blockade increases bone mass and serum sclerostin levels. *Proc Natl Acad Sci U S A,* 111**,** E5187-95.

CHANG, M. K., RAGGATT, L. J., ALEXANDER, K. A., KULIWABA, J. S., FAZZALARI, N. L., SCHRODER, K., MAYLIN, E. R., RIPOLL, V. M., HUME, D. A. & PETTIT, A. R. 2008. Osteal tissue macrophages are intercalated throughout human and mouse bone lining tissues and regulate osteoblast function in vitro and in vivo. *J Immunol,* 181**,** 1232-44.

CHAPPARD, D., LEGRAND, E., BASLE, M. F., FROMONT, P., RACINEUX, J. L., REBEL, A. & AUDRAN, M. 1996. Altered trabecular architecture induced by corticosteroids: a bone histomorphometric study. *J Bone Miner Res,* 11**,** 676-85.

CHEN, L., WEI, X. Q., EVANS, B., JIANG, W. & AESCHLIMANN, D. 2008. IL-23 promotes osteoclast formation by up-regulation of receptor activator of NF-kappaB (RANK) expression in myeloid precursor cells. *Eur J Immunol,* 38**,** 2845-54.

CHENG, T. L., SCHINDELER, A. & LITTLE, D. G. 2015. BMP-2 delivered via sucrose acetate isobutyrate (SAIB) improves bone repair in a rat open fracture model. *J Orthop Res*.

CHO, S. W., SOKI, F. N., KOH, A. J., EBER, M. R., ENTEZAMI, P., PARK, S. I., VAN ROOIJEN, N. & MCCAULEY, L. K. 2014. Osteal macrophages support physiologic skeletal remodeling and anabolic actions of parathyroid hormone in bone. *Proc Natl Acad Sci U S A,* 111**,** 1545-50.

CHO, T. J., GERSTENFELD, L. C. & EINHORN, T. A. 2002. Differential temporal expression of members of the transforming growth factor beta superfamily during murine fracture healing. *J Bone Miner Res,* 17**,** 513-20.

CHOI, H., LEE, R. H., BAZHANOV, N., OH, J. Y. & PROCKOP, D. J. 2011a. Anti-inflammatory protein TSG-6 secreted by activated MSCs attenuates zymosan-induced mouse peritonitis by decreasing TLR2/NF-kappaB signaling in resident macrophages. *Blood,* 118**,** 330-8.

CHOI, H. Y., DIECKMANN, M., HERZ, J. & NIEMEIER, A. 2009. Lrp4, a novel receptor for Dickkopf 1 and sclerostin, is expressed by osteoblasts and regulates bone growth and turnover in vivo. *PLoS One,* 4**,** e7930.

CHOI, S., LEE, Y. A., HONG, S. J., LEE, G. J., KANG, S. W., PARK, J. H., PARK, J. H. & PARK, H. K. 2011b. Evaluation of inflammatory change and bone erosion using a murine type II collagen-induced arthritis model. *Rheumatol Int,* 31**,** 595-603.

CHOY, E. H. & PANAYI, G. S. 2001. Cytokine pathways and joint inflammation in rheumatoid arthritis. *N Engl J Med,* 344**,** 907-16.

CHUNG, C. Y., IIDA-KLEIN, A., WYATT, L. E., RUDKIN, G. H., ISHIDA, K., YAMAGUCHI, D. T. & MILLER, T. A. 1999. Serial passage of MC3T3-E1 cells alters osteoblastic function and responsiveness to transforming growth factor-beta1 and bone morphogenetic protein-2. *Biochem Biophys Res Commun,* 265**,** 246-51.

CLARKE, B. 2008. Normal bone anatomy and physiology. *Clin J Am Soc Nephrol,* 3 Suppl 3**,** S131-9.

CLARKE, B. L. 2014. Anti-sclerostin antibodies: utility in treatment of osteoporosis. *Maturitas,* 78**,** 199-204.

COLLINGE, C. & FAVELA, J. 2016. Use of teriparatide in osteoporotic fracture patients. *Injury,* 47 Suppl 1**,** S36-8.

CONN, P. M. 2013. *Animal models for the study of human disease, Chapter 5, p 392,* London ; Waltham, MA, Elsevier.

CONRON, M., BONDESON, J., PANTELIDIS, P., BEYNON, H. L., FELDMANN, M., DUBOIS, R. M. & FOXWELL, B. M. 2001. Alveolar macrophages and T cells from sarcoid, but not normal lung, are permissive to adenovirus infection and allow analysis of NF-kappa b-dependent signaling pathways. *Am J Respir Cell Mol Biol,* 25**,** 141-9.

COSTA, A. G., BILEZIKIAN, J. P. & LEWIECKI, E. M. 2014. Update on romosozumab : a humanized monoclonal antibody to sclerostin. *Expert Opin Biol Ther,* 14**,** 697-707.

D'AMELIO, P., CRISTOFARO, M. A., TAMONE, C., MORRA, E., DI BELLA, S., ISAIA, G., GRIMALDI, A., GENNERO, L., GARIBOLDI, A., PONZETTO, A., PESCARMONA, G. P. & ISAIA, G. C. 2008. Role of iron metabolism and oxidative damage in postmenopausal bone loss. *Bone,* 43**,** 1010-5.

DAHL, L. B., DAHL, I. M., ENGSTROM-LAURENT, A. & GRANATH, K. 1985. Concentration and molecular weight of sodium hyaluronate in synovial fluid from patients with rheumatoid arthritis and other arthropathies. *Ann Rheum Dis,* 44**,** 817-22.

DAI, X. M., RYAN, G. R., HAPEL, A. J., DOMINGUEZ, M. G., RUSSELL, R. G., KAPP, S., SYLVESTRE, V. & STANLEY, E. R. 2002. Targeted disruption of the mouse colony-stimulating factor 1 receptor gene results in osteopetrosis, mononuclear phagocyte deficiency, increased primitive progenitor cell frequencies, and reproductive defects. *Blood,* 99**,** 111-20.

DALBETH, N., DOYLE, A., BOYER, L., ROME, K., SURVEPALLI, D., SANDERS, A., SHEEHAN, T., LOBO, M., GAMBLE, G. & MCQUEEN, F. M. 2011. Development of a computed tomography method of scoring bone erosion in patients with gout: validation and clinical implications. *Rheumatology (Oxford),* 50**,** 410-6.

DALBETH, N. & SO, A. 2010. Hyperuricaemia and gout: state of the art and future perspectives. *Ann Rheum Dis,* 69**,** 1738-43.

DANCHUK, S., YLOSTALO, J. H., HOSSAIN, F., SORGE, R., RAMSEY, A., BONVILLAIN, R. W., LASKY, J. A., BUNNELL, B. A., WELSH, D. A., PROCKOP, D. J. & SULLIVAN, D. E. 2011. Human multipotent stromal cells attenuate lipopolysaccharide-induced acute lung injury in mice via secretion of tumor necrosis factor-alpha-induced protein 6. *Stem Cell Res Ther,* 2**,** 27.

DAY, A. J., APLIN, R. T. & WILLIS, A. C. 1996. Overexpression, purification, and refolding of link module from human TSG-6 in Escherichia coli: effect of temperature, media, and mutagenesis on lysine misincorporation at arginine AGA codons. *Protein Expr Purif,* 8**,** 1-16.

DAY, A. J. & DE LA MOTTE, C. A. 2005. Hyaluronan cross-linking: a protective mechanism in inflammation? *Trends Immunol,* 26**,** 637-43.

DE GORTER, D. J., VAN DINTHER, M., KORCHYNSKYI, O. & TEN DIJKE, P. 2011. Biphasic effects of transforming growth factor beta on bone morphogenetic protein-induced osteoblast differentiation. *J Bone Miner Res,* 26**,** 1178-87.

DELAISSE, J. M. 2014. The reversal phase of the bone-remodeling cycle: cellular prerequisites for coupling resorption and formation. *Bonekey Rep,* 3**,** 561.

DELANY, A. M., AMLING, M., PRIEMEL, M., HOWE, C., BARON, R. & CANALIS, E. 2000. Osteopenia and decreased bone formation in osteonectin-deficient mice. *J Clin Invest,* 105**,** 1325.

DELANY, A. M., KALAJZIC, I., BRADSHAW, A. D., SAGE, E. H. & CANALIS, E. 2003. Osteonectin-null mutation compromises osteoblast formation, maturation, and survival. *Endocrinology,* 144**,** 2588-96.

DELVES, P. J. & ROITT, I. M. 2000. The immune system. First of two parts. *N Engl J Med,* 343**,** 37-49.

DEMPSTER, D. W., ZHOU, H., RECKER, R. R., BROWN, J. P., BOLOGNESE, M. A., RECKNOR, C. P., KENDLER, D. L., LEWIECKI, E. M., HANLEY, D. A., RAO, S. D., MILLER, P. D., WOODSON, G. C., 3RD, LINDSAY, R., BINKLEY, N., ALAM, J., RUFF, V. A., GALLAGHER, E. R. & TAYLOR, K. A. 2016. A Longitudinal Study of Skeletal Histomorphometry at 6 and 24 Months Across Four Bone Envelopes in Postmenopausal Women with Osteoporosis Receiving Teriparatide or Zoledronic Acid in the SHOTZ Trial. *J Bone Miner Res*.

DEWHIRST, F. E., STASHENKO, P. P., MOLE, J. E. & TSURUMACHI, T. 1985. Purification and partial sequence of human osteoclast-activating factor: identity with interleukin 1 beta. *J Immunol,* 135**,** 2562-8.

DING, L., SAUNDERS, T. L., ENIKOLOPOV, G. & MORRISON, S. J. 2012. Endothelial and perivascular cells maintain haematopoietic stem cells. *Nature,* 481**,** 457-62.

DING, W. G., ZHANG, Z. M., ZHANG, Y. H., JIANG, S. D., JIANG, L. S. & DAI, L. Y. 2010. Changes of substance P during fracture healing in ovariectomized mice. *Regul Pept,* 159**,** 28-34.

DOBNIG, H. & TURNER, R. T. 1995. Evidence that intermittent treatment with parathyroid hormone increases bone formation in adult rats by activation of bone lining cells. *Endocrinology,* 136**,** 3632-8.

DOUGALL, W. C., GLACCUM, M., CHARRIER, K., ROHRBACH, K., BRASEL, K., DE SMEDT, T., DARO, E., SMITH, J., TOMETSKO, M. E., MALISZEWSKI, C. R., ARMSTRONG, A., SHEN, V., BAIN, S., COSMAN, D., ANDERSON, D., MOR-

RISSEY, P. J., PESCHON, J. J. & SCHUH, J. 1999. RANK is essential for osteoclast and lymph node development. *Genes Dev,* 13**,** 2412-24.

DUCY, P., ZHANG, R., GEOFFROY, V., RIDALL, A. L. & KARSENTY, G. 1997. Osf2/Cbfa1: a transcriptional activator of osteoblast differentiation. *Cell,* 89**,** 747-54.

DYER, D. P., THOMSON, J. M., HERMANT, A., JOWITT, T. A., HANDEL, T. M., PROUDFOOT, A. E., DAY, A. J. & MILNER, C. M. 2014. TSG-6 inhibits neutrophil migration via direct interaction with the chemokine CXCL8. *J Immunol,* 192**,** 2177-85.

EGHBALI-FATOURECHI, G., KHOSLA, S., SANYAL, A., BOYLE, W. J., LACEY, D. L. & RIGGS, B. L. 2003. Role of RANK ligand in mediating increased bone resorption in early postmenopausal women. *J Clin Invest,* 111**,** 1221-30.

EINHORN, T. A. 1998. The cell and molecular biology of fracture healing. *Clin Orthop Relat Res***,** S7-21.

EISENER-DORMAN, A. F., LAWRENCE, D. A. & BOLIVAR, V. J. 2009. Cautionary insights on knockout mouse studies: the gene or not the gene? *Brain Behav Immun,* 23**,** 318-24.

EMLEN, W., NIEBUR, J., FLANDERS, G. & RUTLEDGE, J. 1996. Measurement of serum hyaluronic acid in patients with rheumatoid arthritis: correlation with disease activity. *J Rheumatol,* 23**,** 974-8.

ENGHILD, J. J., THOGERSEN, I. B., CHENG, F., FRANSSON, L. A., ROEPSTORFF, P. & RAHBEK-NIELSEN, H. 1999. Organization of the inter-alpha-inhibitor heavy chains on the chondroitin sulfate originating from Ser(10) of bikunin: posttranslational modification of IalphaI-derived bikunin. *Biochemistry,* 38**,** 11804-13.

ENTWISTLE, J., HALL, C. L. & TURLEY, E. A. 1996. HA receptors: regulators of signalling to the cytoskeleton. *J Cell Biochem,* 61**,** 569-77.

ERBEN, R. G. 1997. Embedding of bone samples in methylmethacrylate: an improved method suitable for bone histomorphometry, histochemistry, and immunohistochemistry. *J Histochem Cytochem,* 45**,** 307-13.

ERIKSEN, E. F. 2010. Cellular mechanisms of bone remodeling. *Rev Endocr Metab Disord,* 11**,** 219-27.

ERIKSEN, E. F., GUNDERSEN, H. J., MELSEN, F. & MOSEKILDE, L. 1984. Reconstruction of the formative site in iliac trabecular bone in 20 normal individuals employing a kinetic model for matrix and mineral apposition. *Metab Bone Dis Relat Res,* 5**,** 243-52.

EVANS, N. D., GENTLEMAN, E., CHEN, X., ROBERTS, C. J., POLAK, J. M. & STEVENS, M. M. 2010. Extracellular matrix-mediated osteogenic differentiation of murine embryonic stem cells. *Biomaterials,* 31**,** 3244-52.

EVENEPOEL, P., D'HAESE, P. & BRANDENBURG, V. 2014. Romosozumab in postmenopausal women with osteopenia. *N Engl J Med,* 370**,** 1664.

EVERTS, V., DELAISSE, J. M., KORPER, W., JANSEN, D. C., TIGCHELAARGUTTER, W., SAFTIG, P. & BEERTSEN, W. 2002. The bone lining cell: its role in cleaning Howship's lacunae and initiating bone formation. *J Bone Miner Res,* 17**,** 77-90.

FAKHRY, M., HAMADE, E., BADRAN, B., BUCHET, R. & MAGNE, D. 2013. Molecular mechanisms of mesenchymal stem cell differentiation towards osteoblasts. *World J Stem Cells,* 5**,** 136-48.

FEDARKO, N. S., TERMINE, J. D., YOUNG, M. F. & ROBEY, P. G. 1990. Temporal regulation of hyaluronan and proteoglycan metabolism by human bone cells in vitro. *J Biol Chem,* 265**,** 12200-9.

FEDDE, K. N., BLAIR, L., SILVERSTEIN, J., COBURN, S. P., RYAN, L. M., WEINSTEIN, R. S., WAYMIRE, K., NARISAWA, S., MILLAN, J. L., MACGREGOR, G.

R. & WHYTE, M. P. 1999. Alkaline phosphatase knock-out mice recapitulate the metabolic and skeletal defects of infantile hypophosphatasia. *J Bone Miner Res,* 14**,** 2015-26.

FELIX, R., HOFSTETTER, W., WETTERWALD, A., CECCHINI, M. G. & FLEISCH, H. 1994. Role of colony-stimulating factor-1 in bone metabolism. *J Cell Biochem,* 55**,** 340-9.

FENG, J. Q., WARD, L. M., LIU, S., LU, Y., XIE, Y., YUAN, B., YU, X., RAUCH, F., DAVIS, S. I., ZHANG, S., RIOS, H., DREZNER, M. K., QUARLES, L. D., BONEWALD, L. F. & WHITE, K. E. 2006. Loss of DMP1 causes rickets and osteomalacia and identifies a role for osteocytes in mineral metabolism. *Nat Genet,* 38**,** 1310-5.

FENG, J. Q., YE, L. & SCHIAVI, S. 2009. Do osteocytes contribute to phosphate homeostasis? *Curr Opin Nephrol Hypertens,* 18**,** 285-91.

FENG, P. & LIAU, G. 1993. Identification of a novel serum and growth factor-inducible gene in vascular smooth muscle cells. *J Biol Chem,* 268**,** 21453.

FERNANDES, T. J., HODGE, J. M., SINGH, P. P., EELES, D. G., COLLIER, F. M., HOLTEN, I., EBELING, P. R., NICHOLSON, G. C. & QUINN, J. M. 2013. Cord blood-derived macrophage-lineage cells rapidly stimulate osteoblastic maturation in mesenchymal stem cells in a glycoprotein-130 dependent manner. *PLoS One,* 8**,** e73266.

FERRARI, S. 2012. [Treatment of osteoporosis with Denosumab]. *Ther Umsch,* 69**,** 182-6.

FLORES, M. E., NORGARD, M., HEINEGARD, D., REINHOLT, F. P. & ANDERSSON, G. 1992. RGD-directed attachment of isolated rat osteoclasts to osteopontin, bone sialoprotein, and fibronectin. *Exp Cell Res,* 201**,** 526-30.

FOSKETT, A. M., BAZHANOV, N., TI, X., TIBLOW, A., BARTOSH, T. J. & PROCKOP, D. J. 2014. Phase-directed therapy: TSG-6 targeted to early inflammation improves bleomycin-injured lungs. *Am J Physiol Lung Cell Mol Physiol,* 306**,** L120-31.

FRANCESCHI, C., BONAFE, M., VALENSIN, S., OLIVIERI, F., DE LUCA, M., OTTAVIANI, E. & DE BENEDICTIS, G. 2000. Inflamm-aging. An evolutionary perspective on immunosenescence. *Ann N Y Acad Sci,* 908**,** 244-54.

FRIEDENSTEIN, A. J., CHAILAKHJAN, R. K. & LALYKINA, K. S. 1970. The development of fibroblast colonies in monolayer cultures of guinea-pig bone marrow and spleen cells. *Cell Tissue Kinet,* 3**,** 393-403.

FRIEDENSTEIN, A. J., CHAILAKHYAN, R. K., LATSINIK, N. V., PANASYUK, A. F. & KEILISS-BOROK, I. V. 1974. Stromal cells responsible for transferring the microenvironment of the hemopoietic tissues. Cloning in vitro and retransplantation in vivo. *Transplantation,* 17**,** 331-40.

FROST, H. M. 1966. Relation between bone tissue and cell population dynamics, histology and tetracycline labeling. *Clin Orthop Relat Res,* 49**,** 65-75.

FUJII, T., KITAURA, H., KIMURA, K., HAKAMI, Z. W. & TAKANO-YAMAMOTO, T. 2012. IL-4 inhibits TNF-alpha-mediated osteoclast formation by inhibition of RANKL expression in TNF-alpha-activated stromal cells and direct inhibition of TNF-alpha-activated osteoclast precursors via a T-cell-independent mechanism in vivo. *Bone,* 51**,** 771-80.

FUJIKAWA, Y., QUINN, J. M., SABOKBAR, A., MCGEE, J. O. & ATHANASOU, N. A. 1996. The human osteoclast precursor circulates in the monocyte fraction. *Endocrinology,* 137**,** 4058-60.

FUJIMOTO, T., SAVANI, R. C., WATARI, M., DAY, A. J. & STRAUSS, J. F., 3RD 2002. Induction of the hyaluronic acid-binding protein, tumor necrosis factor-stimulated

gene-6, in cervical smooth muscle cells by tumor necrosis factor-alpha and prostaglandin E(2). *Am J Pathol,* 160**,** 1495-502.

FULLER, K., LAWRENCE, K. M., ROSS, J. L., GRABOWSKA, U. B., SHIROO, M., SAMUELSSON, B. & CHAMBERS, T. J. 2008. Cathepsin K inhibitors prevent matrix-derived growth factor degradation by human osteoclasts. *Bone,* 42**,** 200-11.

FULOP, C., KAMATH, R. V., LI, Y., OTTO, J. M., SALUSTRI, A., OLSEN, B. R., GLANT, T. T. & HASCALL, V. C. 1997. Coding sequence, exon-intron structure and chromosomal localization of murine TNF-stimulated gene 6 that is specifically expressed by expanding cumulus cell-oocyte complexes. *Gene,* 202**,** 95-102.

FULOP, C., SZANTO, S., MUKHOPADHYAY, D., BARDOS, T., KAMATH, R. V., RUGG, M. S., DAY, A. J., SALUSTRI, A., HASCALL, V. C., GLANT, T. T. & MIKECZ, K. 2003. Impaired cumulus mucification and female sterility in tumor necrosis factor-induced protein-6 deficient mice. *Development,* 130**,** 2253-61.

GABORIAUD, C., GREGORY-PAURON, L., TEILLET, F., THIELENS, N. M., BALLY, I. & ARLAUD, G. J. 2011. Structure and properties of the Ca(2+)-binding CUB domain, a widespread ligand-recognition unit involved in major biological functions. *Biochem J,* 439**,** 185-93.

GALIBERT, L., TOMETSKO, M. E., ANDERSON, D. M., COSMAN, D. & DOUGALL, W. C. 1998. The involvement of multiple tumor necrosis factor receptor (TNFR)-associated factors in the signaling mechanisms of receptor activator of NF-kappaB, a member of the TNFR superfamily. *J Biol Chem,* 273**,** 34120-7.

GANDHI, N. S. & MANCERA, R. L. 2008. The structure of glycosaminoglycans and their interactions with proteins. *Chem Biol Drug Des,* 72**,** 455-82.

GANESAN, K., TEKLEHAIMANOT, S., TRAN, T. H., ASUNCION, M. & NORRIS, K. 2005. Relationship of C-reactive protein and bone mineral density in community-dwelling elderly females. *J Natl Med Assoc,* 97**,** 329-33.

GAO, Y., MORITA, I., MARUO, N., KUBOTA, T., MUROTA, S. & ASO, T. 1998. Expression of IL-6 receptor and GP130 in mouse bone marrow cells during osteoclast differentiation. *Bone,* 22**,** 487-93.

GARRISON, K. R., SHEMILT, I., DONELL, S., RYDER, J. J., MUGFORD, M., HARVEY, I., SONG, F. & ALT, V. 2010. Bone morphogenetic protein (BMP) for fracture healing in adults. *Cochrane Database Syst Rev***,** CD006950.

GERSTENFELD, L. C., CHO, T. J., KON, T., AIZAWA, T., TSAY, A., FITCH, J., BARNES, G. L., GRAVES, D. T. & EINHORN, T. A. 2003. Impaired fracture healing in the absence of TNF-alpha signaling: the role of TNF-alpha in endochondral cartilage resorption. *J Bone Miner Res,* 18**,** 1584-92.

GETTING, S. J., MAHONEY, D. J., CAO, T., RUGG, M. S., FRIES, E., MILNER, C. M., PERRETTI, M. & DAY, A. J. 2002. The link module from human TSG-6 inhibits neutrophil migration in a hyaluronan- and inter-alpha -inhibitor-independent manner. *J Biol Chem,* 277**,** 51068-76.

GEUSENS, P. 2012. The role of RANK ligand/osteoprotegerin in rheumatoid arthritis. *Ther Adv Musculoskelet Dis,* 4**,** 225-33.

GINALDI, L., DI BENEDETTO, M. C. & DE MARTINIS, M. 2005. Osteoporosis, inflammation and ageing. *Immun Ageing,* 2**,** 14.

GINGERY, A., BRADLEY, E. W., PEDERSON, L., RUAN, M., HORWOOD, N. J. & OURSLER, M. J. 2008. TGF-beta coordinately activates TAK1/MEK/AKT/NFkB and SMAD pathways to promote osteoclast survival. *Exp Cell Res,* 314**,** 2725-38.

GIRASOLE, G., JILKA, R. L., PASSERI, G., BOSWELL, S., BODER, G., WILLIAMS, D. C. & MANOLAGAS, S. C. 1992. 17 beta-estradiol inhibits interleukin-6 production

by bone marrow-derived stromal cells and osteoblasts in vitro: a potential mechanism for the antiosteoporotic effect of estrogens. *J Clin Invest,* 89**,** 883-91.

GLANT, T. T., CS-SZABO, G., NAGASE, H., JACOBS, J. J. & MIKECZ, K. 1998. Progressive polyarthritis induced in BALB/c mice by aggrecan from normal and osteoarthritic human cartilage. *Arthritis Rheum,* 41**,** 1007-18.

GLANT, T. T., KAMATH, R. V., BARDOS, T., GAL, I., SZANTO, S., MURAD, Y. M., SANDY, J. D., MORT, J. S., ROUGHLEY, P. J. & MIKECZ, K. 2002. Cartilage-specific constitutive expression of TSG-6 protein (product of tumor necrosis factor alpha-stimulated gene 6) provides a chondroprotective, but not antiinflammatory, effect in antigen-induced arthritis. *Arthritis Rheum,* 46**,** 2207-18.

GLANT, T. T., MIKECZ, K., ARZOUMANIAN, A. & POOLE, A. R. 1987. Proteoglycan-induced arthritis in BALB/c mice. Clinical features and histopathology. *Arthritis Rheum,* 30**,** 201-12.

GLASS, G. E., CHAN, J. K., FREIDIN, A., FELDMANN, M., HORWOOD, N. J. & NANCHAHAL, J. 2011. TNF-alpha promotes fracture repair by augmenting the recruitment and differentiation of muscle-derived stromal cells. *Proc Natl Acad Sci U S A,* 108**,** 1585-90.

GLOBUS, R. K., DOTY, S. B., LULL, J. C., HOLMUHAMEDOV, E., HUMPHRIES, M. J. & DAMSKY, C. H. 1998. Fibronectin is a survival factor for differentiated osteoblasts. *J Cell Sci,* 111 (Pt 10)**,** 1385-93.

GONG, Y., SLEE, R. B., FUKAI, N., RAWADI, G., ROMAN-ROMAN, S., REGINATO, A. M., WANG, H., CUNDY, T., GLORIEUX, F. H., LEV, D., ZACHARIN, M., OEXLE, K., MARCELINO, J., SUWAIRI, W., HEEGER, S., SABATAKOS, G., APTE, S., ADKINS, W. N., ALLGROVE, J., ARSLAN-KIRCHNER, M., BATCH, J. A., BEIGHTON, P., BLACK, G. C., BOLES, R. G., BOON, L. M., BORRONE, C., BRUNNER, H. G., CARLE, G. F., DALLAPICCOLA, B., DE PAEPE, A.,

FLOEGE, B., HALFHIDE, M. L., HALL, B., HENNEKAM, R. C., HIROSE, T., JANS, A., JUPPNER, H., KIM, C. A., KEPPLER-NOREUIL, K., KOHLSCHUETTER, A., LACOMBE, D., LAMBERT, M., LEMYRE, E., LETTEBOER, T., PELTONEN, L., RAMESAR, R. S., ROMANENGO, M., SOMER, H., STEICHEN-GERSDORF, E., STEINMANN, B., SULLIVAN, B., SUPERTI-FURGA, A., SWOBODA, W., VAN DEN BOOGAARD, M. J., VAN HUL, W., VIKKULA, M., VOTRUBA, M., ZABEL, B., GARCIA, T., BARON, R., OLSEN, B. R., WARMAN, M. L. & OSTEOPOROSIS-PSEUDOGLIOMA SYNDROME COLLABORATIVE, G. 2001. LDL receptor-related protein 5 (LRP5) affects bone accrual and eye development. *Cell,* 107**,** 513-23.

GORDON, S. & TAYLOR, P. R. 2005. Monocyte and macrophage heterogeneity. *Nat Rev Immunol,* 5**,** 953-64.

GORMAN, J. D., SACK, K. E. & DAVIS, J. C., JR. 2002. Treatment of ankylosing spondylitis by inhibition of tumor necrosis factor alpha. *N Engl J Med,* 346**,** 1349-56.

GOWEN, M., MEIKLE, M. C. & REYNOLDS, J. J. 1983. Stimulation of bone resorption in vitro by a non-prostanoid factor released by human monocytes in culture. *Biochim Biophys Acta,* 762**,** 471-4.

GREENSPAN, S. L., BONE, H. G., ETTINGER, M. P., HANLEY, D. A., LINDSAY, R., ZANCHETTA, J. R., BLOSCH, C. M., MATHISEN, A. L., MORRIS, S. A., MARRIOTT, T. B. & TREATMENT OF OSTEOPOROSIS WITH PARATHYROID HORMONE STUDY, G. 2007. Effect of recombinant human parathyroid hormone (1-84) on vertebral fracture and bone mineral density in postmenopausal women with osteoporosis: a randomized trial. *Ann Intern Med,* 146**,** 326-39.

GREGORY, C. A., GUNN, W. G., PEISTER, A. & PROCKOP, D. J. 2004. An Alizarin red-based assay of mineralization by adherent cells in culture: comparison with cetylpyridinium chloride extraction. *Anal Biochem,* 329**,** 77-84.

GRIGORIADIS, A. E., WANG, Z. Q., CECCHINI, M. G., HOFSTETTER, W., FELIX, R., FLEISCH, H. A. & WAGNER, E. F. 1994. c-Fos: a key regulator of osteoclast-macrophage lineage determination and bone remodeling. *Science,* 266**,** 443-8.

GUHA, M. & MACKMAN, N. 2001. LPS induction of gene expression in human monocytes. *Cell Signal,* 13**,** 85-94.

GUIHARD, P., DANGER, Y., BROUNAIS, B., DAVID, E., BRION, R., DELECRIN, J., RICHARDS, C. D., CHEVALIER, S., REDINI, F., HEYMANN, D., GASCAN, H. & BLANCHARD, F. 2012. Induction of osteogenesis in mesenchymal stem cells by activated monocytes/macrophages depends on oncostatin M signaling. *Stem Cells,* 30**,** 762-72.

HAMIDOUCHE, Z., FROMIGUE, O., RINGE, J., HAUPL, T., VAUDIN, P., PAGES, J. C., SROUJI, S., LIVNE, E. & MARIE, P. J. 2009. Priming integrin alpha5 promotes human mesenchymal stromal cell osteoblast differentiation and osteogenesis. *Proc Natl Acad Sci U S A,* 106**,** 18587-91.

HAMMARSTROM, L. E., HANKER, J. S. & TOVERUD, S. U. 1971. Cellular differences in acid phosphatase isoenzymes in bone and teeth. *Clin Orthop Relat Res,* 78**,** 151-67.

HANCOX, N. M. 1972. *Biology of bone Chapter, 12,* Cambridge, CUP.

HANLEY, D. A., ADACHI, J. D., BELL, A. & BROWN, V. 2012. Denosumab: mechanism of action and clinical outcomes. *Int J Clin Pract,* 66**,** 1139-46.

HARVEY, N., DENNISON, E. & COOPER, C. 2010. Osteoporosis: impact on health and economics. *Nat Rev Rheumatol,* 6**,** 99-105.

HASHIMOTO, Y., ZHANG, S. & BLISSARD, G. W. 2010. Ao38, a new cell line from eggs of the black witch moth, Ascalapha odorata (Lepidoptera: Noctuidae), is permissive for AcMNPV infection and produces high levels of recombinant proteins. *BMC Biotechnol,* 10**,** 50.

HAUGE, E. M., QVESEL, D., ERIKSEN, E. F., MOSEKILDE, L. & MELSEN, F. 2001. Cancellous bone remodeling occurs in specialized compartments lined by cells expressing osteoblastic markers. *J Bone Miner Res,* 16**,** 1575-82.

HELDIN, C. H., MIYAZONO, K. & TEN DIJKE, P. 1997. TGF-beta signalling from cell membrane to nucleus through SMAD proteins. *Nature,* 390**,** 465-71.

HEMINGWAY, F., CHENG, X., KNOWLES, H. J., ESTRADA, F. M., GORDON, S. & ATHANASOU, N. A. 2011. In vitro generation of mature human osteoclasts. *Calcif Tissue Int,* 89**,** 389-95.

HEMINGWAY, F., KASHIMA, T. G., KNOWLES, H. J. & ATHANASOU, N. A. 2013. Investigation of osteoclastogenic signalling of the RANKL substitute LIGHT. *Exp Mol Pathol,* 94**,** 380-5.

HENDRIX, S. L. & MCNEELEY, S. G. 2001. Effect of selective estrogen receptor modulators on reproductive tissues other than endometrium. *Ann N Y Acad Sci,* 949**,** 243-50.

HENTUNEN, T. A., CHOI, S. J., BOYCE, B. F., DALLAS, M. R., DALLAS, S. L., SHENONG, G. L. & ROODMAN, G. D. 2000. A murine model of inflammatory bone disease. *Bone,* 26**,** 183-8.

HIGMAN, V. A., BLUNDELL, C. D., MAHONEY, D. J., REDFIELD, C., NOBLE, M. E. & DAY, A. J. 2007. Plasticity of the TSG-6 HA-binding loop and mobility in the TSG-6-HA complex revealed by NMR and X-ray crystallography. *J Mol Biol,* 371**,** 669-84.

HIGMAN, V. A., BRIGGS, D. C., MAHONEY, D. J., BLUNDELL, C. D., SATTELLE, B. M., DYER, D. P., GREEN, D. E., DEANGELIS, P. L., ALMOND, A., MILNER, C. M. & DAY, A. J. 2014. A refined model for the TSG-6 link module in complex with hyaluronan: use of defined oligosaccharides to probe structure and function. *J Biol Chem,* 289**,** 5619-34.

HILTON, M. J., TU, X., WU, X., BAI, S., ZHAO, H., KOBAYASHI, T., KRONENBERG, H. M., TEITELBAUM, S. L., ROSS, F. P., KOPAN, R. & LONG, F. 2008. Notch signaling maintains bone marrow mesenchymal progenitors by suppressing osteoblast differentiation. *Nat Med,* 14**,** 306-14.

HOCHULI, E., DOBELI, H. & SCHACHER, A. 1987. New metal chelate adsorbent selective for proteins and peptides containing neighbouring histidine residues. *J Chromatogr,* 411**,** 177-84.

HODGE, J. M., KIRKLAND, M. A. & NICHOLSON, G. C. 2007. Multiple roles of M-CSF in human osteoclastogenesis. *J Cell Biochem,* 102**,** 759-68.

HOFBAUER, L. C., KHOSLA, S., DUNSTAN, C. R., LACEY, D. L., BOYLE, W. J. & RIGGS, B. L. 2000. The roles of osteoprotegerin and osteoprotegerin ligand in the paracrine regulation of bone resorption. *J Bone Miner Res,* 15**,** 2-12.

HOFMANN, T. J., OTSURU, S., MARINO, R., RASINI, V., VERONESI, E., MURGIA, A., LAHTI, J., BOYD, K., DOMINICI, M. & HORWITZ, E. M. 2013. Transplanted murine long-term repopulating hematopoietic cells can differentiate to osteoblasts in the marrow stem cell niche. *Mol Ther,* 21**,** 1224-31.

HOLLBERG, K., NORDAHL, J., HULTENBY, K., MENGARELLI-WIDHOLM, S., ANDERSSON, G. & REINHOLT, F. P. 2005. Polarization and secretion of cathepsin K precede tartrate-resistant acid phosphatase secretion to the ruffled border area during the activation of matrix-resorbing clasts. *J Bone Miner Metab,* 23**,** 441-9.

HOROWITZ, M., VIGNERY, A., GERSHON, R. K. & BARON, R. 1984. Thymus-derived lymphocytes and their interactions with macrophages are required for the production of osteoclast-activating factor in the mouse. *Proc Natl Acad Sci U S A,* 81**,** 2181-5.

HORTON, J. E., RAISZ, L. G., SIMMONS, H. A., OPPENHEIM, J. J. & MERGENHAGEN, S. E. 1972. Bone resorbing activity in supernatant fluid from cultured human peripheral blood leukocytes. *Science,* 177**,** 793-5.

HORWOOD, N. J. 2015. Macrophage Polarization and Bone Formation: A review. *Clin Rev Allergy Immunol*.

HORWOOD, N. J., ELLIOTT, J., MARTIN, T. J. & GILLESPIE, M. T. 1998. Osteotropic agents regulate the expression of osteoclast differentiation factor and osteoprotegerin in osteoblastic stromal cells. *Endocrinology,* 139**,** 4743-6.

HORWOOD, N. J., ELLIOTT, J., MARTIN, T. J. & GILLESPIE, M. T. 2001. IL-12 alone and in synergy with IL-18 inhibits osteoclast formation in vitro. *J Immunol,* 166**,** 4915-21.

HORWOOD, N. J., KARTSOGIANNIS, V., QUINN, J. M., ROMAS, E., MARTIN, T. J. & GILLESPIE, M. T. 1999. Activated T lymphocytes support osteoclast formation in vitro. *Biochem Biophys Res Commun,* 265**,** 144-50.

HOWARD, G. A., BOTTEMILLER, B. L., TURNER, R. T., RADER, J. I. & BAYLINK, D. J. 1981. Parathyroid hormone stimulates bone formation and resorption in organ culture: evidence for a coupling mechanism. *Proc Natl Acad Sci U S A,* 78**,** 3204-8.

HUANG, R. L., YUAN, Y., ZOU, G. M., LIU, G., TU, J. & LI, Q. 2014. LPS-stimulated inflammatory environment inhibits BMP-2-induced osteoblastic differentiation through crosstalk between TLR4/MyD88/NF-kappaB and BMP/Smad signaling. *Stem Cells Dev,* 23**,** 277-89.

HUGHES, D. E., SALTER, D. M. & SIMPSON, R. 1994. CD44 expression in human bone: a novel marker of osteocytic differentiation. *J Bone Miner Res,* 9**,** 39-44.

HUME, D. A., LOUTIT, J. F. & GORDON, S. 1984. The mononuclear phagocyte system of the mouse defined by immunohistochemical localization of antigen F4/80: macrophages of bone and associated connective tissue. *J Cell Sci,* 66**,** 189-94.

HUTADILOK, N., GHOSH, P. & BROOKS, P. M. 1988. Binding of haptoglobin, inter-alpha-trypsin inhibitor, and alpha 1 proteinase inhibitor to synovial fluid hyaluronate and the influence of these proteins on its degradation by oxygen derived free radicals. *Ann Rheum Dis,* 47**,** 377-85.

ISHTIAQ, S., FOGELMAN, I. & HAMPSON, G. 2015. Treatment of post-menopausal osteoporosis: beyond bisphosphonates. *J Endocrinol Invest,* 38**,** 13-29.

ITOH, K., UDAGAWA, N., KATAGIRI, T., IEMURA, S., UENO, N., YASUDA, H., HIGASHIO, K., QUINN, J. M., GILLESPIE, M. T., MARTIN, T. J., SUDA, T. & TAKAHASHI, N. 2001. Bone morphogenetic protein 2 stimulates osteoclast differentiation and survival supported by receptor activator of nuclear factor-kappaB ligand. *Endocrinology,* 142**,** 3656-62.

ITOH, S., UDAGAWA, N., TAKAHASHI, N., YOSHITAKE, F., NARITA, H., EBISU, S. & ISHIHARA, K. 2006. A critical role for interleukin-6 family-mediated Stat3 activation in osteoblast differentiation and bone formation. *Bone,* 39**,** 505-12.

JAGER, M., FISCHER, J., DOHRN, W., LI, X., AYERS, D. C., CZIBERE, A., PRALL, W. C., LENSING-HOHN, S. & KRAUSPE, R. 2008. Dexamethasone modulates BMP-2 effects on mesenchymal stem cells in vitro. *J Orthop Res,* 26**,** 1440-8.

JAISWAL, N., HAYNESWORTH, S. E., CAPLAN, A. I. & BRUDER, S. P. 1997. Osteogenic differentiation of purified, culture-expanded human mesenchymal stem cells in vitro. *J Cell Biochem,* 64**,** 295-312.

JAWORSKI, Z. F., DUCK, B. & SEKALY, G. 1981. Kinetics of osteoclasts and their nuclei in evolving secondary Haversian systems. *J Anat,* 133**,** 397-405.

JEMTLAND, R., HOLDEN, M., REPPE, S., OLSTAD, O. K., REINHOLT, F. P., GAUTVIK, V. T., REFVEM, H., FRIGESSI, A., HOUSTON, B. & GAUTVIK, K. M. 2011. Molecular disease map of bone characterizing the postmenopausal osteoporosis phenotype. *J Bone Miner Res,* 26**,** 1793-801.

JENSEN, P. R., ANDERSEN, T. L., HAUGE, E. M., BOLLERSLEV, J. & DELAISSE, J. M. 2015. A joined role of canopy and reversal cells in bone remodeling--lessons from glucocorticoid-induced osteoporosis. *Bone,* 73**,** 16-23.

JESSEN, T. E. & ODUM, L. 2004. TSG-6 and calcium ions are essential for the coupling of inter-alpha-trypsin inhibitor to hyaluronan in human synovial fluid. *Osteoarthritis Cartilage,* 12**,** 142-8.

JIANG, D., LIANG, J. & NOBLE, P. W. 2011. Hyaluronan as an immune regulator in human diseases. *Physiol Rev,* 91**,** 221-64.

JIANG, Y., JAHAGIRDAR, B. N., REINHARDT, R. L., SCHWARTZ, R. E., KEENE, C. D., ORTIZ-GONZALEZ, X. R., REYES, M., LENVIK, T., LUND, T., BLACKSTAD, M., DU, J., ALDRICH, S., LISBERG, A., LOW, W. C., LARGAESPADA, D. A. & VERFAILLIE, C. M. 2002. Pluripotency of mesenchymal stem cells derived from adult marrow. *Nature,* 418**,** 41-9.

JILKA, R. L., HANGOC, G., GIRASOLE, G., PASSERI, G., WILLIAMS, D. C., ABRAMS, J. S., BOYCE, B., BROXMEYER, H. & MANOLAGAS, S. C. 1992. Increased osteoclast development after estrogen loss: mediation by interleukin-6. *Science,* 257**,** 88-91.

JILKA, R. L., WEINSTEIN, R. S., PARFITT, A. M. & MANOLAGAS, S. C. 2007. Quantifying osteoblast and osteocyte apoptosis: challenges and rewards. *J Bone Miner Res,* 22**,** 1492-501.

JONES, S., HORWOOD, N., COPE, A. & DAZZI, F. 2007. The antiproliferative effect of mesenchymal stem cells is a fundamental property shared by all stromal cells. *J Immunol,* 179**,** 2824-31.

KABIRI, M., KUL, B., LOTT, W. B., FUTREGA, K., GHANAVI, P., UPTON, Z. & DORAN, M. R. 2012. 3D mesenchymal stem/stromal cell osteogenesis and autocrine signalling. *Biochem Biophys Res Commun,* 419**,** 142-7.

KAHMANN, J. D., KORUTH, R. & DAY, A. J. 1997. Method for quantitative refolding of the link module from human TSG-6. *Protein Expr Purif,* 9**,** 315-8.

KALLIOLIAS, G. D., ZHAO, B., TRIANTAFYLLOPOULOU, A., PARK-MIN, K. H. & IVASHKIV, L. B. 2010. Interleukin-27 inhibits human osteoclastogenesis by abrogating RANKL-mediated induction of nuclear factor of activated T cells c1 and suppressing proximal RANK signaling. *Arthritis Rheum,* 62**,** 402-13.

KANATANI, M., SUGIMOTO, T., KAJI, H., KOBAYASHI, T., NISHIYAMA, K., FUKASE, M., KUMEGAWA, M. & CHIHARA, K. 1995. Stimulatory effect of bone morphogenetic protein-2 on osteoclast-like cell formation and bone-resorbing activity. *J Bone Miner Res,* 10**,** 1681-90.

KANEKO, H., ARAKAWA, T., MANO, H., KANEDA, T., OGASAWARA, A., NAKAGAWA, M., TOYAMA, Y., YABE, Y., KUMEGAWA, M. & HAKEDA, Y. 2000. Direct stimulation of osteoclastic bone resorption by bone morphogenetic protein (BMP)-2 and expression of BMP receptors in mature osteoclasts. *Bone,* 27**,** 479-86.

KANEMATSU, M., SATO, T., TAKAI, H., WATANABE, K., IKEDA, K. & YAMADA, Y. 2000. Prostaglandin E2 induces expression of receptor activator of nuclear factor-kappa B ligand/osteoprotegrin ligand on pre-B cells: implications for accelerated osteoclastogenesis in estrogen deficiency. *J Bone Miner Res,* 15**,** 1321-9.

KANIS, J. A., MCCLOSKEY, E. V., JOHANSSON, H., COOPER, C., RIZZOLI, R., REGINSTER, J. Y., SCIENTIFIC ADVISORY BOARD OF THE EUROPEAN SOCIETY FOR, C., ECONOMIC ASPECTS OF, O., OSTEOARTHRITIS & THE COMMITTEE OF SCIENTIFIC ADVISORS OF THE INTERNATIONAL OSTEOPOROSIS, F. 2013. European guidance for the diagnosis and management of osteoporosis in postmenopausal women. *Osteoporos Int,* 24**,** 23-57.

KASPER, J. C., WINTER, G. & FRIESS, W. 2013. Recent advances and further challenges in lyophilization. *Eur J Pharm Biopharm,* 85**,** 162-9.

KATAGIRI, T., YAMAGUCHI, A., KOMAKI, M., ABE, E., TAKAHASHI, N., IKEDA, T., ROSEN, V., WOZNEY, J. M., FUJISAWA-SEHARA, A. & SUDA, T. 1994. Bone morphogenetic protein-2 converts the differentiation pathway of C2C12 myoblasts into the osteoblast lineage. *J Cell Biol,* 127**,** 1755-66.

KAUR, G. & DUFOUR, J. M. 2012. Cell lines: Valuable tools or useless artifacts. *Spermatogenesis,* 2**,** 1-5.

KAUR, K., HARDY, R., AHASAN, M. M., EIJKEN, M., VAN LEEUWEN, J. P., FILER, A., THOMAS, A. M., RAZA, K., BUCKLEY, C. D., STEWART, P. M., RABBITT, E. H., HEWISON, M. & COOPER, M. S. 2010. Synergistic induction of local glucocorticoid generation by inflammatory cytokines and glucocorticoids: implications for inflammation associated bone loss. *Ann Rheum Dis,* 69**,** 1185-90.

KE, H. Z., RICHARDS, W. G., LI, X. & OMINSKY, M. S. 2012. Sclerostin and Dickkopf-1 as therapeutic targets in bone diseases. *Endocr Rev,* 33**,** 747-83.

KHAN, I., ZHANG, L., MOHAMMED, M., ARCHER, F. E., ABUKHARMAH, J., YUAN, Z., RIZVI, S. S., MELEK, M. G., RABSON, A. B., SHI, Y., WEINBERGER, B. & VETRANO, A. M. 2015. Effects of Wharton's jelly-derived mesenchymal stem cells on neonatal neutrophils. *J Inflamm Res,* 8**,** 1-8.

KHASHAN, M., INOUE, S. & BERVEN, S. H. 2013. Cell based therapies as compared to autologous bone grafts for spinal arthrodesis. *Spine (Phila Pa 1976),* 38**,** 1885-91.

KHOSLA, S., OURSLER, M. J. & MONROE, D. G. 2012. Estrogen and the skeleton. *Trends Endocrinol Metab,* 23**,** 576-81.

KIM, D. K., CHOI, H., NISHIDA, H., OH, J. Y., GREGORY, C., LEE, R. H., YU, J. M., WATANABE, J., AN, S. Y., BARTOSH, T. J. & PROCKOP, D. J. 2016. Scalable Production of a Multifunctional Protein (TSG-6) That Aggregates with Itself and the CHO Cells That Synthesize It. *PLoS One,* 11**,** e0147553.

KIM, G., COLE, J. H., BOSKEY, A. L., BAKER, S. P. & VAN DER MEULEN, M. C. 2014a. Reduced tissue-level stiffness and mineralization in osteoporotic cancellous bone. *Calcif Tissue Int,* 95**,** 125-31.

KIM, H. H., LEE, D. E., SHIN, J. N., LEE, Y. S., JEON, Y. M., CHUNG, C. H., NI, J., KWON, B. S. & LEE, Z. H. 1999. Receptor activator of NF-kappaB recruits multiple TRAF family adaptors and activates c-Jun N-terminal kinase. *FEBS Lett,* 443**,** 297-302.

KIM, J. A., KO, J. H., KO, A. Y., LEE, H. J., KIM, M. K., WEE, W. R., LEE, R. H., FULCHER, S. F. & OH, J. Y. 2014b. TSG-6 protects corneal endothelium from transcorneal cryoinjury in rabbits. *Invest Ophthalmol Vis Sci,* 55**,** 4905-12.

KIM, S. J., LEE, H. J., YUN, J. H., KO, J. H., CHOI DA, Y. & OH, J. Y. 2015. Intravitreal TSG-6 suppresses laser-induced choroidal neovascularization by inhibiting CCR2+ monocyte recruitment. *Sci Rep,* 5**,** 11872.

KIMBLE, R. B., BAIN, S. & PACIFICI, R. 1997. The functional block of TNF but not of IL-6 prevents bone loss in ovariectomized mice. *J Bone Miner Res,* 12**,** 935-41.

KING, E. J. & ARMSTRONG, A. R. 1934. A Convenient Method for Determining Serum and Bile Phosphatase Activity. *Can Med Assoc J,* 31**,** 376-81.

KIYOMIYA, H., ARIYOSHI, W., OKINAGA, T., KANEUJI, T., MITSUGI, S., SAKURAI, T., HABU, M., YOSHIOKA, I., TOMINAGA, K. & NISHIHARA, T. 2015. IL-33 inhibits RANKL-induced osteoclast formation through the regulation of Blimp-1 and IRF-8 expression. *Biochem Biophys Res Commun,* 460**,** 320-6.

KLAMPFER, L., CHEN-KIANG, S. & VILCEK, J. 1995. Activation of the TSG-6 gene by NF-IL6 requires two adjacent NF-IL6 binding sites. *J Biol Chem,* 270**,** 3677-82.

KLAMPFER, L., LEE, T. H., HSU, W., VILCEK, J. & CHEN-KIANG, S. 1994. NF-IL6 and AP-1 cooperatively modulate the activation of the TSG-6 gene by tumor necrosis factor alpha and interleukin-1. *Mol Cell Biol,* 14**,** 6561-9.

KNOTHE TATE, M. L., ADAMSON, J. R., TAMI, A. E. & BAUER, T. W. 2004. The osteocyte. *Int J Biochem Cell Biol,* 36**,** 1-8.

KODAMA, H., NOSE, M., NIIDA, S. & YAMASAKI, A. 1991. Essential role of macrophage colony-stimulating factor in the osteoclast differentiation supported by stromal cells. *J Exp Med,* 173**,** 1291-4.

KOGA, T., INUI, M., INOUE, K., KIM, S., SUEMATSU, A., KOBAYASHI, E., IWATA, T., OHNISHI, H., MATOZAKI, T., KODAMA, T., TANIGUCHI, T., TAKAYANAGI, H. & TAKAI, T. 2004. Costimulatory signals mediated by the ITAM motif cooperate with RANKL for bone homeostasis. *Nature,* 428**,** 758-63.

KOHDA, D., MORTON, C. J., PARKAR, A. A., HATANAKA, H., INAGAKI, F. M., CAMPBELL, I. D. & DAY, A. J. 1996. Solution structure of the link module: a hyaluronan-binding domain involved in extracellular matrix stability and cell migration. *Cell,* 86**,** 767-75.

KOIDE, M., MURASE, Y., YAMATO, K., NOGUCHI, T., OKAHASHI, N. & NISHIHARA, T. 1999. Bone morphogenetic protein-2 enhances osteoclast formation mediated by interleukin-1alpha through upregulation of osteoclast differentiation factor and cyclooxygenase-2. *Biochem Biophys Res Commun,* 259**,** 97-102.

KOMORI, T., YAGI, H., NOMURA, S., YAMAGUCHI, A., SASAKI, K., DEGUCHI, K., SHIMIZU, Y., BRONSON, R. T., GAO, Y. H., INADA, M., SATO, M., OKAMOTO, R., KITAMURA, Y., YOSHIKI, S. & KISHIMOTO, T. 1997. Targeted disruption of Cbfa1 results in a complete lack of bone formation owing to maturational arrest of osteoblasts. *Cell,* 89**,** 755-64.

KONG, Y. Y., FEIGE, U., SAROSI, I., BOLON, B., TAFURI, A., MORONY, S., CAPPARELLI, C., LI, J., ELLIOTT, R., MCCABE, S., WONG, T., CAMPAGNUOLO, G., MORAN, E., BOGOCH, E. R., VAN, G., NGUYEN, L. T., OHASHI, P. S., LACEY, D. L., FISH, E., BOYLE, W. J. & PENNINGER, J. M. 1999. Activated T cells regulate bone loss and joint destruction in adjuvant arthritis through osteoprotegerin ligand. *Nature,* 402**,** 304-9.

KORNAK, U., KASPER, D., BOSL, M. R., KAISER, E., SCHWEIZER, M., SCHULZ, A., FRIEDRICH, W., DELLING, G. & JENTSCH, T. J. 2001. Loss of the ClC-7 chloride channel leads to osteopetrosis in mice and man. *Cell,* 104**,** 205-15.

KOSTENUIK, P. J. & SHALHOUB, V. 2001. Osteoprotegerin: a physiological and pharmacological inhibitor of bone resorption. *Curr Pharm Des,* 7**,** 613-35.

KOTAKE, S., UDAGAWA, N., TAKAHASHI, N., MATSUZAKI, K., ITOH, K., ISHIYAMA, S., SAITO, S., INOUE, K., KAMATANI, N., GILLESPIE, M. T., MARTIN, T. J. & SUDA, T. 1999. IL-17 in synovial fluids from patients with rheumatoid arthritis is a potent stimulator of osteoclastogenesis. *J Clin Invest,* 103**,** 1345-52.

KRISTENSEN, H. B., ANDERSEN, T. L., MARCUSSEN, N., ROLIGHED, L. & DELAISSE, J. M. 2013. Increased presence of capillaries next to remodeling sites in adult human cancellous bone. *J Bone Miner Res,* 28**,** 574-85.

KRONENBERG, H. M. 2003. Developmental regulation of the growth plate. *Nature,* 423**,** 332-6.

KRUYT, M. C., VAN GAALEN, S. M., ONER, F. C., VERBOUT, A. J., DE BRUIJN, J. D. & DHERT, W. J. 2004. Bone tissue engineering and spinal fusion: the potential of hybrid constructs by combining osteoprogenitor cells and scaffolds. *Biomaterials,* 25**,** 1463-73.

KURIHARA, N., BERTOLINI, D., SUDA, T., AKIYAMA, Y. & ROODMAN, G. D. 1990. IL-6 stimulates osteoclast-like multinucleated cell formation in long term human marrow cultures by inducing IL-1 release. *J Immunol,* 144**,** 4226-30.

KUZNETSOVA, S. A., DAY, A. J., MAHONEY, D. J., RUGG, M. S., MOSHER, D. F. & ROBERTS, D. D. 2005. The N-terminal module of thrombospondin-1 interacts with the link domain of TSG-6 and enhances its covalent association with the heavy chains of inter-alpha-trypsin inhibitor. *J Biol Chem,* 280**,** 30899-908.

KUZNETSOVA, S. A., MAHONEY, D. J., MARTIN-MANSO, G., ALI, T., NENTWICH, H. A., SIPES, J. M., ZENG, B., VOGEL, T., DAY, A. J. & ROBERTS, D. D. 2008. TSG-6 binds via its CUB_C domain to the cell-binding domain of fibronectin and increases fibronectin matrix assembly. *Matrix Biol,* 27**,** 201-10.

LACEY, D. L., TIMMS, E., TAN, H. L., KELLEY, M. J., DUNSTAN, C. R., BURGESS, T., ELLIOTT, R., COLOMBERO, A., ELLIOTT, G., SCULLY, S., HSU, H., SULLIVAN, J., HAWKINS, N., DAVY, E., CAPPARELLI, C., ELI, A., QIAN, Y. X., KAUFMAN, S., SAROSI, I., SHALHOUB, V., SENALDI, G., GUO, J., DELANEY, J. & BOYLE, W. J. 1998. Osteoprotegerin ligand is a cytokine that regulates osteoclast differentiation and activation. *Cell,* 93**,** 165-76.

LAEMMLI, U. K. 1970. Cleavage of structural proteins during the assembly of the head of bacteriophage T4. *Nature,* 227**,** 680-5.

LAINE, C. M., CHUNG, B. D., SUSIC, M., PRESCOTT, T., SEMLER, O., FISKERSTRAND, T., D'EUFEMIA, P., CASTORI, M., PEKKINEN, M., SOCHETT, E., COLE, W. G., NETZER, C. & MAKITIE, O. 2011. Novel mutations affecting LRP5

splicing in patients with osteoporosis-pseudoglioma syndrome (OPPG). *Eur J Hum Genet,* 19**,** 875-81.

LAMKIN, E., CHENG, G., CALABRO, A., HASCALL, V. C., JOO, E. J., LI, L., LINHARDT, R. J. & LAUER, M. E. 2015. Heavy chain transfer by tumor necrosis factor-stimulated gene 6 to the bikunin proteoglycan. *J Biol Chem,* 290**,** 5156-66.

LAMOUREUX, F., BAUD'HUIN, M., DUPLOMB, L., HEYMANN, D. & REDINI, F. 2007. Proteoglycans: key partners in bone cell biology. *Bioessays,* 29**,** 758-71.

LAUER, M. E., CHENG, G., SWAIDANI, S., ARONICA, M. A., WEIGEL, P. H. & HASCALL, V. C. 2013. Tumor necrosis factor-stimulated gene-6 (TSG-6) amplifies hyaluronan synthesis by airway smooth muscle cells. *J Biol Chem,* 288**,** 423-31.

LAURENT, T. C. & FRASER, J. R. 1992. Hyaluronan. *FASEB J,* 6**,** 2397-404.

LE BLANC, K., TAMMIK, L., SUNDBERG, B., HAYNESWORTH, S. E. & RINGDEN, O. 2003. Mesenchymal stem cells inhibit and stimulate mixed lymphocyte cultures and mitogenic responses independently of the major histocompatibility complex. *Scand J Immunol,* 57**,** 11-20.

LEE, J. W., FANG, X., KRASNODEMBSKAYA, A., HOWARD, J. P. & MATTHAY, M. A. 2011. Concise review: Mesenchymal stem cells for acute lung injury: role of paracrine soluble factors. *Stem Cells,* 29**,** 913-9.

LEE, J. Y. & SPICER, A. P. 2000. Hyaluronan: a multifunctional, megaDalton, stealth molecule. *Curr Opin Cell Biol,* 12**,** 581-6.

LEE, R. H., PULIN, A. A., SEO, M. J., KOTA, D. J., YLOSTALO, J., LARSON, B. L., SEMPRUN-PRIETO, L., DELAFONTAINE, P. & PROCKOP, D. J. 2009. Intravenous hMSCs improve myocardial infarction in mice because cells embolized in lung are activated to secrete the anti-inflammatory protein TSG-6. *Cell Stem Cell,* 5**,** 54-63.

LEE, S. E., CHUNG, W. J., KWAK, H. B., CHUNG, C. H., KWACK, K. B., LEE, Z. H. & KIM, H. H. 2001. Tumor necrosis factor-alpha supports the survival of osteoclasts through the activation of Akt and ERK. *J Biol Chem,* 276**,** 49343-9.

LEE, T. H., WISNIEWSKI, H. G. & VILCEK, J. 1992. A novel secretory tumor necrosis factor-inducible protein (TSG-6) is a member of the family of hyaluronate binding proteins, closely related to the adhesion receptor CD44. *J Cell Biol,* 116**,** 545-57.

LEIBBRANDT, A. & PENNINGER, J. M. 2008. RANK/RANKL: regulators of immune responses and bone physiology. *Ann N Y Acad Sci,* 1143**,** 123-50.

LENCEL, P. & MAGNE, D. 2011. Inflammaging: the driving force in osteoporosis? *Med Hypotheses,* 76**,** 317-21.

LESLEY, J., GAL, I., MAHONEY, D. J., CORDELL, M. R., RUGG, M. S., HYMAN, R., DAY, A. J. & MIKECZ, K. 2004. TSG-6 modulates the interaction between hyaluronan and cell surface CD44. *J Biol Chem,* 279**,** 25745-54.

LESLIE, W. D., MAJUMDAR, S. R., LIX, L. M., JOHANSSON, H., ODEN, A., MCCLOSKEY, E., KANIS, J. A. & MANITOBA BONE DENSITY, P. 2012. High fracture probability with FRAX usually indicates densitometric osteoporosis: implications for clinical practice. *Osteoporos Int,* 23**,** 391-7.

LESLIE, W. D. & MORIN, S. N. 2014. Osteoporosis epidemiology 2013: implications for diagnosis, risk assessment, and treatment. *Curr Opin Rheumatol,* 26**,** 440-6.

LEWIECKI, E. M. 2011. Combination therapy: the Holy Grail for the treatment of postmenopausal osteoporosis? *Curr Med Res Opin,* 27**,** 1493-7.

LI, B., BOAST, S., DE LOS SANTOS, K., SCHIEREN, I., QUIROZ, M., TEITELBAUM, S. L., TONDRAVI, M. M. & GOFF, S. P. 2000. Mice deficient in Abl are osteoporotic and have defects in osteoblast maturation. *Nat Genet,* 24**,** 304-8.

LI, J., SAROSI, I., CATTLEY, R. C., PRETORIUS, J., ASUNCION, F., GRISANTI, M., MORONY, S., ADAMU, S., GENG, Z., QIU, W., KOSTENUIK, P., LACEY, D. L.,

SIMONET, W. S., BOLON, B., QIAN, X., SHALHOUB, V., OMINSKY, M. S., ZHU KE, H., LI, X. & RICHARDS, W. G. 2006. Dkk1-mediated inhibition of Wnt signaling in bone results in osteopenia. *Bone,* 39**,** 754-66.

LI, W., WEI, H., XIA, C., ZHU, X., HOU, G., XU, F., SONG, X. & ZHAN, Y. 2015. Gene gun transferring-bone morphogenetic protein 2 (BMP-2) gene enhanced bone fracture healing in rabbits. *Int J Clin Exp Med,* 8**,** 19982-93.

LI, X., OMINSKY, M. S., NIU, Q. T., SUN, N., DAUGHERTY, B., D'AGOSTIN, D., KURAHARA, C., GAO, Y., CAO, J., GONG, J., ASUNCION, F., BARRERO, M., WARMINGTON, K., DWYER, D., STOLINA, M., MORONY, S., SAROSI, I., KOSTENUIK, P. J., LACEY, D. L., SIMONET, W. S., KE, H. Z. & PASZTY, C. 2008. Targeted deletion of the sclerostin gene in mice results in increased bone formation and bone strength. *J Bone Miner Res,* 23**,** 860-9.

LI, X., ZHANG, Y., KANG, H., LIU, W., LIU, P., ZHANG, J., HARRIS, S. E. & WU, D. 2005. Sclerostin binds to LRP5/6 and antagonizes canonical Wnt signaling. *J Biol Chem,* 280**,** 19883-7.

LIN, Q. M., ZHAO, S., ZHOU, L. L., FANG, X. S., FU, Y. & HUANG, Z. T. 2013. Mesenchymal stem cells transplantation suppresses inflammatory responses in global cerebral ischemia: contribution of TNF-alpha-induced protein 6. *Acta Pharmacol Sin,* 34**,** 784-92.

LIU, Y., ZHANG, R., YAN, K., CHEN, F., HUANG, W., LV, B., SUN, C., XU, L., LI, F. & JIANG, X. 2014. Mesenchymal stem cells inhibit lipopolysaccharide-induced inflammatory responses of BV2 microglial cells through TSG-6. *J Neuroinflammation,* 11**,** 135.

LOCKLIN, R. M., KHOSLA, S., TURNER, R. T. & RIGGS, B. L. 2003. Mediators of the biphasic responses of bone to intermittent and continuously administered parathyroid hormone. *J Cell Biochem,* 89**,** 180-90.

LOGAR, D. B., KOMADINA, R., PREZELJ, J., OSTANEK, B., TROST, Z. & MARC, J. 2007. Expression of bone resorption genes in osteoarthritis and in osteoporosis. *J Bone Miner Metab,* 25**,** 219-25.

LOI, F., CORDOVA, L. A., ZHANG, R., PAJARINEN, J., LIN, T. H., GOODMAN, S. B. & YAO, Z. 2016. The effects of immunomodulation by macrophage subsets on osteogenesis in vitro. *Stem Cell Res Ther,* 7**,** 15.

LOMAGA, M. A., YEH, W. C., SAROSI, I., DUNCAN, G. S., FURLONGER, C., HO, A., MORONY, S., CAPPARELLI, C., VAN, G., KAUFMAN, S., VAN DER HEIDEN, A., ITIE, A., WAKEHAM, A., KHOO, W., SASAKI, T., CAO, Z., PENNINGER, J. M., PAIGE, C. J., LACEY, D. L., DUNSTAN, C. R., BOYLE, W. J., GOEDDEL, D. V. & MAK, T. W. 1999. TRAF6 deficiency results in osteopetrosis and defective interleukin-1, CD40, and LPS signaling. *Genes Dev,* 13**,** 1015-24.

LORENZO, J. A., SOUSA, S. L., FONSECA, J. M., HOCK, J. M. & MEDLOCK, E. S. 1987. Colony-stimulating factors regulate the development of multinucleated osteoclasts from recently replicated cells in vitro. *J Clin Invest,* 80**,** 160-4.

LORGET, F., KAMEL, S., MENTAVERRI, R., WATTEL, A., NAASSILA, M., MAAMER, M. & BRAZIER, M. 2000. High extracellular calcium concentrations directly stimulate osteoclast apoptosis. *Biochem Biophys Res Commun,* 268**,** 899-903.

LOSER, K., MEHLING, A., LOESER, S., APELT, J., KUHN, A., GRABBE, S., SCHWARZ, T., PENNINGER, J. M. & BEISSERT, S. 2006. Epidermal RANKL controls regulatory T-cell numbers via activation of dendritic cells. *Nat Med,* 12**,** 1372-9.

LOUTIT, J. F. & SANSOM, J. M. 1976. Osteopetrosis of microphthalmic mice -- a defect of the hematopoietic stem cell.? *Calcif Tissue Res,* 20**,** 251-9.

LOVIBOND, A. C., HAQUE, S. J., CHAMBERS, T. J. & FOX, S. W. 2003. TGF-beta-induced SOCS3 expression augments TNF-alpha-induced osteoclast formation. *Biochem Biophys Res Commun,* 309**,** 762-7.

LU, Z., WANG, G., DUNSTAN, C. R. & ZREIQAT, H. 2012. Short-term exposure to tumor necrosis factor-alpha enables human osteoblasts to direct adipose tissue-derived mesenchymal stem cells into osteogenic differentiation. *Stem Cells Dev,* 21**,** 2420-9.

LYMPERI, S., HORWOOD, N., MARLEY, S., GORDON, M. Y., COPE, A. P. & DAZZI, F. 2008. Strontium can increase some osteoblasts without increasing hematopoietic stem cells. *Blood,* 111**,** 1173-81.

MABILLEAU, G. & SABOKBAR, A. 2009. Interleukin-32 promotes osteoclast differentiation but not osteoclast activation. *PLoS One,* 4**,** e4173.

MAEDA, S., HAYASHI, M., KOMIYA, S., IMAMURA, T. & MIYAZONO, K. 2004. Endogenous TGF-beta signaling suppresses maturation of osteoblastic mesenchymal cells. *EMBO J,* 23**,** 552-63.

MAES, C., KOBAYASHI, T., SELIG, M. K., TORREKENS, S., ROTH, S. I., MACKEM, S., CARMELIET, G. & KRONENBERG, H. M. 2010. Osteoblast precursors, but not mature osteoblasts, move into developing and fractured bones along with invading blood vessels. *Dev Cell,* 19**,** 329-44.

MAGER, D. E. & JUSKO, W. J. 2002. Receptor-mediated pharmacokinetic/pharmacodynamic model of interferon-beta 1a in humans. *Pharm Res,* 19**,** 1537-43.

MAHONEY, D. J., MIKECZ, K., ALI, T., MABILLEAU, G., BENAYAHU, D., PLAAS, A., MILNER, C. M., DAY, A. J. & SABOKBAR, A. 2008. TSG-6 regulates bone remodeling through inhibition of osteoblastogenesis and osteoclast activation. *J Biol Chem,* 283**,** 25952-62.

MAHONEY, D. J., MULLOY, B., FORSTER, M. J., BLUNDELL, C. D., FRIES, E., MILNER, C. M. & DAY, A. J. 2005. Characterization of the interaction between tumor necrosis factor-stimulated gene-6 and heparin: implications for the inhibition of plasmin in extracellular matrix microenvironments. *J Biol Chem,* 280**,** 27044-55.

MAHONEY, D. J., SWALES, C., ATHANASOU, N. A., BOMBARDIERI, M., PITZALIS, C., KLISKEY, K., SHARIF, M., DAY, A. J., MILNER, C. M. & SABOKBAR, A. 2011. TSG-6 inhibits osteoclast activity via an autocrine mechanism and is functionally synergistic with osteoprotegerin. *Arthritis Rheum,* 63**,** 1034-43.

MAIER, R., WISNIEWSKI, H. G., VILCEK, J. & LOTZ, M. 1996. TSG-6 expression in human articular chondrocytes. Possible implications in joint inflammation and cartilage degradation. *Arthritis Rheum,* 39**,** 552-9.

MAINA, V., COTENA, A., DONI, A., NEBULONI, M., PASQUALINI, F., MILNER, C. M., DAY, A. J., MANTOVANI, A. & GARLANDA, C. 2009. Coregulation in human leukocytes of the long pentraxin PTX3 and TSG-6. *J Leukoc Biol,* 86**,** 123-32.

MAJID, H., KHAN, A. H., RIAZ, M., KARIMI, H. & TALATI, J. 2016. Identifying Parathyroid Hormone Disorders and Its Phenotypes through a Bone Health Screening Panel: It's Not Simple Vitamin D Deficiency! *Endocr Pract*.

MALONE, J. D., TEITELBAUM, S. L., GRIFFIN, G. L., SENIOR, R. M. & KAHN, A. J. 1982. Recruitment of osteoclast precursors by purified bone matrix constituents. *J Cell Biol,* 92**,** 227-30.

MALYALA, P. & SINGH, M. 2008. Endotoxin limits in formulations for preclinical research. *J Pharm Sci,* 97**,** 2041-4.

MANI, A., RADHAKRISHNAN, J., WANG, H., MANI, A., MANI, M. A., NELSON-WILLIAMS, C., CAREW, K. S., MANE, S., NAJMABADI, H., WU, D. & LIFTON,

R. P. 2007. LRP6 mutation in a family with early coronary disease and metabolic risk factors. *Science,* 315**,** 1278-82.

MARGERIE, D., FLECHTENMACHER, J., BUTTNER, F. H., KARBOWSKI, A., PUHL, W., SCHLEYERBACH, R. & BARTNIK, E. 1997. Complexity of IL-1 beta induced gene expression pattern in human articular chondrocytes. *Osteoarthritis Cartilage,* 5**,** 129-38.

MARKS, S. C., JR. & POPOFF, S. N. 1988. Bone cell biology: the regulation of development, structure, and function in the skeleton. *Am J Anat,* 183**,** 1-44.

MARKS, S. C., JR. & WALKER, D. G. 1969. The role of the parafollicular cell of the thyroid gland in the pathogenesis of congenital osteopetrosis in mice. *Am J Anat,* 126**,** 299-313.

MARSHALL, M. J., NISBET, N. W. & STOCKDALE, M. 1983. Osteopetrosis in the Gruneberg (mi) mouse can be cured by cultured allogeneic bone marrow. *Calcif Tissue Int,* 35**,** 812-4.

MARTIN, T. J., ALLAN, E. H., HO, P. W., GOOI, J. H., QUINN, J. M., GILLESPIE, M. T., KRASNOPEROV, V. & SIMS, N. A. 2010. Communication between ephrinB2 and EphB4 within the osteoblast lineage. *Adv Exp Med Biol,* 658**,** 51-60.

MARTIN, T. J. & SIMS, N. A. 2005. Osteoclast-derived activity in the coupling of bone formation to resorption. *Trends Mol Med,* 11**,** 76-81.

MARTINO, S., CAULEY, J. A., BARRETT-CONNOR, E., POWLES, T. J., MERSHON, J., DISCH, D., SECREST, R. J., CUMMINGS, S. R. & INVESTIGATORS, C. 2004. Continuing outcomes relevant to Evista: breast cancer incidence in postmenopausal osteoporotic women in a randomized trial of raloxifene. *J Natl Cancer Inst,* 96**,** 1751-61.

MASUZAWA, T., MIYAURA, C., ONOE, Y., KUSANO, K., OHTA, H., NOZAWA, S. & SUDA, T. 1994. Estrogen deficiency stimulates B lymphopoiesis in mouse bone marrow. *J Clin Invest,* 94**,** 1090-7.

MATSABA, T., RAMOSHEBI, L. N., CROOKS, J. & RIPAMONTI, U. 2001. Transforming growth factor-beta1 supports the rapid morphogenesis of heterotopic endochondral bone initiated by human osteogenic protein-1 via the synergistic up-regulation of molecular markers. *Growth Factors,* 19**,** 73-86.

MAURER, P. H. & HUDACK, S. S. 1952. The isolation of hyaluronic acid from callus tissue of early healing. *Arch Biochem Biophys,* 38**,** 49-53.

MCBEATH, R., PIRONE, D. M., NELSON, C. M., BHADRIRAJU, K. & CHEN, C. S. 2004. Cell shape, cytoskeletal tension, and RhoA regulate stem cell lineage commitment. *Dev Cell,* 6**,** 483-95.

MCCLUNG, M. R., GRAUER, A., BOONEN, S., BOLOGNESE, M. A., BROWN, J. P., DIEZ-PEREZ, A., LANGDAHL, B. L., REGINSTER, J. Y., ZANCHETTA, J. R., WASSERMAN, S. M., KATZ, L., MADDOX, J., YANG, Y. C., LIBANATI, C. & BONE, H. G. 2014. Romosozumab in postmenopausal women with low bone mineral density. *N Engl J Med,* 370**,** 412-20.

MCCOY, E. M., HONG, H., PRUITT, H. C. & FENG, X. 2013. IL-11 produced by breast cancer cells augments osteoclastogenesis by sustaining the pool of osteoclast progenitor cells. *BMC Cancer,* 13**,** 16.

MEDZHITOV, R. 2010. Inflammation 2010: new adventures of an old flame. *Cell,* 140**,** 771-6.

MILLER, S. C., DE SAINT-GEORGES, L., BOWMAN, B. M. & JEE, W. S. 1989. Bone lining cells: structure and function. *Scanning Microsc,* 3**,** 953-60; discussion 960-1.

MILNER, C. M. & DAY, A. J. 2003. TSG-6: a multifunctional protein associated with inflammation. *J Cell Sci,* 116**,** 1863-73.

MILNER, C. M., HIGMAN, V. A. & DAY, A. J. 2006. TSG-6: a pluripotent inflammatory mediator? *Biochem Soc Trans,* 34**,** 446-50.

MILNER, C. M., TONGSOONGNOEN, W., RUGG, M. S. & DAY, A. J. 2007. The molecular basis of inter-alpha-inhibitor heavy chain transfer on to hyaluronan. *Biochem Soc Trans,* 35**,** 672-6.

MINDRESCU, C., DIAS, A. A., OLSZEWSKI, R. J., KLEIN, M. J., REIS, L. F. & WISNIEWSKI, H. G. 2002. Reduced susceptibility to collagen-induced arthritis in DBA/1J mice expressing the TSG-6 transgene. *Arthritis Rheum,* 46**,** 2453-64.

MINDRESCU, C., THORBECKE, G. J., KLEIN, M. J., VILCEK, J. & WISNIEWSKI, H. G. 2000. Amelioration of collagen-induced arthritis in DBA/1J mice by recombinant TSG-6, a tumor necrosis factor/interleukin-1-inducible protein. *Arthritis Rheum,* 43**,** 2668-77.

MINKIN, C. 1982. Bone acid phosphatase: tartrate-resistant acid phosphatase as a marker of osteoclast function. *Calcif Tissue Int,* 34**,** 285-90.

MIYAKE, K., UNDERHILL, C. B., LESLEY, J. & KINCADE, P. W. 1990. Hyaluronate can function as a cell adhesion molecule and CD44 participates in hyaluronate recognition. *J Exp Med,* 172**,** 69-75.

MIYAURA, C., ONOE, Y., INADA, M., MAKI, K., IKUTA, K., ITO, M. & SUDA, T. 1997. Increased B-lymphopoiesis by interleukin 7 induces bone loss in mice with intact ovarian function: similarity to estrogen deficiency. *Proc Natl Acad Sci U S A,* 94**,** 9360-5.

MIZOGUCHI, T., MUTO, A., UDAGAWA, N., ARAI, A., YAMASHITA, T., HOSOYA, A., NINOMIYA, T., NAKAMURA, H., YAMAMOTO, Y., KINUGAWA, S., NAKAMURA, M., NAKAMICHI, Y., KOBAYASHI, Y., NAGASAWA, S., ODA, K., TANAKA,

H., TAGAYA, M., PENNINGER, J. M., ITO, M. & TAKAHASHI, N. 2009. Identification of cell cycle-arrested quiescent osteoclast precursors in vivo. *J Cell Biol,* 184**,** 541-54.

MOCSAI, A., HUMPHREY, M. B., VAN ZIFFLE, J. A., HU, Y., BURGHARDT, A., SPUSTA, S. C., MAJUMDAR, S., LANIER, L. L., LOWELL, C. A. & NAKAMURA, M. C. 2004. The immunomodulatory adapter proteins DAP12 and Fc receptor gamma-chain (FcRgamma) regulate development of functional osteoclasts through the Syk tyrosine kinase. *Proc Natl Acad Sci U S A,* 101**,** 6158-63.

MOE, S. M. 2008. Disorders involving calcium, phosphorus, and magnesium. *Prim Care,* 35**,** 215-37, v-vi.

MOHAMMADPOUR, H., POURFATHOLLAH, A. A., ZARIF, M. N. & TAHOORI, M. T. 2015. TNF-alpha modulates the immunosuppressive effects of MSCs on dendritic cells and T cells. *Int Immunopharmacol,* 28**,** 1009-17.

MONTESPAN, F., DESCHASEAUX, F., SENSEBE, L., CAROSELLA, E. D. & ROUAS-FREISS, N. 2014. Osteodifferentiated mesenchymal stem cells from bone marrow and adipose tissue express HLA-G and display immunomodulatory properties in HLA-mismatched settings: implications in bone repair therapy. *J Immunol Res,* 2014**,** 230346.

MOSLEY, J. R. 2000. Osteoporosis and bone functional adaptation: mechanobiological regulation of bone architecture in growing and adult bone, a review. *J Rehabil Res Dev,* 37**,** 189-99.

MOURSI, A. M., DAMSKY, C. H., LULL, J., ZIMMERMAN, D., DOTY, S. B., AOTA, S. & GLOBUS, R. K. 1996. Fibronectin regulates calvarial osteoblast differentiation. *J Cell Sci,* 109 (Pt 6)**,** 1369-80.

MOURSI, A. M., GLOBUS, R. K. & DAMSKY, C. H. 1997. Interactions between integrin receptors and fibronectin are required for calvarial osteoblast differentiation in vitro. *J Cell Sci,* 110 (Pt 18)**,** 2187-96.

MUKHOPADHYAY, D., HASCALL, V. C., DAY, A. J., SALUSTRI, A. & FULOP, C. 2001. Two distinct populations of tumor necrosis factor-stimulated gene-6 protein in the extracellular matrix of expanded mouse cumulus cell-oocyte complexes. *Arch Biochem Biophys,* 394**,** 173-81.

MUNDY, G. R. 1996. Regulation of bone formation by bone morphogenetic proteins and other growth factors. *Clin Orthop Relat Res***,** 24-8.

MUNDY, G. R., LUBEN, R. A., RAISZ, L. G., OPPENHEIM, J. J. & BUELL, D. N. 1974. Bone-resorbing activity in supernatants from lymphoid cell lines. *N Engl J Med,* 290**,** 867-71.

MUNETA, Y., NAGAYA, H., MINAGAWA, Y., ENOMOTO, C., MATSUMOTO, S. & MORI, Y. 2004. Expression and one-step purification of bovine interleukin-21 (IL-21) in silkworms using a hybrid baculovirus expression system. *Biotechnol Lett,* 26**,** 1453-8.

NAGAYA, H., KANAYA, T., KAKI, H., TOBITA, Y., TAKAHASHI, M., TAKAHASHI, H., YOKOMIZO, Y. & INUMARU, S. 2004. Establishment of a large-scale purification procedure for purified recombinant bovine interferon-tau produced by a silkworm-baculovirus gene expression system. *J Vet Med Sci,* 66**,** 1395-401.

NAGAYA, H., KANAYA, T., TOBITA, Y., YOKOMIZO, Y., INUMARU, S. & ONODERA, T. 2008. Development of efficient method for purified recombinant bovine granulocyte-macrophage colony-stimulating factor production with baculovirus-silkworm gene expression system. *Biotechnol Lett,* 30**,** 41-5.

NAGYERI, G., RADACS, M., GHASSEMI-NEJAD, S., TRYNISZEWSKA, B., OLASZ, K., HUTAS, G., GYORFY, Z., HASCALL, V. C., GLANT, T. T. & MIKECZ, K.

2011. TSG-6 protein, a negative regulator of inflammatory arthritis, forms a ternary complex with murine mast cell tryptases and heparin. *J Biol Chem,* 286**,** 23559-69.

NAITO, A., AZUMA, S., TANAKA, S., MIYAZAKI, T., TAKAKI, S., TAKATSU, K., NAKAO, K., NAKAMURA, K., KATSUKI, M., YAMAMOTO, T. & INOUE, J. 1999. Severe osteopetrosis, defective interleukin-1 signalling and lymph node organogenesis in TRAF6-deficient mice. *Genes Cells,* 4**,** 353-62.

NAKAMURA, T., IMAI, Y., MATSUMOTO, T., SATO, S., TAKEUCHI, K., IGARASHI, K., HARADA, Y., AZUMA, Y., KRUST, A., YAMAMOTO, Y., NISHINA, H., TAKEDA, S., TAKAYANAGI, H., METZGER, D., KANNO, J., TAKAOKA, K., MARTIN, T. J., CHAMBON, P. & KATO, S. 2007. Estrogen prevents bone loss via estrogen receptor alpha and induction of Fas ligand in osteoclasts. *Cell,* 130**,** 811-23.

NAKASHIMA, K., ZHOU, X., KUNKEL, G., ZHANG, Z., DENG, J. M., BEHRINGER, R. R. & DE CROMBRUGGHE, B. 2002. The novel zinc finger-containing transcription factor osterix is required for osteoblast differentiation and bone formation. *Cell,* 108**,** 17-29.

NAKASHIMA, T., HAYASHI, M., FUKUNAGA, T., KURATA, K., OH-HORA, M., FENG, J. Q., BONEWALD, L. F., KODAMA, T., WUTZ, A., WAGNER, E. F., PENNINGER, J. M. & TAKAYANAGI, H. 2011a. Evidence for osteocyte regulation of bone homeostasis through RANKL expression. *Nat Med,* 17**,** 1231-4.

NAKASHIMA, T., HAYASHI, M. & TAKAYANAGI, H. 2011b. [Bone and calcium update; bone research update. Osteoclastogenesis and osteoimmunology]. *Clin Calcium,* 21**,** 93-102.

NEER, R. M., ARNAUD, C. D., ZANCHETTA, J. R., PRINCE, R., GAICH, G. A., REGINSTER, J. Y., HODSMAN, A. B., ERIKSEN, E. F., ISH-SHALOM, S., GENANT, H. K., WANG, O. & MITLAK, B. H. 2001. Effect of parathyroid hor-

mone (1-34) on fractures and bone mineral density in postmenopausal women with osteoporosis. *N Engl J Med,* 344**,** 1434-41.

NEFUSSI, J. R., BRAMI, G., MODROWSKI, D., OBOEUF, M. & FOREST, N. 1997. Sequential expression of bone matrix proteins during rat calvaria osteoblast differentiation and bone nodule formation in vitro. *J Histochem Cytochem,* 45**,** 493-503.

NEGISHI-KOGA, T., GOBER, H. J., SUMIYA, E., KOMATSU, N., OKAMOTO, K., SAWA, S., SUEMATSU, A., SUDA, T., SATO, K., TAKAI, T. & TAKAYANAGI, H. 2015. Immune complexes regulate bone metabolism through FcRgamma signalling. *Nat Commun,* 6**,** 6637.

NENTWICH, H. A., MUSTAFA, Z., RUGG, M. S., MARSDEN, B. D., CORDELL, M. R., MAHONEY, D. J., JENKINS, S. C., DOWLING, B., FRIES, E., MILNER, C. M., LOUGHLIN, J. & DAY, A. J. 2002. A novel allelic variant of the human TSG-6 gene encoding an amino acid difference in the CUB module. Chromosomal localization, frequency analysis, modeling, and expression. *J Biol Chem,* 277**,** 15354-62.

NICOLAIDOU, V., WONG, M. M., REDPATH, A. N., ERSEK, A., BABAN, D. F., WILLIAMS, L. M., COPE, A. P. & HORWOOD, N. J. 2012. Monocytes induce STAT3 activation in human mesenchymal stem cells to promote osteoblast formation. *PLoS One,* 7**,** e39871.

NIELSEN, S. P., SLOSMAN, D., SORENSEN, O. H., BASSE-CATHALINAT, B., DE CASSIN, P., ROUX, C. R. & MEUNIER, P. J. 1999. Influence of strontium on bone mineral density and bone mineral content measurements by dual X-ray absorptiometry. *J Clin Densitom,* 2**,** 371-9.

NISBET, N. W., MENAGE, J. & LOUTIT, J. F. 1978. Host-donor cellular interactions in the treatment of experimental osteopetrosis. *Nature,* 271**,** 464-6.

NOH, T., GABET, Y., COGAN, J., SHI, Y., TANK, A., SASAKI, T., CRISWELL, B., DIXON, A., LEE, C., TAM, J., KOHLER, T., SEGEV, E., KOCKERITZ, L., WOODGETT, J., MULLER, R., CHAI, Y., SMITH, E., BAB, I. & FRENKEL, B. 2009. Lef1 haploinsufficient mice display a low turnover and low bone mass phenotype in a gender- and age-specific manner. *PLoS One,* 4**,** e5438.

OCHAREON, P. & HERRING, S. W. 2011. Cell replication in craniofacial periosteum: appositional vs. resorptive sites. *J Anat,* 218**,** 285-97.

OCHSNER, S. A., DAY, A. J., RUGG, M. S., BREYER, R. M., GOMER, R. H. & RICHARDS, J. S. 2003. Disrupted function of tumor necrosis factor-alpha-stimulated gene 6 blocks cumulus cell-oocyte complex expansion. *Endocrinology,* 144**,** 4376-84.

OH, J. Y., LEE, R. H., YU, J. M., KO, J. H., LEE, H. J., KO, A. Y., RODDY, G. W. & PROCKOP, D. J. 2012. Intravenous mesenchymal stem cells prevented rejection of allogeneic corneal transplants by aborting the early inflammatory response. *Mol Ther,* 20**,** 2143-52.

OH, J. Y., RODDY, G. W., CHOI, H., LEE, R. H., YLOSTALO, J. H., ROSA, R. H., JR. & PROCKOP, D. J. 2010. Anti-inflammatory protein TSG-6 reduces inflammatory damage to the cornea following chemical and mechanical injury. *Proc Natl Acad Sci U S A,* 107**,** 16875-80.

OHNAKA, K., TANIGUCHI, H., KAWATE, H., NAWATA, H. & TAKAYANAGI, R. 2004. Glucocorticoid enhances the expression of dickkopf-1 in human osteoblasts: novel mechanism of glucocorticoid-induced osteoporosis. *Biochem Biophys Res Commun,* 318**,** 259-64.

OKAMOTO, K., MATSUURA, T., HOSOKAWA, R. & AKAGAWA, Y. 1998. RGD peptides regulate the specific adhesion scheme of osteoblasts to hydroxyapatite but not to titanium. *J Dent Res,* 77**,** 481-7.

OKER-BLOM, C. & SUMMERS, M. D. 1989. Expression of Sindbis virus 26S cDNA in Spodoptera frugiperda (Sf9) cells, using a baculovirus expression vector. *J Virol,* 63**,** 1256-64.

ONAL, M., XIONG, J., CHEN, X., THOSTENSON, J. D., ALMEIDA, M., MANOLAGAS, S. C. & O'BRIEN, C. A. 2012. Receptor activator of nuclear factor kappaB ligand (RANKL) protein expression by B lymphocytes contributes to ovariectomy-induced bone loss. *J Biol Chem,* 287**,** 29851-60.

ONOE, Y., MIYAURA, C., ITO, M., OHTA, H., NOZAWA, S. & SUDA, T. 2000. Comparative effects of estrogen and raloxifene on B lymphopoiesis and bone loss induced by sex steroid deficiency in mice. *J Bone Miner Res,* 15**,** 541-9.

ORCEL, P., FEUGA, M., BIELAKOFF, J. & DE VERNEJOUL, M. C. 1993. Local bone injections of LPS and M-CSF increase bone resorption by different pathways in vivo in rats. *Am J Physiol,* 264**,** E391-7.

ORRISS, I. R., HAJJAWI, M. O., HUESA, C., MACRAE, V. E. & ARNETT, T. R. 2014. Optimisation of the differing conditions required for bone formation in vitro by primary osteoblasts from mice and rats. *Int J Mol Med,* 34**,** 1201-8.

OZAWA, K., KUWABARA, K., TAMATANI, M., TAKATSUJI, K., TSUKAMOTO, Y., KANEDA, S., YANAGI, H., STERN, D. M., EGUCHI, Y., TSUJIMOTO, Y., OGAWA, S. & TOHYAMA, M. 1999. 150-kDa oxygen-regulated protein (ORP150) suppresses hypoxia-induced apoptotic cell death. *J Biol Chem,* 274**,** 6397-404.

PACIFICI, R. 2010. The immune system and bone. *Arch Biochem Biophys,* 503**,** 41-53.

PADHI, D., ALLISON, M., KIVITZ, A. J., GUTIERREZ, M. J., STOUCH, B., WANG, C. & JANG, G. 2014. Multiple doses of sclerostin antibody romosozumab in healthy men and postmenopausal women with low bone mass: a randomized, double-blind, placebo-controlled study. *J Clin Pharmacol,* 54**,** 168-78.

PAPAPOULOS, S. E. 2015. Anabolic bone therapies in 2014: New bone-forming treatments for osteoporosis. *Nat Rev Endocrinol,* 11**,** 69-70.

PARFITT, A. M. 1979. Quantum concept of bone remodeling and turnover: implications for the pathogenesis of osteoporosis. *Calcif Tissue Int,* 28**,** 1-5.

PARK, J. S., JUNG, Y. O., OH, H. J., PARK, S. J., HEO, Y. J., KANG, C. M., KWOK, S. K., JU, J. H., PARK, K. S., CHO, M. L., SUNG, Y. C., PARK, S. H. & KIM, H. Y. 2012. Interleukin-27 suppresses osteoclastogenesis via induction of interferon-gamma. *Immunology,* 137**,** 326-35.

PARKAR, A. A. & DAY, A. J. 1997. Overlapping sites on the Link module of human TSG-6 mediate binding to hyaluronan and chrondroitin-4-sulphate. *FEBS Lett,* 410**,** 413-7.

PARKAR, A. A., KAHMANN, J. D., HOWAT, S. L., BAYLISS, M. T. & DAY, A. J. 1998. TSG-6 interacts with hyaluronan and aggrecan in a pH-dependent manner via a common functional element: implications for its regulation in inflamed cartilage. *FEBS Lett,* 428**,** 171-6.

PARKS, T. D., LEUTHER, K. K., HOWARD, E. D., JOHNSTON, S. A. & DOUGHERTY, W. G. 1994. Release of proteins and peptides from fusion proteins using a recombinant plant virus proteinase. *Anal Biochem,* 216**,** 413-7.

PAZIANAS, M. 2015. Anabolic effects of PTH and the 'anabolic window'. *Trends Endocrinol Metab,* 26**,** 111-3.

PERRY, S. E., ROBINSON, P., MELCHER, A., QUIRKE, P., BUHRING, H. J., COOK, G. P. & BLAIR, G. E. 2007. Expression of the CUB domain containing protein 1 (CDCP1) gene in colorectal tumour cells. *FEBS Lett,* 581**,** 1137-42.

PETERSON, R. S., ANDHARE, R. A., ROUSCHE, K. T., KNUDSON, W., WANG, W., GROSSFIELD, J. B., THOMAS, R. O., HOLLINGSWORTH, R. E. & KNUDSON,

C. B. 2004. CD44 modulates Smad1 activation in the BMP-7 signaling pathway. *J Cell Biol,* 166**,** 1081-91.

PETREY, A. C. & DE LA MOTTE, C. A. 2014. Hyaluronan, a crucial regulator of inflammation. *Front Immunol,* 5**,** 101.

PETTIT, A. R., CHANG, M. K., HUME, D. A. & RAGGATT, L. J. 2008. Osteal macrophages: a new twist on coupling during bone dynamics. *Bone,* 43**,** 976-82.

PFEILSCHIFTER, J., KODITZ, R., PFOHL, M. & SCHATZ, H. 2002. Changes in proinflammatory cytokine activity after menopause. *Endocr Rev,* 23**,** 90-119.

PIETSCHMANN, P., MECHTCHERIAKOVA, D., MESHCHERYAKOVA, A., FOGER-SAMWALD, U. & ELLINGER, I. 2016. Immunology of Osteoporosis: A Mini-Review. *Gerontology,* 62**,** 128-37.

PITTENGER, M. F., MACKAY, A. M., BECK, S. C., JAISWAL, R. K., DOUGLAS, R., MOSCA, J. D., MOORMAN, M. A., SIMONETTI, D. W., CRAIG, S. & MARSHAK, D. R. 1999. Multilineage potential of adult human mesenchymal stem cells. *Science,* 284**,** 143-7.

PIVONKA, P. & DUNSTAN, C. R. 2012. Role of mathematical modeling in bone fracture healing. *Bonekey Rep,* 1**,** 221.

PIXLEY, F. J. & STANLEY, E. R. 2004. CSF-1 regulation of the wandering macrophage: complexity in action. *Trends Cell Biol,* 14**,** 628-38.

POLAYES, D. A., PARKS, T. D., JOHNSTON, S. A. & DOUGHERTY, W. G. 1998. Application of TEV Protease in Protein Production. *Methods Mol Med,* 13**,** 169-83.

PORATH, J. & FLODIN, P. 1959. Gel filtration: a method for desalting and group separation. *Nature,* 183**,** 1657-9.

POWER, R. A., IWANIEC, U. T., MAGEE, K. A., MITOVA-CANEVA, N. G. & WRONSKI, T. J. 2004. Basic fibroblast growth factor has rapid bone anabolic effects in ovariectomized rats. *Osteoporos Int,* 15**,** 716-23.

PROCKOP, D. J. 2013. Concise review: two negative feedback loops place mesenchymal stem/stromal cells at the center of early regulators of inflammation. *Stem Cells,* 31**,** 2042-6.

PROCKOP, D. J. & OH, J. Y. 2012. Mesenchymal stem/stromal cells (MSCs): role as guardians of inflammation. *Mol Ther,* 20**,** 14-20.

QUINN, J. M., SIMS, N. A., SALEH, H., MIROSA, D., THOMPSON, K., BOURALEXIS, S., WALKER, E. C., MARTIN, T. J. & GILLESPIE, M. T. 2008. IL-23 inhibits osteoclastogenesis indirectly through lymphocytes and is required for the maintenance of bone mass in mice. *J Immunol,* 181**,** 5720-9.

RACZ, G. Z., KADAR, K., FOLDES, A., KALLO, K., PERCZEL-KOVACH, K., KEREMI, B., NAGY, A. & VARGA, G. 2014. Immunomodulatory and potential therapeutic role of mesenchymal stem cells in periodontitis. *J Physiol Pharmacol,* 65**,** 327-39.

RAHMAN, M. S., AKHTAR, N., JAMIL, H. M., BANIK, R. S. & ASADUZZAMAN, S. M. 2015. TGF-beta/BMP signaling and other molecular events: regulation of osteoblastogenesis and bone formation. *Bone Res,* 3**,** 15005.

REY, J. R., CERVINO, E. V., RENTERO, M. L., CRESPO, E. C., ALVARO, A. O. & CASILLAS, M. 2009. Raloxifene: mechanism of action, effects on bone tissue, and applicability in clinical traumatology practice. *Open Orthop J,* 3**,** 14-21.

RIANCHO, J. A. & HERNANDEZ, J. L. 2012. Pharmacogenomics of osteoporosis: a pathway approach. *Pharmacogenomics,* 13**,** 815-29.

RICHTER, W. F. & JACOBSEN, B. 2014. Subcutaneous absorption of biotherapeutics: knowns and unknowns. *Drug Metab Dispos,* 42**,** 1881-9.

RITTMASTER, R. S., BOLOGNESE, M., ETTINGER, M. P., HANLEY, D. A., HODSMAN, A. B., KENDLER, D. L. & ROSEN, C. J. 2000. Enhancement of bone mass in osteoporotic women with parathyroid hormone followed by alendronate. *J Clin Endocrinol Metab,* 85**,** 2129-34.

RIVADENEIRA, F. & MAKITIE, O. 2016. Osteoporosis and Bone Mass Disorders: From Gene Pathways to Treatments. *Trends Endocrinol Metab*.

RIZZOLI, R., AKESSON, K., BOUXSEIN, M., KANIS, J. A., NAPOLI, N., PAPAPOULOS, S., REGINSTER, J. Y. & COOPER, C. 2011. Subtrochanteric fractures after long-term treatment with bisphosphonates: a European Society on Clinical and Economic Aspects of Osteoporosis and Osteoarthritis, and International Osteoporosis Foundation Working Group Report. *Osteoporos Int,* 22**,** 373-90.

ROBLING, A. G. & TURNER, C. H. 2009. Mechanical signaling for bone modeling and remodeling. *Crit Rev Eukaryot Gene Expr,* 19**,** 319-38.

RODAN, G. A. & FLEISCH, H. A. 1996. Bisphosphonates: mechanisms of action. *J Clin Invest,* 97**,** 2692-6.

RODAN, G. A. & MARTIN, T. J. 1981. Role of osteoblasts in hormonal control of bone resorption--a hypothesis. *Calcif Tissue Int,* 33**,** 349-51.

RODDY, G. W., OH, J. Y., LEE, R. H., BARTOSH, T. J., YLOSTALO, J., COBLE, K., ROSA, R. H., JR. & PROCKOP, D. J. 2011. Action at a distance: systemically administered adult stem/progenitor cells (MSCs) reduce inflammatory damage to the cornea without engraftment and primarily by secretion of TNF-alpha stimulated gene/protein 6. *Stem Cells,* 29**,** 1572-9.

ROGGIA, C., GAO, Y., CENCI, S., WEITZMANN, M. N., TORALDO, G., ISAIA, G. & PACIFICI, R. 2001. Up-regulation of TNF-producing T cells in the bone marrow: a key mechanism by which estrogen deficiency induces bone loss in vivo. *Proc Natl Acad Sci U S A,* 98**,** 13960-5.

ROSSOL, M., HEINE, H., MEUSCH, U., QUANDT, D., KLEIN, C., SWEET, M. J. & HAUSCHILDT, S. 2011. LPS-induced cytokine production in human monocytes and macrophages. *Crit Rev Immunol,* 31**,** 379-446.

RUGG, M. S., WILLIS, A. C., MUKHOPADHYAY, D., HASCALL, V. C., FRIES, E., FULOP, C., MILNER, C. M. & DAY, A. J. 2005. Characterization of complexes formed between TSG-6 and inter-alpha-inhibitor that act as intermediates in the covalent transfer of heavy chains onto hyaluronan. *J Biol Chem,* 280**,** 25674-86.

RUSSELL, R. G. 2007. Bisphosphonates: mode of action and pharmacology. *Pediatrics,* 119 Suppl 2**,** S150-62.

RUSSELL, R. G., WATTS, N. B., EBETINO, F. H. & ROGERS, M. J. 2008. Mechanisms of action of bisphosphonates: similarities and differences and their potential influence on clinical efficacy. *Osteoporos Int,* 19**,** 733-59.

SABOKBAR, A. & ATHANASOU, N. S. 2003. Generating human osteoclasts from peripheral blood. *Methods Mol Med,* 80**,** 101-11.

SAIDENBERG-KERMANAC'H, N., COHEN-SOLAL, M., BESSIS, N., DE VERNEJOUL, M. C. & BOISSIER, M. C. 2004. Role for osteoprotegerin in rheumatoid inflammation. *Joint Bone Spine,* 71**,** 9-13.

SALZMAN, G. C., CROWELL, J. M., MARTIN, J. C., TRUJILLO, T. T., ROMERO, A., MULLANEY, P. F. & LABAUVE, P. M. 1975. Cell classification by laser light scattering: identification and separation of unstained leukocytes. *Acta Cytol,* 19**,** 374-7.

SAMBROOK, P. N., HUGHES, D. R., NELSON, A. E., ROBINSON, B. G. & MASON, R. S. 2003. Osteocyte viability with glucocorticoid treatment: relation to histomorphometry. *Ann Rheum Dis,* 62**,** 1215-7.

SANGER, F., NICKLEN, S. & COULSON, A. R. 1977. DNA sequencing with chain-terminating inhibitors. *Proc Natl Acad Sci U S A,* 74**,** 5463-7.

SANGGAARD, K. W., HANSEN, L., SCAVENIUS, C., WISNIEWSKI, H. G., KRISTENSEN, T., THOGERSEN, I. B. & ENGHILD, J. J. 2010. Evolutionary conservation

of heavy chain protein transfer between glycosaminoglycans. *Biochim Biophys Acta,* 1804**,** 1011-9.

SANGGAARD, K. W., SONNE-SCHMIDT, C. S., KROGAGER, T. P., KRISTENSEN, T., WISNIEWSKI, H. G., THOGERSEN, I. B. & ENGHILD, J. J. 2008. TSG-6 transfers proteins between glycosaminoglycans via a Ser28-mediated covalent catalytic mechanism. *J Biol Chem,* 283**,** 33919-26.

SASAKI, N., KUSANO, E., ANDO, Y., YANO, K., TSUDA, E. & ASANO, Y. 2001. Glucocorticoid decreases circulating osteoprotegerin (OPG): possible mechanism for glucocorticoid induced osteoporosis. *Nephrol Dial Transplant,* 16**,** 479-82.

SCHLESSINGER, J. 2000. Cell signaling by receptor tyrosine kinases. *Cell,* 103**,** 211-25.

SHAH, A. K., LAZATIN, J., SINHA, R. K., LENNOX, T., HICKOK, N. J. & TUAN, R. S. 1999. Mechanism of BMP-2 stimulated adhesion of osteoblastic cells to titanium alloy. *Biol Cell,* 91**,** 131-42.

SHERR, C. J., MATSUSHIME, H. & ROUSSEL, M. F. 1992. Regulation of CYL/cyclin D genes by colony-stimulating factor 1. *Ciba Found Symp,* 170**,** 209-19; discussion 219-26.

SHIMADA, T., KAKITANI, M., YAMAZAKI, Y., HASEGAWA, H., TAKEUCHI, Y., FUJITA, T., FUKUMOTO, S., TOMIZUKA, K. & YAMASHITA, T. 2004. Targeted ablation of Fgf23 demonstrates an essential physiological role of FGF23 in phosphate and vitamin D metabolism. *J Clin Invest,* 113**,** 561-8.

SIMONET, W. S., LACEY, D. L., DUNSTAN, C. R., KELLEY, M., CHANG, M. S., LUTHY, R., NGUYEN, H. Q., WOODEN, S., BENNETT, L., BOONE, T., SHIMAMOTO, G., DEROSE, M., ELLIOTT, R., COLOMBERO, A., TAN, H. L., TRAIL, G., SULLIVAN, J., DAVY, E., BUCAY, N., RENSHAW-GEGG, L., HUGHES, T. M., HILL, D., PATTISON, W., CAMPBELL, P., SANDER, S., VAN,

G., TARPLEY, J., DERBY, P., LEE, R. & BOYLE, W. J. 1997. Osteoprotegerin: a novel secreted protein involved in the regulation of bone density. *Cell,* 89**,** 309-19.

SIMS, N. A. & MARTIN, T. J. 2014. Coupling the activities of bone formation and resorption: a multitude of signals within the basic multicellular unit. *Bonekey Rep,* 3**,** 481.

SIMS, N. A. & MARTIN, T. J. 2015. Coupling Signals between the Osteoclast and Osteoblast: How are Messages Transmitted between These Temporary Visitors to the Bone Surface? *Front Endocrinol (Lausanne),* 6**,** 41.

SINCLAIR, A. M. & ELLIOTT, S. 2005. Glycoengineering: the effect of glycosylation on the properties of therapeutic proteins. *J Pharm Sci,* 94**,** 1626-35.

SONG, X., XIE, S., LU, K. & WANG, C. 2015. Mesenchymal stem cells alleviate experimental asthma by inducing polarization of alveolar macrophages. *Inflammation,* 38**,** 485-92.

SPINELLA-JAEGLE, S., ROMAN-ROMAN, S., FAUCHEU, C., DUNN, F. W., KAWAI, S., GALLEA, S., STIOT, V., BLANCHET, A. M., COURTOIS, B., BARON, R. & RAWADI, G. 2001. Opposite effects of bone morphogenetic protein-2 and transforming growth factor-beta1 on osteoblast differentiation. *Bone,* 29**,** 323-30.

SRIDHARAN, G. & SHANKAR, A. A. 2012. Toluidine blue: A review of its chemistry and clinical utility. *J Oral Maxillofac Pathol,* 16**,** 251-5.

ST-JACQUES, B., HAMMERSCHMIDT, M. & MCMAHON, A. P. 1999. Indian hedgehog signaling regulates proliferation and differentiation of chondrocytes and is essential for bone formation. *Genes Dev,* 13**,** 2072-86.

STAEHLING-HAMPTON, K., PROLL, S., PAEPER, B. W., ZHAO, L., CHARMLEY, P., BROWN, A., GARDNER, J. C., GALAS, D., SCHATZMAN, R. C., BEIGHTON, P., PAPAPOULOS, S., HAMERSMA, H. & BRUNKOW, M. E. 2002. A 52-kb de-

letion in the SOST-MEOX1 intergenic region on 17q12-q21 is associated with van Buchem disease in the Dutch population. *Am J Med Genet,* 110**,** 144-52.

STANLEY, E. R., BERG, K. L., EINSTEIN, D. B., LEE, P. S., PIXLEY, F. J., WANG, Y. & YEUNG, Y. G. 1997. Biology and action of colony--stimulating factor-1. *Mol Reprod Dev,* 46**,** 4-10.

STOVE, J., HUCH, K., GUNTHER, K. P. & SCHARF, H. P. 2000. Interleukin-1beta induces different gene expression of stromelysin, aggrecan and tumor-necrosis-factor-stimulated gene 6 in human osteoarthritic chondrocytes in vitro. *Pathobiology,* 68**,** 144-9.

SUDA, T., TAKAHASHI, N. & MARTIN, T. J. 1992. Modulation of osteoclast differentiation. *Endocr Rev,* 13**,** 66-80.

SUDA, T., TAKAHASHI, N., UDAGAWA, N., JIMI, E., GILLESPIE, M. T. & MARTIN, T. J. 1999. Modulation of osteoclast differentiation and function by the new members of the tumor necrosis factor receptor and ligand families. *Endocr Rev,* 20**,** 345-57.

SUDO, H., KODAMA, H. A., AMAGAI, Y., YAMAMOTO, S. & KASAI, S. 1983. In vitro differentiation and calcification in a new clonal osteogenic cell line derived from newborn mouse calvaria. *J Cell Biol,* 96**,** 191-8.

SUPERSAXO, A., HEIN, W. R. & STEFFEN, H. 1990. Effect of molecular weight on the lymphatic absorption of water-soluble compounds following subcutaneous administration. *Pharm Res,* 7**,** 167-9.

SZANTO, S., BARDOS, T., GAL, I., GLANT, T. T. & MIKECZ, K. 2004. Enhanced neutrophil extravasation and rapid progression of proteoglycan-induced arthritis in TSG-6-knockout mice. *Arthritis Rheum,* 50**,** 3012-22.

TAKAGI, M., PARMLEY, R. T., SPICER, S. S., DENYS, F. R. & SETSER, M. E. 1982. Ultrastructural localization of acidic glycoconjugates with the low iron diamine method. *J Histochem Cytochem,* 30**,** 471-6.

TAKAHASHI, N., YAMANA, H., YOSHIKI, S., ROODMAN, G. D., MUNDY, G. R., JONES, S. J., BOYDE, A. & SUDA, T. 1988. Osteoclast-like cell formation and its regulation by osteotropic hormones in mouse bone marrow cultures. *Endocrinology,* 122**,** 1373-82.

TAKAYANAGI, H. 2007a. Osteoimmunology: shared mechanisms and crosstalk between the immune and bone systems. *Nat Rev Immunol,* 7**,** 292-304.

TAKAYANAGI, H. 2007b. The role of NFAT in osteoclast formation. *Ann N Y Acad Sci,* 1116**,** 227-37.

TAKAYANAGI, H. 2010. New immune connections in osteoclast formation. *Ann N Y Acad Sci,* 1192**,** 117-23.

TAKAYANAGI, H., JUJI, T., MIYAZAKI, T., IIZUKA, H., TANAKA, S., ODA, H. & NAKAMURA, K. 2000a. [Amelioration of adjuvant arthritis by gene therapy suppressing Src activity]. *Nihon Rinsho Meneki Gakkai Kaishi,* 23**,** 547-9.

TAKAYANAGI, H., KIM, S., KOGA, T., NISHINA, H., ISSHIKI, M., YOSHIDA, H., SAIURA, A., ISOBE, M., YOKOCHI, T., INOUE, J., WAGNER, E. F., MAK, T. W., KODAMA, T. & TANIGUCHI, T. 2002. Induction and activation of the transcription factor NFATc1 (NFAT2) integrate RANKL signaling in terminal differentiation of osteoclasts. *Dev Cell,* 3**,** 889-901.

TAKAYANAGI, H., OGASAWARA, K., HIDA, S., CHIBA, T., MURATA, S., SATO, K., TAKAOKA, A., YOKOCHI, T., ODA, H., TANAKA, K., NAKAMURA, K. & TANIGUCHI, T. 2000b. T-cell-mediated regulation of osteoclastogenesis by signalling cross-talk between RANKL and IFN-gamma. *Nature,* 408**,** 600-5.

TANABE, N., MAENO, M., SUZUKI, N., FUJISAKI, K., TANAKA, H., OGISO, B. & ITO, K. 2005. IL-1 alpha stimulates the formation of osteoclast-like cells by increasing M-CSF and PGE2 production and decreasing OPG production by osteoblasts. *Life Sci,* 77**,** 615-26.

TANG, Y., WU, X., LEI, W., PANG, L., WAN, C., SHI, Z., ZHAO, L., NAGY, T. R., PENG, X., HU, J., FENG, X., VAN HUL, W., WAN, M. & CAO, X. 2009. TGF-beta1-induced migration of bone mesenchymal stem cells couples bone resorption with formation. *Nat Med,* 15**,** 757-65.

TATSUMI, S., ISHII, K., AMIZUKA, N., LI, M., KOBAYASHI, T., KOHNO, K., ITO, M., TAKESHITA, S. & IKEDA, K. 2007. Targeted ablation of osteocytes induces osteoporosis with defective mechanotransduction. *Cell Metab,* 5**,** 464-75.

TAXEL, P., KANEKO, H., LEE, S. K., AGUILA, H. L., RAISZ, L. G. & LORENZO, J. A. 2008. Estradiol rapidly inhibits osteoclastogenesis and RANKL expression in bone marrow cultures in postmenopausal women: a pilot study. *Osteoporos Int,* 19**,** 193-9.

TAYLOR, K. R. & GALLO, R. L. 2006. Glycosaminoglycans and their proteoglycans: host-associated molecular patterns for initiation and modulation of inflammation. *FASEB J,* 20**,** 9-22.

TERAUCHI, M. 2011. [Role of the immune system in the pathophysiology of postmenopausal osteoporosis]. *Nihon Rinsho,* 69**,** 1215-9.

TERPOS, E. & DIMOPOULOS, M. A. 2011. Interaction between the skeletal and immune systems in cancer: mechanisms and clinical implications. *Cancer Immunol Immunother,* 60**,** 305-17.

THEILL, L. E., BOYLE, W. J. & PENNINGER, J. M. 2002. RANK-L and RANK: T cells, bone loss, and mammalian evolution. *Annu Rev Immunol,* 20**,** 795-823.

TORALDO, G., ROGGIA, C., QIAN, W. P., PACIFICI, R. & WEITZMANN, M. N. 2003. IL-7 induces bone loss in vivo by induction of receptor activator of nuclear factor kappa B ligand and tumor necrosis factor alpha from T cells. *Proc Natl Acad Sci U S A,* 100**,** 125-30.

TOWBIN, H., STAEHELIN, T. & GORDON, J. 1979. Electrophoretic transfer of proteins from polyacrylamide gels to nitrocellulose sheets: procedure and some applications. *Proc Natl Acad Sci U S A,* 76**,** 4350-4.

TROY, K. L. & MORSE, L. R. 2015. Measurement of Bone: Diagnosis of SCI-Induced Osteoporosis and Fracture Risk Prediction. *Top Spinal Cord Inj Rehabil,* 21**,** 267-74.

TSUKAHARA, S., IKEDA, R., GOTO, S., YOSHIDA, K., MITSUMORI, R., SAKAMOTO, Y., TAJIMA, A., YOKOYAMA, T., TOH, S., FURUKAWA, K. & INOUE, I. 2006. Tumour necrosis factor alpha-stimulated gene-6 inhibits osteoblastic differentiation of human mesenchymal stem cells induced by osteogenic differentiation medium and BMP-2. *Biochem J,* 398**,** 595-603.

TU, B., LIU, S., LIU, G., YAN, W., WANG, Y., LI, Z. & FAN, C. 2015. Macrophages derived from THP-1 promote the osteogenic differentiation of mesenchymal stem cells through the IL-23/IL-23R/beta-catenin pathway. *Exp Cell Res,* 339**,** 81-9.

TU, X., CHEN, J., LIM, J., KARNER, C. M., LEE, S. Y., HEISIG, J., WIESE, C., SURENDRAN, K., KOPAN, R., GESSLER, M. & LONG, F. 2012a. Physiological notch signaling maintains bone homeostasis via RBPjk and Hey upstream of NFATc1. *PLoS Genet,* 8**,** e1002577.

TU, X., RHEE, Y., CONDON, K. W., BIVI, N., ALLEN, M. R., DWYER, D., STOLINA, M., TURNER, C. H., ROBLING, A. G., PLOTKIN, L. I. & BELLIDO, T. 2012b. Sost downregulation and local Wnt signaling are required for the osteogenic response to mechanical loading. *Bone,* 50**,** 209-17.

UCCELLI, A. & DE ROSBO, N. K. 2015. The immunomodulatory function of mesenchymal stem cells: mode of action and pathways. *Ann N Y Acad Sci,* 1351**,** 114-26.

USAMI, A., ISHIYAMA, S., ENOMOTO, C., OKAZAKI, H., HIGUCHI, K., IKEDA, M., YAMAMOTO, T., SUGAI, M., ISHIKAWA, Y., HOSAKA, Y., KOYAMA, T., TOBITA, Y., EBIHARA, S., MOCHIZUKI, T., ASANO, Y. & NAGAYA, H. 2011. Comparison of recombinant protein expression in a baculovirus system in insect cells (Sf9) and silkworm. *J Biochem,* 149**,** 219-27.

VAN BEZOOIJEN, R. L., ROELEN, B. A., VISSER, A., VAN DER WEE-PALS, L., DE WILT, E., KARPERIEN, M., HAMERSMA, H., PAPAPOULOS, S. E., TEN DIJKE, P. & LOWIK, C. W. 2004. Sclerostin is an osteocyte-expressed negative regulator of bone formation, but not a classical BMP antagonist. *J Exp Med,* 199**,** 805-14.

VAN STAA, T. P., LEUFKENS, H. G., ABENHAIM, L., ZHANG, B. & COOPER, C. 2000. Use of oral corticosteroids and risk of fractures. *J Bone Miner Res,* 15**,** 993-1000.

VAUGHN, J. L., GOODWIN, R. H., TOMPKINS, G. J. & MCCAWLEY, P. 1977. The establishment of two cell lines from the insect Spodoptera frugiperda (Lepidoptera; Noctuidae). *In Vitro,* 13**,** 213-7.

VENKATRAMAN GIRIJA, U., GINGRAS, A. R., MARSHALL, J. E., PANCHAL, R., SHEIKH, M. A., GAL, P., SCHWAEBLE, W. J., MITCHELL, D. A., MOODY, P. C. & WALLIS, R. 2013. Structural basis of the C1q/C1s interaction and its central role in assembly of the C1 complex of complement activation. *Proc Natl Acad Sci U S A,* 110**,** 13916-20.

VERBORGT, O., GIBSON, G. J. & SCHAFFLER, M. B. 2000. Loss of osteocyte integrity in association with microdamage and bone remodeling after fatigue in vivo. *J Bone Miner Res,* 15**,** 60-7.

VI, L., BAHT, G. S., WHETSTONE, H., NG, A., WEI, Q., POON, R., MYLVAGANAM, S., GRYNPAS, M. & ALMAN, B. A. 2015. Macrophages promote osteoblastic differentiation in-vivo: implications in fracture repair and bone homeostasis. *J Bone Miner Res,* 30**,** 1090-102.

WAKEYAMA, H., AKIYAMA, T., TAKAHASHI, K., AMANO, H., KADONO, Y., NAKAMURA, M., OSHIMA, Y., ITABE, H., NAKAYAMA, K. I., NAKAYAMA, K., NAKAMURA, K. & TANAKA, S. 2007. Negative feedback loop in the Bim-caspase-3 axis regulating apoptosis and activity of osteoclasts. *J Bone Miner Res,* 22**,** 1631-9.

WALKER, D. G. 1975. Bone resorption restored in osteopetrotic mice by transplants of normal bone marrow and spleen cells. *Science,* 190**,** 784-5.

WANG, D., CHRISTENSEN, K., CHAWLA, K., XIAO, G., KREBSBACH, P. H. & FRANCESCHI, R. T. 1999. Isolation and characterization of MC3T3-E1 preosteoblast subclones with distinct in vitro and in vivo differentiation/mineralization potential. *J Bone Miner Res,* 14**,** 893-903.

WANG, H., WU, G., ZHANG, J., ZHOU, K., YIN, B., SU, X., QIU, G., YANG, G., ZHANG, X., ZHOU, G. & WU, Z. 2016. Osteogenic effect of controlled released rhBMP-2 in 3D printed porous hydroxyapatite scaffold. *Colloids Surf B Biointerfaces,* 141**,** 491-8.

WANG, S. S., HU, S. W., ZHANG, Q. H., XIA, A. X., JIANG, Z. X. & CHEN, X. M. 2015. Mesenchymal Stem Cells Stabilize Atherosclerotic Vulnerable Plaque by Anti-Inflammatory Properties. *PLoS One,* 10**,** e0136026.

WANG, Y., AZAIS, T., ROBIN, M., VALLEE, A., CATANIA, C., LEGRIEL, P., PEHAU-ARNAUDET, G., BABONNEAU, F., GIRAUD-GUILLE, M. M. & NASSIF, N. 2012. The predominant role of collagen in the nucleation, growth, structure and orientation of bone apatite. *Nat Mater,* 11**,** 724-33.

WATANABE, J., SHETTY, A. K., HATTIANGADY, B., KIM, D. K., FORAKER, J. E., NISHIDA, H. & PROCKOP, D. J. 2013. Administration of TSG-6 improves memory after traumatic brain injury in mice. *Neurobiol Dis,* 59**,** 86-99.

WATSON, W. C. & TOWNES, A. S. 1985. Genetic susceptibility to murine collagen II autoimmune arthritis. Proposed relationship to the IgG2 autoantibody subclass response, complement C5, major histocompatibility complex (MHC) and non-MHC loci. *J Exp Med,* 162**,** 1878-91.

WATT, F. E., PATERSON, E., FREIDIN, A., KENNY, M., JUDGE, A., SAKLATVALA, J., WILLIAMS, A. & VINCENT, T. L. 2016. Acute molecular changes in synovial fluid following human knee injury are associated with early clinical outcomes. *Arthritis Rheumatol*.

WEI, S., KITAURA, H., ZHOU, P., ROSS, F. P. & TEITELBAUM, S. L. 2005. IL-1 mediates TNF-induced osteoclastogenesis. *J Clin Invest,* 115**,** 282-90.

WEINSTEIN, R. S., JILKA, R. L., PARFITT, A. M. & MANOLAGAS, S. C. 1998. Inhibition of osteoblastogenesis and promotion of apoptosis of osteoblasts and osteocytes by glucocorticoids. Potential mechanisms of their deleterious effects on bone. *J Clin Invest,* 102**,** 274-82.

WEITZMANN, M. N. 2014. T-cells and B-cells in osteoporosis. *Curr Opin Endocrinol Diabetes Obes,* 21**,** 461-7.

WESSELING-PERRY, K. 2014. The BRC canopy: an important player in bone remodeling. *Am J Pathol,* 184**,** 924-6.

WIKTOR-JEDRZEJCZAK, W., BARTOCCI, A., FERRANTE, A. W., JR., AHMED-ANSARI, A., SELL, K. W., POLLARD, J. W. & STANLEY, E. R. 1990. Total absence of colony-stimulating factor 1 in the macrophage-deficient osteopetrotic (op/op) mouse. *Proc Natl Acad Sci U S A,* 87**,** 4828-32.

WILDE, M., KLAUSBERGER, M., PALMBERGER, D., ERNST, W. & GRABHERR, R. 2014. Tnao38, high five and Sf9--evaluation of host-virus interactions in three different insect cell lines: baculovirus production and recombinant protein expression. *Biotechnol Lett,* 36**,** 743-9.

WINKLER, I. G., SIMS, N. A., PETTIT, A. R., BARBIER, V., NOWLAN, B., HELWANI, F., POULTON, I. J., VAN ROOIJEN, N., ALEXANDER, K. A., RAGGATT, L. J. & LEVESQUE, J. P. 2010. Bone marrow macrophages maintain hematopoietic stem cell (HSC) niches and their depletion mobilizes HSCs. *Blood,* 116**,** 4815-28.

WISNIEWSKI, H. G., BURGESS, W. H., OPPENHEIM, J. D. & VILCEK, J. 1994. TSG-6, an arthritis-associated hyaluronan binding protein, forms a stable complex with the serum protein inter-alpha-inhibitor. *Biochemistry,* 33**,** 7423-9.

WISNIEWSKI, H. G., COLON, E., LIUBLINSKA, V., KARIA, R. J., STABLER, T. V., ATTUR, M., ABRAMSON, S. B., BAND, P. A. & KRAUS, V. B. 2014. TSG-6 activity as a novel biomarker of progression in knee osteoarthritis. *Osteoarthritis Cartilage,* 22**,** 235-41.

WISNIEWSKI, H. G., HUA, J. C., POPPERS, D. M., NAIME, D., VILCEK, J. & CRONSTEIN, B. N. 1996. TNF/IL-1-inducible protein TSG-6 potentiates plasmin inhibition by inter-alpha-inhibitor and exerts a strong anti-inflammatory effect in vivo. *J Immunol,* 156**,** 1609-15.

WISNIEWSKI, H. G., MAIER, R., LOTZ, M., LEE, S., KLAMPFER, L., LEE, T. H. & VILCEK, J. 1993. TSG-6: a TNF-, IL-1-, and LPS-inducible secreted glycoprotein associated with arthritis. *J Immunol,* 151**,** 6593-601.

WISNIEWSKI, H. G., SNITKIN, E. S., MINDRESCU, C., SWEET, M. H. & VILCEK, J. 2005. TSG-6 protein binding to glycosaminoglycans: formation of stable complexes with hyaluronan and binding to chondroitin sulfates. *J Biol Chem,* 280**,** 14476-84.

WISNIEWSKI, H. G. & VILCEK, J. 1997. TSG-6: an IL-1/TNF-inducible protein with anti-inflammatory activity. *Cytokine Growth Factor Rev,* 8**,** 143-56.

WISNIEWSKI, H. G. & VILCEK, J. 2004. Cytokine-induced gene expression at the crossroads of innate immunity, inflammation and fertility: TSG-6 and PTX3/TSG-14. *Cytokine Growth Factor Rev,* 15**,** 129-46.

WONG, B. R., BESSER, D., KIM, N., ARRON, J. R., VOLOGODSKAIA, M., HANAFUSA, H. & CHOI, Y. 1999. TRANCE, a TNF family member, activates Akt/PKB through a signaling complex involving TRAF6 and c-Src. *Mol Cell,* 4**,** 1041-9.

WONG, B. R., JOSIEN, R., LEE, S. Y., VOLOGODSKAIA, M., STEINMAN, R. M. & CHOI, Y. 1998. The TRAF family of signal transducers mediates NF-kappaB activation by the TRANCE receptor. *J Biol Chem,* 273**,** 28355-9.

WONG, D. A., KUMAR, A., JATANA, S., GHISELLI, G. & WONG, K. 2008. Neurologic impairment from ectopic bone in the lumbar canal: a potential complication of off-label PLIF/TLIF use of bone morphogenetic protein-2 (BMP-2). *Spine J,* 8**,** 1011-8.

WOZNEY, J. M. 1995. The potential role of bone morphogenetic proteins in periodontal reconstruction. *J Periodontol,* 66**,** 506-10.

WOZNEY, J. M., ROSEN, V., CELESTE, A. J., MITSOCK, L. M., WHITTERS, M. J., KRIZ, R. W., HEWICK, R. M. & WANG, E. A. 1988. Novel regulators of bone formation: molecular clones and activities. *Science,* 242**,** 1528-34.

WU, A. C., RAGGATT, L. J., ALEXANDER, K. A. & PETTIT, A. R. 2013. Unraveling macrophage contributions to bone repair. *Bonekey Rep,* 2**,** 373.

WYTHE, S. E., NICOLAIDOU, V. & HORWOOD, N. J. 2014. Cells of the immune system orchestrate changes in bone cell function. *Calcif Tissue Int,* 94**,** 98-111.

XU, J., ZHEN, J., ZHU, J. & LIN, Q. 2016. Tumor necrosis factor-alpha induced protein 6 attenuates acute lung injury following paraquat exposure. *Toxicol Mech Methods,* 26**,** 32-5.

YANAGISHITA, M. 1993. Function of proteoglycans in the extracellular matrix. *Acta Pathol Jpn,* 43**,** 283-93.

YANG, H., APRECIO, R. M., ZHOU, X., WANG, Q., ZHANG, W., DING, Y. & LI, Y. 2014. Therapeutic effect of TSG-6 engineered iPSC-derived MSCs on experimental periodontitis in rats: a pilot study. *PLoS One,* 9**,** e100285.

YANG, J., ANDRE, P., YE, L. & YANG, Y. Z. 2015. The Hedgehog signalling pathway in bone formation. *Int J Oral Sci,* 7**,** 73-9.

YANG, Y. 2013. *Skeletal morphogenesis and embryonic development,* Ames, Iowa, Wiley-Blackwell.

YASUDA, H., SHIMA, N., NAKAGAWA, N., MOCHIZUKI, S. I., YANO, K., FUJISE, N., SATO, Y., GOTO, M., YAMAGUCHI, K., KURIYAMA, M., KANNO, T., MURAKAMI, A., TSUDA, E., MORINAGA, T. & HIGASHIO, K. 1998a. Identity of osteoclastogenesis inhibitory factor (OCIF) and osteoprotegerin (OPG): a mechanism by which OPG/OCIF inhibits osteoclastogenesis in vitro. *Endocrinology,* 139**,** 1329-37.

YASUDA, H., SHIMA, N., NAKAGAWA, N., YAMAGUCHI, K., KINOSAKI, M., MOCHIZUKI, S., TOMOYASU, A., YANO, K., GOTO, M., MURAKAMI, A., TSUDA, E., MORINAGA, T., HIGASHIO, K., UDAGAWA, N., TAKAHASHI, N. & SUDA, T. 1998b. Osteoclast differentiation factor is a ligand for osteoprotegerin/osteoclastogenesis-inhibitory factor and is identical to TRANCE/RANKL. *Proc Natl Acad Sci U S A,* 95**,** 3597-602.

YAVROPOULOU, M. P., XYGONAKIS, C., LOLOU, M., KARADIMOU, F. & YOVOS, J. G. 2014. The sclerostin story: from human genetics to the development of novel anabolic treatment for osteoporosis. *Hormones (Athens),* 13**,** 323-37.

YAVROPOULOU, M. P. & YOVOS, J. G. 2008. Osteoclastogenesis--current knowledge and future perspectives. *J Musculoskelet Neuronal Interact,* 8**,** 204-16.

YE, L., MORA, R., AKHAYANI, N., HAUDENSCHILD, C. C. & LIAU, G. 1997. Growth factor and cytokine-regulated hyaluronan-binding protein TSG-6 is localized to the injury-induced rat neointima and confers enhanced growth in vascular smooth muscle cells. *Circ Res,* 81**,** 289-96.

YOKOYAMA, M., UKAI, T., AYON HARO, E. R., KISHIMOTO, T., YOSHINAGA, Y. & HARA, Y. 2011. Membrane-bound CD40 ligand on T cells from mice injected with lipopolysaccharide accelerates lipopolysaccharide-induced osteoclastogenesis. *J Periodontal Res,* 46**,** 464-74.

YONA, S., KIM, K. W., WOLF, Y., MILDNER, A., VAROL, D., BREKER, M., STRAUSS-AYALI, D., VIUKOV, S., GUILLIAMS, M., MISHARIN, A., HUME, D. A., PERLMAN, H., MALISSEN, B., ZELZER, E. & JUNG, S. 2013. Fate mapping reveals origins and dynamics of monocytes and tissue macrophages under homeostasis. *Immunity,* 38**,** 79-91.

YONGTAO, Z., KUNZHENG, W., JINGJING, Z., HU, S., JIANQIANG, K., RUIYU, L. & CHUNSHENG, W. 2014. Glucocorticoids activate the local renin-angiotensin system in bone: possible mechanism for glucocorticoid-induced osteoporosis. *Endocrine,* 47**,** 598-608.

YOSHIDA, H., HAYASHI, S., KUNISADA, T., OGAWA, M., NISHIKAWA, S., OKAMURA, H., SUDO, T., SHULTZ, L. D. & NISHIKAWA, S. 1990. The murine mutation osteopetrosis is in the coding region of the macrophage colony stimulating factor gene. *Nature,* 345**,** 442-4.

YOSHIDA, K., KOBAYASHI, K., YAMAGATA, N., IWABUCHI, H., KATSURA, T., SUGIHARA, S., NEGISHI, M., IDE, H., MORI, Y. & TAKAHASHI, T. 1992. Inflammatory cytokines and enzymes in synovial fluid of patients with rheumatoid arthritis and other arthritides. *Int Arch Allergy Immunol,* 98**,** 286-92.

YOSHIKO, Y., CANDELIERE, G. A., MAEDA, N. & AUBIN, J. E. 2007. Osteoblast autonomous Pi regulation via Pit1 plays a role in bone mineralization. *Mol Cell Biol,* 27**,** 4465-74.

YOSHITAKE, F., ITOH, S., NARITA, H., ISHIHARA, K. & EBISU, S. 2008. Interleukin-6 directly inhibits osteoclast differentiation by suppressing receptor activator of NF-kappaB signaling pathways. *J Biol Chem,* 283**,** 11535-40.

YOSHITAKE, H., RITTLING, S. R., DENHARDT, D. T. & NODA, M. 1999. Osteopontin-deficient mice are resistant to ovariectomy-induced bone resorption. *Proc Natl Acad Sci U S A,* 96**,** 8156-60.

YOUSEFZADEH, G., LARIJANI, B., MOHAMMADIRAD, A., HESHMAT, R., DEHGHAN, G., RAHIMI, R. & ABDOLLAHI, M. 2006. Determination of oxidative stress status and concentration of TGF-beta 1 in the blood and saliva of osteoporotic subjects. *Ann N Y Acad Sci,* 1091**,** 142-50.

YUN, A. J. & LEE, P. Y. 2004. Maldaptation of the link between inflammation and bone turnover may be a key determinant of osteoporosis. *Med Hypotheses,* 63**,** 532-7.

ZAISS, M. M., KUROWSKA-STOLARSKA, M., BOHM, C., GARY, R., SCHOLTYSEK, C., STOLARSKI, B., REILLY, J., KERR, S., MILLAR, N. L., KAMRADT, T., MCINNES, I. B., FALLON, P. G., DAVID, J. P., LIEW, F. Y. & SCHETT, G. 2011. IL-33 shifts the balance from osteoclast to alternatively activated macrophage differentiation and protects from TNF-alpha-mediated bone loss. *J Immunol,* 186**,** 6097-105.

ZANIER, E. R., MARCHESI, F., ORTOLANO, F., PEREGO, C., ARABIAN, M., ZOERLE, T., SAMMALI, E., PISCHIUTTA, F. & DE SIMONI, M. G. 2015. Fractalkine Receptor Deficiency Is Associated with Early Protection but Late Worsening of Outcome following Brain Trauma in Mice. *J Neurotrauma*.

ZARBOCK, A., KEMPF, T., WOLLERT, K. C. & VESTWEBER, D. 2012. Leukocyte integrin activation and deactivation: novel mechanisms of balancing inflammation. *J Mol Med (Berl),* 90**,** 353-9.

ZHANG, C. 2010. Transcriptional regulation of bone formation by the osteoblast-specific transcription factor Osx. *J Orthop Surg Res,* 5**,** 37.

ZHANG, J., NIU, C., YE, L., HUANG, H., HE, X., TONG, W. G., ROSS, J., HAUG, J., JOHNSON, T., FENG, J. Q., HARRIS, S., WIEDEMANN, L. M., MISHINA, Y. & LI, L. 2003. Identification of the haematopoietic stem cell niche and control of the niche size. *Nature,* 425**,** 836-41.

ZHANG, K., BARRAGAN-ADJEMIAN, C., YE, L., KOTHA, S., DALLAS, M., LU, Y., ZHAO, S., HARRIS, M., HARRIS, S. E., FENG, J. Q. & BONEWALD, L. F. 2006. E11/gp38 selective expression in osteocytes: regulation by mechanical strain and role in dendrite elongation. *Mol Cell Biol,* 26**,** 4539-52.

ZHAO, C., IRIE, N., TAKADA, Y., SHIMODA, K., MIYAMOTO, T., NISHIWAKI, T., SUDA, T. & MATSUO, K. 2006. Bidirectional ephrinB2-EphB4 signaling controls bone homeostasis. *Cell Metab,* 4**,** 111-21.

ZUO, D., TANG, Q., FAN, H., SHOU, Z., LIU, X., CAO, D. & ZOU, Z. 2015. Modulation of nuclear factor-kappaB-mediated pro-inflammatory response is associated with exogenous administration of bone marrow-derived mesenchymal stem cells for treatment of experimental colitis. *Mol Med Rep,* 11**,** 2741-8.